

**An Exploration of the Mechanism of Hydrophilic Interaction Chromatography
(HILIC) and the Application of HILIC in Metabolomic Profiling**

**A thesis submitted to the Strathclyde Institute of Pharmacy and Biomedical Sciences in
Partial Fulfilment of the Requirement for the award of Doctor of Philosophy of
Strathclyde University.**

By

Sami Salim A Bawazeer

2016

Declaration

'This thesis is the result of the author's original research. It has been composed by the author and has not been previously submitted for examination which has led to the award of a degree.'

'The copyright of this thesis belongs to the author under the terms of the United Kingdom Copyright Acts as qualified by University of Strathclyde Regulation 3.50. Due acknowledgement must always be made of the use of any material contained in, or derived from, this thesis.'

Signed:

Date:

Acknowledgements

I would like to thank, first and foremost, my supervisor Dr David Watson for his constant guidance throughout the PhD research and during the writing of this thesis. Thanks also go to all my colleagues and friends in Dr David Watson's laboratory for having a great time together.

Secondly, my heartfelt gratitude goes to my Dad, Mum and my son for bearing with me and for supporting me during this whole time. I am also very grateful to my brother Dr Saud Bawazeer for all his guidance in this research work. I am also grateful to the entire family. May Allah bless you all!

I am also grateful to the Saudi Cultural Bureau for the funding and support.

Dedication

This work is dedicated to my lovely son.

Contents

Declaration	i
Acknowledgements	ii
Dedication	iii
List of Figures	viii
List of Tables.....	xvii
List of Abbreviations.....	xix
Abstract	xxi
1 Introduction.....	2
1.1 Chromatographic Theory	2
1.2 Chromatographic Performance.....	3
1.3 Separation Techniques	6
1.3.1 Normal Phase Liquid Chromatography	6
1.3.2 Reversed Phase Liquid Chromatography (RPLC):.....	6
1.3.3 Hydrophilic interaction liquid chromatography (HILIC):	8
1.4 Types of HILIC columns.....	13
1.4.1 Bare Silica:	13
1.4.2 Silicon Hydride Columns (Type C Silica):	15
1.4.3 HILIC columns based on silica gel with neutral surface ligands:.....	18
1.5 Factors affecting the separation in HILIC.....	25
1.5.1 Column Temperature:	26
1.5.2 The Effect of the Mobile phase	28
1.5.3 The effect of pH	31
1.5.4 The effect of the buffer concentration on retention in HILIC.....	32
1.6 Applications of HILIC.....	33

1.6.1	Analysis of Formulations:	33
1.6.2	Analysis of Drug Impurities:.....	33
1.6.3	Bioanalysis and Drug Metabolism:	33
1.6.4	Miscellaneous Applications of HILIC:	33
1.6.5	High Performance Liquid Chromatograph (HPLC):	34
1.6.6	Liquid chromatography- Mass spectrometry (LC-MS):	35
1.7	Metabolomics	38
1.7.1	Definition of metabolomics.....	38
1.7.2	Application of Mass Spectrometry in Metabolomics.....	39
1.7.3	Applications of Metabolomics	40
1.7.4	Software in Metabolomics	41
1.8	Aims and Objectives	42
2	Investigation of the effect of different anions on hydrophilic interaction with silica gel.....	44
2.1	Introduction	44
2.2	Aims	47
2.3	Materials and methods.....	47
2.3.1	Chemicals and columns.....	47
2.3.2	Buffer preparation	48
2.3.3	Mobile phase preparation.....	48
2.3.4	Chromatographic System	49
2.3.5	Sample preparation.....	49
2.4	Results	50
2.4.1	Retention of Test Probes on a Kromasil Column with Ammonium Acetate as the Mobile phase modifier.....	50

2.4.2	Retention of Test Probes on a Kromasil Column with Ammonium Formate as the Mobile phase modifier	59
2.4.3	Retention of Test Probes on a Kromasil Column with Ammonium Bicarbonate as the Mobile phase modifier	68
2.4.4	Retention of Test Probes on a Kromasil Column with Ammonium Chloride as the Mobile phase modifier.....	72
2.4.5	Retention of Test Probes on a Kromasil Column with Ammonium Propionate As the Mobile phase modifier	76
2.5	Separation of Sugars Using a Kromasil 60 Column with LC-MS Detection	81
2.6	Application of a Nucleodur core shell column to separation of sugars.....	84
3	A study of some hydride columns for the separation of biomolecules.....	91
3.1	Introduction	91
3.2	Aims of this chapter	91
3.3	Materials and Methods	91
3.3.1	Mobile phase	91
3.3.2	Samples	91
3.3.3	LC-MS Conditions.....	92
3.4	Results and Discussion.....	92
4	A study of the reductive amination of sugars.....	101
4.1	Introduction	101
4.2	Aims	107
4.2.1	Overall objective	107
4.2.2	Specific objectives	107
4.3	Materials and methods.....	108
4.3.1	Test probes and tagging agents	108

4.3.2	Derivatisation of the hexose sugars.....	108
4.3.3	Quantification of sugars in brain samples.....	108
4.3.4	LC-MS conditions.....	110
4.4	Results.....	110
4.4.1	Aniline derivatives of hexose sugars.....	110
4.4.2	Aniline derivatives of hexose sugar phosphates.....	117
4.5	Deuterated aniline derivatives.....	121
4.6	Procainamide Derivatives.....	123
4.7	Analysis of sugars in brain samples.....	128
5	Application of hydrophilic interaction chromatography methods to the profiling of mammalian milks.....	136
5.1	Introduction.....	136
5.2	Materials and methods.....	138
5.2.1	Chemicals and reagents.....	138
5.2.2	Milk Samples.....	139
5.2.3	Preparation of milk samples.....	139
5.2.4	HILIC–HRMS and multiple tandem HRMS analysis and data processing.....	139
5.2.5	Multivariate analysis.....	140
5.3	Results.....	140
5.4	Analysis of Lipids in Seal Milk.....	177
6	Conclusion and Future Work.....	196
	References.....	199

List of Figures

Figure 1.1: Typical chromatogram for a single analyte showing key parameters	4
Figure 1.2: Use of polar embedded groups in reversed phase liquid chromatography	7
Figure 1.3: The partition mechanism in HILIC chromatography	9
Figure 1.4: Retention time of the benzene with different percentage of the water content in a water/acetonitrile mobile phase using an Atlantis silica column.	10
Figure 1.5: Chromatographs for nortriptyline, diphenhydramine, benzylamine, and procainamide with different stationary phases.....	12
Figure 1.6: Surface chemistry of bare silica HILIC stationary phase	13
Figure 1.7: Types of silanol groups.....	13
Figure 1.8: The hydrosilanisation process	14
Figure 1.9: The types of interaction which can occur between and analyte and the silica gel surface in HILIC mode.	15
Figure 1.10: The hydrosilation reaction of the Silica gel and triethoxysilane (TES) resulting in a silicon hydride surface [10].....	16
Figure 1.11: Chemical structure of the silicon hydride, UDC cholesterol hydride and bidentate C18 hydride phases.	17
Figure 1.12: Chemical structures of the mixed mode diol, cross-linked diol and polyethelene glycol phases.....	19
Figure 1.13: The surface of aminopropyl silica without end-capping.	19
Figure 1.14: Chemical reaction of a primary amine and aldehyde group to produce a Schiff's base.	20
Figure 1.15: The surface chemistry of amide silica without endcapping.	21
Figure 1.16: Surface chemistry of (1) aminopropyl silica, (2) poly(succinimide) silica, (a) Poly(aspartic acid) silica, (b) Poly(2-hydroxyethyl) aspartamide silica, and (c) Poly(2-sulfoethyl) aspartamide silica.	22
Figure 1.17: Chemistry surface of a cyclodextrin phase and a toroid structure showing the interaction of a polar analyte with the column surface.....	23
Figure 1.18: Surface chemistry of cyanopropyl silica without end-capping.	24
Figure 1.19: The chemical structure the ZIC-HILIC and ZIC-cHILIC.	25
Figure 1.20: Plot of ln k against the column temperature for (◇) urea, (■) sucrose and (▲) glycine.....	27

Figure 1.21: The van't Hoff plots for (A) aspirin and (B) cytosine on (■) an amine stationary phase (YMC-Pack NH ₂), (◆) an amide stationary phase (TSKgel Amide-80), (▲) a silica stationary phase (HILIC Silica), and (×) a zwitterionic stationary phase (ZIC-HILIC).....	28
Figure 1.22: Effect of different types of the mobile phase organic modifiers on the separation of (1) epidaunorubicin, (2) daunorubicin, (3) epirubicin, (4) doxorubicin..	30
Figure 1.23: Chemical structures for (A) daunorubicin and (B) epirubicin [43].	30
Figure 1.24: The effect of the different mobile phase pH for the aspirin on (◆) amide, (■) silica and (▲) sulfobetaine phases.....	32
Figure 1.25: Schematic diagram of a HPLC system	34
Figure 1.26: A Thermo Scientific Exactive mass spectrometer.....	35
Figure 1.27: Electrospray ionisation process.	36
Figure 1.28: Orbitrap instrument [65].....	37
Figure 2.1: Nicotinic acid run with 5 mM ammonium acetate in acetonitrile/water (90:10) on a Kromasil 60 column.	51
Figure 2.2: Maleic acid run with 5 mM ammonium acetate in acetonitrile/water (90:10) on a Kromasil 60 column.	52
Figure 2.3: Inosine run with 5 mM ammonium acetate in acetonitrile/water (90:10) on a Kromasil 60 column.	52
Figure 2.4: Xanthine run with 5 mM ammonium acetate in acetonitrile/water (90:10) on a Kromasil 60 column.	53
Figure 2.5: Riboflavin run with 5 mM ammonium acetate in acetonitrile/water (90:10) on a Kromasil 60 column.	53
Figure 2.6: Nicotinic acid run with 10 mM ammonium acetate in acetonitrile/water (90:10) on a Kromasil 60 column.	54
Figure 2.7: Maleic acid run with 10 mM ammonium acetate in acetonitrile/water (90:10) on a Kromasil 60 column.	54
Figure 2.8: Inosine run with 10 mM ammonium acetate in acetonitrile/water (90:10) on a Kromasil 60 column.	55
Figure 2.9: Xanthine run with 10 mM ammonium acetate in acetonitrile/water (90:10) on a Kromasil 60 column.	55

Figure 2.10: Riboflavin run with 10 mM ammonium acetate in acetonitrile/water (90:10) on a Kromasil 60 column.	56
Figure 2.11: Nicotinic acid run with 20 mM ammonium acetate in acetonitrile/water (90:10) on a Kromasil 60 column.	56
Figure 2.12: Maleic acid run with 20 mM ammonium acetate in acetonitrile/water (90:10) on a Kromasil 60 column.	57
Figure 2.13: Inosine run with 20 mM ammonium acetate in acetonitrile/water (90:10) on a Kromasil 60 column.	57
Figure 2.14: Xanthine run with 20 mM ammonium acetate in acetonitrile/water (90:10) on a Kromasil 60 column.	58
Figure 2.15: Riboflavin run with 20 mM ammonium acetate in acetonitrile/water (90:10) on a Kromasil 60 column.	58
Figure 2.32: Nicotinic acid run with 10 mM ammonium bicarbonate in acetonitrile/water (90:10) on a Kromasil 60 column.	69
Figure 2.33: Nicotinic acid run with 20 mM ammonium bicarbonate in acetonitrile/water (90:10) on a Kromasil 60 column.	70
Figure 2.34: Inosine run with 5 mM ammonium bicarbonate in acetonitrile/water (90:10) on a Kromasil 60 column.	70
Figure 2.35: Inosine run with 10 mM ammonium bicarbonate in acetonitrile/water (90:10) on a Kromasil 60 column.	71
Figure 2.36: Inosine run with 20 mM ammonium bicarbonate in acetonitrile/water (90:10) on a Kromasil 60 column.	71
Figure 2.37: Nicotinic acid run with 5 mM ammonium chloride in acetonitrile/water (90:10) on a Kromasil 60 column.	73
Figure 2.38: Maleic acid run with 5 mM ammonium chloride in acetonitrile/water (90:10) on a Kromasil 60 column.	73
Figure 2.39: Nicotinic acid run with 10 mM ammonium chloride in acetonitrile/water (90:10) on a Kromasil 60 column.	74
Figure 2.40: Maleic acid run with 10 mM ammonium chloride in acetonitrile/water (90:10) on a Kromasil 60 column.	74
Figure 2.52: The structure of glucose showing the α - and β -furanose and pyranose forms respectively.	82

Figure 2.55: Extracted ion traces (negative ion m/z 259.02-259.03) showing the chromatography of sugar phosphates on a Nucleodur hydrophilic interaction column (150 x 4.6 mm, 2.5 μ m)..	85
Figure 2.56: Extracted ion traces (m/z 179.05-179.06 negative ion) showing separation of sugars on a Nucleodur hydrophilic interaction column (150 x 4.6 mm, 2.5 μ m).	86
Figure 2.57: Extracted ion traces (m/z 259.02-259.03 negative ion) showing separation of sugar phosphates on a Nucleodur hydrophilic interaction column (150 x 4.6 mm, 2.5 μ m).	87
Figure 2.59: Extracted ion traces (m/z 179.05-179.06 negative ion) showing separation of sugars on a Nucleodur hydrophilic interaction column (150 x 4.6 mm, 2.5 μ m).	89
Figure 2.60: Extracted ion traces (m/z 259.02-259.03 negative ion) showing separation of sugar phosphates on a Nucleodur hydrophilic interaction column (150 x 4.6 mm, 2.5 μ m).	89
Figure 3.1 EICs for taurocholic acid (m/z 516.29-516.3) run in HILIC and RP modes on three silicon hydride columns	97
Figure 3.2 EIC for acetylcarnitine (m/z 204.12-204.14) on silicon hydride columns.	97
Figure 3.3 EICs for benzyl sulphate (m/z 187.0-187.02) in urine in HILIC and RP modes on hydride columns.	98
Figure 3.4 EICs for menthol glucuronide (m/z 331.17-331.18) in urine in HILIC and RP modes on hydride columns.	99
Figure 4.1 The equilibrium forms of glucose where the aldehyde group can react to form 5 (furan) or six membered ring via formation of a hemiacetal.	101
Figure 4.2 Chromatograms for glucose and galactose on a ZICpHILIC column (150 x 4.6 mm, 5 μ m) with gradient conditions as specified in section 4.3.4.	102
Figure 4.3 Formation of pyranose ring.	104
Figure 4.4 Reductive amination of a sugar.	105
Figure 4.5 Equilibrium between the hemi-acetal ring form of glucose and its open chain aldehyde form.	106
Figure 4.6 Structures of aniline and aminobenzamide.	107

Figure 4.7: Derivatisation reaction for 4-aminobenzamide derivatives.....	112
Figure 4.8 Aniline derivative of glucose.....	113
Figure 4.9: Chromatograms of the aniline derivatives of the four sugars galactose, glucose, mannose and fructose.....	114
Figure 4.10 Aniline derivatives of the milk sugars showing the presence of glucose, galactose and lactose.....	115
Figure 4.11 Aniline derivatives of sialyl lactose isomers present in milks with the mass spectrum for sialyl lactose.....	116
Figure 4.12 Aniline tagged sialyl lactose sugar.....	117
Figure 4.13 Chemical structure of glucose-6-phosphate in its protonated and ionised forms.....	117
Figure 4.14 Chemical structures of mannose-6, galactose-6 and fructose-1-phosphates.....	118
Figure 4.15 Extracted ion chromatogram of the aniline derivative of glucose-6-phosphate (a) and its mass spectrum (b) showing the exact mass of the stable derivative product formed.....	120
Figure 4.16 Chromatograms showing the separation of aniline derivatives for fructose-1-phosphate and galactose-6, glucose-6 and mannose-6 phosphates.....	121
Figure 4.17 Reductive amination of a sugar using pentadeutero aniline and picoline borane.....	122
Figure 4.18 Sugar standards as deuterioaniline derivatives analysed on a ZICHILIC column using the conditions described in section 4.3.2.....	123
Figure 4.19 The chemical structure of procainamide, whose chemical name is 4-amino-N-(2-diethylaminoethyl) benzamide.....	124
Figure 4.20 Reductive amination of glucose with procainamide in the presence of picoline borane complex.....	124
Figure 4.21 Extracted ion chromatogram of the procainamide derivative of galactose.....	125
Figure 4.22 Extracted ion chromatograms of the procainamide derivative of galactose, glucose, mannose and fructose.....	126
Figure 4.23 Extracted ion chromatograms of the procainamide derivative of galactose-6-phosphate.....	127

Figure 4.24 Extracted ion chromatograms showing the separation of procainamide derivatives of galactose-6, glucose-6, mannose-6 and fructose-1 phosphates.....	128
Figure 4.25 Chromatograms showing peaks of glucose, galactose and mannose as derivatives formed reductive amination with pentadeuterated aniline in the calibration series.....	129
Figure 4.26 Chromatogram showing peaks of ¹³ C glucose internal standard as a derivative pentadeuterated aniline spiked into each point in the calibration series...	129
Figure 4.27 Calibration curve for glucose.....	131
Figure 4.28 Calibration curve for galactose.....	131
Figure 4.29 Calibration curve for mannose.....	132
Figure 4.30 Sugars as their deuterioaniline derivatives. The levels of glucose in affected and control samples were estimated as 2.62µg/ml and 2.03 µg/ml respectively.	133
Figure 4.31 An unidentified abundant pentose present in affected and control brain samples.....	134
Figure 5.1 PCA analysis of mammalian milks showing the separation between cow, goat and camel and seal milk at 8 and 13 days post-partum.....	141
Figure 5.2 Most important components for discriminating land based mammalian milks from seal milk.	141
Figure 5.3 Extracted ion traces for lactose as its chloride adduct in seal, camel, goat and cow milks.	142
Figure 5.4 Extracted ion traces for sialyl lactose in seal, camel, goat and cow milks.	144
Figure 5.5 Extracted ion traces showing lysophosphatidic acid (LPA; C16:0) in seal, camel, goat and cow milk.....	145
Figure 5.6 The relative levels of taurine in different mammalian milks.....	148
Figure 5.7 The relative levels of taurocholic acid in different mammalian milks...	149
Figure 5.8 PCA separation of cow, goat, camel and seal milks based on positive ion mass spectrometry data.	150
Figure 5.9 Extracted ion traces for anthranilic acid (upper) and nicotinamide in 8 day seal milk samples.	153

Figure 5.10 Nicotinamide in the milk of terrestrial mammals in comparison with seal milk.	154
Figure 5.11 Anthranilic acid in the milk of terrestrial mammals in comparison with seal milk.	154
Figure 5.12 N-methyl nicotinamide acid in the milk of terrestrial mammals in comparison with seal milk.	155
Figure 5.13 Biosynthesis of nicotinamide and N-methylpyridone carboxamides. ...	156
Figure 5.14 N1-methyl-2-pyridone-5-carboxamide in the milk of terrestrial mammals in comparison with seal milk.	156
Figure 5.15 Carnitine in the milk of terrestrial mammals in comparison with seal milk.	157
Figure 5.16 Acetyl carnitine in the milk of terrestrial mammals in comparison with seal milk.	158
Figure 5.17 Propionyl carnitine in the milk of terrestrial mammals in comparison with seal milk.	159
Figure 5.18 Butyl carnitine in the milk of terrestrial mammals in comparison with seal milk.	159
Figure 5.19 Extracted ion trace for acetyl carnitine in seal, camel, goat and cow milk.	160
Figure 5.20 Docosahexanoyl carnitine in the milk of terrestrial mammals in comparison with seal milk.	161
Figure 5.21 Oleoyl carnitine in the milk of terrestrial mammals in comparison with seal milk.	161
Figure 5.22 Palmitoyl carnitine in the milk of terrestrial mammals in comparison with seal milk.	162
Figure 5.23 Palmitoleyl carnitine in the milk of terrestrial mammals in comparison with seal milk.	162
Figure 5.24 PCA with hierarchical cluster analysis (HCA) showing no clear separation between the seal milks with time based on 969 metabolites.	166
Figure 5.25 OPLS plot based on eight metabolites of day of milk collection versus predicted day of milk collection.	166

Figure 5.26 Cross validation plot for the OPLS for seal milk composition versus day of collection.....	167
Figure 5.27 Variation of creatinine between day 2 and day 18 in seal milk samples.	168
Figure 5.28 Variation of creatine between day 2 and day 18 in seal milk samples .	169
Figure 5.29 Variation of glycerophosphocholine between day 2 and day 18 in seal milk samples.	169
Figure 5.30 Variation of betaine between day 2 and day 18 in seal milk samples. .	170
Figure 5.31 Variation of carnitine between day 2 and day 18 in seal milk samples.	170
Figure 5.32 Variation of acetyl carnitine between day 2 and day 18 in seal milk samples.....	171
Figure 5.33 Variation of nicotinamide between day 2 and day 18 in seal milk samples.....	171
Figure 5.34 Variation of amino octanoic acid between day 2 and day 18 in seal milk samples.....	172
Figure 5.35 PCA analysis with HCA analysis of negative ion data for seal milk samples based on 650 metabolites.	174
Figure 5.36 OPLS plot for predicted against actual day for seal milk collected over 18 days based on three metabolites detected in negative ion mode.....	175
Figure 5.37 Variation of amino taurine between day 2 and day 18 in seal milk samples.....	176
Figure 5.38 Variation of hexanoic acid between day 2 and day 18 in seal milk samples.....	176
Figure 5.39 Variation of hexadecanoic acid between day 2 and day 18 in seal milk samples.....	177
Figure 5.40 Separation of seal milk samples according to day by PCA with HCA analysis based on 1198 metabolites.	178
Figure 5.41 OPLS model based on eight metabolites detected in negative ion mode showing predicted against actual day of collection for seal milk samples.	178
Figure 5.42 Variation of docosahexanoic acid with day of collection of seal milk sample.	179

Figure 5.43 Variation of eicosapentanoic acid with day of collection of seal milk sample.	180
Figure 5.44 Variation of oxooctadecanoic acid with day of collection of seal milk sample.	181
Figure 5.45 Variation of octadecatrienoic acid with day of collection of seal milk sample.	182
Figure 5.46 Variation of pantothenic acid with day of collection of seal milk sample.	182
Figure 5.47 Variation of oxohexanoic acid with day of collection of seal milk sample.	183
Figure 5.48 Variation of octadecanoic acid with day of collection of seal milk sample.	183
Figure 5.49 Variation of docosatetraenoic acid with day of collection of seal milk sample.	184
Figure 5.50 Extracted ion traces for sialyl lactose in seal, camel, goat and cow milks.	187
Figure 5.51 Variation in sialyl lactose levels in seal milk with time.	187
Figure 5.52 PCA with HCA for seal milk sample lipid profiles in positive ion mode.	188
Figure 5.53 Plot of actual against predicted day based on OPLS model of seal milk lipid data in positive ion mode.	189
Figure 5.54 Variation in PC 32:1 levels in seal milk with time.	190
Figure 5.55 Variation in PC 34:1 levels in seal milk with time.	190
Figure 5.56 Variation in PC 34:0 levels in seal milk with time.	191
Figure 5.57 Variation in triglycerides with time in seal milk.	194

List of Tables

Table 2.1: Factors governing the HILIC effect for acidic and neutral compounds. ..	44
Table 2.2: The elemental compositions, molecular weight and chemical structures of the various test probes used in this chapter.	46
Table 2.3: The hydration energies of the ions in the five mobile phase modifiers used.	47
Table 2.4: Preparation of the buffers of ammonium acetate, bicarbonate, chloride and propionate.....	49
Table 2.5: Mean retention times of the test probes under different strengths of ammonium acetate mobile phase modifier.	50
Table 2.6: Mean retention times of the test probes under different strengths of ammonium formate mobile phase modifier.	59
Table 2.7: Mean retention times of the test probes under different strengths of ammonium bicarbonate mobile phase modifier.....	68
Table 2.8: Mean retention times of the test probes under different strengths of ammonium chloride mobile phase modifier.	72
Table 2.9: Mean retention times of the test probes under different strengths of ammonium propionate mobile phase modifier.	76
Table 3.1 Retention times of some standards for biomolecules on hydride columns in A HILIC mode B reversed phase mode.	94
Table 4.1: Gradient conditions in the analysis of hexose sugar derivatives	110
Table 4.2 Summary table showing peaks areas and peak area ratios (vs. ¹³ C glucose internal standard) of glucose, galactose and mannose.	130
Table 5.1 Fatty acid content (% of total fat content) of fur seal milk during different periods of lactation (analysed by gas chromatography) by Iverson <i>et al.</i> , 1997 [112].	138
Table 5.2 The most important metabolites observed in negative ion mode distinguishing seal milk from camel/goat/cow (CGC) milk.	143
Table 5.3 Top ten features by intensity in camel, cow, goat and seal milks in negative ion mode.....	147
Table 5.4 The most important metabolites in positive ion mode distinguishing seal milk from camel/goat/cow (CGC) milk.	150

Table 5.5 The ten most intense metabolites by absolute response in camel, goat, cow and seal milks	164
Table 5.6 Eight variables used to classify the seal milk samples according to day of collection.	168
Table 5.7 Ten most abundant metabolites by absolute response in positive ion mode in seal milks at four time points.	173
Table 5.8 Metabolites with the greatest impact on the OPLS model for seal milk samples in relation to day of collection in negative ion mode.	175
Table 5.9 Metabolites detected in negative ion mode predicting day of collection of seal milk.	179
Table 5.10 Variation in the absolute abundance of metabolites detected in negative ion mode with day of collection of seal milk.	185
Table 5.11 Lipids used to predict the day of collection of seal milk.	189
Table 5.12 Variation in the absolute abundance of metabolites detected in negative ion mode with day of collection of seal milk.	192

List of Abbreviations

ACN	Acetonitrile
A _s	Asymmetry Factor
ATP	Adenosine Triphosphate
BDM	Benzyltrimethylhexyl Ammonium Chloride
BTE	Benzyltriethyl Ammonium Chloride
BTM	Benzyltrimethyl Ammonium Chloride
CD	Cyclodextrin
CI	Chemical Ionisation
CN	Cyanopropyl Silica
EI	Electron Impact
EIC	Extracted Ion Chromatogram
ESI	Electrospray Ionisation
ESI-MS	Electrospray Ionisation Mass Spectrometry
EtOH	Ethanol
HCA	Hierarchical Cluster Analysis
HILIC	Hydrophilic Interaction Chromatography
HILIC-HRMS	Hydrophilic Interaction Liquid Chromatography - High Resolution Mass Spectrometry
HPLC	High Performance Liquid Chromatography
HRMS	High Resolution Mass Spectrometry
ICA	Independent Component Analysis
k	Capacity Factor
LC	Liquid Chromatography
LC-MS	Liquid Chromatography Mass Spectrometry
LLE	Liquid-Liquid Extraction
LPA	Lysophosphatidic Acid
m/z	Mass to Charge Ratio
MS	Mass Spectrometry
MW	Molecular Weight

N	Number of Theoretical Plates
NAD ⁺	Nicotinamide Adenine Dinucleotide (oxidised)
NADH	Nicotinamide Adenine Dinucleotide (reduced)
NMN	N-Methylnicotinamide
NMR	Nuclear Magnetic Resonance
NPLC	Normal phase liquid chromatography
OPLS	Orthogonal Partial Least Squares
OPLS-DA	Orthogonal Partial Least Squares Discriminant Analysis
PCA	Principal Component Analysis
PEGs	Polar Embedded Groups
PLS	Partial Least Squares
PP	Protein Precipitation
RP	Reversed Phase
RPLC	Reversed Phase Liquid Chromatography
R _s	Resolution
RT	Retention Time
SIM	Selective Ion Monitoring
SIMCA	Soft-Independent Modelling of Class Analogy
SPE	Solid Phase Extraction
SRM	Selective Reaction Monitoring
t ₀	Void Time
TES	Triethoxysilane
TFA	Trifluoroacetic Acid
THF	Tetrahydrofuran
TMS	Trimethylsilane
t _R	Retention Time
UHRMS	Ultra-High Resolution Mass Spectrometry
UV	Ultraviolet
V ₀	Void Volume
ZIC	Zwitterionic
α	Selectivity Factor

Abstract

The aim of this study was to investigate hydrophilic interaction chromatography (HILIC) and its application to metabolic profiling. The effect of different mobile phase modifiers on the retention behaviour of acidic and neutral test probes was studied on silica gel based columns which confirmed the hypothesis that HILIC is due to a combination of hydrophilic interactions and electrostatic interactions. Among the acidic probes tested, the more negatively charged maleic acid was not strongly retained until the strength of the ammonium ion in the mobile phase was high enough to shield the acid from repulsion by charged silanol groups on the silica gel surface. The neutral test probes were increasingly retained with increasing ionic strength of the mobile phase suggesting that the thickness of the water layer on the surface of the silica gel increased with the strength of the ionic modifier. The utility of three silica hydride columns, Cogent silica C, Cogent Phenyl Hydride and Cogent UDC cholesterol, for separating mixture of metabolites was successfully assessed with an alternating gradient from high organic to high aqueous and then from high aqueous to high organic, thus permitting two orthogonal selectivities to be obtained on the same column. A method for the reductive amination was developed for the analysis of sugars and sugar phosphates. This method was very successful with deuterated aniline as a tag which led to the separation of the three common hexoses glucose, galactose and mannose. The method was applied to the profiling of sugars in milk and in brain tissue. An extensive study of seal milk in comparison with other mammalian milks was also conducted which found that unlike the milks of terrestrial mammals, seal milk had very little lactose. Thus seal pups appear to rely on fat metabolism to produce energy. A notable feature of the milk was that it contained high levels of nicotinamide, an essential precursor for the production of the cofactor NAD⁺ which is required for the β -oxidation of fats.

Chapter One:

General Introduction

1 Introduction

1.1 Chromatographic Theory

Chromatography is the term used to describe a technique of separation based on physical interaction between an analyte and two phases, namely: a stationary phase and a mobile phase. The former normally consists of a substance, either hydrophilic, neutral, or hydrophobic, held on a rigid support, commonly silica. On the other hand, the mobile phase is normally a solvent, or mixture of solvents, consisting of polar and organic components which are miscible with each other. The mobile phase serves to carry the analyte through the stationary phase, usually contained in a column, and during which time separation of the components of the analyte occurs.

For a given column and at a fixed mobile phase composition at a constant temperature, the retention factor, of an analyte is a characteristic parameter. And described the affinity with which the analyte is retained by the column in question. It is defined by the equation:

$$k = \frac{t_R - t_0}{t_0} \dots\dots\dots \text{(Equation 1)}$$

Where: t_R = retention time of the analyte in question; t_0 = retention time of an un-retained compound.

There are various techniques used in chromatography which are classified on the basis of mobile phases and stationary phases used in the separation process. They can also be classified by virtue of the retention mechanisms and chemical interactions that occur in the column during the separation process. Based on the stationary and mobile phases used, the commonest separation techniques [1] include:

(1) **Partition chromatography**, which involves the components of the analyte distributing between the stationary and mobile phases, in accordance with their partition coefficients. In this case the analytes which partition strongly in the stationary phase move more slowly as compared to those that partition strongly into the mobile phase;

(2) *Adsorption chromatography*, which occurs by molecules of the analyte adhering to the column through electrostatic, hydrophobic, or van der Waals forces, so that molecules that are strongly held are retained longer than those that are loosely held to the column;

(3) *Ion-exchange chromatography*, in which charged analytes form temporary ion pairs with oppositely charged ion exchange resins in the column. Again here those which form stronger ion pairs are held in the column longer than those which form weaker ion pairs; and

(4) *Size exclusion chromatography*. This uses a mesh of varying pore sizes to regulate the rates of movement of analytes through the column bed. It is normally applied for larger molecular weight substances such as proteins.

Generally speaking the method of separation selected for a given analyte depends on the nature of the analyte itself. Volatile compounds require gas chromatography for their separation; ionisable compounds will require ion exchange chromatography; size exclusion will be required for higher molecular weight compounds of differing sizes; while high performance liquid chromatography will work for a range of non-volatile compounds, whether weakly ionisable or neutral.

1.2 Chromatographic Performance

For any developed chromatographic method, its performance is key. The performance of a chromatographic method is dependent on how narrow and sharp the peaks are. This performance also goes hand in hand with robustness of the method, which deals with how stable to small perturbations a method is. The ideal chromatography system should offer stable retention times, a high efficiency, good peak shape and a high resolution of peaks.

The Figure 1.1 below shows a typical chromatogram for a single analyte.

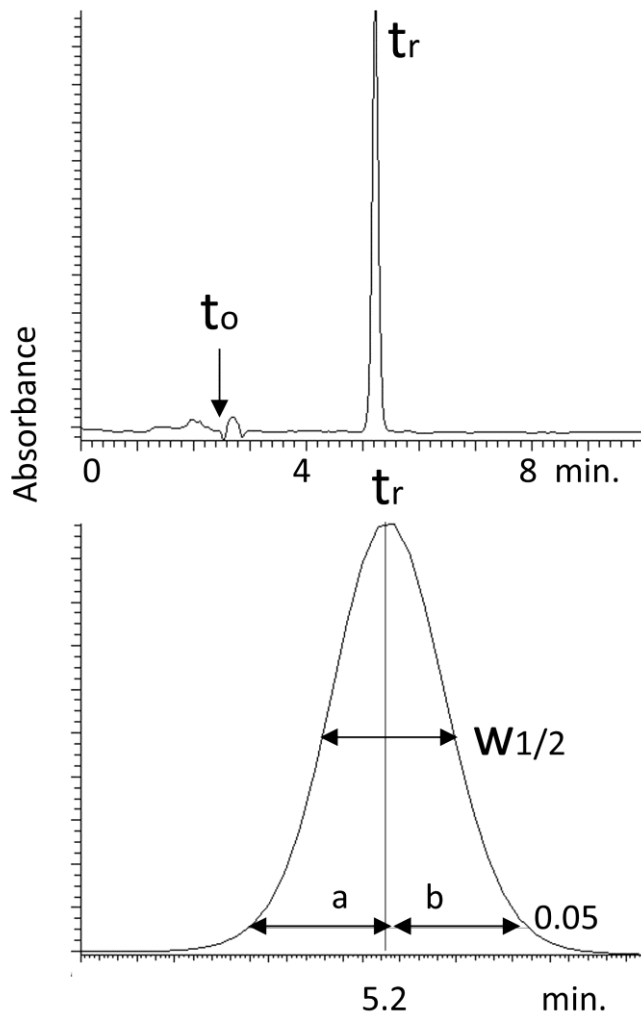


Figure 1.1: Typical chromatogram for a single analyte showing key parameters

In the above chromatogram, t_r represents the retention time of the component while t_0 is an important marker which represents the retention time of an un-retained compound. It is a measure of the void volume of the column – the volume traversed by an un-retained analyte from injection point to the detector. This void volume (abbreviated as V_0) can be estimated (in ml) from equation:

$$V_0 = 0.6\pi r^2 l \dots\dots\dots \text{(Equation 2)}$$

Where: V_0 = void volume of the column; r^2 = radius of the column; and l = length of the column.

Assuming a column to be 15 cm x 4.6 mm in dimensions, V_0 would be $(0.6 \times 3.14 \times 0.23^2 \times 15 = 1.495 \text{ ml})$ which is *ca* 1.5 ml and at a flow rate of 1 ml/min the value of t_0 would be 1.5 min.

From the peak in Fig. 1.1, the capacity factor, k' , can be estimated using equation 1. The efficiency of the column, which practically represents how slim and sharp the peaks are, is given by equation 3 below. N represents the number of theoretical plates, t_R is the retention time, while $W_{0.5}$ is the peak width at half height. The higher the value of N , the higher the efficiency of the column and the better the column at separation of the analyte in question.

$$N = 5.54 \left(\frac{t_R}{w_{0.5}} \right)^2 \dots\dots\dots \text{(Equation 3)}$$

The symmetry of the peak, A_s , is another measure of peak quality and is given by the ratio of a/b (Figure 1.1), measured at 1/20 of the peak height. Perfect symmetry of the peak is obtained when this ratio is 1.0. A_s values below 1.0 represent peak fronting while those greater than 1.0 represent peak tailing. Generally, values between 0.8-1.5 are acceptable.

The sole aim of chromatography is to separate peak of one or more compounds in a mixture. Therefore one of the most important relationships is the peak resolution, R_s , given in the equation below for two analytes A and B.

$$R_s = \left(\frac{1}{4} \right) N^{0.5} \left(\frac{\alpha - 1}{\alpha} \right) \left(\frac{\bar{k}'}{1 + \bar{k}'} \right) \dots\dots\dots \text{(Equation 4)}$$

Where: N = efficiency for one of the analytes; k'_A = capacity factor of peak A, k'_B = capacity factor for peak B, $\alpha = \frac{k'_B}{k'_A}$ = selectivity and $\bar{k}' = \frac{k'_A + k'_B}{2}$.

From the above equation it can be seen that the selectivity (α) is the factor that has the greatest direct effect on resolution since it also affects capacity (k). It is dependent on both the column type and mobile phase chemistry. For a good separation both selectivity and column efficiency conditions have to be appropriate.

1.3 Separation Techniques

1.3.1 Normal Phase Liquid Chromatography

Normal phase liquid chromatography (NPLC) uses a non-polar mobile phase, such as hexane, and a polar stationary phase, such as unmodified silica gel or silica gel with diol, cyano-alkyl, amide-alkyl or amino-alkyl attached, in order to retain the polar analytes. The commonest solvent mixtures are non-polar solvents with a slightly polar one as a modifier, for example hexane/ethyl acetate or hexane/isopropanol.

The retention mechanism involves polar compounds adsorbing onto the stationary phase more strongly than the non-polar ones. The adsorption forces are mainly due to hydrogen bonding between polar analytes and the polar stationary phase. NPLC has a different selectivity when compared to the reversed phase type although the latter has a wider applicability. In fact, NPLC has several limitations including: poor solubility of polar analytes in the highly non-polar mobile phases used; difficulty in ionizing analytes when interfaced with an electrospray mass spectrometer; slow equilibration between analytes and stationary phase leading to peak tailing, fronting, or variable retention times as concentration changes; and phase instability. Due to these problems there has been an increased popularity of reversed phase systems whose mode of separation is opposite to that of NPLC [1].

1.3.2 Reversed Phase Liquid Chromatography (RPLC):

This offers an opposite mode of operation when compared to normal phase type. The mobile phase is a polar one, containing a high proportion of water with an organic modifier, while the amount the stationary phase is hydrophobic, such as octadecyl (C₁₈), octyl (C₈) or butyl (C₄) bonded to silica support.

Partitioning is the main mechanism of the separation of the analyte whereby lipophilic analytes are held up in the column longer than the hydrophilic ones due to the higher partitioning of the former into the stationary phase. The RPLC type offers a reliable and excellent method of separation of non-polar compounds as these can partition easily into the lipophilic stationary phase for separation to occur. However the retention of the polar ones is a challenging process in RPLC. The solution might be to use a high amount of water in the mobile phase, however, this also leads to phase collapse, or phase de-wetting, and thus loss of all chromatographic efficiency. This frequently results in unstable retention times and

poor resolution of peaks resulting from poor wettability in highly aqueous mobile phase compositions [2, 3].

Poor wettability problems of RPLC separations have been overcome, at least partly, through the use of polar embedded groups (PEGs) (Figure 1.2) which stop the lipophilic stationary phase from shrinking at high aqueous concentrations of the mobile phase.

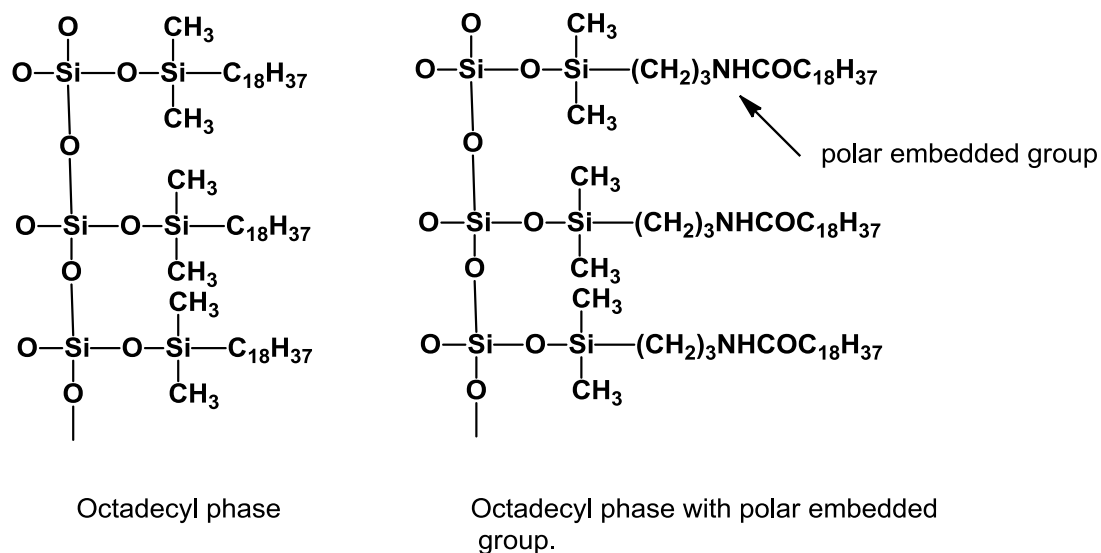


Figure 1.2: Use of polar embedded groups in reversed phase liquid chromatography

It has been observed that using polar embedded groups does not significantly improve the retention of polar compounds in RPLC. Thus due to the difficulty in retaining polar compounds on a lipophilic stationary phase as the analytes will elute at t_0 , as part of the void volume, V_0 .

Polar analyte retention in reversed phase chromatography may be possible if the analyte is ionisable and therefore can form charged species in a reasonable pH range. The charged ions can in turn be made for form neutral ion pairs with ion-pair reagents such as alkyl sulfonates (if the analyte is positively charged) or tetrabutylammonium (for negatively charged analyte ions). This technique is inexpensive, simple and can provide a good efficiency of separation. However, this approach it is not compatible with analyses that use mass spectrometry as the detector. The other setbacks are: (a) the possibility for complexation between the ions and, (b) slow equilibration rates with the ion pair reagent which might lead unstable retention times.

The other possibility for improving separation of polar analytes in reversed phase liquid chromatography is by derivatisation of the analytes. In doing so, a hydrophobic group is attached, through chemical reaction, to one or more polar groups of the analyte. If successful, the new product formed will be able to partition better in the column as it now contains a non-polar group that can interact with the lipophilic stationary phase. There are challenges, however, with this approach such as new impurities being introduced from side reactions, time consuming, poor reaction with derivatising agents, etc. An alternative approach to this is hydrophilic interaction liquid chromatography (HILIC) technique [1, 4].

1.3.3 Hydrophilic interaction liquid chromatography (HILIC):

HILIC is a technique used to separate polar analytes using a polar stationary phase and a less polar mobile phase. It works in an orthogonal manner to reversed phase chromatography, for example, whereas the organic solvent is the strong solvent in reversed phase partition, water is the stronger one in HILIC. It has recently established itself as the method of choice for highly polar and hydrophilic compounds instead of RPLC.

Given that both HILIC and normal phase chromatography appear to be opposite of the reversed phase technique, there is possibility that the two can often be confused. The key differentiator, however, is that in HILIC water is used as a strong solvent to elute strongly held analytes, which is not the case in normal phase. An advantage of HILIC is that it can increase mass spectrometry sensitivity in ESI mode due to increased ionisation efficiency. The latter occurs as a result of a high proportion of organic solvent (such as acetonitrile) in HILIC mobile phase. This high organic content of the mobile phase in HILIC also means that biological samples need not be evaporated and re-constituted following protein precipitation with acetonitrile. This simplifies the whole process of sample preparation in bioanalysis [5-7]. The other advantages include ability to separate counter ions including chloride, sodium, and potassium that are common components of pharmaceuticals formulated in salt forms; low viscosity of the high organic mobile phase permits the use of higher flow rates and leads to lower back pressures; and a wide selection of HILIC stationary phases is now available.

The key challenges with the HILIC mechanism include column overload leading to peak fronting, longer equilibration times, and the fact that there may be mixed mechanisms in the separation process which are not easily understood and therefore not easily controllable [8].

1.3.3.1 The Mechanism of separation in HILIC

In HILIC, the higher the polarity of the analyte, the longer is the retention times. Other factors that increase retention times are: increased stationary phase polarity and decreased percentage of water in the mobile phase. It has been suggested [6] that the separation is dependent on the partitioning effect between the non-polar mobile phase and an aqueous layer which adsorbs onto the surface of the polar stationary phase as shown in the Figure 1.3 below.

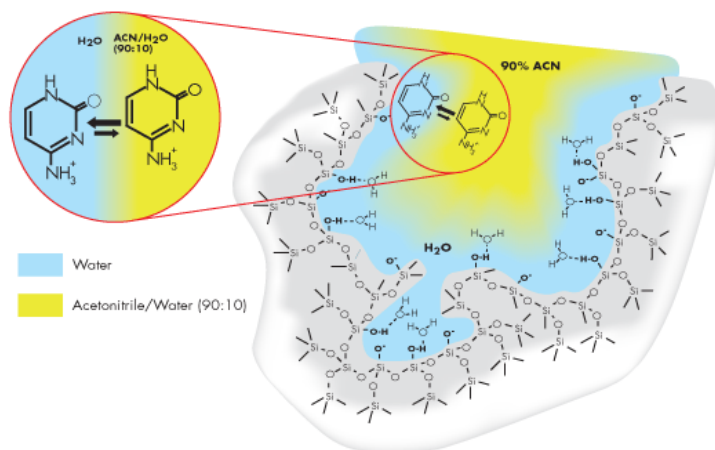


Figure 1.3: The partition mechanism in HILIC chromatography [4]

In 2008, McCally and Neue showed that the retention time of benzene depended on the thickness of the water layer formed in the stationary phase when using bare silica [9]. It can be seen from Figure 1.4 below that the retention time of benzene first decreases as the water content in the mobile phase is increased from 0 to 20%, but subsequently increases again. In the first part is where water equilibrates in the column to form an aqueous layer and thus retaining the slightly polar benzene. Increasing the water content beyond 20% breaks down the interaction and causes faster elution; or it could be an issue of poor solubility of benzene in higher aqueous solvents.

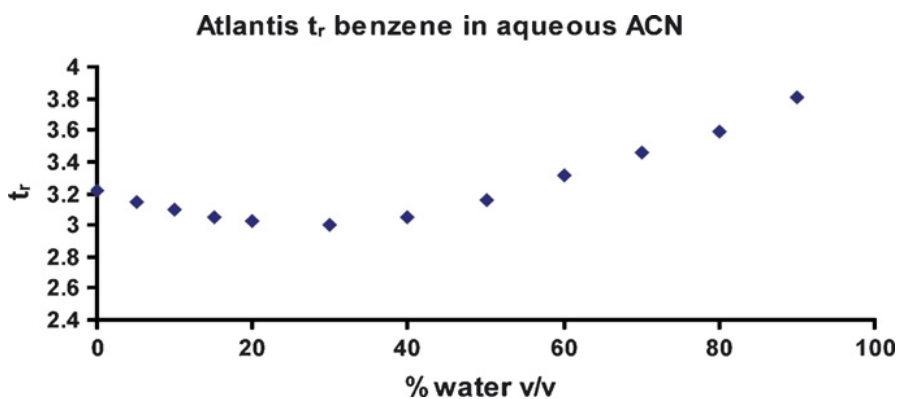


Figure 1.4: Retention time of the benzene with different percentage of the water content in a water/acetonitrile mobile phase using an Atlantis silica column [7].

The main mechanism of retention in HILIC is the partitioning of polar compounds between a layer of water adhering on the polar stationary phase and the mobile phase that is more non polar. Other interactions for example adsorption, ion-exchange and hydrophobic ones might play a role as well in HILIC separations. The adsorption mechanism in HILIC separations was demonstrated by McCalley [8] during the study of retention of various chemical compounds including basic, neutral and acidic analytes on varying stationary phases including silica, amide, diol, and zwitterionic ones.

The retention process in adsorption chromatography may be represented by the equation: $\log k = \log k_B - n \log X_B$, where X_B is the mole fraction of water in the mobile phase, k_B the retention factor aqueous phase, and n is the number of water molecules. Thus a plot of $\log k$ against mole fraction of water is expected to give a straight line if the adsorption mechanism is the only interaction mode in play during chromatography. This outcome was demonstrated for cross-linked diol and amide stationary phases [8], which indicated that adsorption mechanism was present with these HILIC phases. The other phases including zwitterionic, silica and mixed-mode did not produce linear plots because of mixed interactions in those columns.

Ion exchange was also confirmed as one of the separation mechanisms that applies to the HILIC retention mechanism by different methods [8]. This was initially done by comparing the behaviour of acids, bases and neutral compounds with one type of stationary phase (bare silica), using different buffers. Next, the behaviour of acidic, neutral and basic compounds was compared using different stationary phases.

In the first approach it was shown that un-modified silica retained bases probably because it has silanol groups which can be ionized. Alternatively the retention of the bases might be because the silanol forms a bigger hydration layer with the mobile phase and thus retains the bases more.

However the second explanation could not be supported by evidence since an increased hydration layer would have retained both acidic and the basic compounds alike. Instead, the silica phase demonstrated only poor retention of acidic analytes, due possibly to repulsion of the negatively charged acidic groups by the similarly charged silanols. This hypothesis was proved by using trifluoroacetic acid (TFA) in order to lower the pH of the weakly acidic analytes below their pKa values in order to suppress their ionisation. The result was an increased retention of the acids as well on the silica column which in this case were retained purely according to their water solubility. Ammonium formate buffer did not give better results as it makes the analytes and the silanols to ionise similarly and therefore lead to repulsion.

When the retention factor (k) was plotted against the concentration of counter ions in the mobile phase for various types of columns in HILIC conditions, basic compounds produced curved lines while neutral compounds produced a straight line. Caffeine was the neutral compound while procainamide, benzylamine, nortriptyline, and diphenhydramine were the bases. These results confirmed that the mechanism of retention in HILIC also contained some ion exchange interactions for basic compounds [8].

It is generally known that unmodified silica phases are the most ionisable of all stationary phases because they consist only of silanol groups. On the other hand, zwitter-ionic phases contain sulphonic acid groups which act as sites for cation exchange and quaternary ammonium groups which act as sites of anion exchange. Relatively neutral phases including amide and diol also have residual silanol groups that remain after ligand bonding and these ionise negatively at various pH ranges and act as sites of cationic exchange.

Hydrophobic processes have also been demonstrated in HILIC [8]. McCalley showed the behaviour of different bases consisting both hydrophilic and lipophilic ones using HILIC phases including silica, amide, cross linked diol, mixed mode diol and zwitterionic. He found that hydrophobic bases (nortriptyline and diphenhydramine) eluted before hydrophilic bases (benzylamine and procainamide) on all stationary phases as expected of a HILIC

separation. However, mixed mode diol phases gave different separation order for hydrophobic basic analytes. Nortriptyline was unexpectedly retained longer than the more hydrophilic bases (Figure 1.5). This effect might be explained since mixed mode phases produce some hydrophobic interactions with compounds that are significantly more hydrophobic.

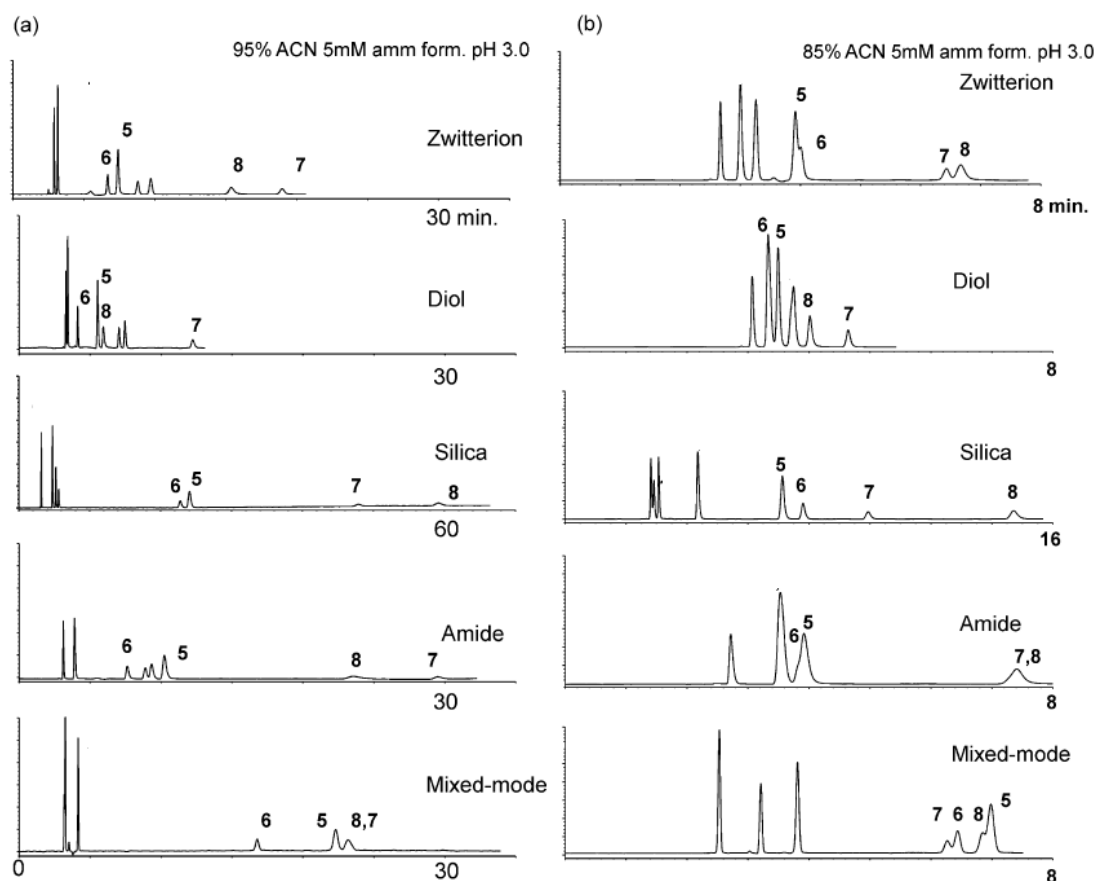


Figure 1.5: Chromatograms for 5. nortriptyline, 6. diphenhydramine, 7. benzylamine, 8. procainamide, with different stationary phases. Mobile phases are (a) acetonitrile:water (95:5, v/v) and (b) Acetonitrile:water (85:15, v/v) both containing 5 mM ammonium formate buffer pH 3.0 [8].

It can be realised from the foregoing discussion that the retention mechanisms in HILIC separations is a complex mixture of liquid partitioning between the bulk mobile phase and the surface aqueous layer on the stationary phase, adsorption through hydrogen bonding or/and dipole/dipole interactions, ionic interactions between a charged stationary phase (or charged Si-OH on silica support) and charged analytes, and sometimes even hydrophobic interaction between hydrophobic analytes and a partly hydrophobic stationary phase. Thus

the HILIC separation mechanism is dependent on solute characteristics, type and nature of the stationary phase, and mobile phase composition.

1.4 Types of HILIC columns

HILIC phases can be classified according to their chemical properties which reflect the different mechanisms that each phase offers to aid the separation of analytes. They are as follows:

1.4.1 Bare Silica:

Figure 1.6 represents the structure of silica gel (bare silica). The surface consists of hydroxyl groups bonded to the silicon atoms to form silanols throughout the entire surface of the particle.

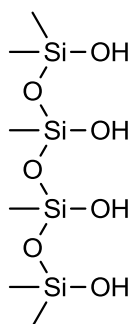


Figure 1.6: Surface chemistry of bare silica HILIC stationary phase

Silanols are of different types and these types vary in their acidic strength. Siloxanes are the least acidic while metal activated silanols are the most acidic (Figure 1.7).

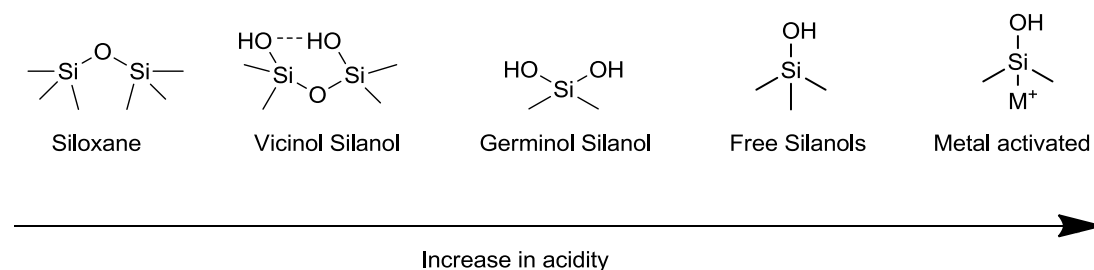


Figure 1.7: Types of silanol groups [9]

The silica phases can be divided into three different types according to particle shape, proportion of metal contamination, and the silanol group type. Silica type A has a high metal content, type B is based deactivated, while type C is silicon hydride. Type A was the earliest silica to be introduced into chromatographic use and has been used for almost every purpose. Its main problem is that it is highly acidic, the acidity being due to presence of various metal contaminants which can have adverse effects on chromatographic output. At the same time this type of silica has irregular particle sizes which can affect reproducibility of the chromatographic results.

On the other hand, type B silica is the second generation silica gel that came after type A and is almost free from metal impurities due to treatment with a mineral acid. It is also spherical in shape and more regular than type A. Type C silica has a silicon hydride surface which is prepared by hydrosilylation of the silanol (Si-OH) groups to convert them into Si-H (Figure 1.8).

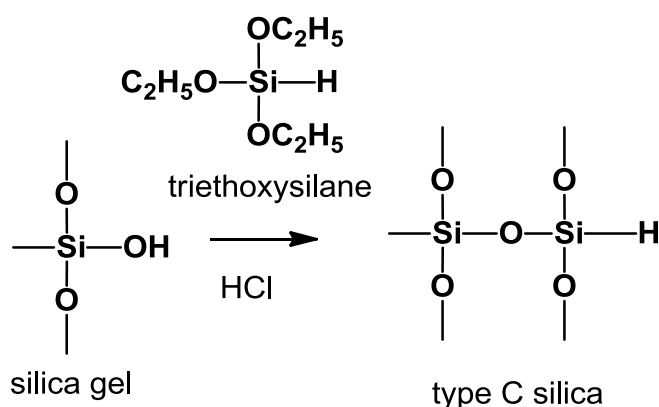


Figure 1.8: The hydrosilylation process

There are quite a number of bare silica columns commercially available today. These are manufactured by various companies including Hypersil and Kromasil. Properties of columns supplied by different manufacturers are different even when they are labelled to be the same type [2]. This is perhaps due to the differences in purity levels of the silicas or different processes of column manufacture.

For a bare silica column under HILIC conditions the mechanism of separation may be partition or cation exchange depending on the properties of the analyte under separation and the mobile phase used. Cationic analytes will be strongly retained if the Si-OH groups are ionized leading to longer retention times. For an acidic analyte the retention process can only

be partitioning if the analyte is un-ionised. Ionisation can result into some partitioning into the aqueous layer associated with the silica gel surface but there may also be charge repulsion from the negative charged silanol groups. This can be summarised in Figure 1.9 for an analyte possessing acidic, basic, and neutral groups.

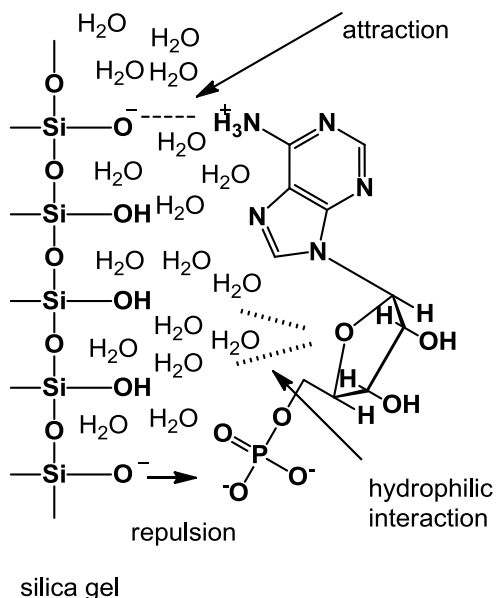


Figure 1.9: The types of interaction which can occur between an analyte and the silica gel surface in HILIC mode.

The main advantage of unmodified silica is the absence of bonded ligands which simplifies interactions with the stationary phase. Furthermore, if bare silica under HILIC mode is compared to the one under normal phase mode, the former is more compatible with biological extracts where compounds of interest are polar and exist in a complex matrix. Such highly polar compounds may not easily dissolve in high organic solvent mixtures associated with normal phase chromatography.

1.4.2 Silicon Hydride Columns (Type C Silica):

The type C silica columns overcome the effects of free silanols and offer a different degree of selectivity than traditional silica gel. They are prepared by hydrosilation of the silica surface. The latest approach is to react triethoxysilane with the normal silica in the presence of hydrochloric acid catalyst (Figure 1.10). This gives a 95% conversion rate for silanols into silicon hydrides. The resulting Si-H surface is more stable for a long time in water or air.

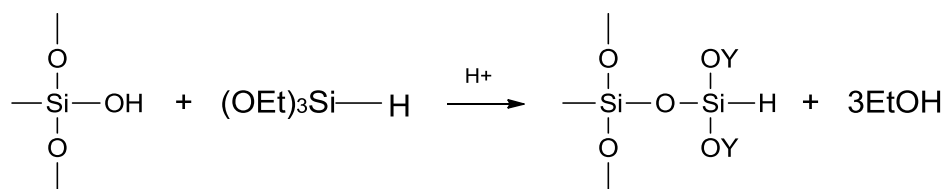
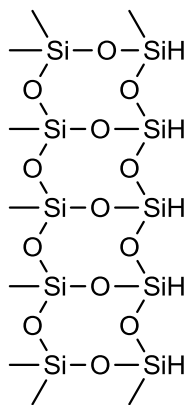


Figure 1.10: The hydrosilation reaction of the Silica gel and triethoxysilane (TES) resulting in a silicon hydride surface [10].

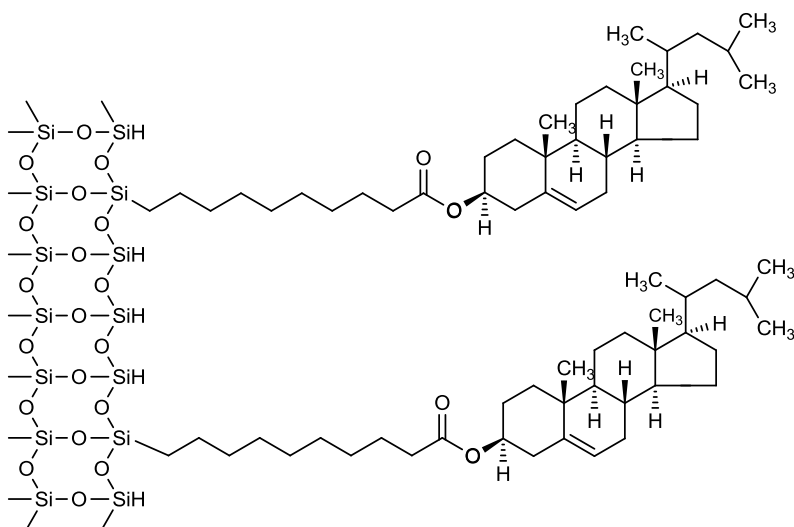
The Si-H surface is less polar than silica gel and is less attractive to water; thus providing alternative selectivity in HILIC for non-polar compounds and improves reproducibility of the separation [11]. The Si-H groups also produce a mixed mode of separation which includes both reversed phase and HILIC. At higher aqueous concentration of mobile phase, the reversed phase interaction occurs but when the aqueous content in the mobile phase is low (usually 5-30%), HILIC interaction predominates reversed phase [12]. This situation does not occur in bare silicas which have strong hydrophilic properties and so do not retain non-polar compounds in a reversed phase manner [11].

Various Si-H bonded phases including UDC Cholesterol and bidentate C18 silicon hydride (Figure 1.11) are available. Soukup and Jandera compared these phases in the separation of flavonoids in HILIC mode with identical conditions and found that elution pattern was identical although retention times increased with increase in polarity of the phases [13].

(A) Silica hydride



(B) Cholesterol hydride



(C) Bidentate C18 hydride

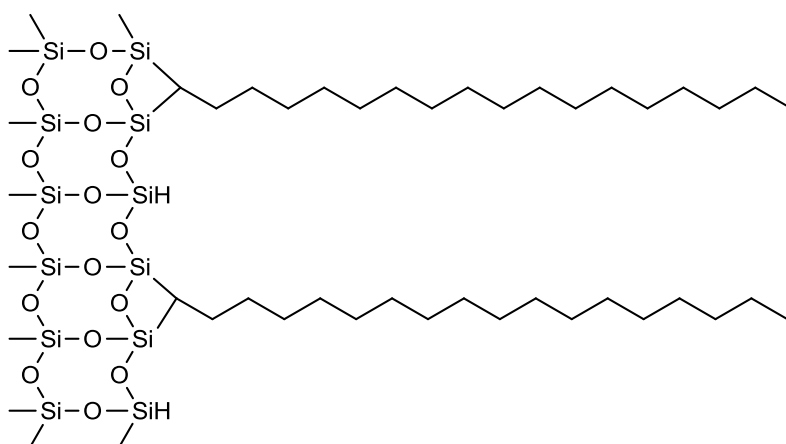


Figure 1.11: Chemical structure of the (A) Silicon hydride, (B) UDC Cholesterol hydride and (C) Bidentate C18 hydride phases.

1.4.3 HILIC columns based on silica gel with neutral surface ligands:

1.4.3.1 Diol silica

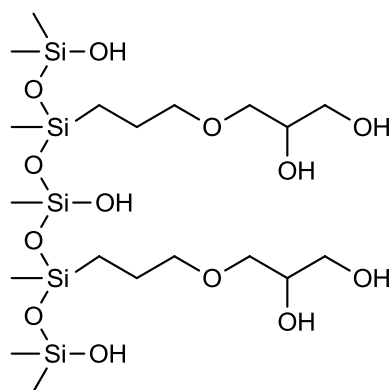
Although diol silica phases are bonded stationary phases, their surface chemistry closely resembles that of bare silica (Figure 1.12) when compared in terms of their degree of polarity. Their main difference is that they are not ionized save for any unreacted silanol groups which can be removed to some extent by way of end-capping using silylating agents such as trimethylsilane (TMS).

The diol stationary phase may be classified as neutral [14] but it is likely that even when end-capping is carried out there are still significant numbers of residual silanol groups that remain on the surface un-reacted. One of the main reasons for developing the diol phase was to overcome the irreversible adsorption properties of bare silica and at the same time offer a different selectivity for separation of analytes. Because of its high polarity, the diol stationary phase is appropriate for use in HILIC mode. The high polarity of the phase enables it to accept and donate hydrogen bonds necessary to form the hydration layer on its surface. The mode of operation is similar in diol phase to that of bare silica and as such the presence of high amounts of organic solvent with a low aqueous content is used to obtain the separation [15].

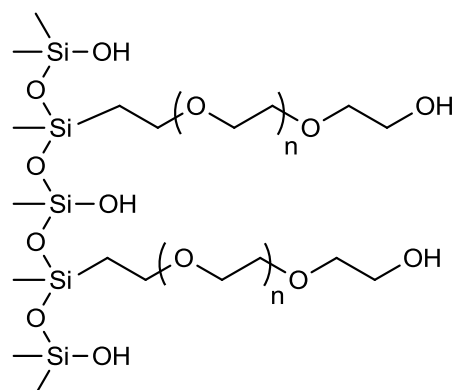
At the same time at high proportions of water in the mobile phase, lipophilic compounds can be retained in a reversed phase manner due to the fact that the diol phase possesses a lipophilic alkyl chain functionality which interacts with non-polar analytes, unlike on bare silica columns. The other advantage of diol stationary phases when used in HILIC mode is their ability to determine the mutarotation of the sugars such as monosaccharides [16].

Their disadvantage results from their tendency to lose the bonded phase under highly acidic conditions. This problem has been partly overcome by using cross-linked diol columns which are more stable (Figure 1.12). These cross-linked diol phases also offer stronger hydrophobic interactions, better peak shape, and higher resolutions when compared to the ordinary diol silica types [17]. Some of the brands of cross-linked diol columns available on the market include Luna HILIC which possesses properties resembling both the polyethylene glycol phase and the diol phase since it has both oxyethylene and hydroxyl groups within its core [18].

(A) Diol



(C) Polyethylene glycol



(B) Cross-linked diol.

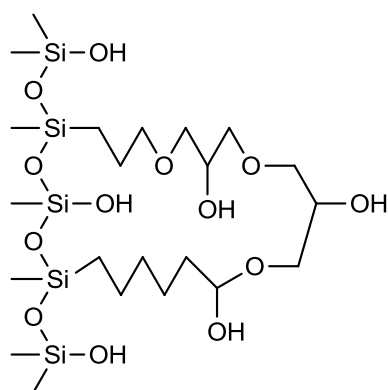


Figure 1.12: Chemical structures of the mixed mode diol, cross-linked diol and polyethelene glycol phases. None of these stationary phases are end-capped.

1.4.3.2 Aminopropyl silica:

In these types of columns the silica is chemically bonded to aminopropyl chains implying that there is a positive charge on the primary amino group at low values of pH (e.g. below pH 8.0) (Figure 1.13) [19].

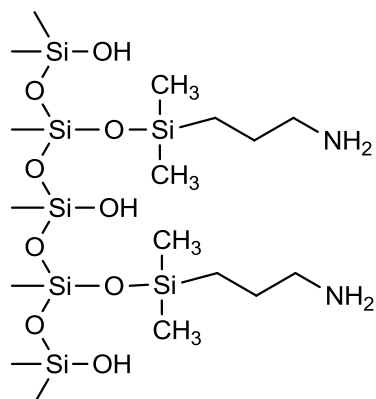


Figure 1.13: The surface of aminopropyl silica without end-capping.

The aminopropyl stationary phase is essentially a polar phase which makes it appropriate for use under HILIC conditions. Negatively charged analytes become strongly attracted to the positively charged aminopropyl groups by way of an anion exchange process. In this case the retention of charged basic analytes by this type of column is reduced due to charge repulsion. Under these conditions an increase in the ionic strength of the mobile phase also results in a reduction in retention time of acidic compounds.

Challenges with aminopropyl type columns include longer equilibration times with buffers, sometimes requiring several hundred column volumes, and poor stability resulting from hydrolysis when aqueous mobile phases are used [20, 21]. As a result of this hydrolysis, the aminopropyl ligand is broken from the silica support leading to deterioration of peak shape under HILIC conditions. This lack of stability may be overcome by using a polymer instead of silica for bonding with the aminopropyl ligand [22].

Generally primary aminopropyl phases are not used for separation of carbohydrates as they react together to form Schiff bases. This reaction causes the chemistry of the stationary phase to change (Figure 1.14) leading to poor chromatographic separation [23].

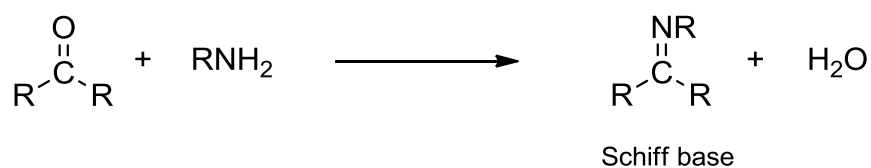


Figure 1.14: Chemical reaction of a primary amine and aldehyde group to produce a Schiff's base.

On the other hand stationary phases with 2° or 3° amino groups may result in improved column performance since they do not react with carbonyl compounds to form Schiff's bases as the primary amines do. For bonded phases containing aromatic amine linked to silica support, they have also been used in HILIC for analysis of polar compounds and show short elution times and symmetrical peaks [24].

Among the applications of aminopropyl columns is they can eliminate formation of two peaks for anomeric compounds but combine them into a single peak, providing better peak shape, which is an opposite effect to the diol column [24].

1.4.3.3 Amide silica:

Amide stationary phases consist of an amide containing ligand bonded to silica gel via a short alkyl spacer. Amide phases do not have basic properties, but are neutral instead, and therefore ion exchange mechanisms do not take place during their use in chromatography. In this way they are different from aminopropyl phases. Due to their neutrality, amide phases have better stability compared to aminopropyl phases mainly because they do not possess strong analyte adsorption [4].

The main advantage of the amide phase is that the eluent does not have to be buffered since the stationary phase is un-ionisable. Amide stationary phases have been demonstrated to be able to separate various mono- and oligosaccharides, sugar derivatives, amino acids, and peptides in the HILIC mode with evaporative light scattering as a detector [25]. Examples of amide phases include: the carbamoyl-silica HILIC TSK-gel Amide-80 which has been developed specially for HILIC (Figure 1.15).

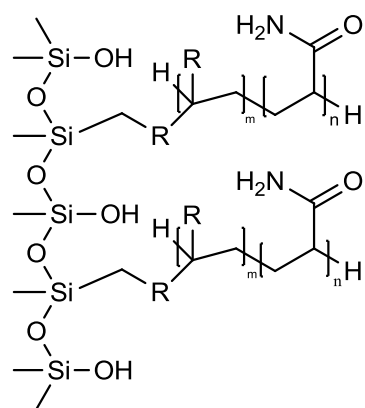


Figure 1.15: The surface chemistry of amide silica (TSK-Gel Amide-80) without endcapping.

Different attempts have been made to develop aminopropyl columns with different functional groups. For instance Alpert [26] proposed a reaction of between aminopropyl silica and polysuccinimide which yields a reactive surface to which further ligands can be bonded. The first stage involves the preparation of polysuccinimide silica, after that there is further modification to obtain various silica chemistries (Figure 1.16). For example the weak cation exchanger known as polyaspartic acid was prepared by the alkali hydrolysis of the polysuccinimide surface, poly(2-hydroxyethyl aspartamide) silica gel was obtained with 2-aminoethanol and finally the strong cation exchangers could be prepared from the reaction with 2-aminoethylsulfonic acid which formed poly(2-sulfoethyl aspartamide) silica (Figure 1.16).

1.4.3.4 Poly(succinimide)-bonded silica:

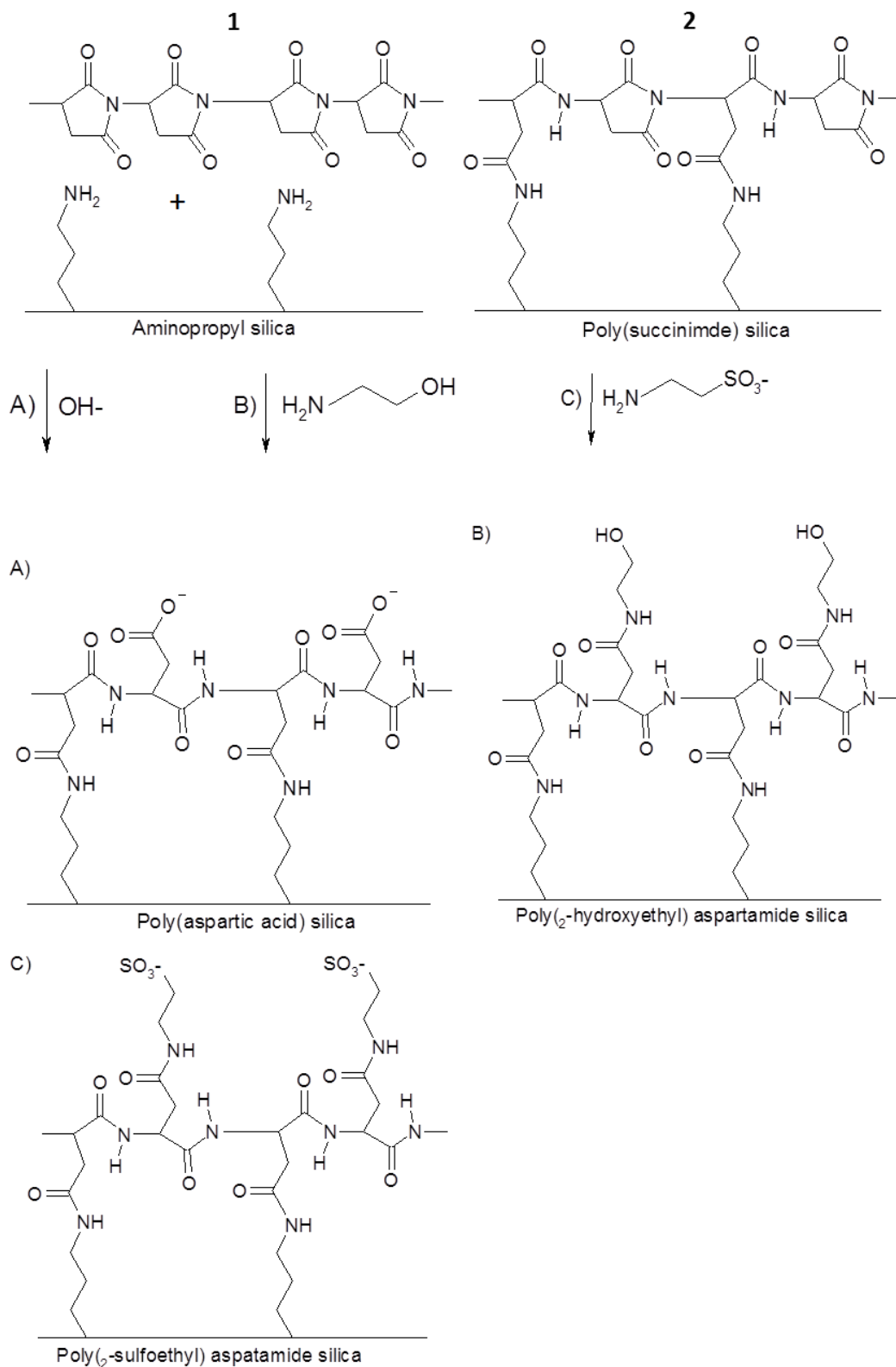


Figure 1.16: Surface chemistry of (1) aminopropyl silica, (2) poly(succinimide) silica, (a) Poly(aspartic acid) silica, (b) Poly(2-hydroxyethyl) aspartamide silica, and (c) Poly(2-sulfoethyl) aspartamide silica.

These phases exhibit mixed separation modes under HILIC conditions including varying degrees of ion exchange and partitioning mechanisms [27]. Some of the disadvantages associated with the use of poly(2-hydroxyethyl aspartamide) HILIC phases are loss of performance during separation of polar compounds, which leads to lower efficiency when compared with more recent HILIC columns such as ZIC-HILIC. Problems with long term stability and column bleeding can occur with the polysulfoethyl aspartamide phases [25, 28].

1.4.3.5 Cyclodextrin based columns:

The cyclodextrin (CD) consists of five or more glucose units which are 1-4 linked-D-glucopyranoside residues forming toroid ring structures. Each of these structures has a narrow end and a wide entrance from which hydroxyl groups protrude facing towards the surrounding solvent. The interior cavity is relatively hydrophobic (Figure 1.17).

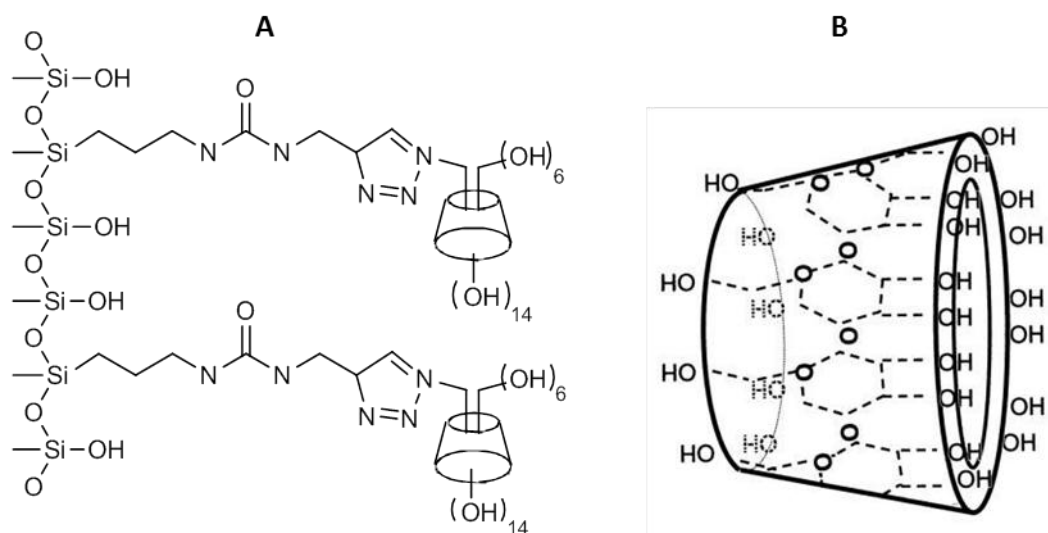


Figure 1.17: (A) Chemistry surface of a cyclodextrin phase and (B) a toroid structure showing the interaction of a polar analyte with the column surface.

The inside of the toroid of the cyclodextrin (CD) is less polar compared to the outside. Therefore it can provide a hydration shield between the water and the external part of the toroid thus making cyclodextrin phases appropriate for use in HILIC separations. The cyclodextrin phase can perform chiral recognition due to the fact that CDs are made from optically active sugars. Thus they can be used as achiral selectors in chromatographic or electrophoretic separations [29].

During HILIC the analyte is retained in the aqueous layer on the outer part of the cyclodextrin rather than on the inside of the toroid, contrary to what would occur in chiral separations. The polarity of the CD can be further enhanced by increasing the number of the monosaccharide residues used to form it. It goes without saying that increased polarity of the CD leads to increased retention of polar analytes [30, 31].

1.4.3.6 Cyanopropyl silica:

In cyanopropyl silica (CN) based columns, a cyano group is linked to the silica support through an alkyl propyl group (Figure 1.18). These columns are polar because the $C\equiv N$ bond is polar. The lack of hydrogen bonding ability causes the cyanopropyl phase to possess unique separation properties.

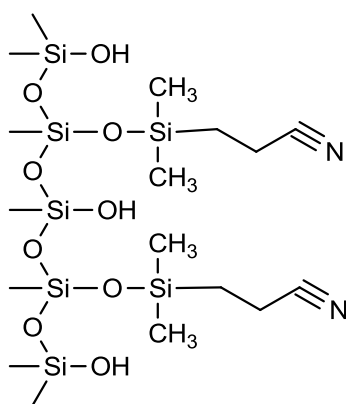


Figure 1.18: Surface chemistry of cyanopropyl silica without end-capping.

Both normal and reversed phase liquid chromatographic separations have been performed with CN columns. But the application of the CN column in HILIC is limited to analysis of denaturants in alcohol. Furthermore, studies have shown that CN columns do not offer appreciable retention for peptides even at high levels of organic solvent composition. But perhaps the main problem with cyanopropyl columns is their low stability in intermediate polarity solvents due, at least in part, to breakage of inter-particulate linkages [32-34].

1.4.3.7 Sulfobetaine and phosphorylcholine silica:

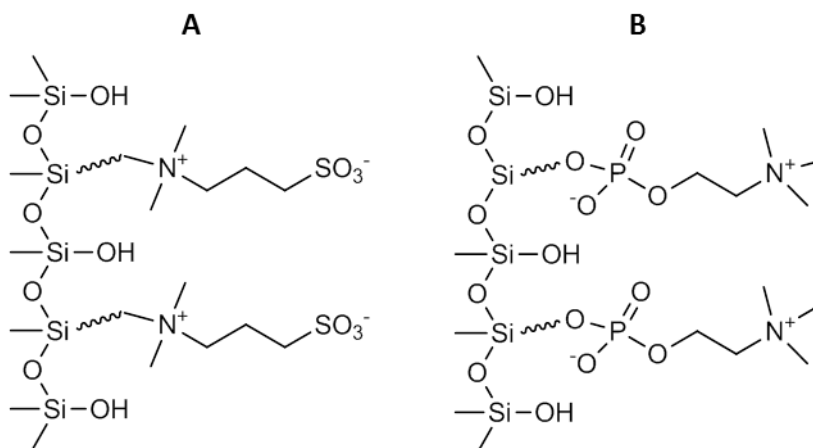


Figure 1.19: The chemical structure the (A) ZIC-HILIC and (B) ZIC-cHILIC. ZIC-HILIC has a sulfobetaine functional group while ZIC-cHILIC has a phosphorylcholine.

The need to reduce ionic exchange interactions in HILIC led to the development of zwitterionic phases which are charge neutral. Their surfaces are able to form a hydration layer but they do not exhibit ion exchange interactions due to cancellation of the positive and negative charge effects.

Guo *et al* [35] compared the separation of various chemical compounds on zwitterionic, silica, amino and amide stationary phases. The zwitterionic phase was the least affected by pH change and provided a totally different selectivity when compared to the amino column. The zwitterionic phase contains a strongly base (a quaternary amino group) linked to a strongly acidic sulfonic acid group via a short alkyl spacer (Figure 1.19). The positive and the negative charge on the phase exist in a 1 to 1.01 ratio and so there is a minor excess of negative charge which aids the separation of negatively and positively charged analytes [36-39].

1.5 Factors affecting the separation in HILIC

Various factors affect the order of elution, retention time, separation efficiency or even the chemical properties of analytes and stationary phase during HILIC separations. These factors include: type of the organic solvent (mobile phase), pH, buffer type and salt concentration, and temperature of the column.

1.5.1 Column Temperature:

The retention factor (k) of analytes in a column at different temperatures can be calculated using the van't Hoff equation below:

$$\ln k' = \ln \beta - \frac{\Delta H^\circ}{RT} + \frac{\Delta S^\circ}{R} \dots\dots\dots \text{(Equation 5)}$$

Where: (H) is the standard enthalpy change relating to the movement of the analyte from the mobile phase to the stationary phase, (S) is the corresponding standard entropy change, (R) is the molar gas constant (value $8.314 \text{ JK}^{-1}\text{mol}^{-1}$), (T) is the absolute temperature and (β) is the phase ratio of the stationary phase.

The effect of temperature on molecular interactions during HILIC can lead to improved or controlled analyte separation. Column temperature affects the diffusivity of the solute, viscosity of the mobile phase, and ease of transfer of solutes between the mobile phase and stationary phase, all of which are important considerations in HPLC separations. A change in column temperature can improve HPLC performance by increasing the diffusion coefficients of analytes thereby producing sharper peaks within shorter run times. The effect of temperature on neutral, charged, and zwitterionic HILIC columns has been investigated. The diol and amide columns which are neutral do not have ion-exchange interactions with analytes and thus they give a negative slope on a van't Hoff plot for analytes such as urea, sucrose and glycine. For these columns, as temperature increases, their $\log_e k$ values decrease because of improved solubility of the analyte in the mobile phase [40] (Figure 1.20).

On the other hand, ionisable HILIC phases such as bare silica and amines give a different effect when used for acidic and basic analytes. For example bare silica gives a negative slope for aspirin (acidic) and cytosine (basic) on the van't Hoff plot. This result is probably due to reduced viscosity of mobile phase as well as an increased diffusibility of the analytes.

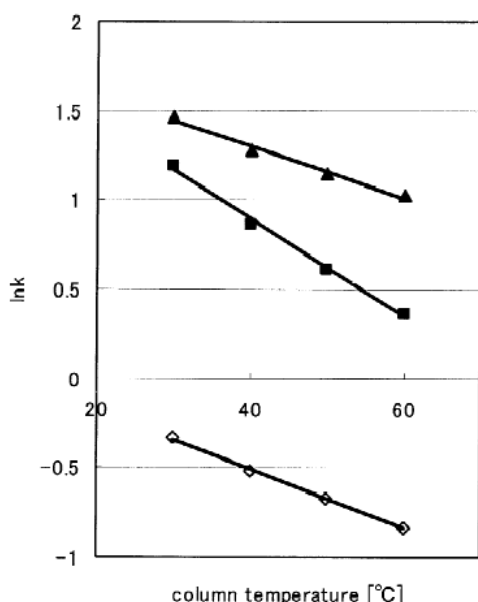


Figure 1.20: Plot of $\ln k$ against the column temperature for (\diamond) urea, (\blacksquare) sucrose and (\blacktriangle) glycine. Mobile phase water/ACN (20:80, v/v), diol stationary phase, flow rate 1.0 ml/min, refractive index detector.

However, the slope of the van't Hoff plot is positive when an amino HILIC column (positively charged) is used for the analysis of aspirin, a negatively charged analyte [35] (Figure 1.21). This outcome is due to increased ionic interaction between the analyte and stationary phase at higher temperature as well as a decrease in solvation strength between the ionic analyte and the mobile phase. The latter causes the analyte to be less solvated by the mobile phase thereby having an increased activity towards ion exchange sites on the stationary phase [41].

The zwitterionic HILIC stationary phases such as ZIC-HILIC provide a more unique selectivity as they have their own way of forming a partitioning layer with water and have only weak electrostatic interactions with charged compounds. A negative van't Hoff plot is obtained for both acidic (aspirin) and basic (cytosine) analytes on the zwitterionic HILIC phase [35] (Figure 1.21) indicating that the thickness of the solvating aqueous layer probably decreases as temperature increases.

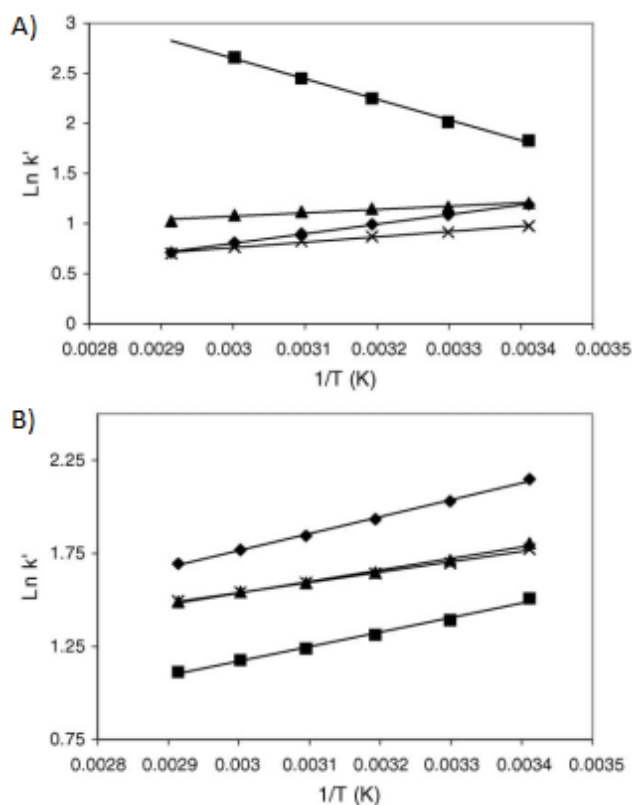


Figure 1.21: The van't Hoff plots for (A) aspirin and (B) cytosine on (■) an amine stationary phase (YMC-Pack NH₂), (◆) an amide stationary phase (TSKgel Amide-80), (▲) a silica stationary phase (HILIC Silica), and (×) a zwitterionic stationary phase (ZIC--HILIC). Mobile phase: 10 mM ammonium acetate in water/acetonitrile (10/90, v/v).

1.5.2 The Effect of the Mobile phase

The role of mobile phase is to dissolve the sample to be analysed and act as the medium for the movement of the sample through the column and detection systems. It also plays a key role in the process of separation because it can control the level of ionisation of analytes in the sample. In the HILIC mode, the mobile phase composition resembles that of a reversed phase type but the difference is that HILIC uses a mobile phase that has water as the strong solvent instead of the organic one, the latter being the case in reversed phase mode.

The main mechanism of separation in HILIC is by partitioning of the analyte between mobile phase and the layer of water adsorbed onto the stationary phase. The more polar an analyte is, the longer it will be retained by the column. It is very important to choose a suitable organic solvent for the mobile phase in order to improve the selectivity of the separation by forming a stable hydration layer in the column.

Organic mobile solvents can be subdivided into protic and aprotic ones. Protic organic solvents are those that have hydrogen that is capable of forming hydrogen bonds and they include: methanol, ethanol and isopropanol. On the other hand, tetrahydrofuran and acetonitrile are the commonly used aprotic solvents. While protic solvents can accept and donate hydrogen bonds, aprotic solvents can only accept them. As a result, protic solvents are able to compete for polar sites on the stationary phase with consequent displacement of the water molecules forming the aqueous layer on the HILIC phase surface. This replacement of the water by the protic organic solvent makes the stationary phase more hydrophobic and as a result reduces the retentivity of the column towards polar analytes [42].

For instance Li and Huang [43] compared the retention of epirubicin analogues on a bare silica HILIC column using different organic mobile phases. All four analytes eluted at the same time (Figure 1.22) when methanol was used. However isopropanol gave a slightly better resolved elution profile because, being more hydrophobic than methanol due to its longer alkyl residue, it competes less with the aqueous layer on the stationary phase and the polar analytes can be retained longer. In addition, when the mobile phase was changed from protic to the aprotic solvent tetrahydrofuran (THF), even greater resolution was obtained for the analytes and selectivity was further improved when acetonitrile is used.

Although both THF and acetonitrile are weak hydrogen acceptors, the former is the stronger one of the two. So when acetonitrile is used as the organic modifier, the mechanism of retention of analytes is by partitioning. However, when THF or protic solvents are used as organic modifiers, the retention mechanism reverses to polar interactions and ion-exchange.

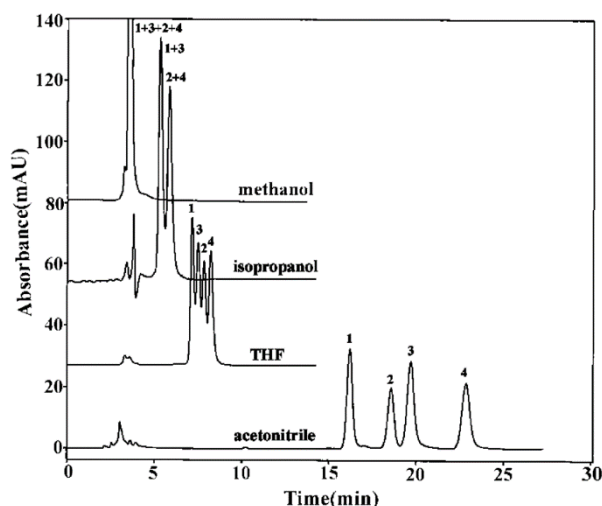
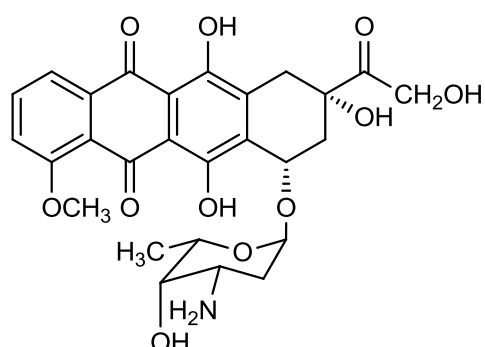


Figure 1.22: Effect of different types of the mobile phase organic modifiers on the separation of (1) epidaunorubicin, (2) daunorubicin, (3) epirubicin, (4) doxorubicin. The stationary phase was Kromasil KR100-5SIL and the mobile phase was isocratic water with different organic solvents (10:90, v/v) containing sodium formate (20 mM, pH 2.9).

Daunorubicin (peak 2) and epirubicin (peak 3) possess identical chemical structures but different configurations of the OH group (Figure 1.23). They are epimers. Whereas one can form a hydrogen bond internally with the amine group (daunorubicin), the other cannot (epirubicin) - thus causing it to interact more strongly with the polar stationary phase leading to a higher retention time.

Thus, in HILIC, acetonitrile is traditionally the weakest solvent (with regard to hydrogen donation and acceptance) hence provides a better separation than methanol; also acetonitrile gives sharper peaks than the rest of the organic solvents.

A) Daunorubicin



B) Epirubicin

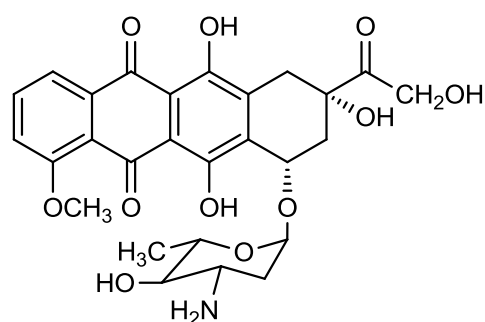


Figure 1.23: Chemical structures for (A) daunorubicin and (B) epirubicin [43].

1.5.3 *The effect of pH*

The pH of a solution is a measure of its hydrogen ion activity. Through pH control of the buffer, it is possible to control the degree of ionisation of acidic and basic analytes thus also controlling the level of interaction of analytes and the stationary phase in the column during separation. Generally pH affects selectivity of ionisable analytes in HILIC. When a chargeable analyte acquires a charge, it becomes more polar than its neutral form. This means that analytes become more strongly retained by HILIC as they partition into the aqueous layer forming the stationary phase.

It is known generally that opposite charges attract while similar ones repel each other. So when ionisable analytes acquire a charge similar to that of the stationary phase, they get repelled and their retention times decrease drastically. However, when their charges are opposite each other they form ion pairs which increases their retention times on the column. Early elution is detrimental to chromatography and, as a rule of thumb, better chromatography is obtained when an analyte stays long enough in the column so that its retention factor is at least equal to 2.

The pH at which ionisable analytes completely ionise is dependent on their p*K*_a. Thus bases are completely ionised at 2 pH units below their p*K*_a while acids are completely ionised at 2 pH units above their p*K*_a values [1]. Ionisation of a compound makes it more polar and less retained on a reversed phase column. For this reason, acidic and basic analytes are analysed in ionisation suppression modes. But for bases, because their p*K*_as are high, ionisation suppression can only occur at high pH values which may not be safe for some types of columns.

When acidic analytes are run on silica gel, various modes of interaction can occur, including partition, silanophilic, adsorption, and even repulsive. Thus it is sometimes difficult to predict the effect of increased pH on the retention of acids on this type of column. But the general rule is that retention times increase with an increase in pH for acidic compounds [35] (Figure 1.24).

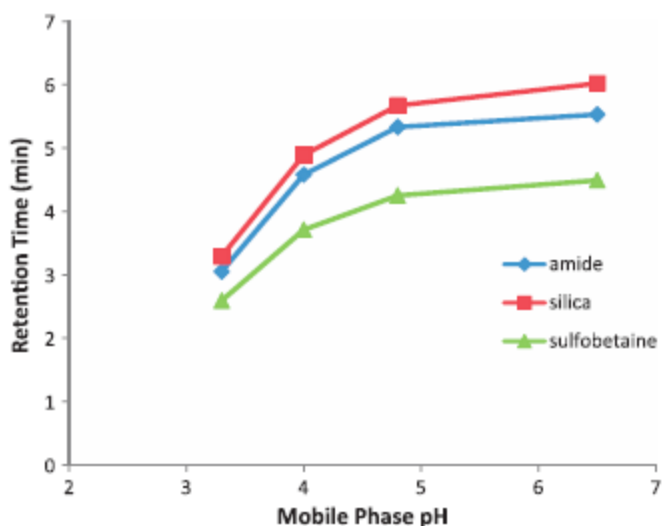


Figure 1.24: The effect of the different mobile phase pH for the aspirin on (♦) amide, (■) silica and (▲) sulfobetaine phases. The mobile phase was 10mM ammonium formate in water/ACN (10:90 v/v). Taken from Guo and Gaiki, 2005 [35].

But for a basic compound such as cytidine retention on silica is increased as pH increases because the stationary phase and the analyte are oppositely charged. This results in increased electrostatic/ionic interactions in addition to the partitioning mechanism. Positively charged stationary phases such as aminopropyl behave in the opposite manner.

On the other hand, zwitterionic columns like ZIC-HILIC have similar retention behaviour to silica gel because both have a negatively charged group although the effect in ZIC-HILIC is smaller [44]. Neutral columns may behave like negatively charged ones because of residual silanols which become negatively ionised as pH increases [45].

1.5.4 The effect of the buffer concentration on retention in HILIC

Other than controlling pH, a buffer can provide ions which act as competing species for the sites in the column thereby causing faster elution of the compounds being analysed in HILIC mode. This causes displacement of the bound analyte ions and hence faster elution.

However, these buffer ions can also act to minimise repulsion from columns which carry the same charge as the compounds being analysed. In this case the buffer ions cancel out the repulsive forces and improve the retention of analytes on the column [46]. A detailed description of the effect of buffer and its ionic strength on the elution of ionisable compounds in HILIC has been presented by Guo *et al.* [35].

1.6 Applications of HILIC

Because of its excellent performance in the separation of polar compounds in complex mixtures, HILIC has been used for various applications in the food, pharmaceutical, biological, and environmental analytical situations [47].

1.6.1 Analysis of Formulations:

HILIC has been shown to work well on bare silica in the simultaneous analysis of pseudoephedrine, dextromethorphan, and diphenhydramine in a cough preparation [48].

1.6.2 Analysis of Drug Impurities:

The HILIC technique has been used for the separation of oxprenolol from its impurities on a cyanopropyl column by Al-Tannak *et al.* [34]. In addition, six impurities of mildronate have been separated using both ZIC-HILIC and silica gel type HILIC columns [49]. Other successful applications of the HILIC technique in impurity analysis have been done for streptomycin, dihydrostreptomycin, and atenolol [50-53].

1.6.3 Bioanalysis and Drug Metabolism:

Because many bioanalytical components are polar, HILIC plays a major role there. For example: separation of choline from acetylcholine on a bare silica gel type HILIC column carried out by Grumbatch *et al* [54]; separation of nicotinic acid and its metabolites by Hsieh and Chen [55]; and pharmacokinetic monitoring of antibiotics e.g. neomycin in plasma by Oertel *et al.* [56]. The other key applications include analysis of cocaine and its metabolites in hair [7] and body fluids [57] among others in the fight against drug abuse [58].

1.6.4 Miscellaneous Applications of HILIC:

The other pharmaceutical and analytical applications of HILIC are especially useful in herbal drug development [59, 60], natural products analysis, and in the analysis of active ingredients as well as contaminants in foods and beverages [22] and in the environment [47, 61]. The others include protein and protein digests analysis [62] and metabolomics [63].

1.6.5 High Performance Liquid Chromatograph (HPLC):

The HPLC equipment consists of five components which are: mobile phase, pump, injection manifold, stationary phase and detector (Figure 1.25). The purpose of the HPLC is to pass the injected sample through the column which is carried by the mobile phase due to the pressure provided by pump. There are three types of elution techniques: isocratic, gradient and stepwise. The interaction between the compounds and the stationary phase is different depend on the characteristic of the analytes and the properties of the stationary and the mobile phases. After eluting an analyte from the stationary phase, it is then detected by an appropriate detector. The chemical properties of the analyte determine the most suitable detector to be used but the main ones include: ultraviolet (UV), fluorescence, refractive index, evaporative light scattering and mass spectrometry (MS) detectors.

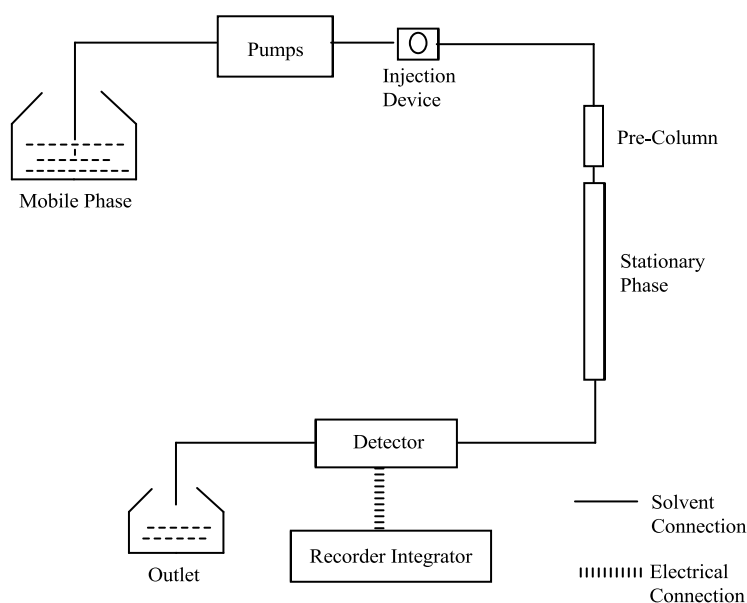


Figure 1.25: Schematic diagram of a HPLC system

For compounds that possess a chromophore, for example a benzene group, a UV detector is preferred because it is cheaper and easy to use. But for those compounds which are not amenable to detection by UV, evaporative light scattering or refractive index may be used. And yet still for the few compounds that possess a fluorophore, fluorescence detectors can be employed. But perhaps the most powerful and versatile detector is the mass spectrometer which offers the highest sensitivity and selectivity, and it can be used for almost all compounds. In addition, it provides supplementary data such as chemical formulae, ion spectra, and charge magnitude for the analytes detected [1].

1.6.6 Liquid chromatography- Mass spectrometry (LC-MS):

The main components of the mass spectrometer are the ionisation source, ion separation device and detection device. The role of the MS component is to form ions of the analytes in order for them to be detected and controlled by the mass analysers. Initially analytes eluting from the LC column pass into the ionisation chamber which is responsible for producing either positive or negative ions, or both, of the analytes. Following the ionization, ions are transferred to the mass analyser maintained at a high vacuum. This analyser in turn controls the movement of these ions.

Within the mass analyser, ions are separated based on their mass to charge ratios (m/z) to form a mass spectrum. From the mass spectrum, identification of individual components giving rise to various ion spectra is then carried out before the signals are transferred to an output (Figure 1.26).

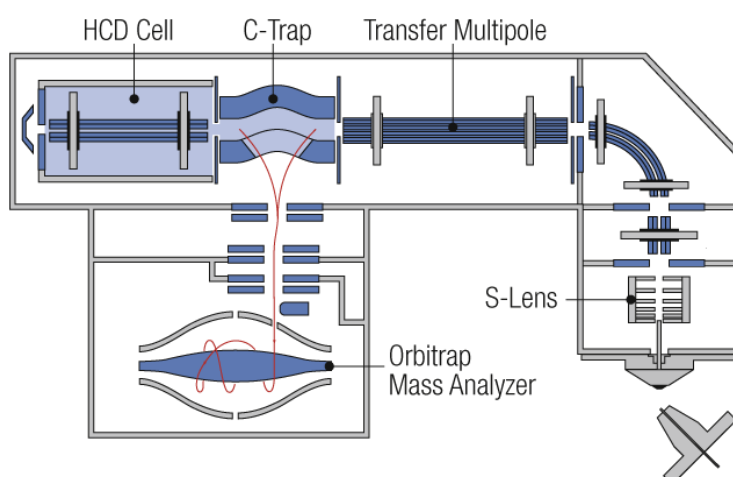


Figure 1.26: A Thermo Scientific Exactive mass spectrometer.

The ionisation process in the mass spectrometer can be affected by various, including: type of analyte, nature and strength of buffer used, and mode of ion formation. The main mechanisms of ion formation in LC-MS are chemical ionisation (CI), electron impact (EI) ionization and electrospray ionisation (ESI). The latter is used for the majority of analytical assays because it does not cause significant fragmentation of analytes being analysed. For this reason, it is called a soft ionisation technique [64].

During electrospray ionization (ESI) the sample is introduced into the source via a fine, high voltage, capillary needle. As the analytes flow towards the mass spectrometer within the needle, they acquire a charge. The charged ions first form a Taylor cone as the spray exits the needle at its tip. Ions of the charge opposite to that of the capillary are attracted away from this cone leaving the ions of the same charge within the spray. Then by way of coulombic repulsive force, the high charge concentration of ions within the droplets causes them to break up further. This is enhanced by the flow of nitrogen gas and heating, both of which cause evaporation of solvent until a single charged molecule is obtained (Figure 1.27). These charged molecules are then sucked into a high vacuum analyser region for mass measurement.

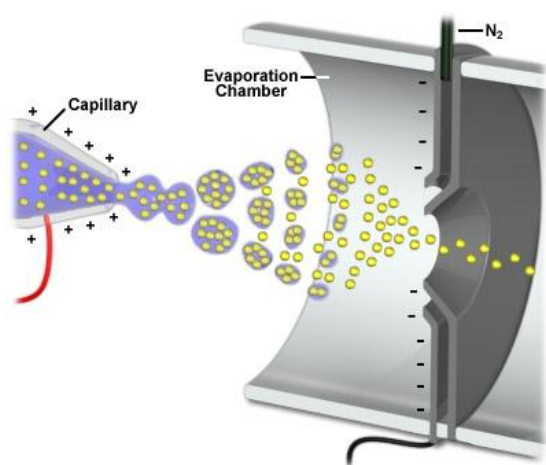


Figure 1.27: Electrospray ionisation process.

Various types of mass analysers are currently commercially available, including: quadrupoles, time-of-flight instruments and Orbitraps. The latter is one of the latest technologies with the advantages of high mass resolution and accurate mass measurement [64]. Essentially the Orbitrap is a form of ion trap which is designed to trap ions within an electrostatic field. This electrostatic attraction occurs towards a central spindle shaped electrode because the centrifugal force of the ions resulting from their velocity is balanced by their attraction towards the central electrode. The electrostatic field that the ions in the trap are subjected to forces them to move in complex, spiral pattern (Figure 1.28).

The high resolution detection of the trapped ions is based on the principle of image current measurement which itself is derived from axial oscillations of the ion packets orbiting the

central electrode. This image current, once detected, is converted, by way of Fourier mathematical transformation, into a mass spectrum [65].

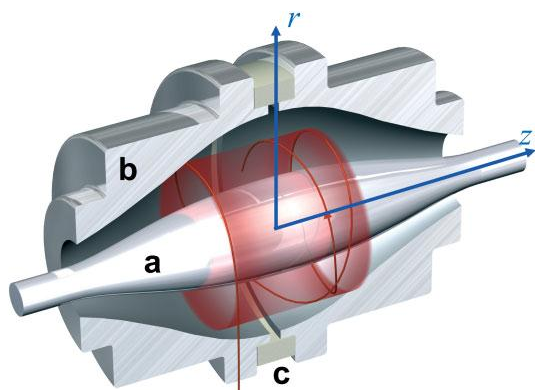


Figure 1.28: Orbitrap instrument [65].

The mass spectrometer is the method of choice for detecting analytes in biological samples because of its high selectivity and specificity in detection, and its applicability to reaction monitoring (e.g. SRM and SIM). Because bioanalytical samples contain mainly polar compounds, it provides a necessity to use HILIC in bioanalysis. It because of these reasons that direct coupling of HILIC-based LC to mass spectrometry has gained significant attention in the recent past [66].

It has already been discussed that reversed phase does not present the best option for the analysis of polar compounds because of poor retention and therefore its application to bioanalysis is problematic. Whereas ion-pair approach improves retention of ionisable polar analytes, it also leads to ion suppression which results into decreased efficiency droplet fragmentation during ESI by reducing the spray needle's charge separation [67].

At the same time, using HILIC coupled to mass spectrometry means that the more volatile high organic mobile phases used in the technique will increase ESI-MS sensitivity by improving the efficiency by which gas phase ions are formed in the ionisation chamber [68].

During sample preparation of bioanalytical samples it is a common dilemma that extracts obtained after liquid-liquid extraction (LLE), solid phase extraction (SPE), and protein precipitation (PP) contain far too much organic content than would be suitable for sample

injection in reversed phase LC-MS. This is because doing so would result in poor chromatography owing to peak fronting. Thus the extraction solvent would have to be evaporated and the sample reconstituted in a more appropriate solvent mixture prior to the injection. The use of HILIC can eliminate this need because, after all, samples containing high levels of organic solvent are already compatible with this technique [69].

1.7 Metabolomics

1.7.1 Definition of metabolomics

The term ‘metabolomics’ was first introduced in 1998 to describe the metabolic conduct of microbial systems. Since then, the term has gradually gained significant popularity within the scientific community. The suffix –ome in the word ‘metabolome’ indicates the aspiration of the field to “direct attention to holistic abstractions” based only on those observations that are possible although being only part of that whole [70]. Currently, there are four different approaches to metabolomic studies and these are: metabolic profiling, target analysis, footprinting and metabolic fingerprinting [70]. The ultimate goal of metabolomics is to identify, quantify, and classify all metabolites in a given sample which may be cell lysates, plasma, urine, or body tissue. For this reason, metabolomics, a rapidly emerging field, can be described as a comprehensive study of all metabolites – the end products of regulatory developments in a cell [71]. The level of a given metabolite in a sample indicates the response of a biological system to environmental and genetic changes [72]. In response to these changes, a biological system produces a set of metabolites which constitute its metabolome. The analysis of metabolomes can help to explain how metabolite levels vary in response to such changes as genetic variations and environmental alterations such as drug treatments [71]. In a broader context, the analysis of metabolomes is important for understanding of cellular function; it helps to unveil the dynamic nature of metabolism by supplying essential knowledge about types and quantities of existing metabolites, and the environment which exists in cell systems and living organisms [73]. Better understanding of metabolism leads to a better understanding of the overall physiological state of organisms. In metaphorical terms, metabolomics has been described as a direct ‘functional readout of the physiological state’ of a living organism [74]. Despite its seeming specificity – a focus on metabolites – metabolomics is a powerful tool capable of shaping the knowledge of underlying principles of the function of living organisms.

1.7.2 Application of Mass Spectrometry in Metabolomics

Metabolomics studies can follow one of two research directions, namely, metabolic profiling and metabolic fingerprinting. Metabolic profiling is concerned with the analysis of a set of metabolites which relate to specific biochemical pathways or treatments [75]. In pharmacology, the aim of metabolic profiling is to determine the catabolic outcome of administered drugs [72]. Metabolic profiling is often hypothesis-driven rather than hypothesis-generating: metabolites are selected for investigation on the basis of the hypothesis. Hence, the constraints of metabolic profiling are obvious: while this method can corroborate or refute the hypothesis, its capacity to reveal new aspects is limited. Another disadvantage of metabolic profiling is that it is not global due to its focus on specific groups of metabolites [75].

Metabolic fingerprinting is focused on comparing the changing patterns of metabolites. It is widely used as a diagnostic tool in medicine because it allows the identification and separation of diseased and normal subjects, and helps in assessing the dynamics of biotic, abiotic, and genetic perturbations [76]. Metabolic fingerprinting can be performed on a wide variety of biomaterials including urine, tissues, cells, and plasma. Unlike metabolic profiling, metabolic fingerprinting is a true 'omics' approach since it can be applied concurrently to a wide range of metabolites. In other words, metabolic fingerprinting is a more global method [75]. Both metabolic profiling and metabolic fingerprinting rely on various analytical tools which include nuclear magnetic resonance spectroscopy (NMR) and mass spectrometry (MS). The strength of NMR is that it is non-destructive, implying that the sample can be used for further analysis by other techniques, and it is highly selective, with the ability to distinguish between several closely related chemical compounds. In addition, NMR sets forth minimal requirements for sample preparation. The disadvantage of the technique is that it can only detect medium and high level metabolites within a sample because of its limited sensitivity [77].

The limitation of using NMR in metabolomics can be overcome with MS analysis. MS is a highly selective and sensitive instrument which can potentially identify metabolites using their accurate masses for online database search or by employing customised databases using standards. MS techniques provide spectral information such as fragmentation patterns and the precise masses of molecular ions which allow for identification of the metabolites. For this reason, there has been a rapid increase of MS-based metabolomics studies.

MS analysis is often used in combination with liquid chromatography (LC) analysis. Such a combination is often referred to as LC-MS based metabolomics. In LC-MS analysis, prepared biological samples are introduced into a mass spectrometer through the LC system. In simple terms, LC-MS analysis works as follows: comparative abundances of metabolites are estimated, data is processed using appropriate software, and data analysis is performed to compare relative abundances of each metabolite between different samples [78]. The development of LC-MS technology was primarily driven by the pharmaceutical industry: the industry requires high sensitivity and precision for studying xenobiotics, that is, drugs and their metabolic effects [79]. LC-MS based metabolomics has been applied in the studies of drug metabolism, invasive ovarian carcinomas, and ovarian borderline tumors [80].

In metabolic profiling, the MS serves as a separation technique; it differentiates metabolites based on their mass-to-charge ratio. LC technique alone is not able to provide a comprehensive analysis due to its limited sensitivity and selectivity of the ultraviolet (UV) detectors. However, in combination with MS, a higher degree of sensitivity and specificity is possible to achieve. For instance, pyrolysis-MS is able to identify metabolic markers that distinguish certain bacteria species and to classify bacteria species. Also, it is reported that MS-technology was applied to distinguish fungi species [72].

In metabolic fingerprinting, the role of LC-MS analysis is not so much to differentiate the analytes but to provide as accurate as possible data for further identification and analysis of biomarkers. This task also requires a high degree of sensitivity which the LC-MS technique provides. The primary advantage of the MS technique in metabolic fingerprinting is its capability to render high mass accuracy which allows for accurate metabolite identification. This further implies that the number of potential identities for candidate markers is reduced [81]. Hence, the overall process of identification and analysis is facilitated.

1.7.3 Applications of Metabolomics

Metabolomics has a number of applications. Traditionally, metabolite profiling has been conducted for medical and diagnostic purposes. In addition, metabolomics has been employed in advanced classification and description of plants and fungi. For instance, detection and quantification of mycotoxins is a means of characterization of fungi. The study of mycotoxins was also used to advance regulations related to food safety [82]. Also, metabolomics is an important instrument in functional genomics. Specifically, it helps in the understanding the role of specific genes. For instance, metabolomics can provide

classification of molecular signatures which account for phenotypes of unknown and silent mutations. In addition, metabolomics tools allowed the development of hypotheses about an impact of a certain phenotype on amino acid and carbohydrate metabolism [82]. Metabolomics has also potential application in evolution studies. The point is that certain secondary metabolites are very species-specific and such metabolites are considered to be potential markers for phylogenetics and taxonomy [74]. Therefore, they can help to reveal the evolution of certain species.

Metabolomics research is widely used in pharmacology for purposes of drug discovery and development. Specifically it is applied in lead compound discovery. Furthermore, metabolomics helps to identify biomarkers which are necessary to monitor diseases and to assess drug efficiency. Also, metabolomics is used in drug metabolism studies. Finally, metabolite research is a part of drug toxicity assessment, clinical trials and post-approval drug monitoring [83]. Thus one may observe that metabolomics accompanies virtually all stages of drug development – from discovery to post-approval maintenance.

1.7.4 Software in Metabolomics

Metabolomics uses various statistical methods for data analysis. The choice of the method depends upon the objective of the study. Thus, if the objective is to classify samples and if there is no prior information about the sample identity, then principal component analysis (PCA), hierarchical clustering analysis (HCA) and independent component analysis (ICA) are applied to find out about the properties of biomarkers. However, if the sample identity is known, then such supervised methods as orthogonal partial least squares discriminant analysis (OPLS-DA) and partial least squares (PLS) can be used [75].

PCA is one of the most popular statistical methods. This tool is used to reduce complexity in large datasets or by focusing on the essential parameters that show the greatest degrees of variance. PCA identifies an optimal linear conversion for a group of data points such as characteristics of the sample studied. PCA allows observation of differences among samples and identifying the main contributors to such differences. Also, PCA is a powerful visualization tool as it allows visual detection of sample patterns. The visualization is achieved through projection of multidimensional data on 2D and 3D sketches.

HCA is an unsupervised method which produces a ‘tree-like’ dendrogram. It, as well as other clustering methods, is used to evaluate in a multivariate way the similarity of set of

samples on the basis the metabolite profiles of these samples. The application of the HCA allows classifying unknown samples according to their closeness to the known ones. This method, however, is criticized as poorly reproducible and mathematically unjustified. It is also claimed that this method lacks adequate measurement for the quality of clusters [84].

On the other hand, OPLS-DA is a supervised model which tries to cluster samples based on their classifications. For instance, a dataset may contain metabolites in both treatment and control groups. These two classes are specified in the software and when OPLS-DA is employed, it will try to separate the subjects based on whether they belong to the treatment or control groups. In this way, it assigns greater significance to the metabolites that are different between the two groups already in the data set. This approach has been used in determining the biomarkers for certain treatment interventions or disease states in comparison to controls. It has also been employed in the metabolomics study of milks from the giant panda mothers [77, 85, 86].

1.8 Aims and Objectives

The aims of the work described in this thesis were as follows:

- (i) To investigate the effect of different anions on hydrophilic interaction liquid chromatography (HILIC) retention on silica gel.
- (ii) To investigate the effect of counter ions on retention behaviour in HILIC.
- (iii) To assess the usefulness of a silica C column for the analysis of metabolites and metabolomics profiling.
- (iv) To study the reductive amination of sugars in order to produce separation of common sugars in HILIC mode.
- (v) To examine the metabolomics profile of post-partum seal milk by LC-MS and compare seal milk with land based mammals (camel, goat and cow) in order better understand differences in nutritional requirements in mammalian neonates.

Chapter 2:

Investigation of the interaction of different anions and neutral compounds on hydrophilic interaction with silica gel

2 Investigation of the effect of different anions on hydrophilic interaction with silica gel

2.1 Introduction

There is still a lack of knowledge of the processes which occur on the simplest HILIC phase, silica gel and this is a hindrance to fully exploiting the HILIC mechanism. While different silica gels have been explored previously with regard to their HILIC properties there has been no systematic study of the influence of silica gel surface area on HILIC. McCalley proposed a model [8] which was later used by Bicker *et al* to dissect out the relative contributions of ion-exchange and HILIC for different HILIC columns [87]. In a previous study it was clearly observed that an increase in silica gel surface area led to an increase in hydrophilic interaction [88]. For bases the contribution of HILIC to overall retention increases as the ionic strength of the competing counter ion is increased and if it is desired that the contribution of HILIC to retention should be promoted then it would be better to work at higher ionic strength. Although we have yet to study this, the ionic strength of the mobile phase modifier is likely to be much higher in the HILIC layer than in the bulk since ionic modifiers will partition strongly into the aqueous layer. The level of such modifier partitioning should also depend on the particular counter ions used, both anions and cations and this is the subject of the current chapter. For essentially a very simple system the possible interactions between the silica stationary phase, water, buffer salts and analytes is extremely complex. Table 2.1 summarises some of the possible interactions which could occur leading effects on analyte retention. In the work described in this chapter the cation exchange effects were not explored since these were evaluated in an earlier study [88] and the test probes used were either neutral or acidic.

Table 2.1: Factors governing the HILIC effect for acidic and neutral compounds.

Effect	Comments
HILIC.	The HILIC effect depends on the solubility of the analyte in a water layer on the surface of the column. The thicker the water layer and the greater the effect. The thickness of the water layer could depend on the solvation energy of the ions used in the mobile phase. The higher the hydration energy of the ion the more water it will associate with the thicker the HILIC layer. In addition the

greater the concentration of modifier the greater the concentration of ions in the HILIC layer, the thicker the HILIC layer. In addition ionisation of silanol groups on the silica gel surface will cause greater association of water with the surface. Ionisation of silanols increases as pH increases.

Charge repulsion.

Acids carry a negative charge as does the surface of the silica gel and thus the higher the pH the more the surface and acidic analytes will become negatively charged and repel each other. The presence of positively charged ions from the mobile phase modifier can shield the negatively charged surface reducing repulsion. Thus higher concentrations of cations should reduce charge repulsion and increase the retention of acids.

Anion exchange interactions

The presence of a high concentration of positively charged ions in the HILIC layer might promote anion exchange type interactions with negatively charged analytes.

This chapter discusses the effect of different strengths of four buffers namely: ammonium acetate, ammonium formate, ammonium chloride, ammonium propionate and ammonium bicarbonate, on the retention of various test probes in HILIC mode on silica gel. Initially, the effects of different ionic strengths of ammonium acetate, ammonium formate, and ammonium bicarbonate buffers on the retention of analytes on a Kromasil column were investigated using five probes: riboflavin (very weak acid), xanthine (weak acid), nicotinic acid (acidic), maleic acid (doubly charged acid) and inosine (weak acid). The structures of the probes are shown in Table 2.2. The effect of the ionic strength of ammonium chloride and ammonium propionate buffers on retention on the Kromasil was investigated. In this case, four probes nicotinic acid, maleic acid, ketoprofen and hydroxybenzoic acid were used for ammonium chloride, while riboflavin, xanthine, inosine and maleic acid were used for ammonium propionate. The variation in the anion in the buffer modifier allowed assessment of its effects on the acid test probes. It might be expected that buffer anions with higher solvation energies would tend to displace the acidic probes to a greater extent from the HILIC layer. The solvation energies of most of the counter anions are shown in Table 2.3.

Table 2.2: The elemental compositions, molecular weight and chemical structures of the various test probes used in this chapter.

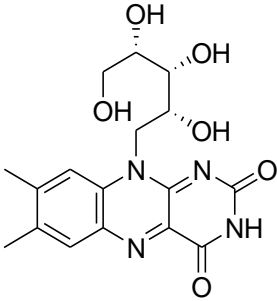
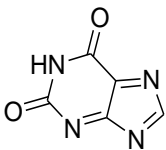
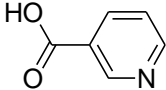
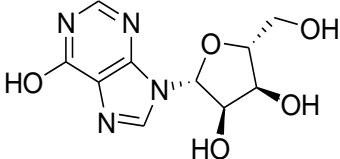
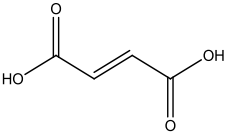
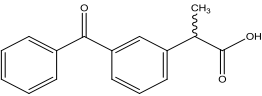
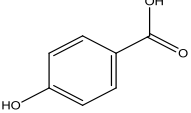
Probe	Elemental composition	MW	Structure	logP	pKa
Riboflavin	$C_{17}H_{20}N_4O_6$	376.36		-1.46	10.2
Xanthine	$C_5H_4N_4O_2$	152.11		-0.7	7.53
Nicotinic acid	$C_6H_5NO_2$	123.11		0.36	4.75
Inosine	$C_{10}H_{12}N_4O_5$	268.23		-2.1	8.6
Maleic acid	$HO_2CCH=CHCO_2H$	116.07		-0.48	1.83
Ketoprofen	$C_{16}H_{14}O_3$	254.28		3.12	4.45
4-Hydroxybenzoic acid	$C_7H_6O_3$	138.12		1.58	4.54

Table 2.3: The hydration energies of the ions in the five mobile phase modifiers used.

Modifier	Energy (kJ mol ⁻¹)	Modifier	Energy (kJ mol ⁻¹)
NH ₄ ⁺	-307 kJ mol ⁻¹	CH ₃ COO ⁻	-389 kJ mol ⁻¹
Cl ⁻	-378 kJ mol ⁻¹	HCOO ⁻	-368 kJ mol ⁻¹
HCO ₃ ⁻	-380 kJ mol ⁻¹	C ₂ H ₅ COO ⁻	-328 kJ mol ⁻¹

D.W. Smith, J. Chem. Educ., 54, 540 (1977) and Kang et al., J. Phys. Chem. 1987, 91, 4118-4120 [89].

2.2 Aims

- To investigate the effect of **ammonium acetate** buffer strength on analyte retention on Kromasil column using the probes riboflavin, xanthine, nicotinic acid, maleic acid, hydroxybenzoic acid and inosine.
- To investigate the effect of **ammonium bicarbonate** buffer on analyte retention on Kromasil column using the probes riboflavin, xanthine, nicotinic acid, maleic acid hydroxy benzoic acid and inosine.
- To investigate the effect of ionic strength of **ammonium chloride** buffer on Kromasil column and measure the amount of water using the probes, riboflavin xanthine, nicotinic acid, maleic acid hydroxy benzoic acid and inosine.
- To investigate the effect of ionic strength of **ammonium formate** buffer on Kromasil column and measure the amount of water using the probes, riboflavin xanthine, nicotinic acid, maleic acid hydroxy benzoic acid and inosine.
- To investigate the effect of ionic strength of **ammonium propionate** buffer on analyte retention on the Kromasil column using riboflavin, xanthine, inosine, maleic acid, nicotinic acid, ketoprofen and hydroxybenzoic acid as the probes.
- To investigate some HILIC methods for the separation of some common sugar isomers.

2.3 Materials and methods

2.3.1 Chemicals and columns

The HPLC grade solvents methanol, acetonitrile, formic acid and acetic acid were purchased from Fisher Scientific (Loughborough, UK). HPLC water was produced in the lab using a

Millipore water purification system. The test probes pentyl benzene, riboflavin, xanthine, nicotinic acid, inosine, maleic acid, ketoprofen, and hydroxybenzoic acid, ammonium acetate, ammonium formate, ammonium carbonate, ammonium chloride, and propionic acid were all obtained from Sigma Aldrich (Dorset, UK). The HPLC column was a Kromasil 60-5SIL column (150 mm×4.6 mm×4 μm, pore size 60Å) obtained from HiChrom Ltd (Reading, U.K).

2.3.2 Buffer preparation

Ammonium acetate buffer (200 mM) was prepared by dissolving 7.8 g of ammonium acetate in about 400 ml of purified water in a 500 ml volumetric flask and adding 50 ml of methanol (the methanol was intended to stop bacteria growing in the ammonium acetate buffer). Thereafter, the solution was made up to the 500 ml mark with water. For the preparation of 100 mM ammonium acetate buffer, 3.9 g of ammonium acetate was used instead of 7.8 g.

Ammonium bicarbonate buffer (100 mM) was prepared by dissolving 3.9 g of ammonium bicarbonate in about 400 ml of purified water in a 500 ml volumetric flask and adding 50 ml of methanol. The solution was then made up to the 500 ml mark with water.

Ammonium chloride buffer (200 mM) was prepared by dissolving 5.4 g of ammonium chloride in about 400 ml of purified water in a 500 ml volumetric flask and adding 50 ml of methanol. The solution was then made up to the 500 ml mark with water. To prepare 100 mM of the buffer, the same procedure was used but with only 2.7 g of ammonium chloride.

Ammonium propionate buffer (200 mM) was prepared by dissolving 7.4 g of propionic acid in about 300 ml of purified water. The pH was adjusted to 6.8 using ammonia solution and then 50 ml of methanol was added in order to stop bacteria from growing in the buffer. To prepare 100 mM of the buffer, the same procedure was used but with only 3.7 g of ammonium carbonate sample.

2.3.3 Mobile phase preparation

Twenty different mobile phases each with a different strength or anion were used. These mobile phase were prepared using the respective buffers prepared in 2.3.2 above by transferring either 50 or 25 ml of each of the stock buffers (Table 2.4) into a suitable container and then adding 450 ml of acetonitrile. For the preparation of the 5mM strengths of the buffers, 25ml of water was first added to the buffers before the 450ml of acetonitrile was added.

Table 2.4: Preparation of the buffers of ammonium acetate, bicarbonate, chloride and propionate

<i>Buffer</i>	<i>Molarity (mM) and volumes (mL) of stock solutions used</i>							
	Buffer mM	Acetate 200	100	Bicarbonate 100	Chloride 200	100	Propionate 200	100
Acetate	20	50						
	10	50						
Bicarbonate	5	25						
Chloride	20	50						
	10	50						
	5	25						
Propionate	20	50						
	10	50						
	5	25						

2.3.4 Chromatographic System

A Thermo Separations P2000 HPLC pump was used in the studies. The HPLC system was equipped with a variable wavelength UV detector. The isocratic method employed the pre-mixed mobile phases as described above at a flow rate of 1.0 ml/min and detection was carried out UV at a wavelength of 254 nm. The system was fully equilibrated before each experiment by running the mobile phase for 30 minutes.

2.3.5 Sample preparation

The seven test compounds riboflavin, xanthine, nicotinic acid, inosine, maleic acid, ketoprofen, and hydroxybenzoic acid were separately prepared by mixing 50 mg of each sample with 50 ml of methanol/water (1:1). After thorough mixing, 50 µl of each solution was pipetted and transferred into a separate HPLC vial and diluted to 1ml with the relevant mobile phase prior to the analysis. Due to their limited solubility, the xanthine and riboflavin stock solutions were filtered prior to dilution in order to remove any suspended insoluble material that could have damaged the column. Thus their concentration might have been less than the 0.05mg/ml used with the other probes but this could not affect the data as the experiment was qualitative.

2.4 Results

2.4.1 Retention of Test Probes on a Kromasil Column with Ammonium Acetate as the Mobile phase modifier

Table 2.5: Mean retention times of the test probes under different strengths of ammonium acetate mobile phase modifier.

Compound	Mean Retention Times (Min)					
	5 mM		10 mM		20 mM	
	Mean	SD	Mean	SD	Mean	SD
Nicotinic acid	10.8		10.0		26.4	
Ketoprofen	4.9		5.5		5.1	
Maleic acid	2.6		6.4		28.2	
Hydroxybenzoic acid	6.1		8.1		14.3	
Toluene	1.8		1.8		1.7	
Pentylbenzene	1.8		1.7		1.6	
Riboflavin	4.9		8.4		11.3	
Xanthine	4.5		7.3		11.5	
Inosine	6.0		11.1		20.4	

Figures 2.1-2.15 show chromatograms for nicotinic, maleic acid, xanthine, riboflavin and inosine run on the Kromasil column at 5, 10 and 20 mM ammonium acetate in acetonitrile/water (90:10). Both analytes are well retained on the silica gel column under these conditions since they have high water solubility. The lipophilic acid ketoprofen has only low water solubility and is only weakly retained by the column (Table 2.4) at all the ammonium acetate strengths. The retention of maleic, nicotinic and hydroxybenzoic acids increases with ammonium acetate strength. There are at least two mechanisms which could produce this increase. The increase in ammonium acetate strength could promote an increase in the thickness of the water layer on the surface of the silica gel or increasing amounts of ammonium ion could shield the negative charge on the surface of the silica gel reducing the repulsion of the acids by the surface. Maleic acid is more water soluble than nicotinic acid but it is also more highly charged, having two carboxylic acid groups in comparison to one for nicotinic acid, and thus it has a shorter retention time due to charge repulsion. At the highest ammonium acetate concentration, in the case of maleic acid, water solubility dominates over charge repulsion and it is retained more than nicotinic acid. Riboflavin,

xanthine and inosine are very weak acids and are effectively neutral at the pH of the mobile phase. Therefore any increase in their retention time must be due to an increase in the thickness of the aqueous HILIC layer since charge does not play a role. Inosine in particular shows a marked increase in retention at 20mM ammonium acetate and this suggests much of the increase in retention with increased ionic strength is due to the higher salt concentration producing more separation between the organic and aqueous phases and thus an increase in the thickness of the aqueous phase on the column surface, although there may be a component due to a reduction in charge repulsion in the case of the acids. The pentyl benzene was included to test this as well and provide some evidence of a thicker aqueous layer. The retention time of the pentyl benzene decreases by 0.2 min between 5 and 20 mM ammonium acetate and this possibly indicates a thicker water layer which excludes pentyl benzene from the water filled pores of the silica gel because of its lack of water solubility.

Figure 2.1: Nicotinic acid run with 5 mM ammonium acetate in acetonitrile/water (90:10) on a Kromasil 60 column.

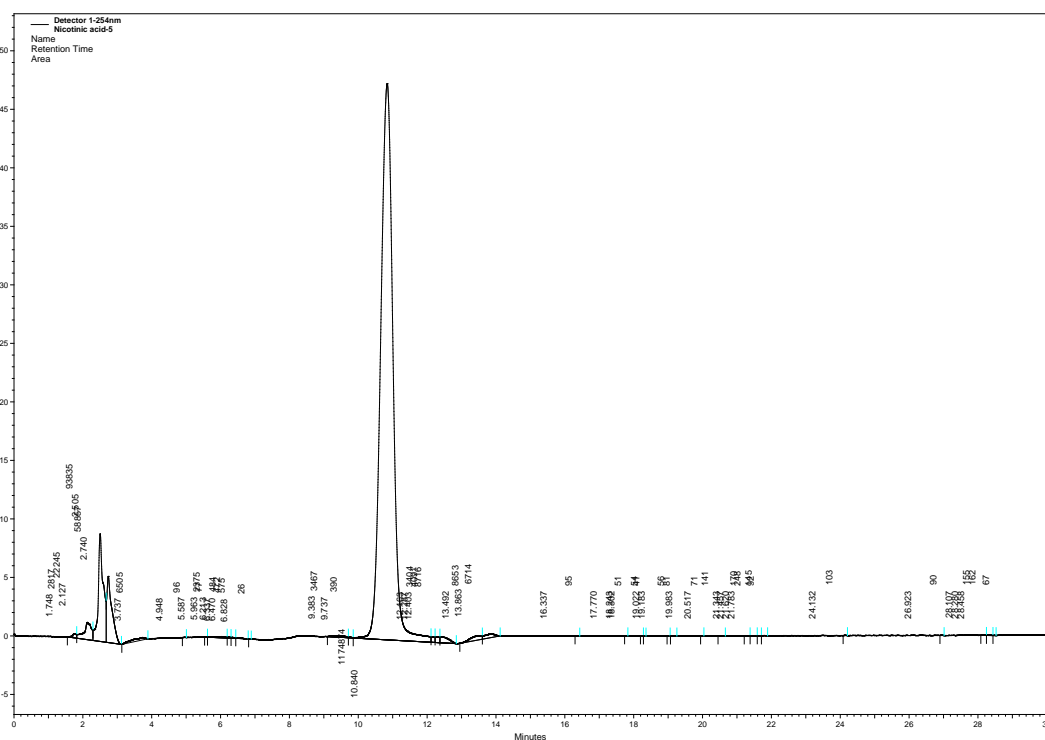


Figure 2.2: Maleic acid run with 5 mM ammonium acetate in acetonitrile/water (90:10) on a Kromasil 60 column.

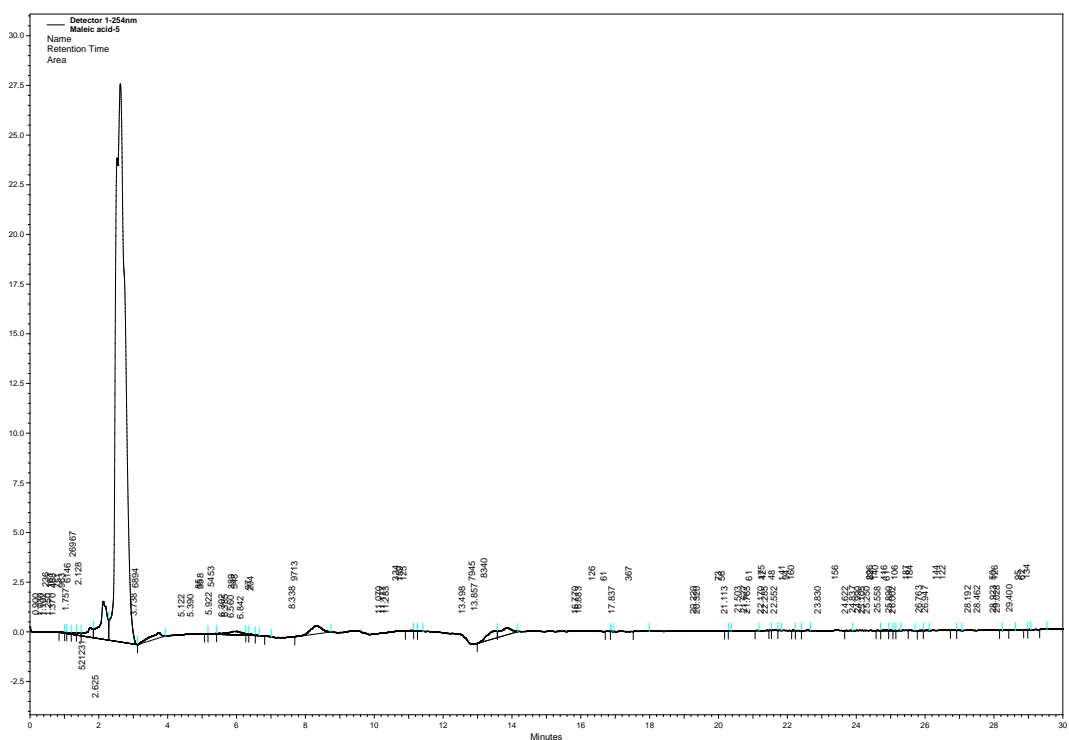


Figure 2.3: Inosine run with 5 mM ammonium acetate in acetonitrile/water (90:10) on a Kromasil 60 column.

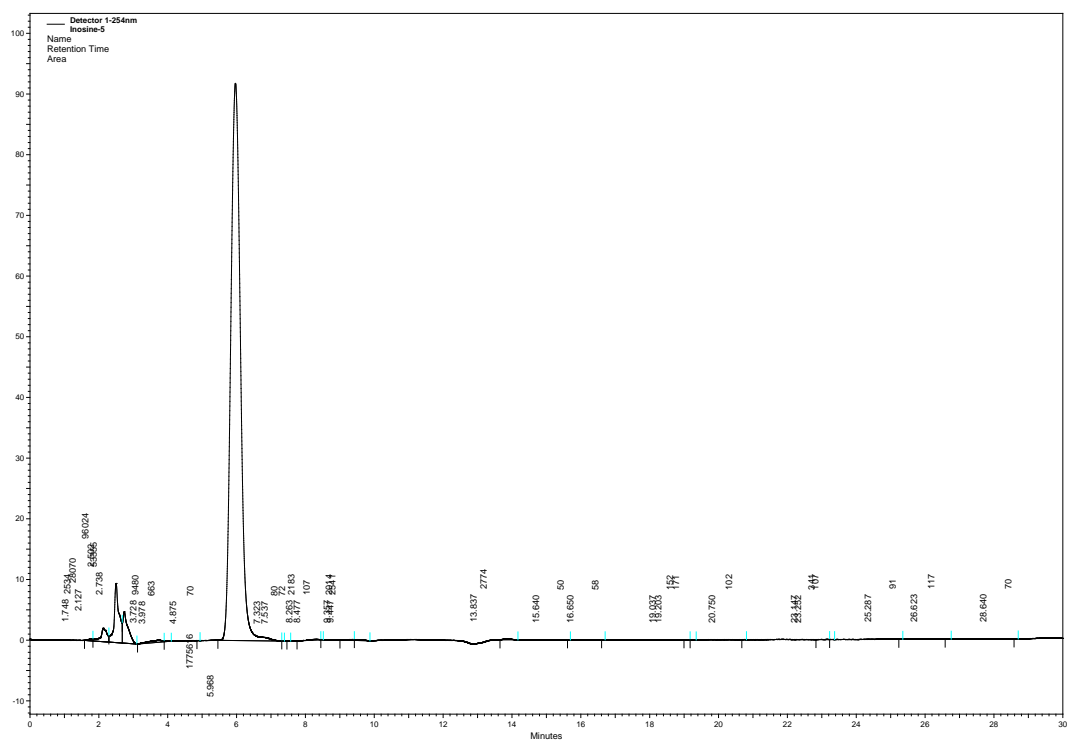


Figure 2.4: Xanthine run with 5 mM ammonium acetate in acetonitrile/water (90:10) on a Kromasil 60 column.

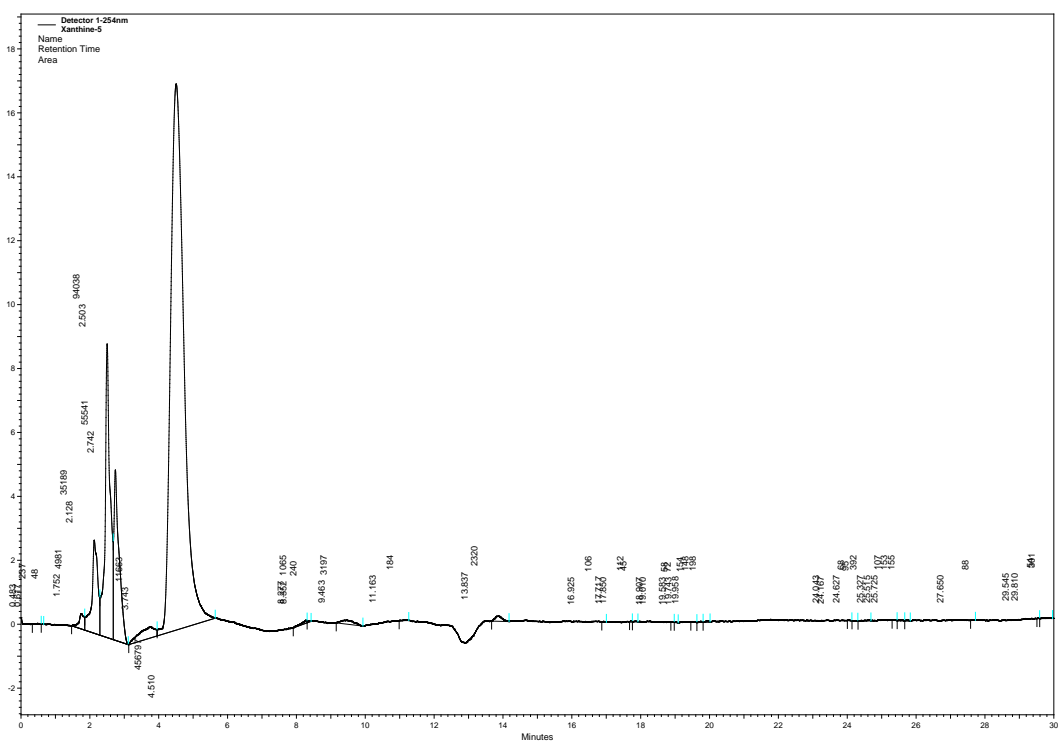


Figure 2.5: Riboflavin run with 5 mM ammonium acetate in acetonitrile/water (90:10) on a Kromasil 60 column.

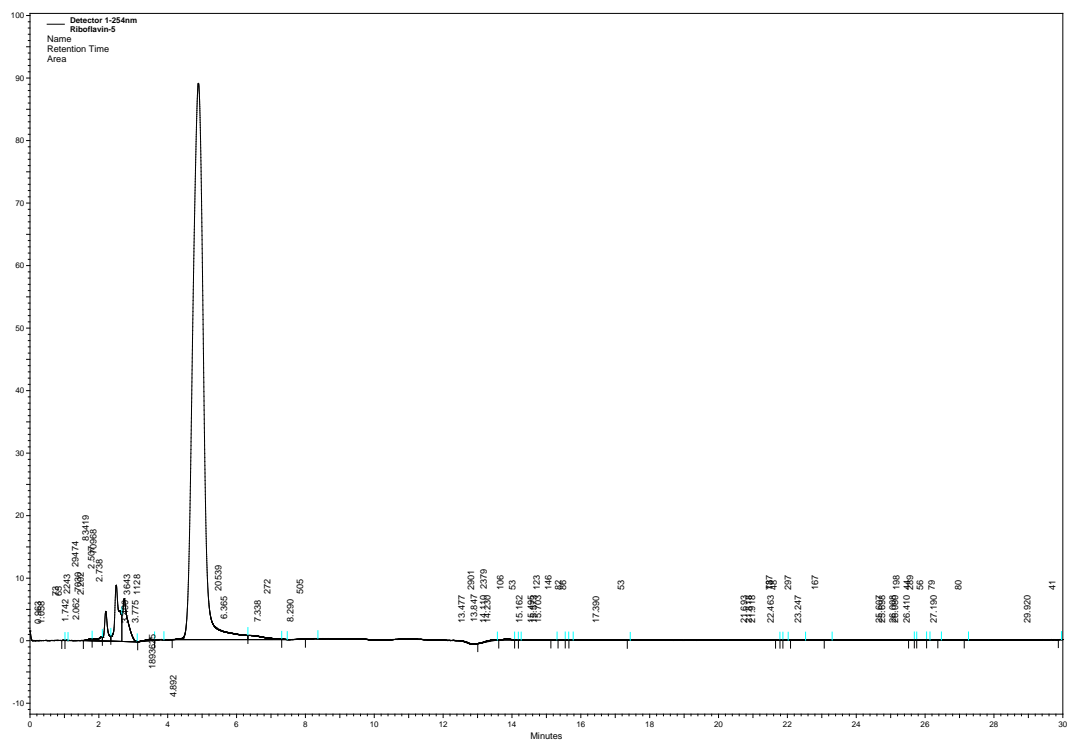


Figure 2.6: Nicotinic acid run with 10 mM ammonium acetate in acetonitrile/water (90:10) on a Kromasil 60 column.

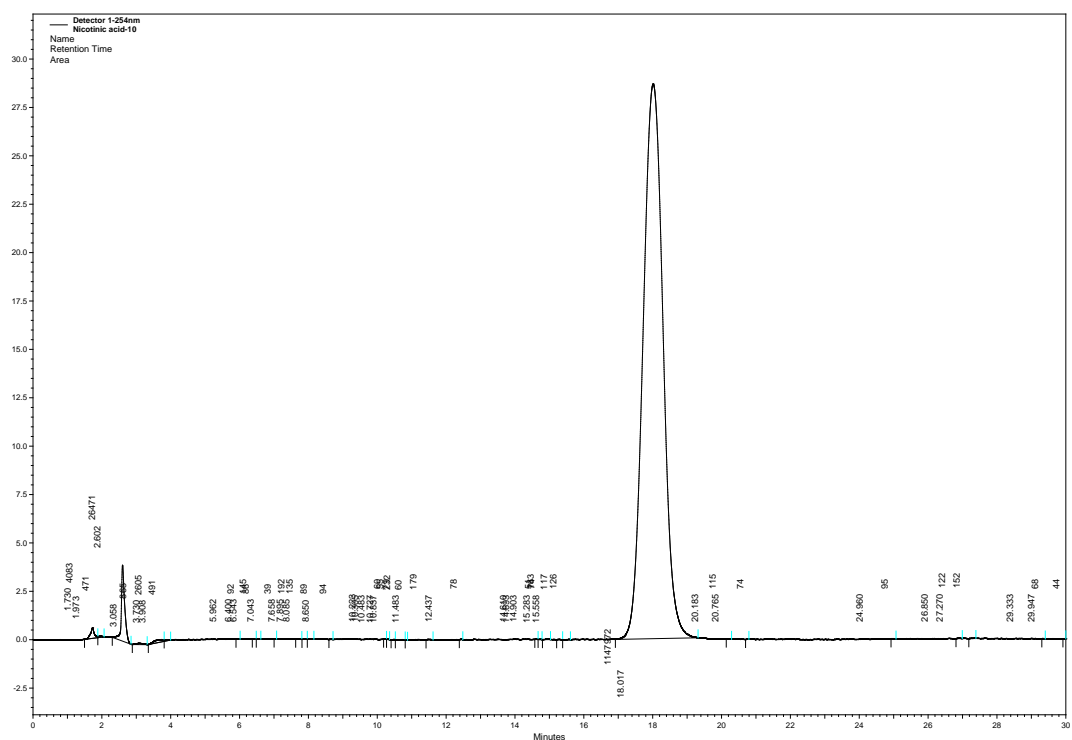


Figure 2.7: Maleic acid run with 10 mM ammonium acetate in acetonitrile/water (90:10) on a Kromasil 60 column.

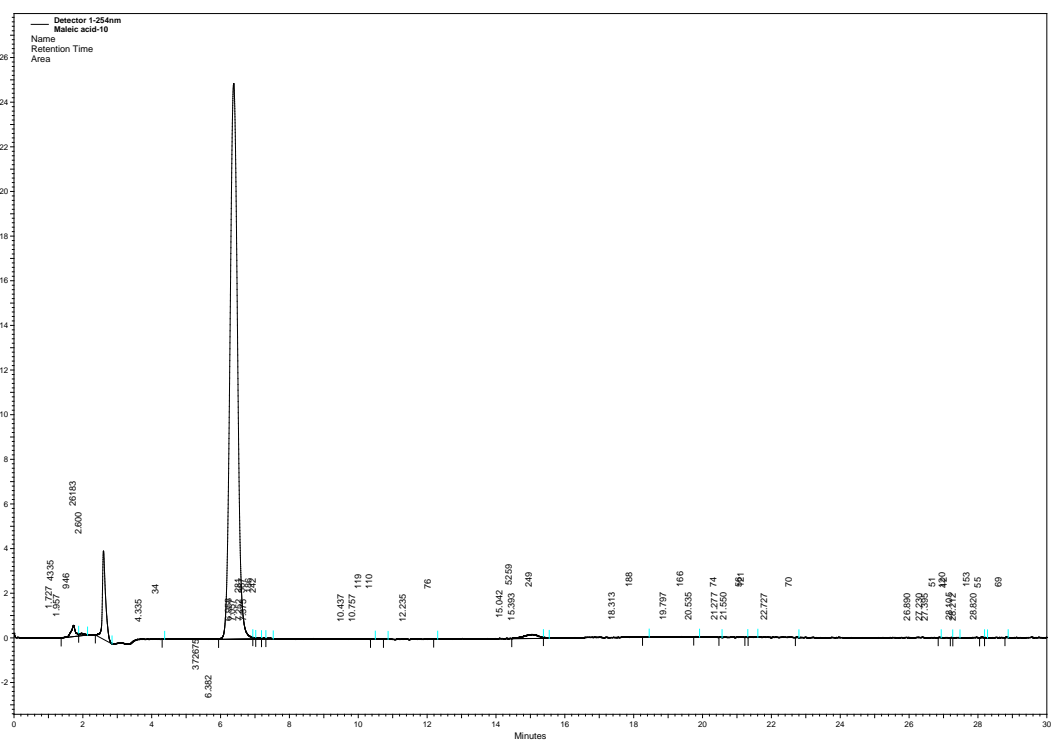


Figure 2.8: Inosine run with 10 mM ammonium acetate in acetonitrile/water (90:10) on a Kromasil 60 column.

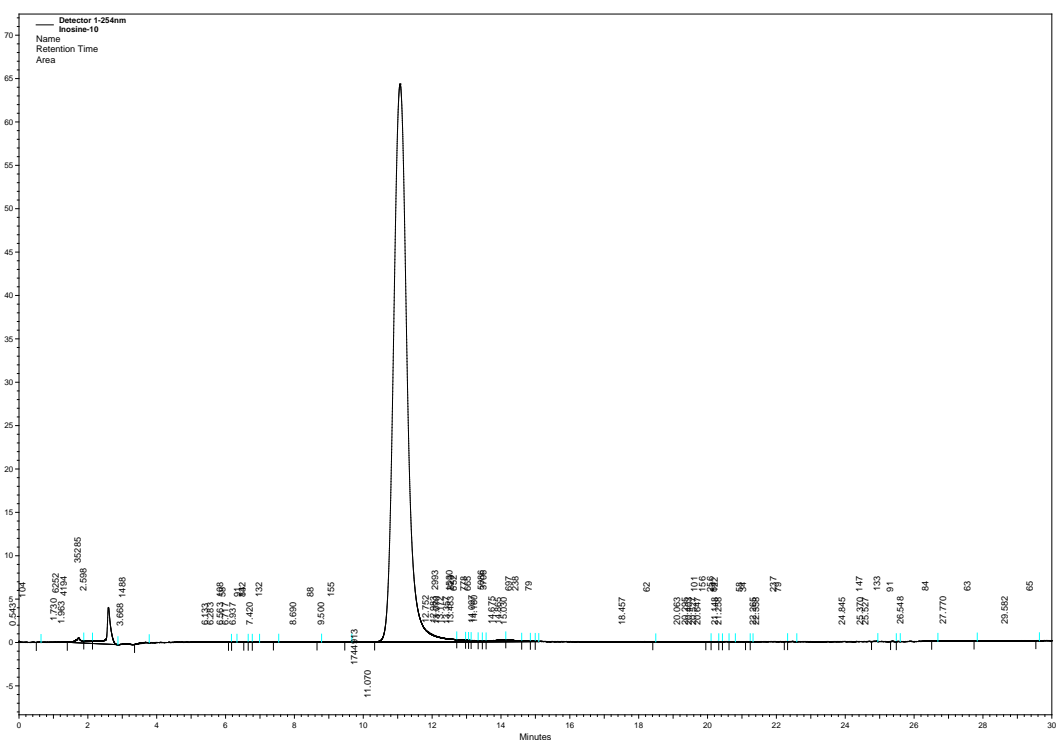


Figure 2.9: Xanthine run with 10 mM ammonium acetate in acetonitrile/water (90:10) on a Kromasil 60 column.

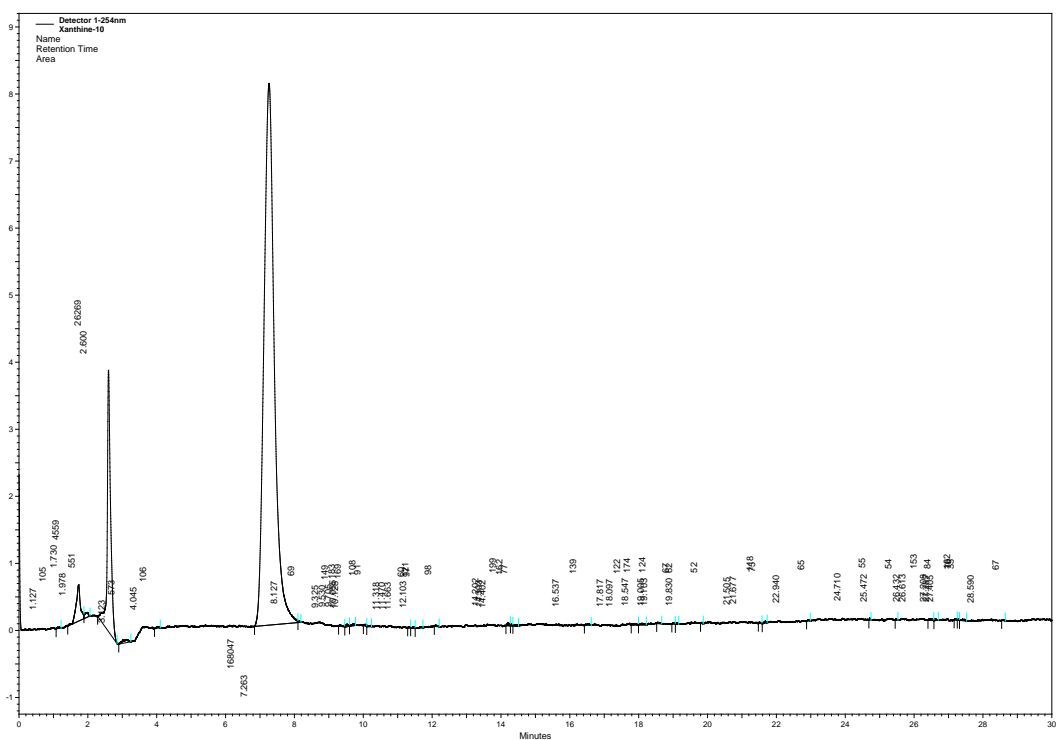


Figure 2.12: Maleic acid run with 20 mM ammonium acetate in acetonitrile/water (90:10) on a Kromasil 60 column.

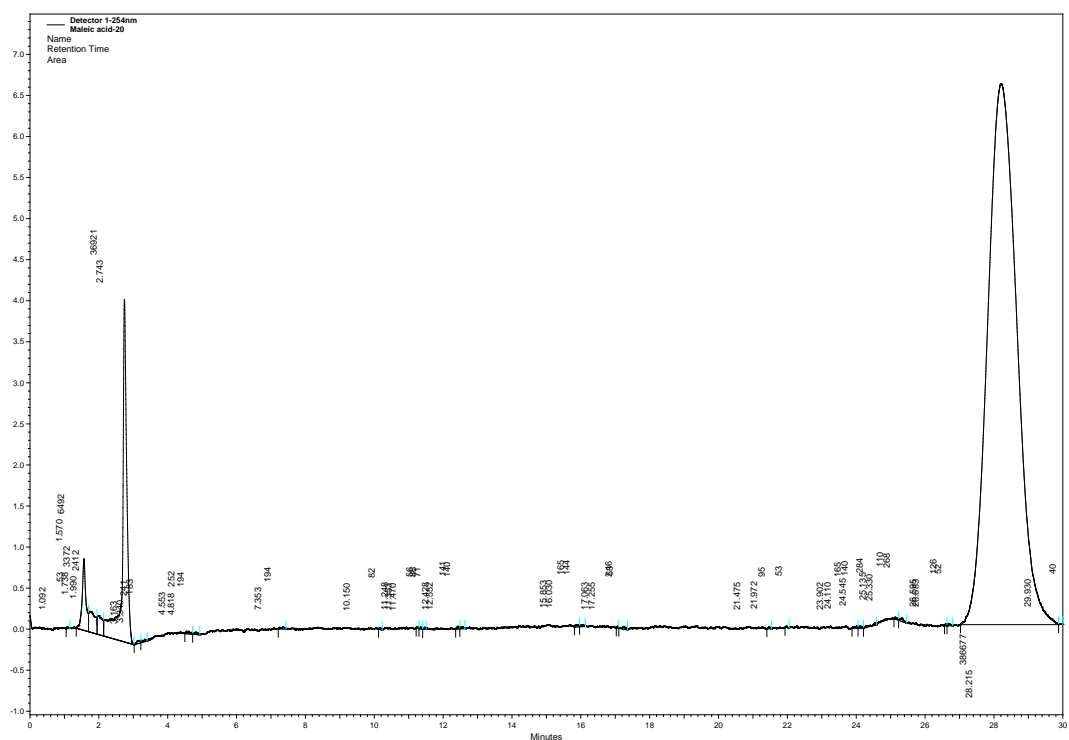
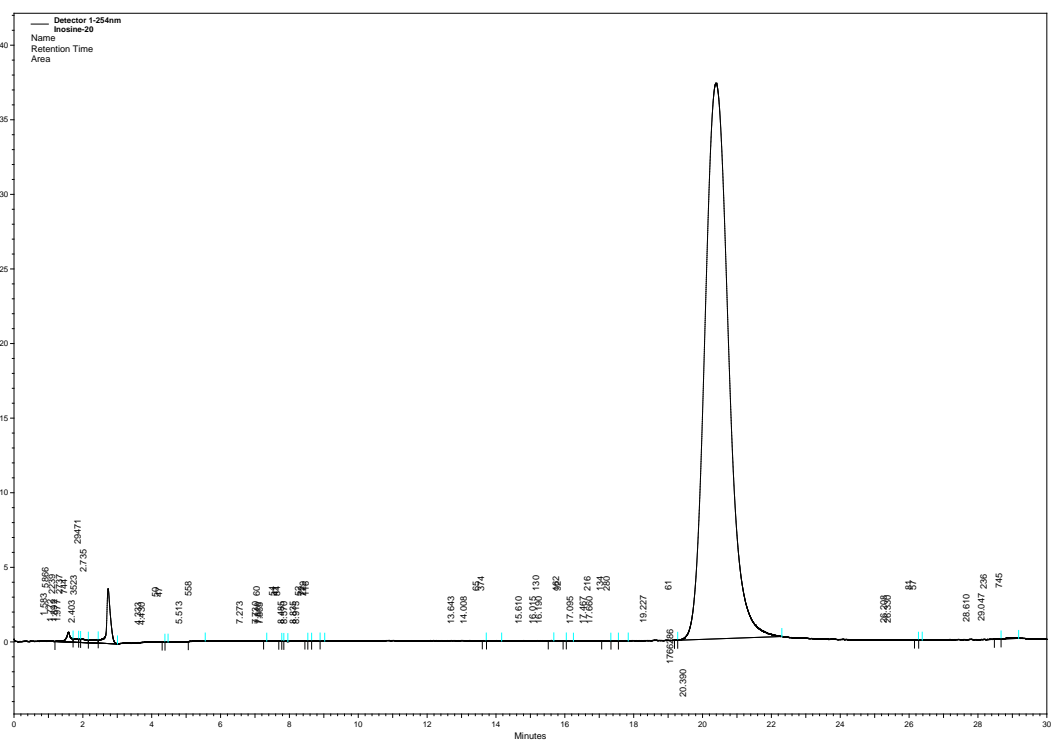


Figure 2.13: Inosine run with 20 mM ammonium acetate in acetonitrile/water (90:10) on a Kromasil 60 column.



2.4.2 Retention of Test Probes on a Kromasil Column with Ammonium Formate as the Mobile phase modifier

Table 2.6: Mean retention times of the test probes under different strengths of ammonium formate mobile phase modifier.

Compound	Mean Retention Times (Min)		
	5 mM	10 mM	20 mM
Nicotinic acid	20.7	23.8	30.5
Riboflavin	6.5	8.0	11.5
Xanthine	5.6	6.1	9.1
Inosine	7.6	9.4	19.3
Ketoprofen	4.7	5.0	4.1
Maleic acid	2.5	4.0	14.0
Hydroxybenzoic acid	4.8	5.5	10.6
Toluene	1.8	1.8	1.8
Pentylbenzene	1.8	1.8	1.7

Table 2.5 shows the retention times for the test probes run on the Kromasil column with different strengths of ammonium formate. Figures 2.16-2.30 show chromatograms for nicotinic, maleic acid, xanthine, riboflavin and inosine run on the Kromasil column at 5, 10 and 20 mM ammonium formate in acetonitrile/water (95:5). The retention of nicotinic acid on the Kromasil column is high at all ammonium formate strengths and there is not as great an increase between 5 mM and 20mM as there was with ammonium acetate. This suggests that the water layer may not be increasing as much as the formate strength increases and this is reflected in the behaviour of riboflavin, inosine and xanthine where their retention times do not increase as much as they did in response to increasing ammonium acetate strength. This might be explained according to the lower solvation energy for formate shown in Table 2.3 in comparison to acetate which might result in less water being drawn into the HILIC layer. The pH of ammonium formate (*ca* 5.5) is about 1 unit below that of ammonium acetate (*ca* 6.9) so the silica gel surface will bear less negative charge than when ammonium acetate is used but it will still be charged. The higher retention time of nicotinic acid at 5 mM ammonium formate in comparison with 5 mM ammonium acetate suggests that charge repulsion is less significant at the pH of ammonium formate. Of the three acids maleic acid is the strongest and can carry two negative charges, in the case of ammonium formate its retention time does not overtake that of nicotinic acid suggesting the charge repulsion of

Figure 2.17: Maleic acid run with 5 mM ammonium formate in acetonitrile/water (90:10) on a Kromasil 60 column.

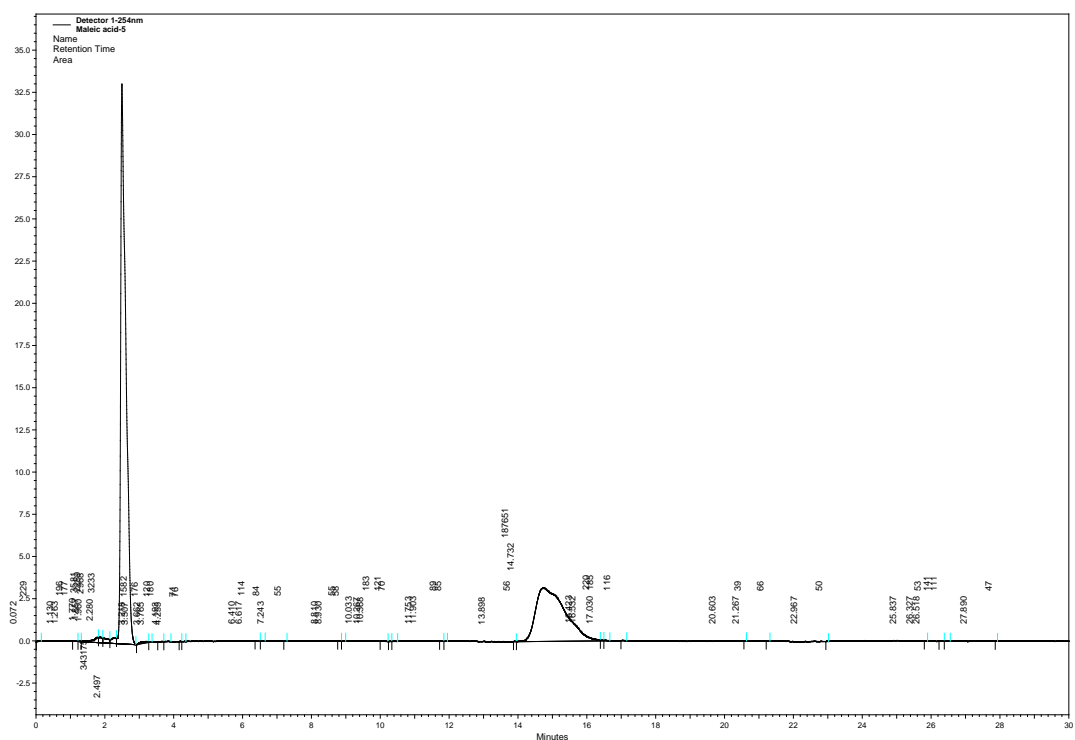


Figure 2.18: Inosine run with 5 mM ammonium formate in acetonitrile/water (90:10) on a Kromasil 60 column.

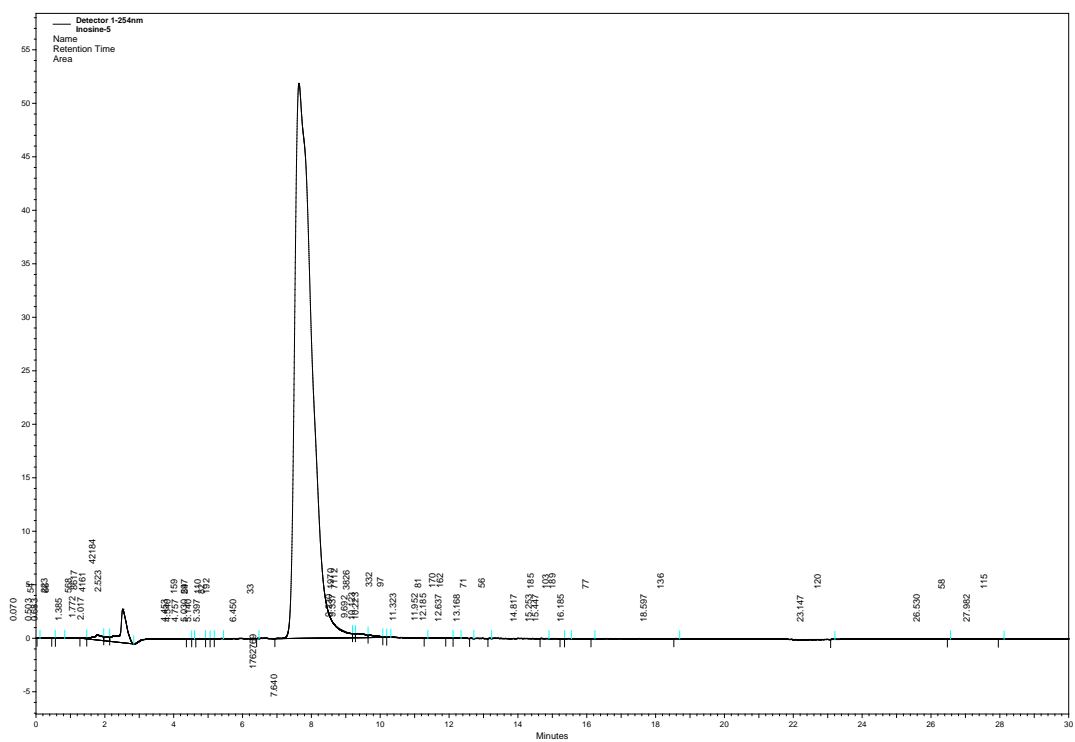


Figure 2.19: Xanthine run with 5 mM ammonium formate in acetonitrile/water (90:10) on a Kromasil 60 column.

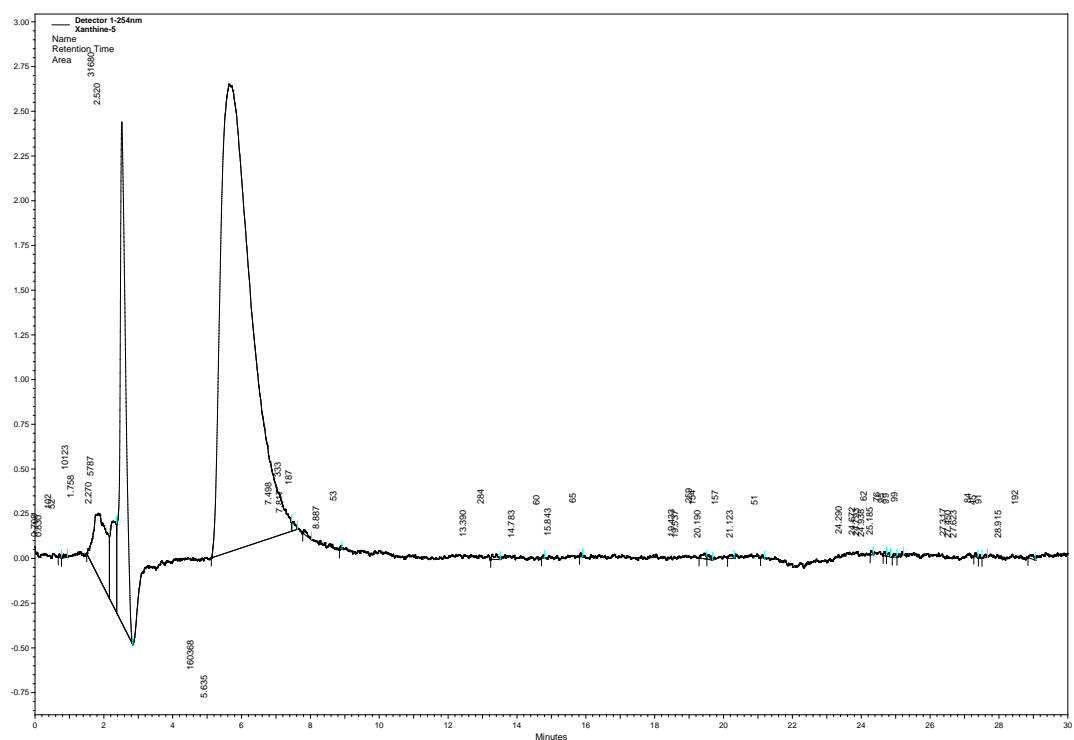


Figure 2.20: Riboflavin run with 5 mM ammonium formate in acetonitrile/water (90:10) on a Kromasil 60 column.

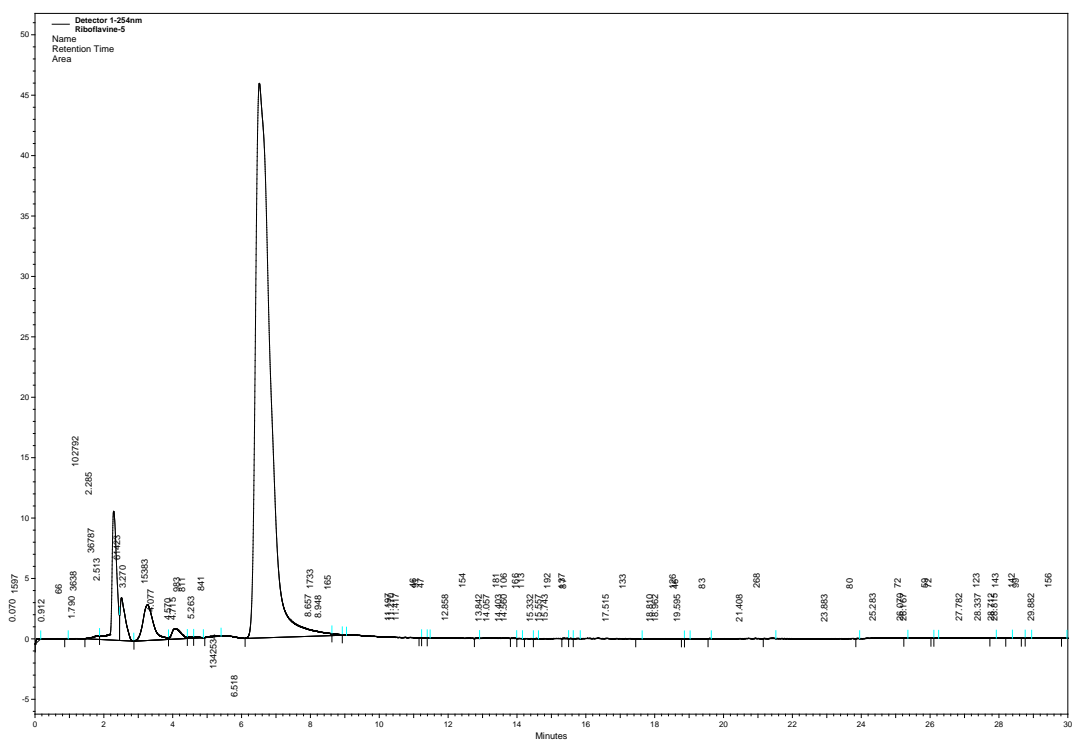


Figure 2.21: Nicotinic acid run with 10 mM ammonium formate in acetonitrile/water (90:10) on a Kromasil 60 column.

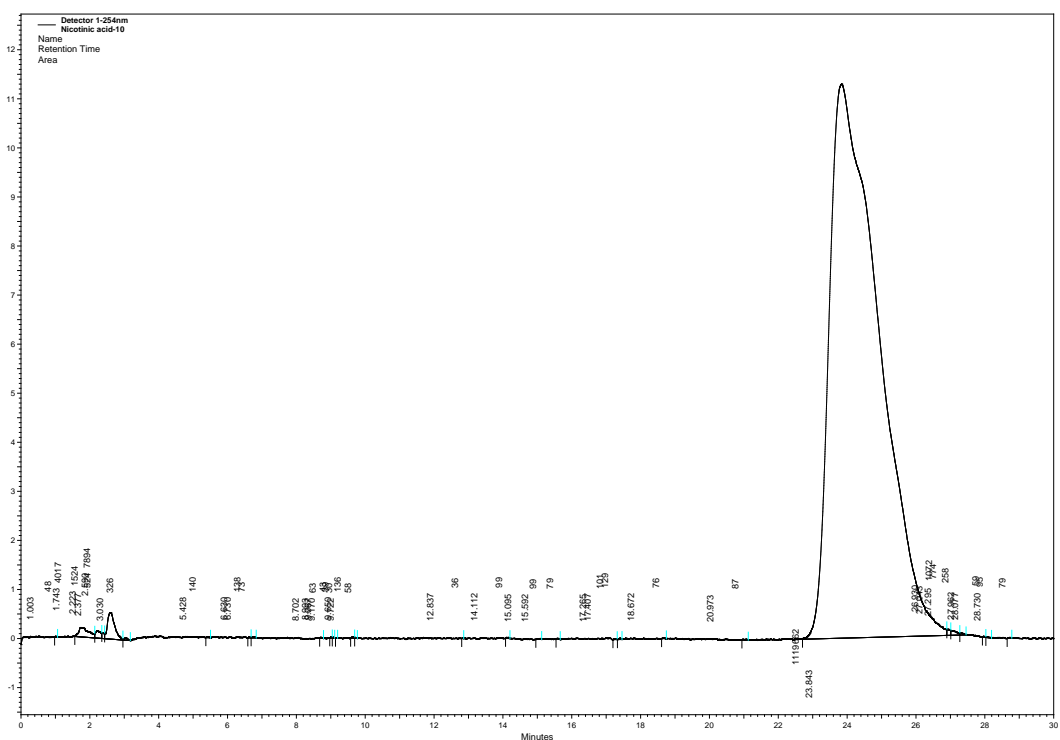


Figure 2.22: Maleic acid run with 10 mM ammonium formate in acetonitrile/water (90:10) on a Kromasil 60 column.

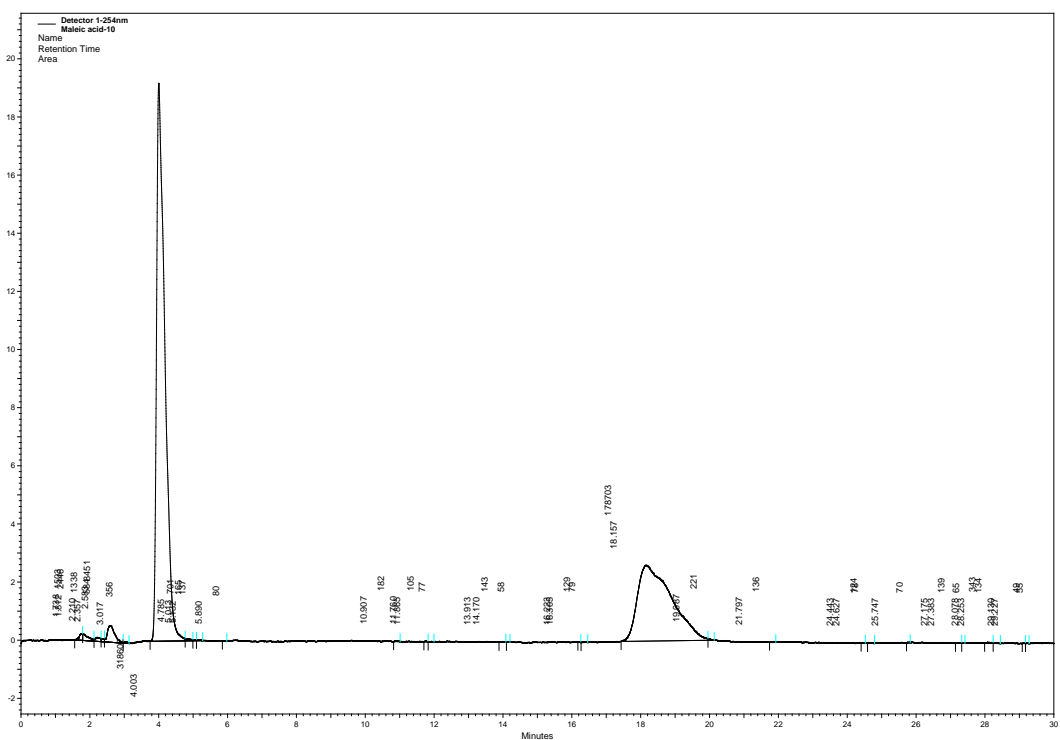


Figure 2.27: Maleic acid run with 20 mM ammonium formate in acetonitrile/water (90:10) on a Kromasil 60 column.

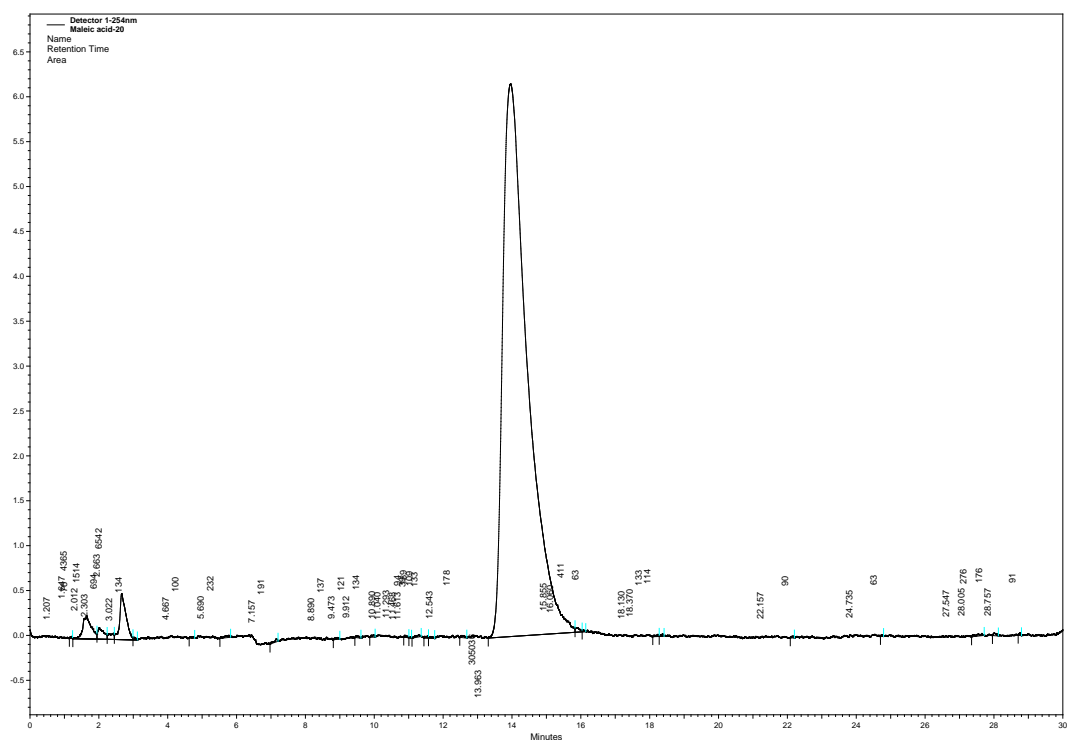
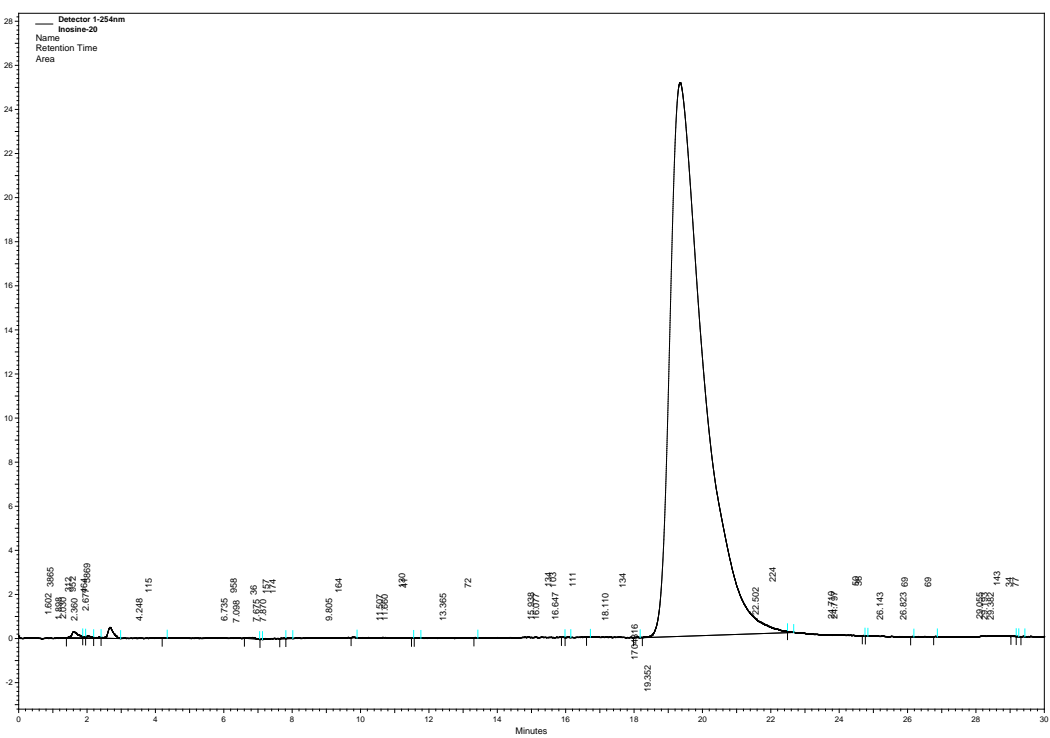


Figure 2.28: Inosine run with 20 mM ammonium formate in acetonitrile/water (90:10) on a Kromasil 60 column.



2.4.3 Retention of Test Probes on a Kromasil Column with Ammonium Bicarbonate as the Mobile phase modifier

Table 2.7: Mean retention times of the test probes under different strengths of ammonium bicarbonate mobile phase modifier.

Compound	t_R at 5 mM	t_R at 10 mM	t_R at 20 mM
Nicotinic acid	2.60	3.87	5.15
Riboflavin	7.51	8.57	9.78
Xanthine	4.83	5.83	7.57
Inosine	9.05	10.84	13.11
Ketoprofen	1.8	2.3	2.5
Maleic acid	1.54	2.35	4.92
Hydroxybenzoic acid	2.2	3.0	4.3
Toluene	1.9	1.8	1.9
Pentylbenzene	1.8	1.8	1.8

Table 2.6 shows the retention times for the test probes run on the Kromasil column with different strengths of ammonium bicarbonate in the mobile phase. Figures 2.31-2.36 show chromatograms for nicotinic and inosine run on the Kromasil column at 5, 10 and 20 mM ammonium bicarbonate in acetonitrile/water (95:5). When ammonium bicarbonate is used as the mobile phase, the retention times of all of the acids are very short. This indicates at the pH of ammonium carbonate (*ca* 8.0) both the silica gel and the acids are completely ionised so that there is strong charge repulsion. Even at the highest concentration of ammonium bicarbonate charge repulsion prevents the acids from retaining to any great extent. The increases in retention of xanthine and inosine indicate that increasing concentration of ammonium bicarbonate increases the thickness of the water layer but this is not reflected in the case of the acids. The most strongly retained neutral probe inosine is only retained to about half the extent in comparison with its retention when ammonium acetate and ammonium formate as used as modifiers. This suggests that ammonium bicarbonate does not promote the formation of a water layer as much as the other two modifiers. This might be due to a tendency of the ammonium bicarbonate to dissociate into ammonium and carbonic acid since both ions at pH 8.0 are not far from their pKa values. This would reduce the

concentration of ions available for promoting the formation of an aqueous layer on the surface of the silica gel.

Figure 2.31 Nicotinic acid run with 5 mM ammonium bicarbonate in acetonitrile/water (90:10) on a Kromasil 60 column.

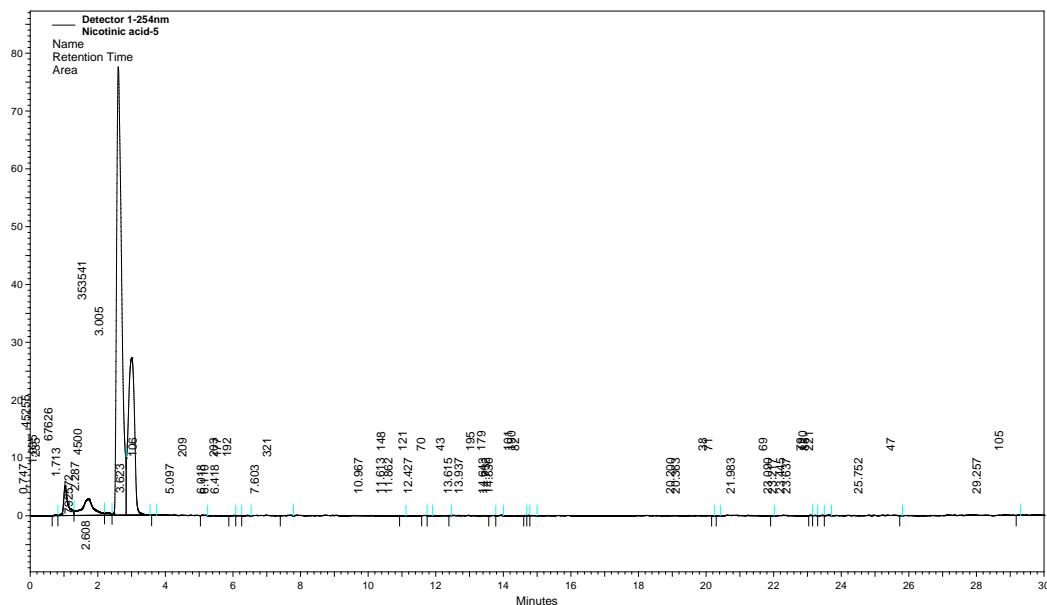


Figure 2.16: Nicotinic acid run with 10 mM ammonium bicarbonate in acetonitrile/water (90:10) on a Kromasil 60 column

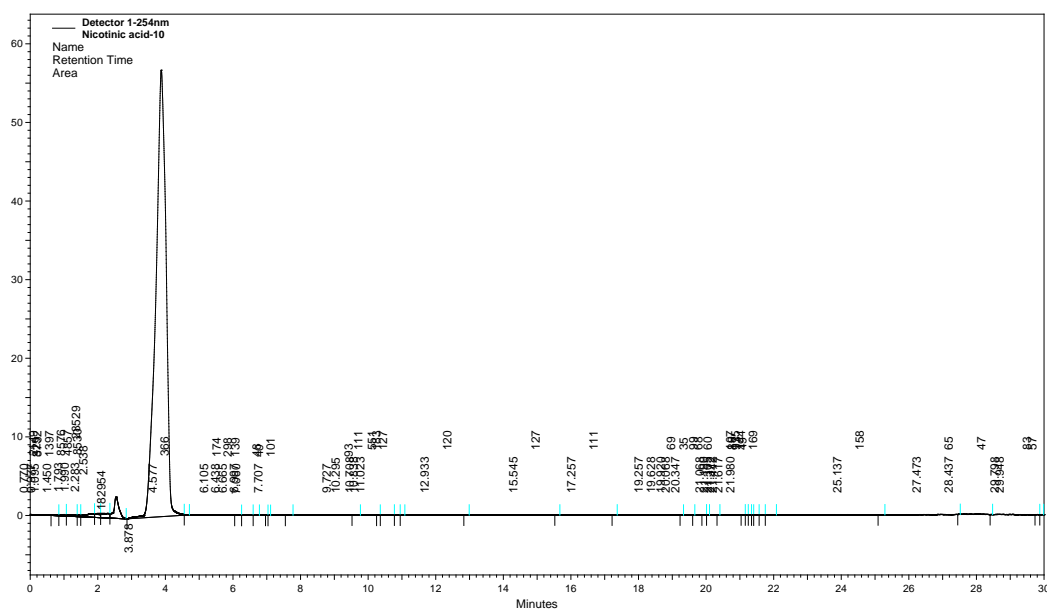


Figure 2.17: Nicotinic acid run with 20 mM ammonium bicarbonate in acetonitrile/water (90:10) on a Kromasil 60 column.

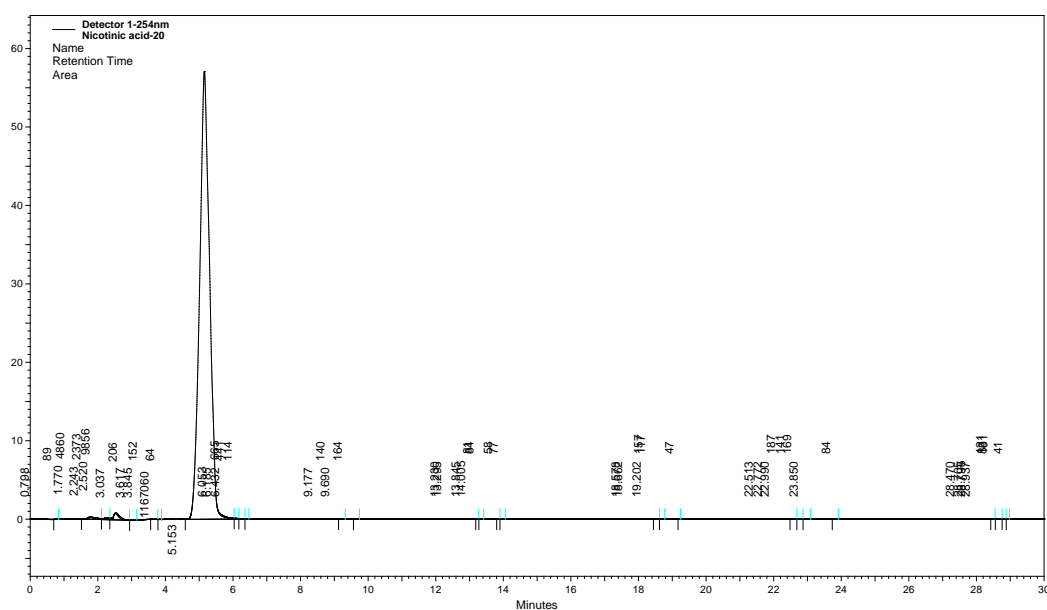


Figure 2.18: Inosine run with 5 mM ammonium bicarbonate in acetonitrile/water (90:10) on a Kromasil 60 column

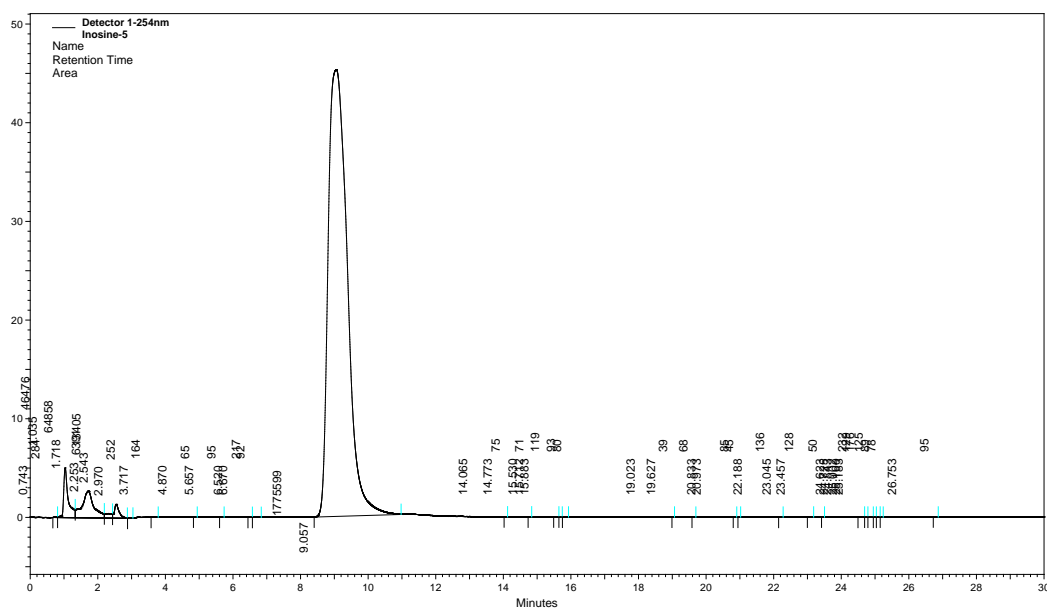


Figure 2.19: Inosine run with 10 mM ammonium bicarbonate in acetonitrile/water (90:10) on a Kromasil 60 column

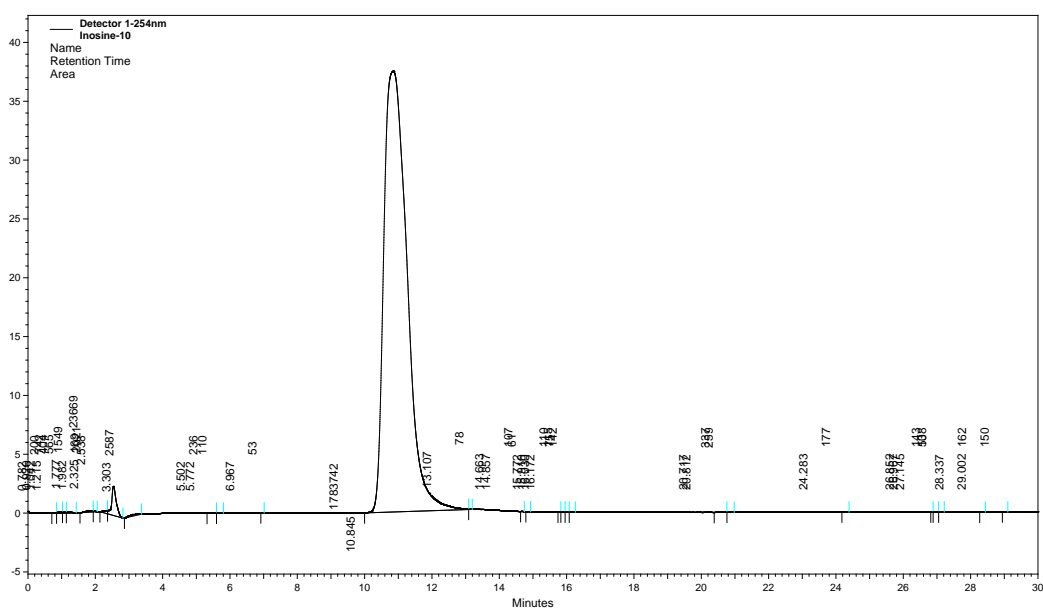
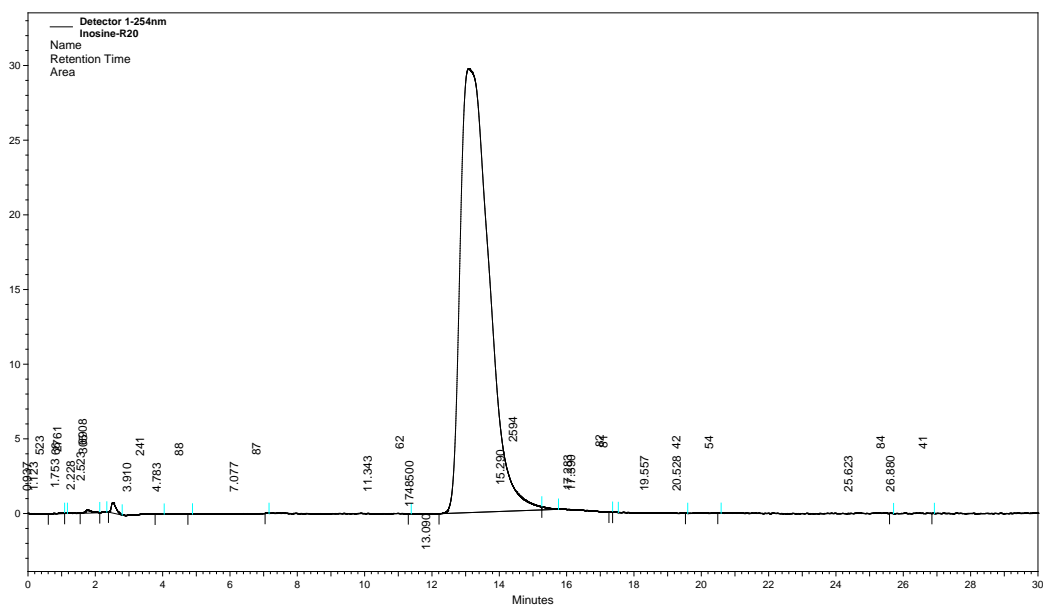


Figure 2.20: Inosine run with 20 mM ammonium bicarbonate in acetonitrile/water (90:10) on a Kromasil 60 column.



2.4.4 Retention of Test Probes on a Kromasil Column with Ammonium Chloride as the Mobile phase modifier

Table 2.8: Mean retention times of the test probes under different strengths of ammonium chloride mobile phase modifier.

Compound	5mM	10mM	20mM
Nicotinic acid	7.8	6.3	5.8
Riboflavin	4.6	4.9	5.3
Pentylbenzene	4.7	1.8	5.2
Xanthine	4.7	3.6	5.3
Inosine	4.7	5.5	5.3
Toluene	4.7	1.9	5.2
Ketoprofen	2.0	2.0	2.0
Maleic acid	(18.5)	3.1	3.5
Hydroxybenzoic acid	2.1	2.1	2.1

Table 2.7 shows the retention times for the test probes run on the Kromasil column with different strengths of ammonium chloride in the mobile phase. Figures 2.31-2.36 show chromatograms for maleic acid, nicotinic and inosine run on the Kromasil column at 5, 10 and 20 mM ammonium chloride in acetonitrile/water (95:5). Ammonium chloride produces a low pH of 4.5 and thus neither the acids nor the silica gel are extensively ionised at this low pH. This both reduces the hydrophilicity of the acids and the thickness of the water layer since less water binds to the unionised silica gel surface and the retention times of the acids are short. The neutral compounds are not strongly retained either indicating that the water layer on the surface of the silica gel is not thick. Thus working at such a low pH is not really suitable for producing HILIC interactions on silica gel.

Figure 2.21: Nicotinic acid run with 5 mM ammonium chloride in acetonitrile/water (90:10) on a Kromasil 60 column.

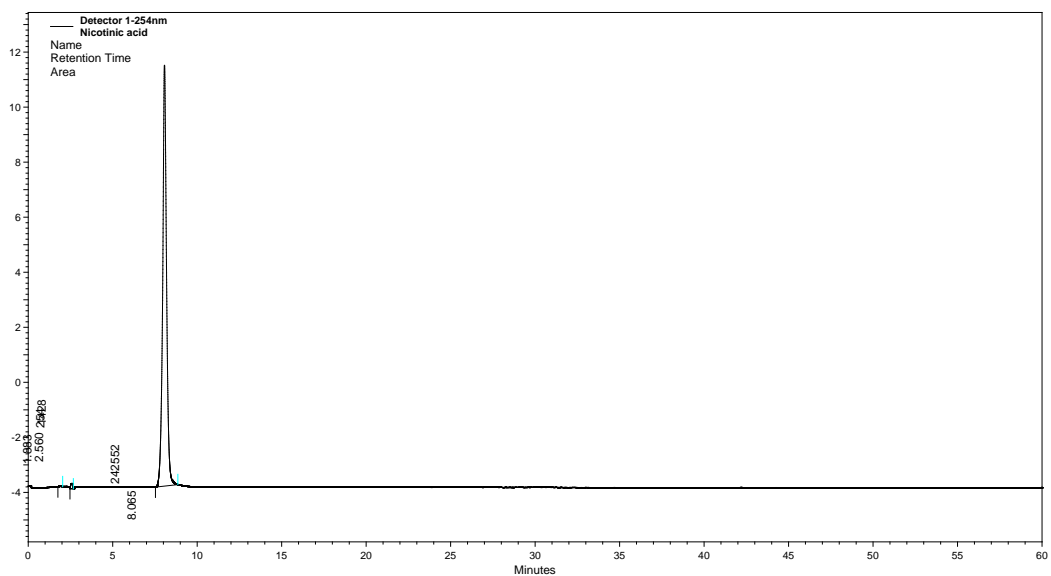


Figure 2.22: Maleic acid run with 5 mM ammonium chloride in acetonitrile/water (90:10) on a Kromasil 60 column.

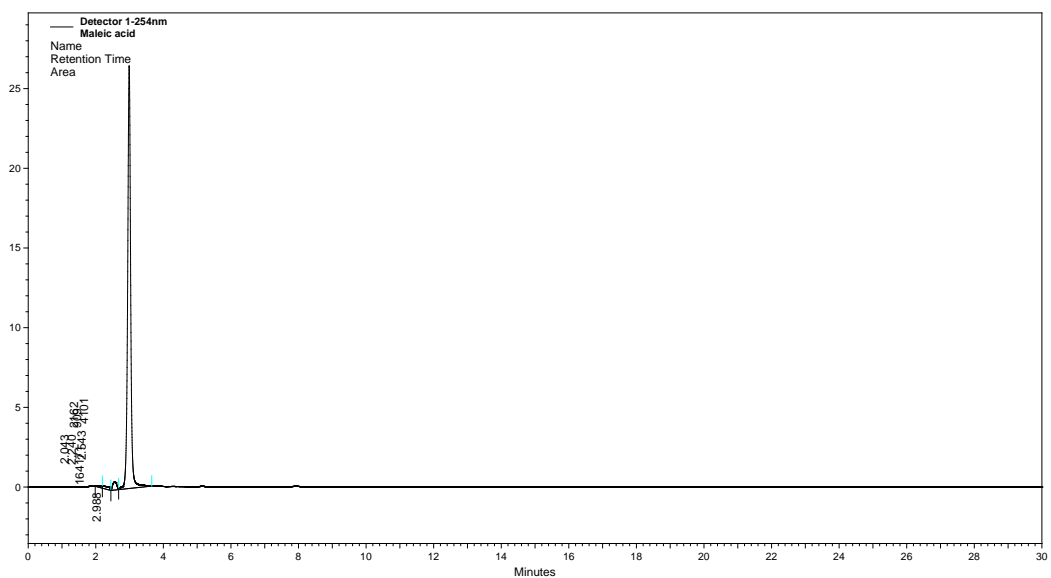


Figure 2.23: Nicotinic acid run with 10 mM ammonium chloride in acetonitrile/water (90:10) on a Kromasil 60 column.

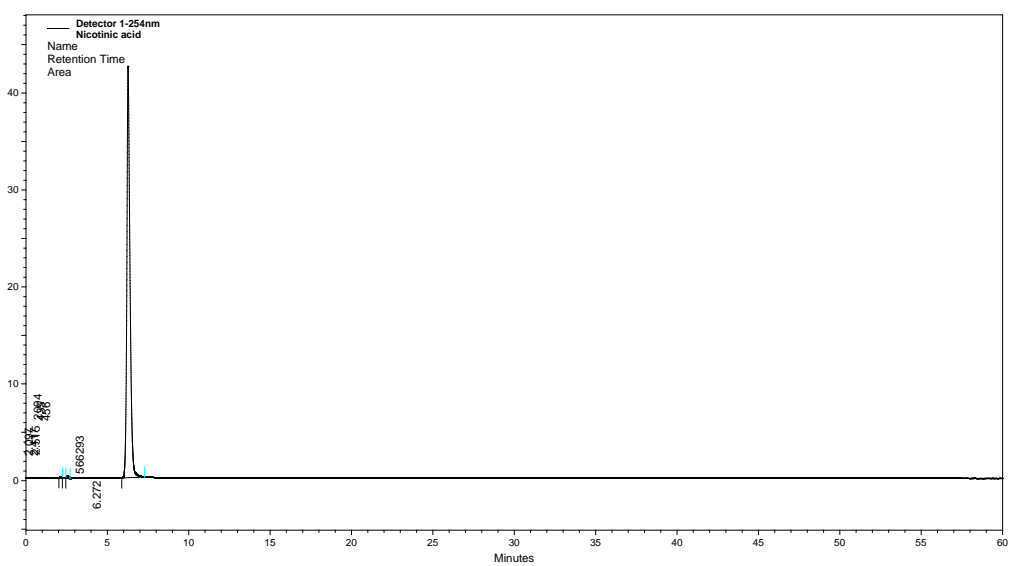


Figure 2.24: Maleic acid run with 10 mM ammonium chloride in acetonitrile/water (90:10) on a Kromasil 60 column.

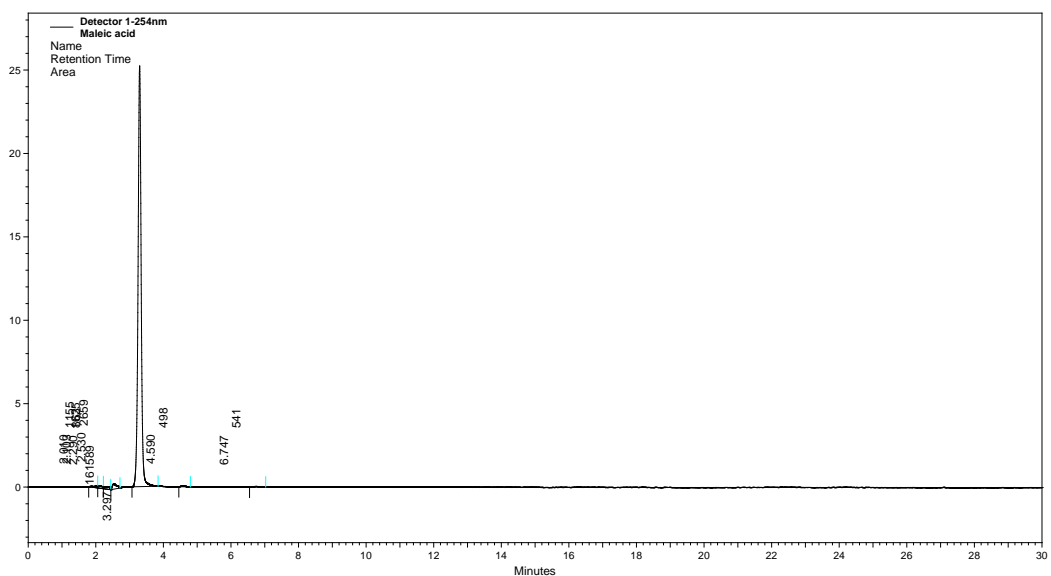


Figure 2.41: Nicotinic acid run with 20 mM ammonium chloride in acetonitrile/water (90:10) on a Kromasil 60 column.

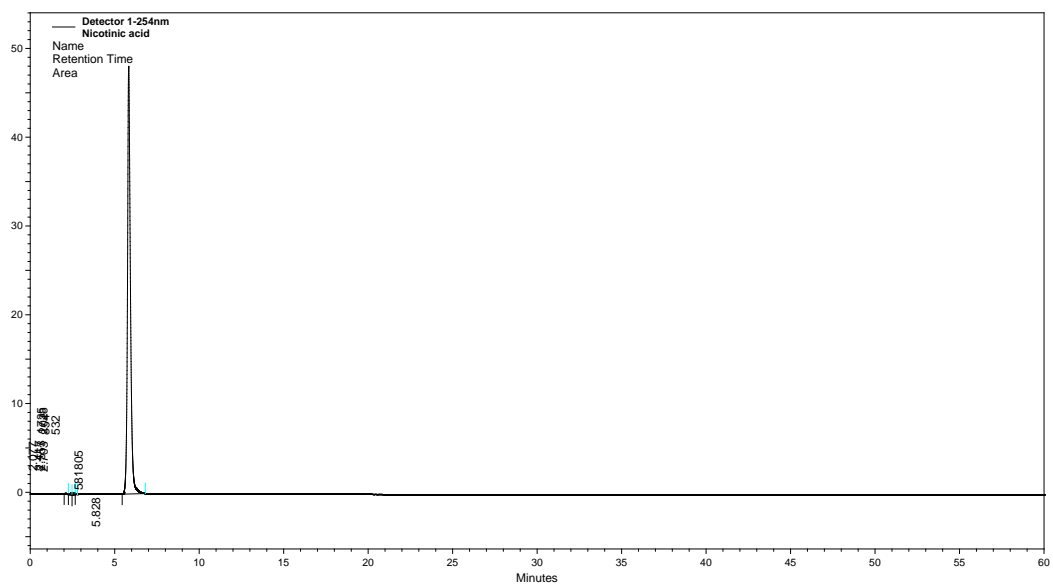


Figure 2.42: Inosine acid run with 20 mM ammonium chloride in acetonitrile/water (90:10) on a Kromasil 60 column.

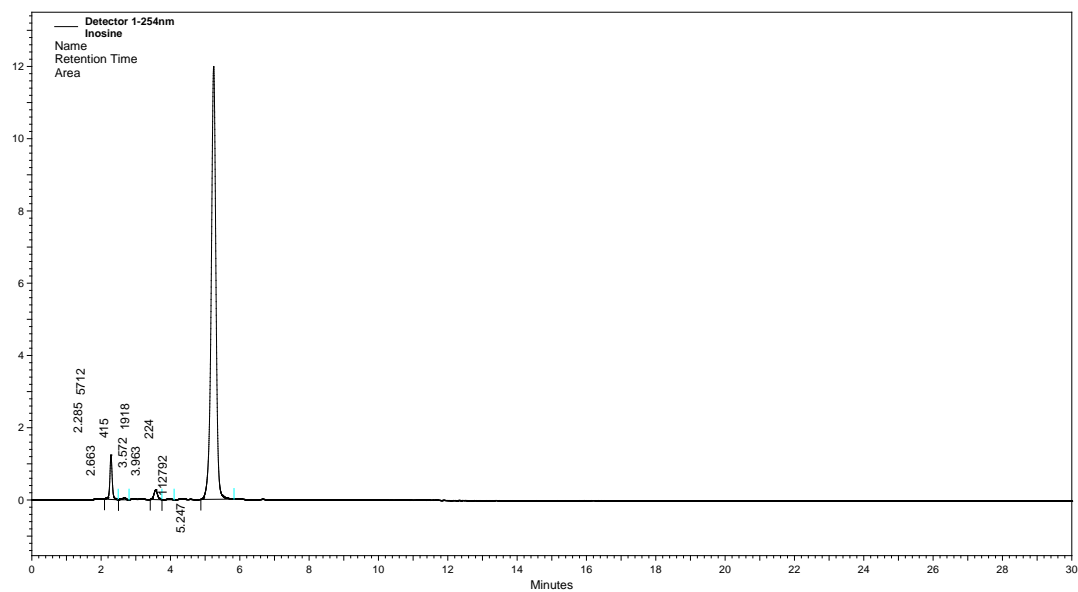
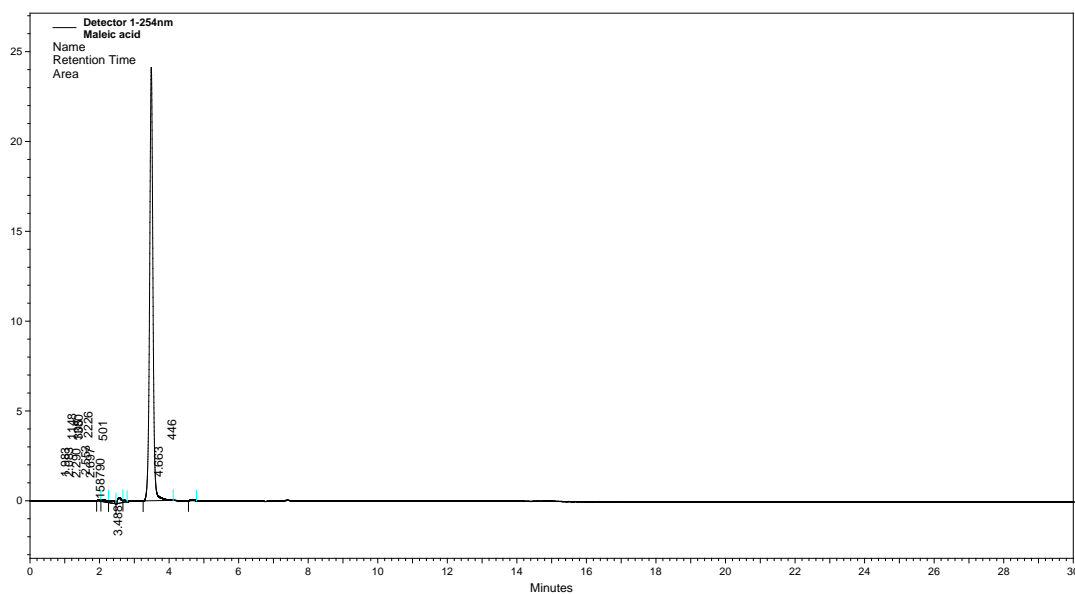


Figure 2.43: Maleic acid run with 20 mM ammonium chloride in acetonitrile/water (90:10) on a Kromasil 60 column.



2.4.5 Retention of Test Probes on a Kromasil Column with Ammonium Propionate As the Mobile phase modifier

Table 2.9: Mean retention times of the test probes under different strengths of ammonium propionate mobile phase modifier.

Compound	Rt at 5 mM	Rt at 10 mM	Rt at 20 mM
Nicotinic acid	13.9	16.5	18.2
Riboflavin	6.1	7.5	9.8
Xanthine	8.7	6.2	9.0
Inosine	7.7-9.2	5.6-6.3	3.6
Ketoprofen	5.3	6.1	6.1
Maleic acid	3.6	6.8	18.6
Hydroxybenzoic acid	7.0	9.0	11.8
Toluene	1.9	1.9	1.8
Pentylbenzene	1.8	1.8	1.8

Table 2.8 shows the retention times for the test probes run on the Kromasil column with different strengths of ammonium chloride in the mobile phase. Figures 2.44-2.51 show chromatograms for maleic acid, nicotinic and inosine run on the Kromasil column at 5, 10 and 20 mM ammonium propionate in acetonitrile/water (95:5). Propionic acid has almost the same pK_a value as acetic acid and thus adjusting it to the pH of ammonium acetate (6.9) should produce a similar ionic strength. The modifier should thus produce a similar effect to ammonium acetate but since the solvation energy for propionate is lower than that of acetate then the concentration of ammonium propionate in aqueous phase might be relatively lower and thus the water layer produced on the silica gel surface will be thinner. Both maleic acid and nicotinic acid, although they are quite well retained, have shorter retention times when ammonium propionate is used as a modifier in comparison with when ammonium acetate is used which fits the theory that the ammonium propionate partitions less into the aqueous layer. In addition the partitioning of the neutral compounds riboflavin and xanthine is lower again supporting the hypothesis of lower partitioning of ammonium propionate in comparison with ammonium acetate thus a thinner water layer.

Figure 2.44: Nicotinic acid run with 5 mM ammonium propionate in acetonitrile/water (90:10) on a Kromasil 60 column.

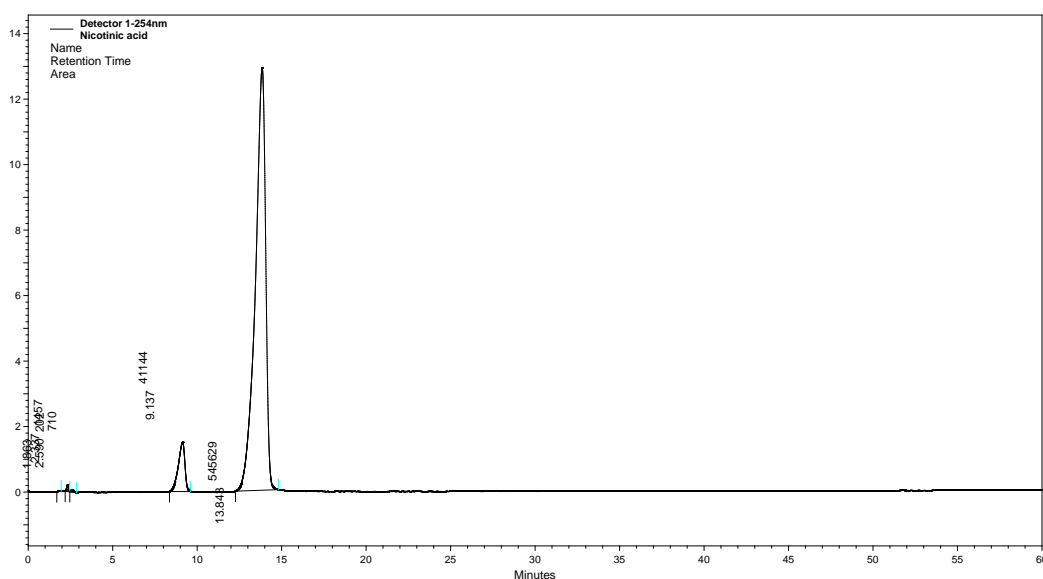


Figure 2.47: Nicotinic acid run with 10 mM ammonium propionate in acetonitrile/water (90:10) on a Kromasil 60 column.

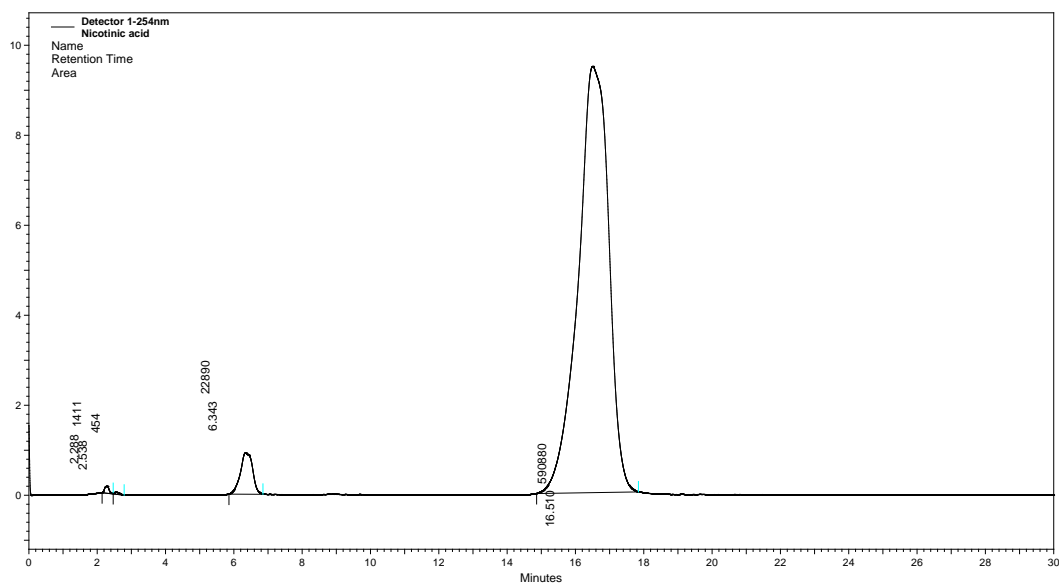


Figure 2.48: Inosine run with 10 mM ammonium propionate in acetonitrile/water (90:10) on a Kromasil 60 column.

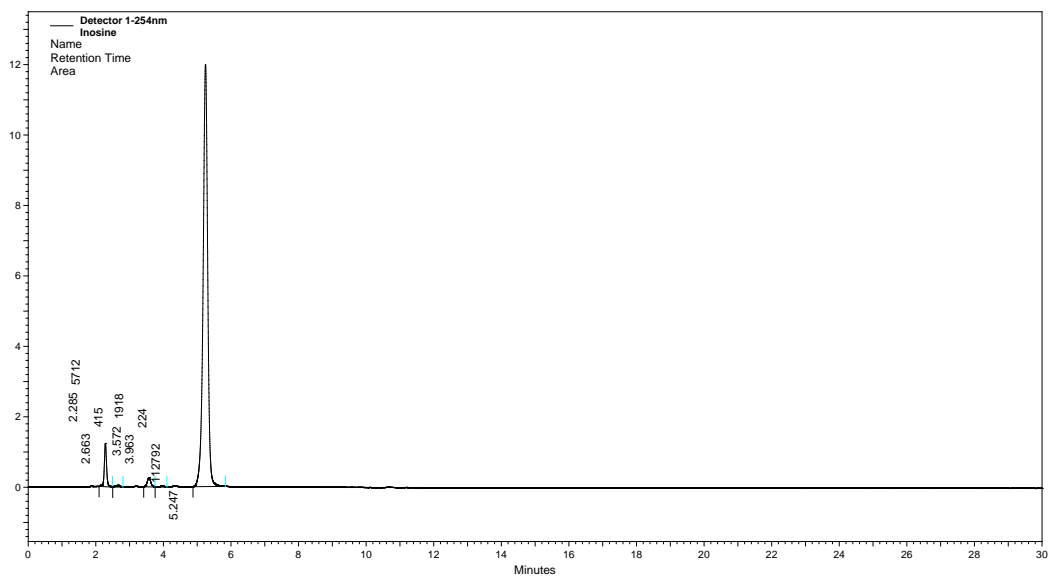


Figure 2.49: Nicotinic acid run with 20 mM ammonium propionate in acetonitrile/water (90:10) on a Kromasil 60 column.

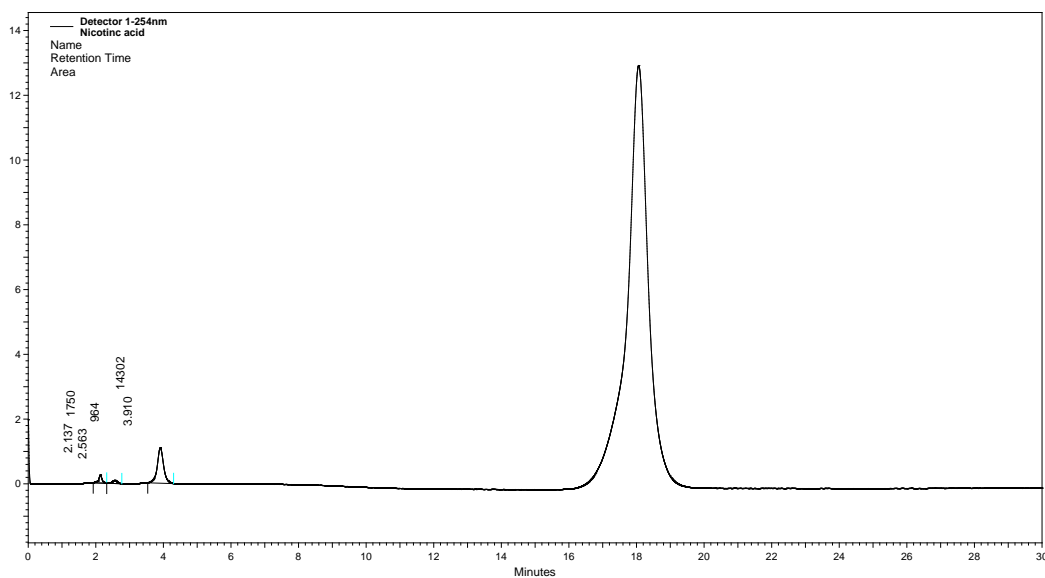


Figure 2.50: Maleic acid run with 20 mM ammonium propionate in acetonitrile/water (90:10) on a Kromasil 60 column.

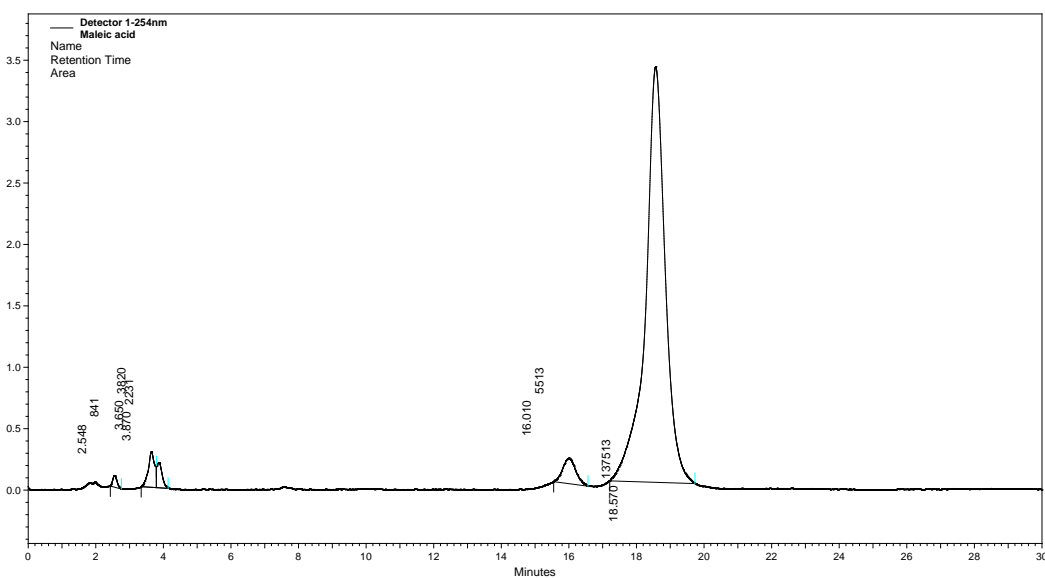
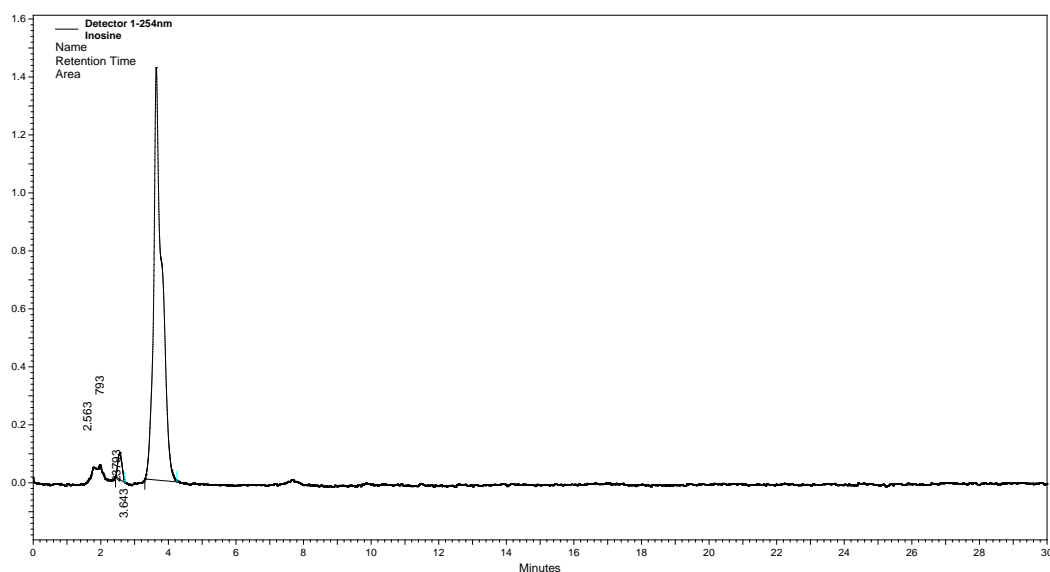


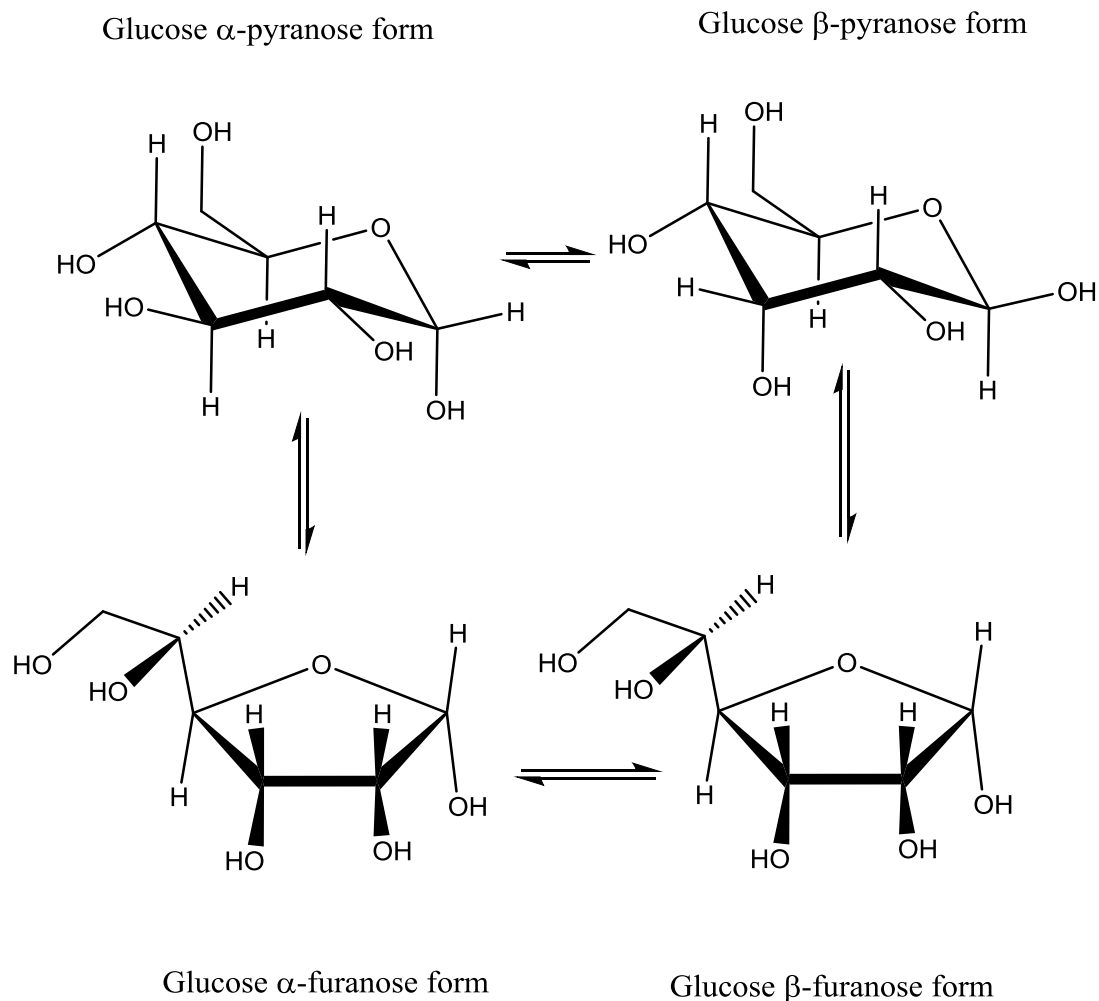
Figure 2.51: Inosine run with 20 mM ammonium propionate in acetonitrile/water (90:10) on a Kromasil 60 column.



2.5 Separation of Sugars Using a Kromasil 60 Column with LC-MS Detection

Having gained some insight into the factors governing retention of neutral and acidic compounds on Kromasil, the column was applied in an attempt to separate sugars. The ability to separate sugar isomers by hydrophilic interaction chromatography would be very useful in metabolomics studies. The separation of sugars is challenging. Taking glucose as an example, it can be seen in Figure 2.52 that glucose can exist in four different configurations, the α - and β -forms of the furanose and pyranose forms, of which are all in equilibrium with each other. This leads to chromatographic peak broadening and thus poor separation of different sugar isomers.

Figure 2.25: The structure of glucose showing the α - and β -furanose and pyranose forms respectively. The linear form of glucose makes up just less than 3% of glucose molecules in solution with the rest being cyclic. Up 99% of the pyranose forms are in solution, of which 36% is the α -anomer, while 64% is the β -anomer.



Sugars cannot be detected by using UV detection thus mass spectrometry was used to analyse the sugars in negative ion mode. Figures 2.53 and 2.54 show the extracted ion chromatograms for glucose, mannose, galactose and fructose on Kromasil column indicating peak broadening and no difference in retention times. The performance of the method was better when ammonium acetate was used as the mobile phase modifier probably because the equilibrium between the four forms of the sugars is more rapid at the higher pH of ammonium acetate. However, there is no difference in the retention times of the four common hexose isomers.

Figure 2.53: Kromasil 60-5SIL column with mobile phase (A) H₂O: methanol (95:5) containing 20mM ammonium acetate and mobile phase (B) ACN:water (95:5) containing 20 mM ammonium acetate in negative ion ESI mode. The gradient conditions were 0 min A: B (90:10) and at 30 min A: B (50:50) at a flow rate of 0.6 ml/min. Detection was with an Orbitrap Exactive instrument. The extracted ion traces are for the masses of the negative ions of each of the sugars.

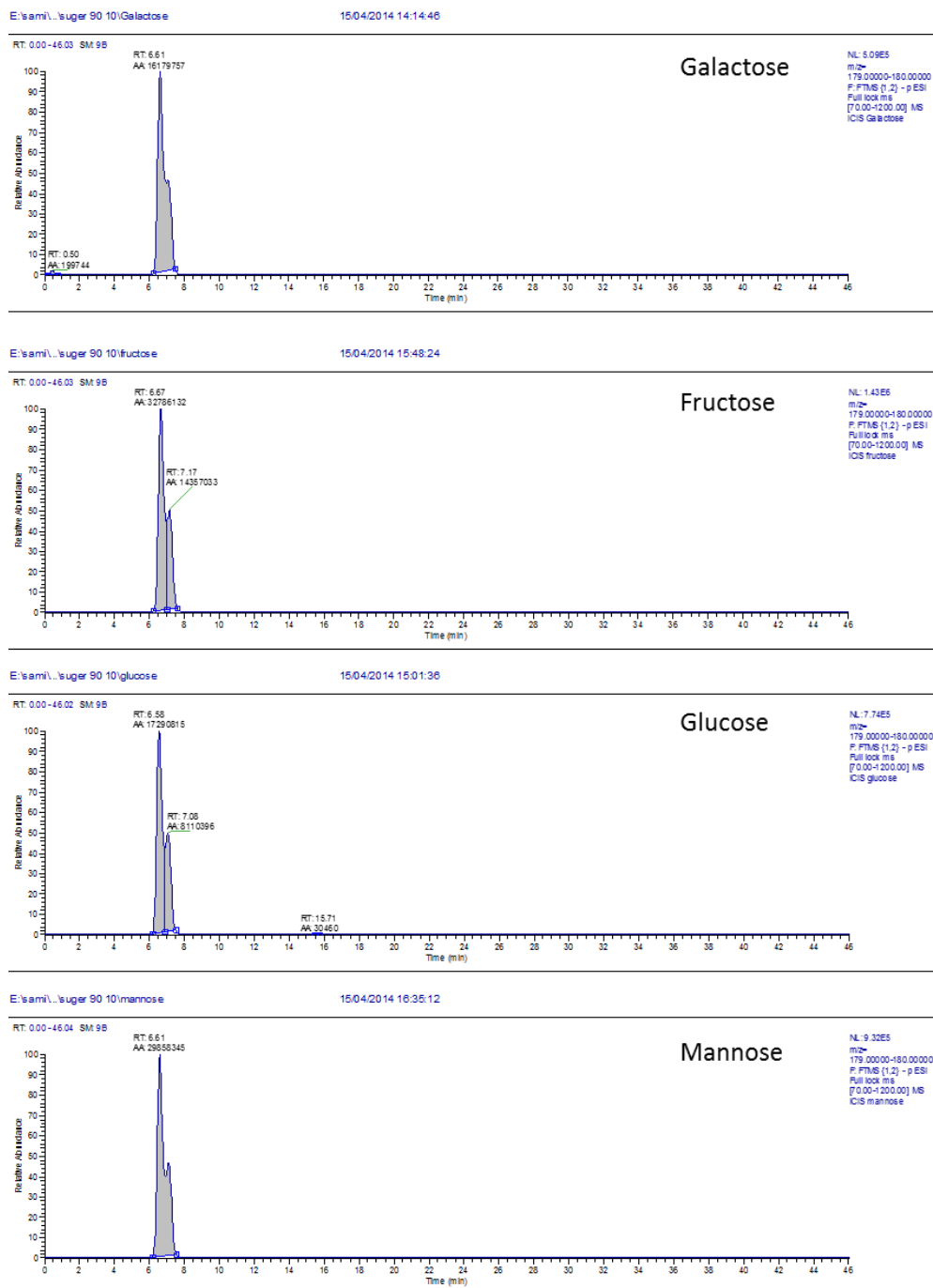
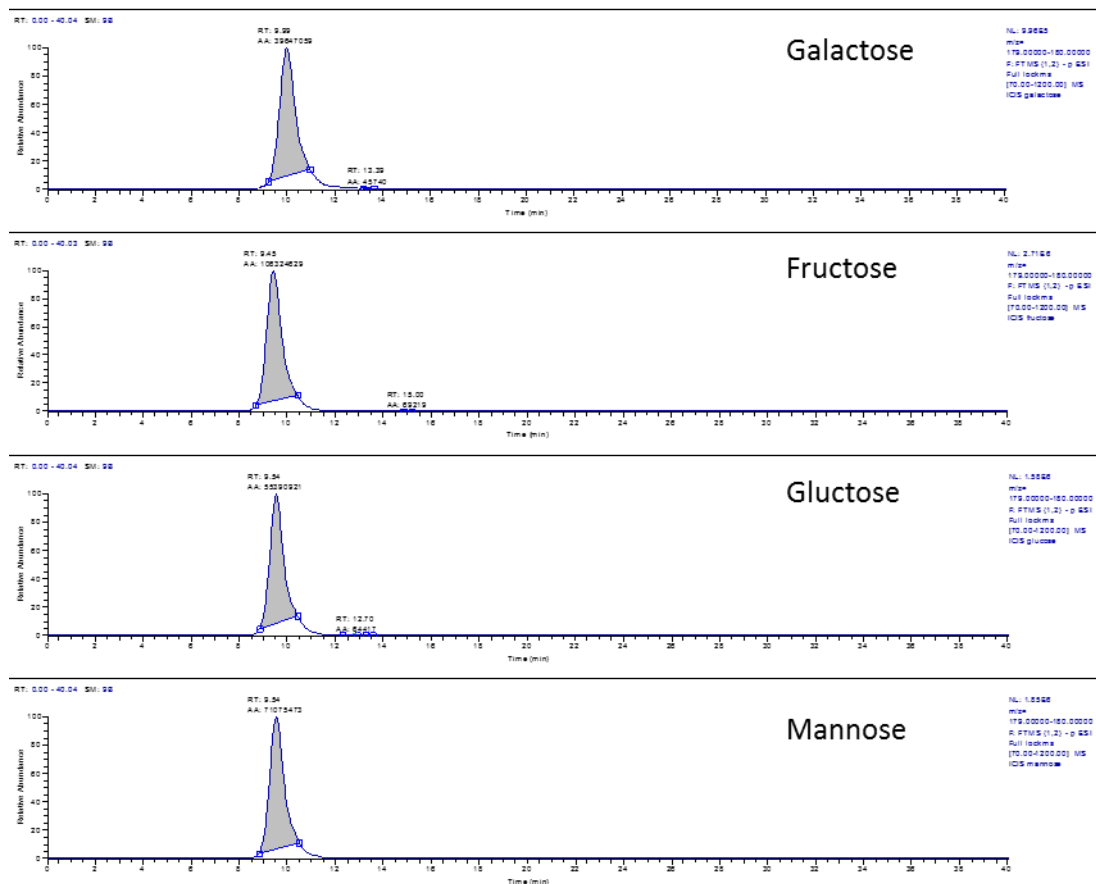


Figure 2.54: Kromasil 60-5SIL Column with mobile phase (A) H₂O: methanol (95:5) containing 20mM ammonium acetate and mobile phase (B) ACN: water (95:5) containing 20 mM ammonium acetate in negative ion ESI mode. The samples were run isocratically with mobile phase A:B (20:80) for 40 min at a flow rate of 0.6 ml/min.

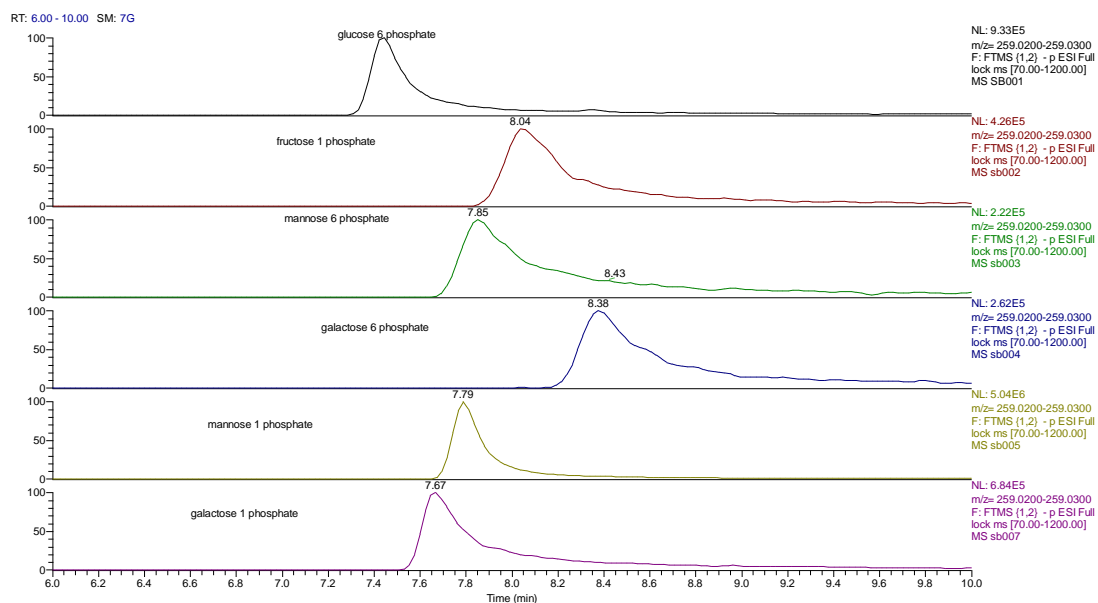


2.6 Application of a Nucleodur core shell column to separation of sugars

There was not much evidence that silica gel would be able to separate neutral sugars by hydrophilic interaction chromatography. Recently a new column has appeared in the Nucleodur series of columns which has a zwitterionic coating like that of ZIC-HILIC but is available in core shell format with a particle size of 2.5 μm . Core shell particles have a reduced pore volume offering a reduced back pressure in comparison with porous particles enabling a smaller particle size to be used without increases in back pressure. The reduced pore volume also offers a reduction in mass transfer effects and thus reduced contribution from mass transfer (C term) in the van Deemter equation. The sugar phosphates are important in biological systems since many of them are involved in glycolysis. The phosphates do not produce good chromatography on silica gel because their high negative charge causes them to be repelled from the negatively charged surface and peak shapes are

often poor. Figure 2.55 shows the chromatography of six sugar phosphates on the Nucleodur core shell column. The chromatographic peak shapes are quite good but there is not much chromatographic separation between the sugars. However, there is evidence of a systematic separation between the 1- and 6-phosphates.

Figure 2.26: Extracted ion traces (negative ion m/z 259.02-259.03) showing the chromatography of sugar phosphates on a Nucleodur hydrophilic interaction column (150 x 4.6 mm, 2.5 μ m). Mobile phase A 0.1% formic acid in water B 0.1% formic acid in ACN. Gradient: 80-20% B (0-30 min); flow rate: 0.3 ml/min.



The chromatography of the neutral sugars on the Nucleodur column is shown in Figure 2.55. There was again not a strong separation between the four common neutral hexoses and galactose and mannose have double peaks which result from the equilibrium shown in figure 2.56. Fructose produces a good peak shape suggesting that the equilibration between its different forms is more rapid than for the aldoses. Fructose cannot form a pyranose and only forms α - and β -furanoses.

Figure 2.27: Extracted ion traces (m/z 179.05-179.06 negative ion) showing separation of sugars on a Nucleodur hydrophilic interaction column (150 x 4.6 mm, 2.5 μ m). Mobile phase A 0.1% formic acid in water B 0.1% formic acid in ACN. Gradient: 80-20% B (0-30 min); flow rate: 0.3 ml/min.

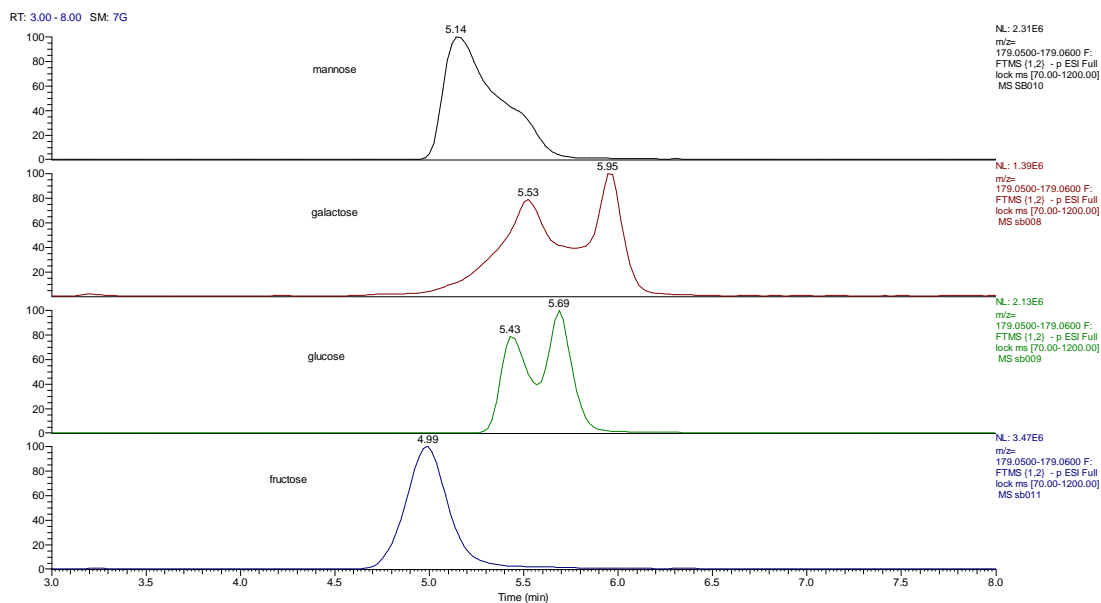


Figure 2.57 shows the chromatography of the sugar phosphates on the Nucleodur column with ammonium acetate as the mobile phase modifier rather than formic acid. The ammonium acetate raises the pH of the mobile phase promoting ionisation of the phosphates and of the surface of the stationary phase. The sugar phosphates retain longer with the higher pH mobile phase but the peak shapes are poor, possibly due to increased ionic repulsion and there is not much evidence of separation between the different phosphates.

Figure 2.28: Extracted ion traces (m/z 259.02-259.03 negative ion) showing separation of sugar phosphates on a Nucleodur hydrophilic interaction column (150 x 4.6 mm, 2.5 μ m). Mobile phase A 20 mM ammonium acetate in water B ACN. Gradient: 80-20% B (0-30 min); flow rate: 0.3 ml/min.

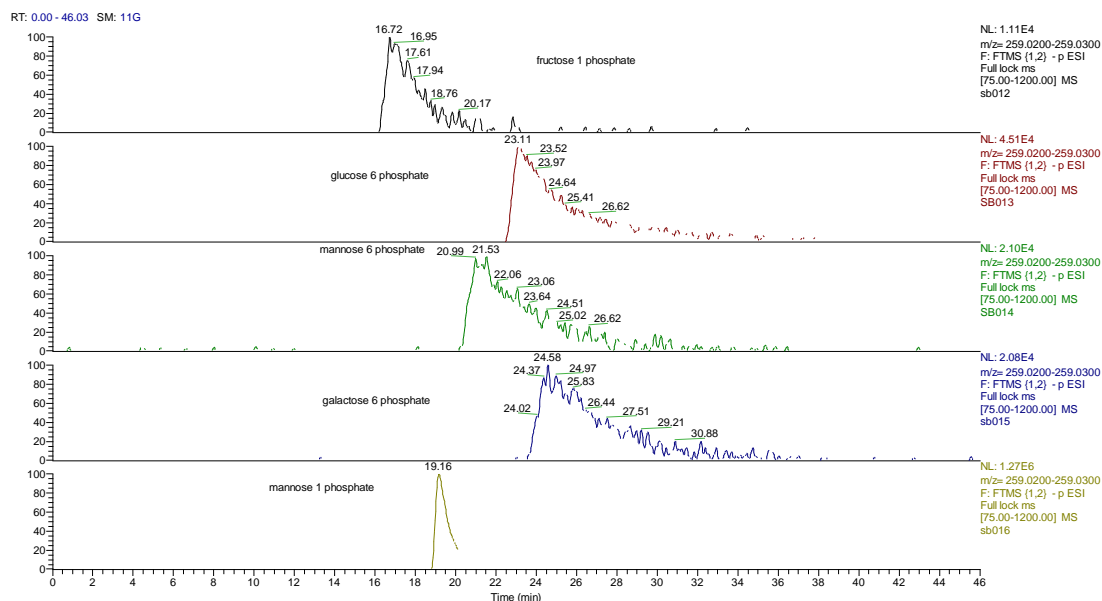


Figure 2.58 shows the separation of the common neutral sugars on the Nucleodur column with ammonium acetate as the mobile phase modifier. Unlike the sugar phosphates there is no marked increase in retention with the increased pH of the mobile phase since there are no ionisable groups in the neutral sugars. However, the peak shape of mannose is improved under these conditions and this is probably due to the fact that the equilibrium between the different forms of the sugars show in figure 2.59 is faster at higher pH values. Galactose and glucose still give double peaks but with shallower valleys again indicating faster equilibration between the four forms. The more rapid the equilibration the more the peak will tend towards being a single peak. If it was possible to raise the pH enough to increase the rate of equilibration still further then there might be a chance of separating the four sugars. It is thus recommended that future studies should investigate this possibility.

Figure 2.58: Extracted ion traces (m/z 179.05-179.06 negative ion) showing separation of sugars on a Nucleodur hydrophilic interaction column (150 x 4.6 mm, 2.5 μ m). Mobile phase A 20 mM ammonium acetate in water B ACN. Gradient: 80-20% B (0-30 min); flow rate: 0.3 ml/min.

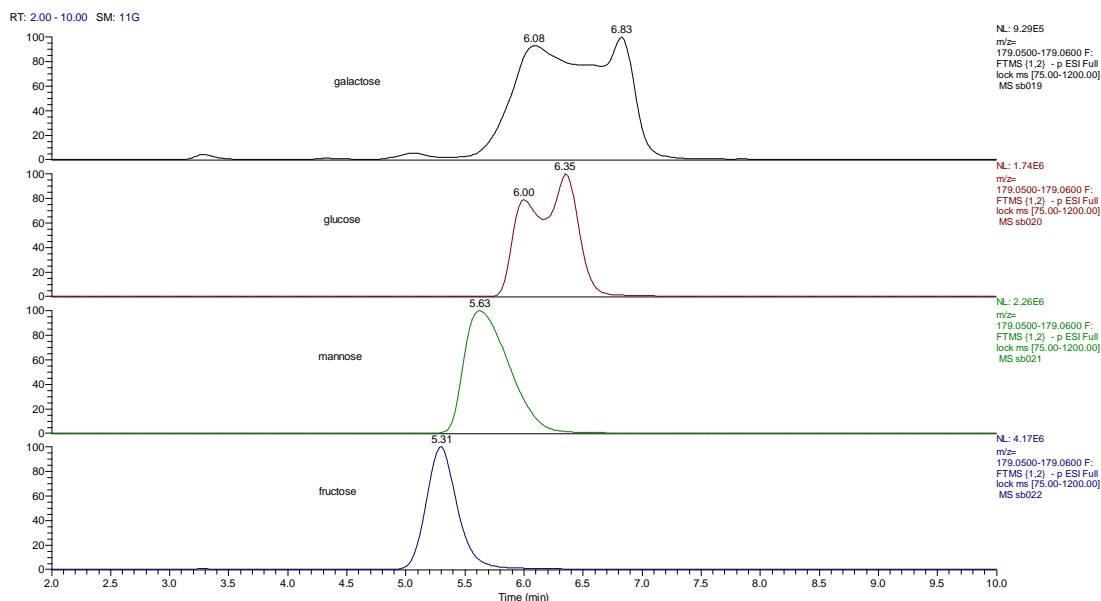


Figure 2.59 shows the chromatograms obtained for the neutral sugars on the Nucleodur column with ammonium bicarbonate as the mobile phase modifier. As predicted the equilibration between the different forms of the sugars is very rapid at this higher pH and they have formed single peaks. However, unfortunately as can be seen in figure 2.60 the retention times of the sugar phosphates were very short under the conditions where ammonium bicarbonate was used as the mobile phase modifier and this suggested that the surface coating of the column may have been removed by using the higher pH. Ammonium bicarbonate generates a pH of around 8.0 and the pH range of the column was specified as being up to 8.5. However, it would appear that the column could not tolerate a higher pH and this approach had to be abandoned. The work was resumed as described in chapter 4 where derivatisation was used as a strategy for separating sugars.

Figure 2.29: Extracted ion traces (m/z 179.05-179.06 negative ion) showing separation of sugars on a Nucleodur hydrophilic interaction column (150 x 4.6 mm, 2.5 μ m). Mobile phase A 20 mM ammonium bicarbonate in water B ACN. Gradient: 80-20% B (0-30 min); flow rate: 0.3 ml/min.

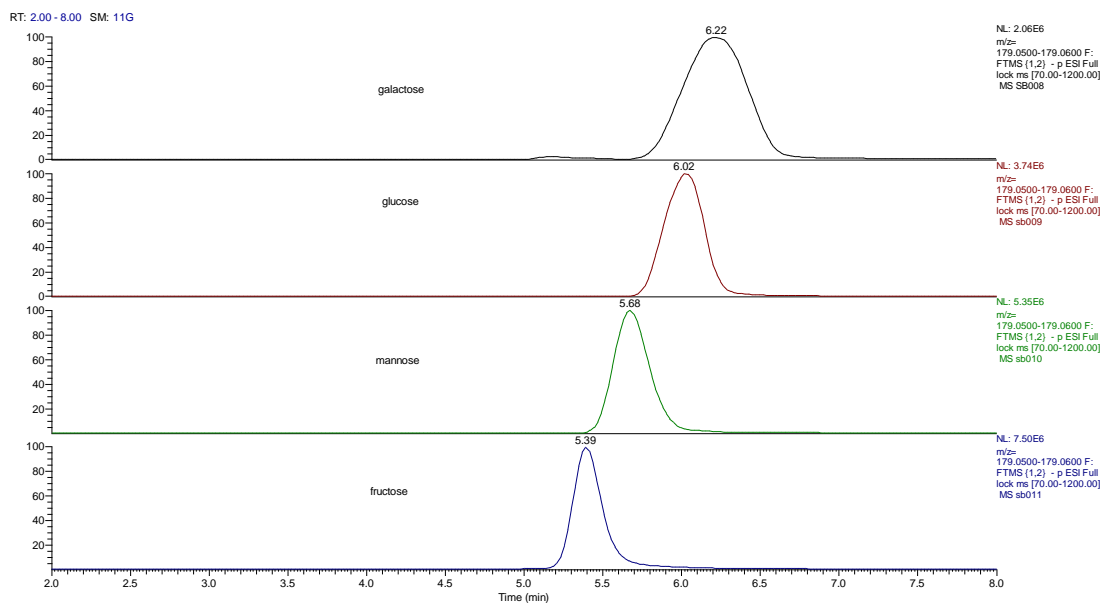
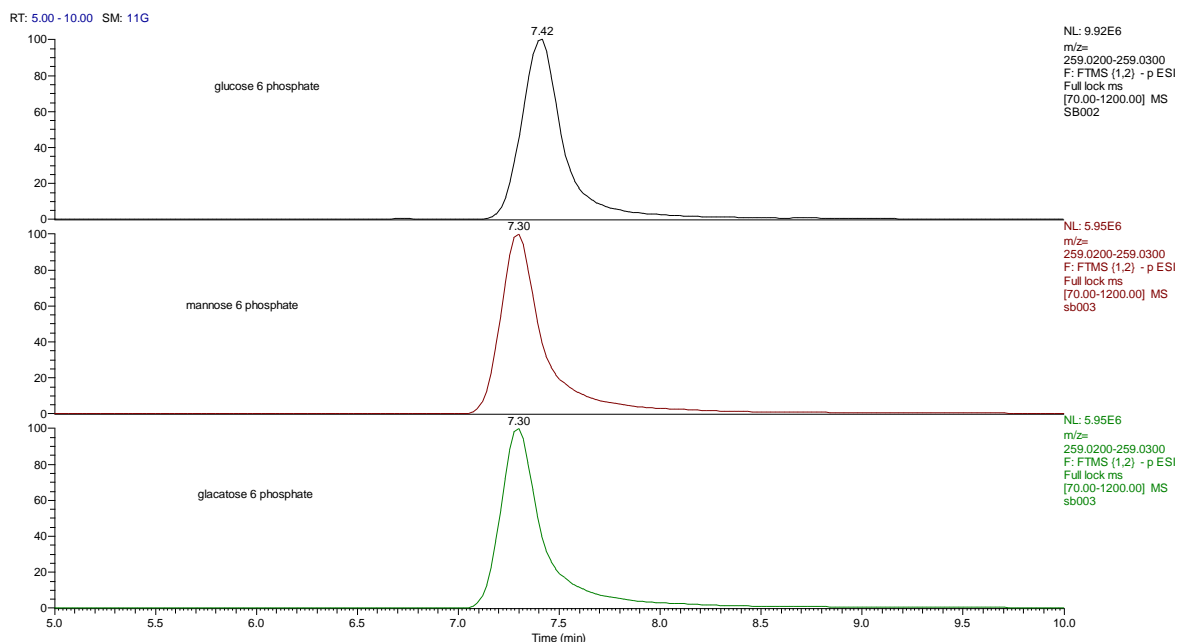


Figure 2.30: Extracted ion traces (m/z 259.02-259.03 negative ion) showing separation of sugar phosphates on a Nucleodur hydrophilic interaction column (150 x 4.6 mm, 2.5 μ m). Mobile phase A 20 mM ammonium bicarbonate in water B ACN. Gradient: 80-20% B (0-30 min); flow rate: 0.3 ml/min.



Chapter 3:

A study of the application of Cogent Hydride columns for the Chromatography of Biomolecules

3 A study of some hydride columns for the separation of biomolecules

3.1 Introduction

Silica C phases offer some interesting properties and it was of interest to see how well they could be applied in metabolomics screens. The structure of type C silica gel was reviewed in the general introduction. There are a number of different phases now commercially available and for this chapter three different phases were examined an unmodified Silica C phase, a phenyl hydride phase and a cholesterol hydride phase. Although some work has been done on these phases this has not been extensive and the aim was to evaluate whether or not these phases might be useful in metabolomics screens and it might be possible to carry out orthogonal screening on the same column using both the lipophilic and hydrophilic properties of the column.

3.2 Aims of this chapter

- a) To study the family of silicon hydride columns more closely and to apply them in metabolomics and drug purity profiling studies.
- b) To develop quantitative methods for certain key metabolites using these methods.

3.3 Materials and Methods

3.3.1 Mobile phase

The mobile phases consisted of 20 mM ammonium acetate in water (A) and acetonitrile (B).

3.3.2 Samples

The urine sample (0.2 ml) was either diluted with acetonitrile (0.8 ml) and centrifuged a 3000 g and the supernatant analysed in HILIC mode or urine (0.2 ml) was diluted with water (0.8 ml), centrifuged a 3000 g and analysed in reversed phase mode. All of the biomolecule

standards were obtained from Sigma Aldrich, Dorset, UK and prepared at 1mg/ml in methanol/water (1:1) before diluting to 10µg/ml with mobile phase starting composition in a standard mixture.

3.3.3 LC-MS Conditions

The LC-MS was carried out on an Orbitrap Exactive. The gas flows in the ESI source were sheath gas 60 (arbitrary units) and auxiliary gas 25 (arbitrary units), the capillary temperature was 275°C and the needle voltage was 4.5kV. The instrument was freshly tuned with the manufacturer's tuning standard solution with the addition of pyridine to calibrate the lower mass range. The residual caffeine peak from the tuning solution was used as a lock mass. Analyses were carried out on a Cogent Silica C, Cogent Phenyl Hydride and Cogent UDC cholesterol columns (150 x 4.6 mm x 4 µm). The mobile phase used was 10 mM ammonium acetate in water 95:5 (A) and acetonitrile (B). A flow rate of 0.3 ml/ min was used with gradient between 20% A 80% B at 0 min and 80% A 20% B at 30 min, then hold 80% A 20% B for 10 minutes (HILIC mode) followed by reinjection of the sample and return to 20% A 80% B for 30 min and hold 20% A 80% to 40 min (reversed phase mode). Standard mixtures containing 46 test compounds were used to evaluate the columns and also urine samples.

3.4 Results and Discussion

Table 3.1 shows the retention times of some selected standards run on the three hydride columns. The best coverage of the metabolites was provided by the Silica C column which produced interesting complementary retention time information when used in HILIC mode followed by reversed phase mode. For instance taurocholate (TC), highlighted in yellow (Table 3.1), is well retained in HILIC mode, although it is quite a lipophilic compound, and also displays what appears to be lipophilic interaction with the Silica C column when run in reversed phase mode, also being well retained in this mode. TC is less strongly retained in

HILIC mode on the surface modified hydride columns but exhibits strong lipophilic interaction with these columns in reversed phase mode (Figure 3.1). The efficiencies achieved for lipophilic compounds such as cholic acid on the alkyl columns were very high. The exact mechanism of interaction with the silicon hydride surface remains unclear. Figure 3.2 shows extracted ion chromatograms for acetyl carnitine analysed on three silicon hydride columns with solvent programming from high to low organic and low to high organic. Acetyl carnitine has some degree of lipophilicity but it is most strongly retained in both solvent programming modes on the Silica C column indicating the main mode of interaction in this case is with the Si-H surface rather than with bonded chains. The Silica C column also exhibits good selectivity for the isomers highlighted in blue in Table 3.1.

Table 3.1 Retention times of some standards for biomolecules on hydride columns in A HILIC mode B reversed phase mode.

Compound	Silica C A	Silica C B	UDC Chol A	UDC Chol B	Ph Hyd. A	Ph Hyd. B
Glycine	21.4	7.0	17.2	5.8	-	5.2
Pyruvate	6.7	-	4.9	-	3.8	
Alanine	21.3	7.1	16.8	5.9	14.5	5.3
β -Alanine	22.5	7.5	18.3	6.1	16.1	-
Sarcosine	21.6	7.7	17.6	6.3	15.7	5.7
3-Hydroxy butanoic	13.4	4.2	10.1	3.9	8.6	3.7
2-Hydroxy butanoic	12.7	4.2	9.6	3.9	8.4	3.7
Serine	20.3	6.8	17.1	5.7	-	5.2
Cytosine	18.0	8.5	14.3	9.5	12.5	-
Fumarate	14.3	-	10.0	3.5	-	-
Succinate	11.0	3.7	9.3	3.6	-	3.4
Betaine	24.1	11.7	20.4	10.1	19.1	6.3
Nicotinate	13.1	3.7	9.8	4.2	9.7	4.2
Picolinate	6.6	4.1	5.0	4.2	6.2	4.0
Aminolevulinate	23.1	7.9	18.6	6.4	16.4	5.5
Hydroxyproline	22.0	7.6	18.0	6.3	15.9	5.7
Malic acid	17.3	-	14.5	3.5	8.2	-
Adenine	16.4	10.5	15.0	15.2	13.8	15.1
Inosine	16.2	7.6	11.8	11.4	9.6	12.1
Phosphoethanolamine	24.6	4.5	-	4.1	-	3.7
Glutamine	21.5	7.0	17.2	5.9	14.5	5.4
Lysine	23.6	8.6	-	6.9	15.9	6.9
Guanine	16.9	7.7	13.2	12.0	9.9	12.3
Allantoin	12.2	19.4	14.2	20.8	7.4	14.0
Coumaric acid	11.1	4.1	-	5.6	6.1	5.0

Arginine	25.0	21.8	-	-	-	-
Glucosamine	16.2	6.8, 7.6	11.9 12.5	11.4	9.7,10.8	11.7,12.1
Caffeic acid	11.3	6.5	-	5.0	9.9	5.2
Fructose	13.5	-	11.0/11.2	-	5.7	-
Galactose	12.2	-	10.6	15.1	-	-
Glucose	12.4	-	10.9	-	-	-
Mannitol	16.9	6.6	12.6	5.7	10.0	5.3
Sorbitol	17.8	6.6	12.8	5.6	10.1	5.2
Hydroxy indole AA	11.5	4.1	-	5.1	-	13.6
Acetylcarnitine	28.1	15.3	24.1	13.4	22.1	13.2
Kynurenine	17.6	8.9	16.8	12.7	-	13.5
N-acetylglucosamine	12.2	6.7	10.6 12.3	6.1	9.8	6.1
N-acetylmannosamine	16.6	6.7	12.5	6.1	9.9	5.8
Adenosine	15.4	7.8	12.7	13.5	10.5	13.4
Guanosine	16.8	6.9	12.3	12.0	10.0	11.9

Methylthio adenosine	13.4	9.3	12.2	16.7	10.0	16.4
CMP	17.3	3.7	-	3.7	-	3.4
Maltose	17.6	6.4	-	11.8	9.8	11.8
Sucrose	17.4	-	-	11.7	9.7	-
AMP	17.1	3.7	-	3.8	-	-
Taurocholate	8.5	12.4	7.7	16.4	4.5	15.1

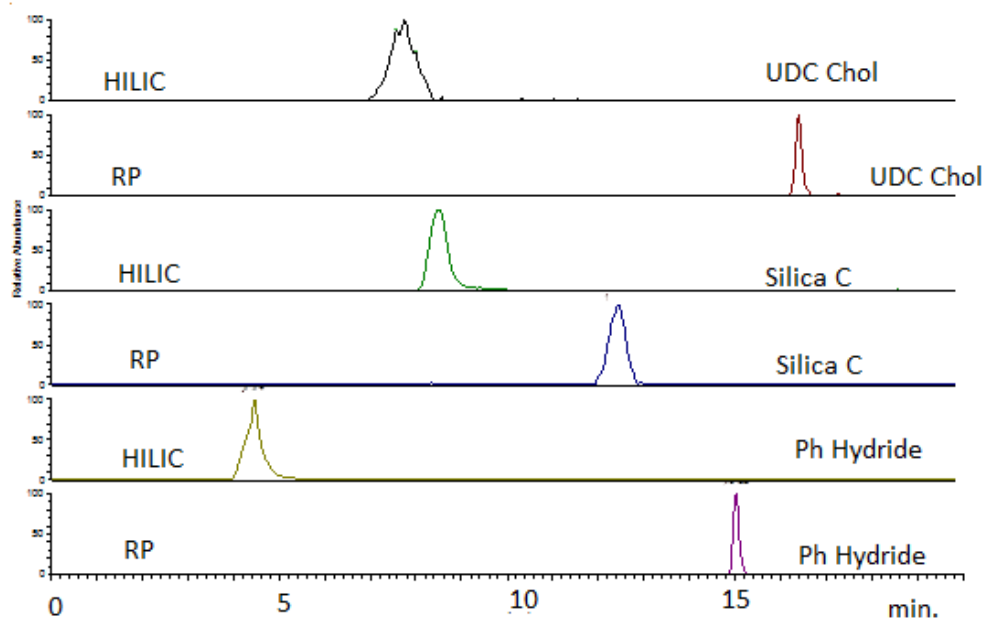


Figure 3.1 EICs for taurocholic acid (m/z 516.29-516.3) run in HILIC and RP modes on three silicon hydride columns

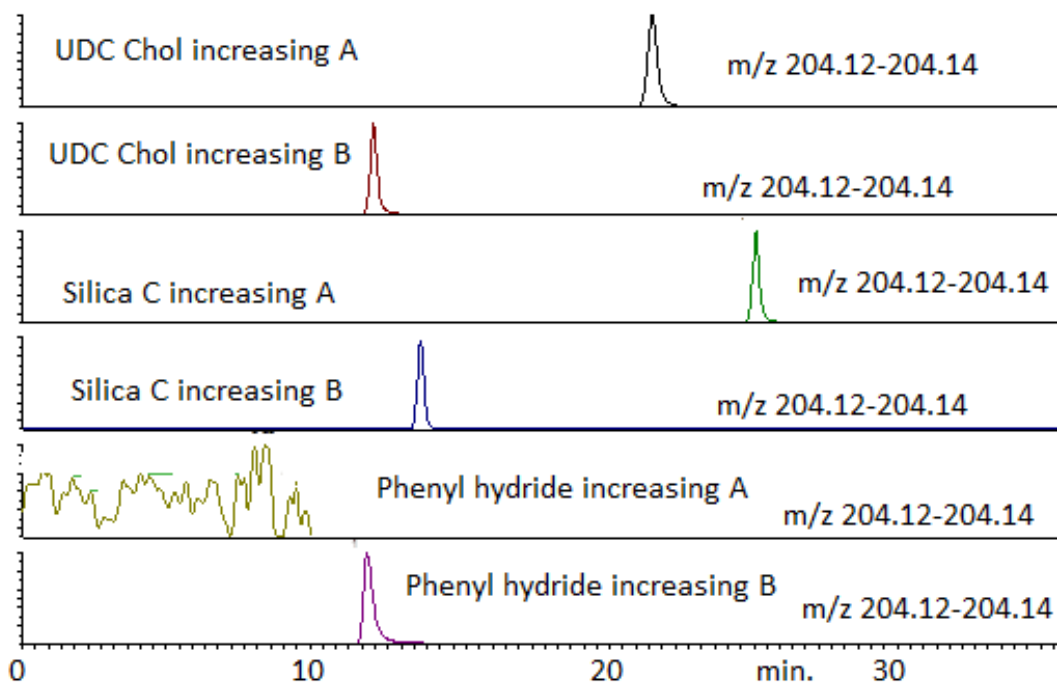


Figure 3.2 EIC for acetylcarnitine (m/z 204.12-204.14) on silicon hydride columns.

Figure 3.3 shows extracted ion chromatograms for the xenobiotic metabolite benzyl sulphate. Sulphates tend not to be strongly retained under HILIC conditions but complementary

information is obtained by running on the hydride columns where the analyte is retained on all the columns in reversed phase mode. Similar selectivity can be seen in the case of the dietary xenobiotic menthol glucuronide which is well retained both in HILIC and RP mode on all three hydride columns (Figure 3.4).

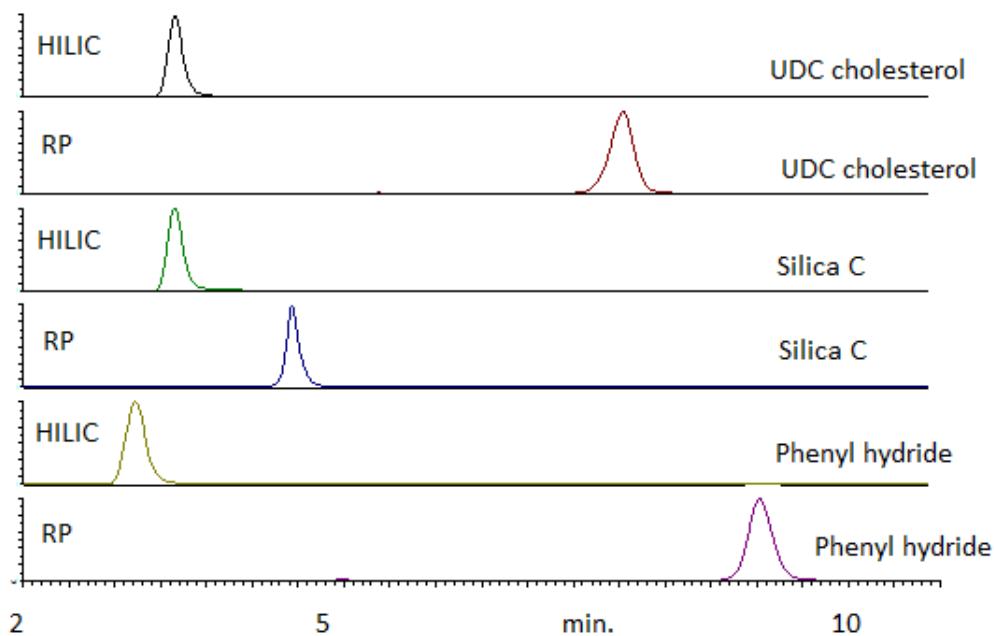


Figure 3.3 EICs for benzyl sulphate (m/z 187.0-187.02) in urine in HILIC and RP modes on hydride columns.

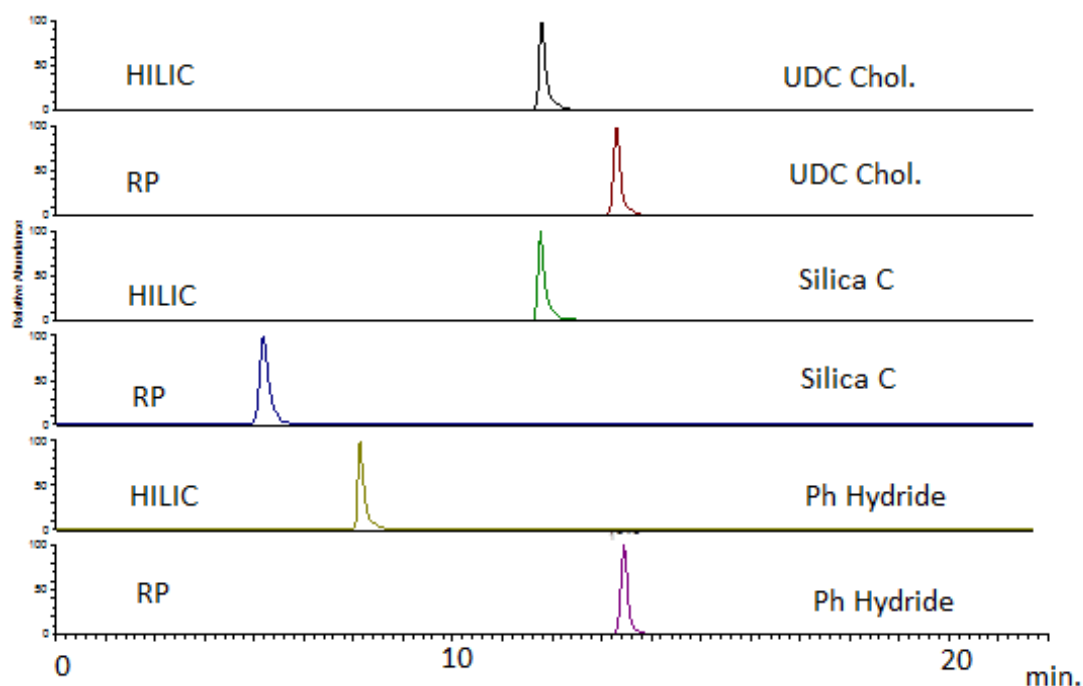


Figure 3.4 EICs for menthol glucuronide (m/z 331.17-331.18) in urine in HILIC and RP modes on hydride columns.

Thus silicon hydride columns offer an interesting alternative selectivity to conventional HILIC methods and reversed phase. The exact retention mechanism for analytes on these columns remains unclear, however, it is clear that even the unmodified silicon hydride phase Silica C offers both reversed phase and HILIC like activity and this permits sequential runs where metabolites can be characterised by their retention times in both modes. The reversed phase retention probably originates from interaction with the siloxane bond within the underlying silica gel since this bond is surprisingly lipophilic. The next stage in this work would be to develop some specific quantitative methods for bile acids and possibly for sulphates and glucuronides of xenobiotics. There is still no universal method for the analysis of all metabolites which occur in biological systems.

Chapter 4:

**A study of reductive amination of
sugars in order to produce
separation of the common sugars by
using HILIC chromatography**

4 A study of the reductive amination of sugars

4.1 Introduction

Reducing sugars can exist as alpha and beta anomers and also in pyranose and furanose ring forms. This is illustrated for glucose in Figure 4.1. The pyranose form of glucose is a 6-membered hemiacetal while the furanose form is a 5-membered hemiacetal. In the alpha anomers, the hydroxyl group on the anomeric carbon is below the plane of the structure while in the beta anomers the hydroxyl group attached to the anomeric carbon is above the plane of the structure. This configuration is also observed in other hexose sugars such as galactose, fructose, and mannose.

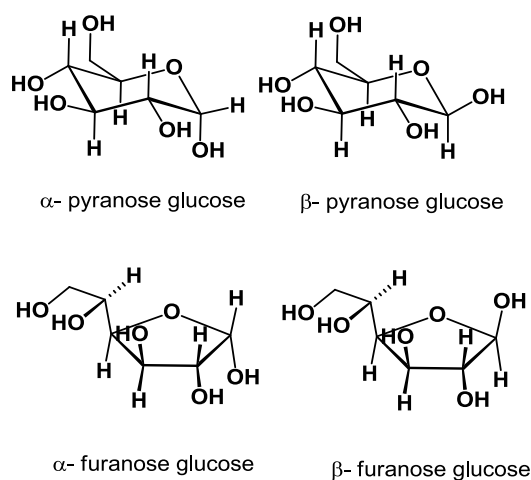
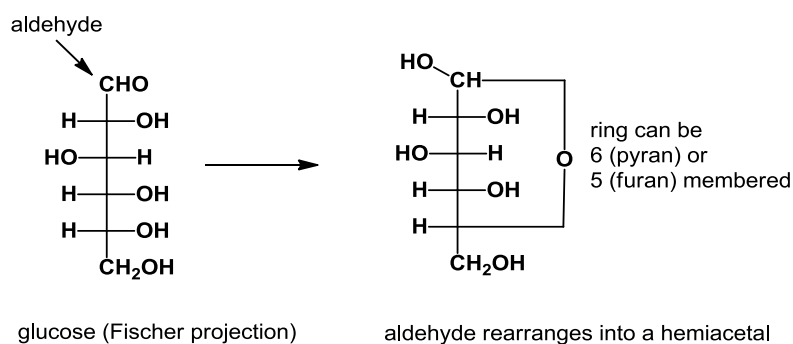


Figure 4.1 The equilibrium forms of glucose where the aldehyde group can react to form 5 (furan) or six membered ring via formation of a hemiacetal. The hydroxyl group generated can be in the α - or β -position.

This means each of the hexose sugars can adopt four forms all of which are in equilibrium. The challenge for the chromatographer is that the resulting chromatogram for an individual hexose sugar consists of broad and misshapen peaks since the four forms are continuously interconverting. Figure 4.2 shows chromatograms for glucose and galactose on a ZICpHILIC column. There is little chance of getting a good separation as long as all the four forms are present.

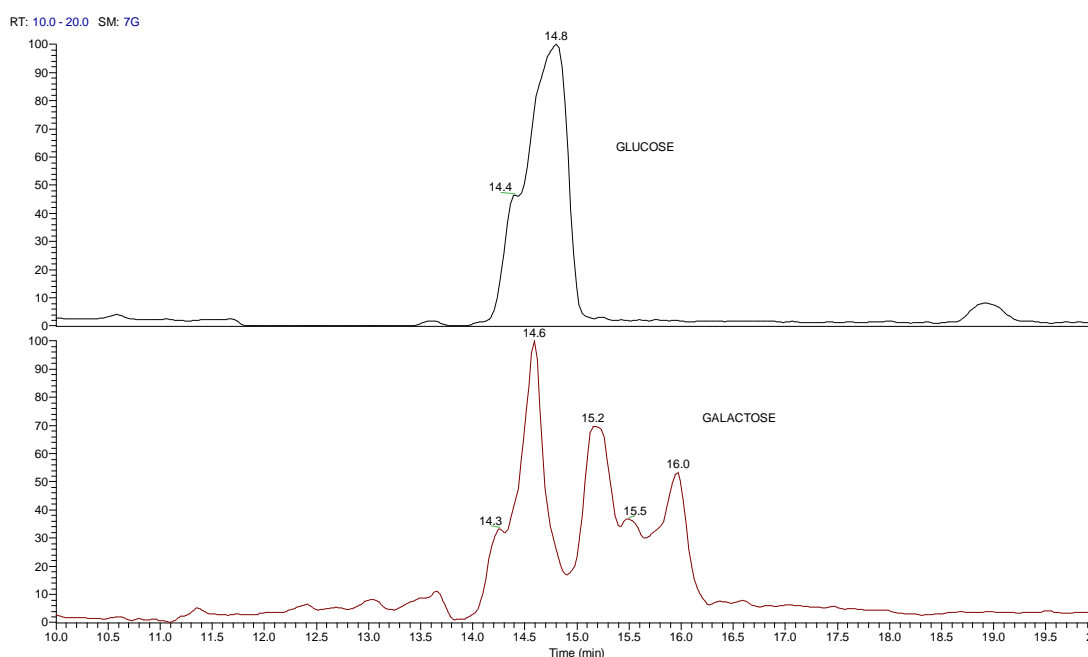


Figure 4.2 Chromatograms for glucose and galactose on a ZICpHILIC column (150 x 4.6 mm, 5 μ m) with gradient conditions as specified in section 4.3.4.

Sugars are some of the most difficult analytes to detect during metabolomics analyses by LC-MS. This is mainly because of two reasons: Firstly, they do not ionise properly given their lack of ionisable groups, and, secondly as discussed above, they tend to give jagged peaks which are broad because they can exist in four different ring forms (α - and β -anomers of pyranose and furanose respectively). These two major problems can be overcome through the use of derivatising agents. The derivatising agent needs to be able to impart on the sugar ionising property and avoid the formation of several various isoforms. When compared to

unlabelled metabolites, the detection sensitivity of analytes can be improved by up to 3 orders of magnitude following derivatisation [90]. Derivatising agents (also called tagging agents) introduce ionizable functional groups to the sugars thereby improving the detection of the poorly ionising sugars. In addition, the tag alters the overall polarity of the resulting derivative which modifies its chromatographic profile leading to better separation [91]. For instance, tagging facilitates the analysis of polar and even ionic metabolites in reversed phase LC by increasing the lipophilicity of the tagged molecule. Tagging also increases the likelihood of successful analysis of both positively and negatively charged compounds within the same sample by, for instance, derivatising all acids with a positively charged tagging agent before analysing the samples in a positive mode. In this case, a more comprehensive analysis of a given sub-metabolome can be obtained. Some derivatising agents are labelled with stable isotopes such as ^2H (deuterium) and ^{13}C . These stable isotopes can also be used as internal standards in quantification experiments to overcome the problem of matrix and ion suppression effects [91]. In this case, a light isotope tag is introduced on the analytes in one sample while a heavy isotope tag is introduced on a comparative sample [92]. The common functional metabolites can then be easily recognised by both similar retention times and characteristic mass difference between the isotopes. Thus each peak is a doublet one unlabelled and stable isotope labelled derivative. Quantification can be performed by fixing the concentration of the heavy isotope as an internal standard [90]. Whereas derivatisation is an essential technique in metabolomics to detect and analyse new biomarkers in different disease conditions, its major challenge comes from complex sample preparation especially when isotope labelling is involved [93].

Sugars exist predominantly in their ring forms (>97%) at neutral pH in water. In this form, the hydroxyl group on C_5 bonds to the aldehyde group on C_1 to form a pyranose ring (Figure 4.3). On the other hand, a furanose ring is formed when the C_4 hydroxyl group bonds to the aldehyde. As derivatisation reactions occur between the aldehyde and an amine of a tagging

agent, the ring forms do not derivatise. In order for the derivatisation to be effective, the reaction has to be carried out at acidic pH where most of the sugar is in the ring open form.

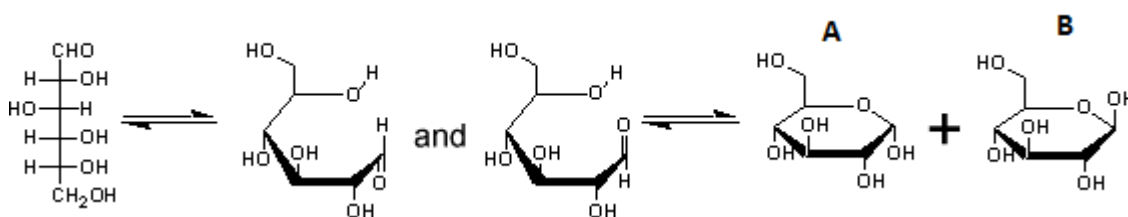


Figure 4.3 Formation of pyranose ring. A is α -pyranose and B is β -pyranose.

A frequently adopted strategy for removing this problem in liquid chromatography is to carry out reductive amination of the sugars at low pH. This is illustrated in Figure 4.4. The aldehyde group of the sugar reacts with the amine to form a Schiff's base and then, since the Schiff's base can exist in syn- and anti-forms and is also not particularly stable, the reaction is pushed to completion by reducing the Schiff's base to produce a single product which is stable.

The reaction mechanism between the aldehyde and the amine follows a nucleophilic attack on the carbonyl carbon by the basic nitrogen of the base containing unbonded lone pairs of electrons. There is a loss of one molecule of water during the reaction leading to the formation of the Schiff's base. Both the syn- and anti- forms are formed during the reaction owing to the lack of rotation about the C=N double bond. Reduction of the double bond by hydrogenation leads to the formation of a single final product which is stable.

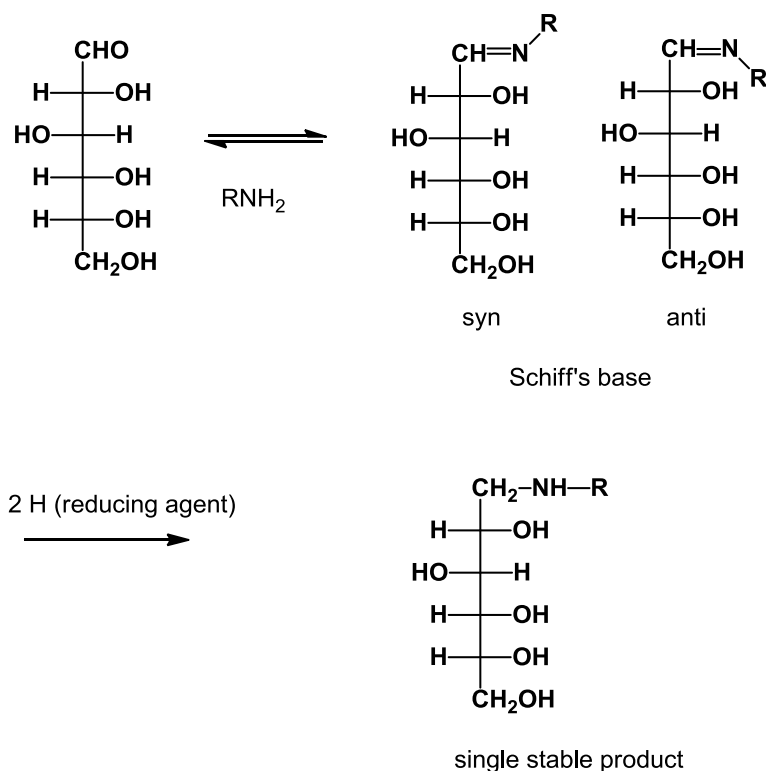


Figure 4.4 Reductive amination of a sugar. The reduction pulls the equilibrium to the right producing a single stable product.

There have been several reviews of methods for derivatising sugars and three basic rules have been established [94-105]. The reaction should be conducted at low pH so that the acyclic form of the sugar is favoured over the cyclic form (Figure 4.5) since it is the aldehyde form that reacts to form the Schiff base. Thus it is better to carry out the reaction at a fairly low pH (e.g. in dilute formic acid).

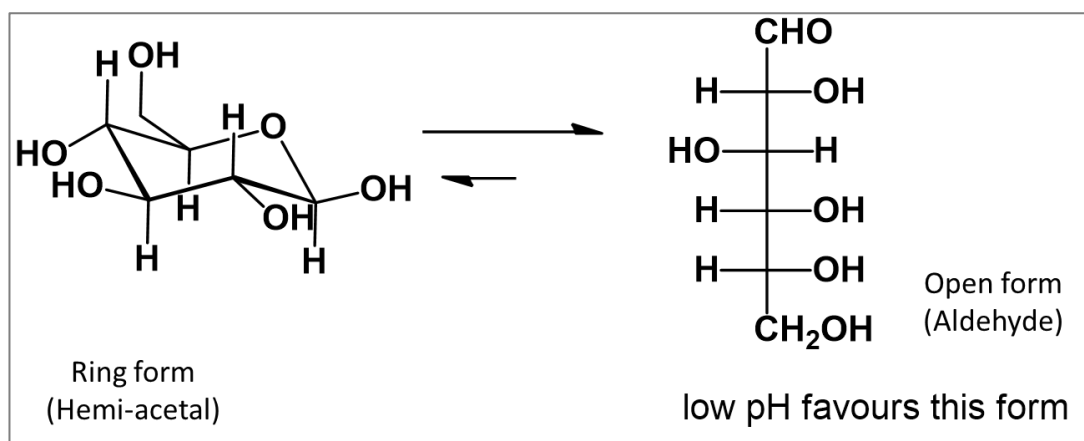


Figure 4.5 Equilibrium between the hemi-acetal ring form of glucose and its open chain aldehyde form.

Having to work at low pH determines the second rule. Since bases are protonated at a low pH, and it is the unprotonated form of a base that reacts with the aldehyde, then to get a successful reaction it is necessary to use a weak base that is not fully protonated at low pH. A good example of such a base is aniline (Figure 4.6) which has been used for many years to detect sugars. The pK_a value of aniline is about 4.5 so even working say at pH 3.5 there is still enough of the unprotonated form of the base to react with the sugar. A base such as aminobenzamide (Figure 4.6) has an even lower pK_a value (~ 2.0) and may be even better than aniline for the derivatisation of the sugars. The presence of the amide group at the para-position to the amino group increased the electron withdrawing effect away from the nitrogen of the basic group, which weakens the latter. This means that aminobenzamine is largely in its unprotonated form at a pH of 3.5.

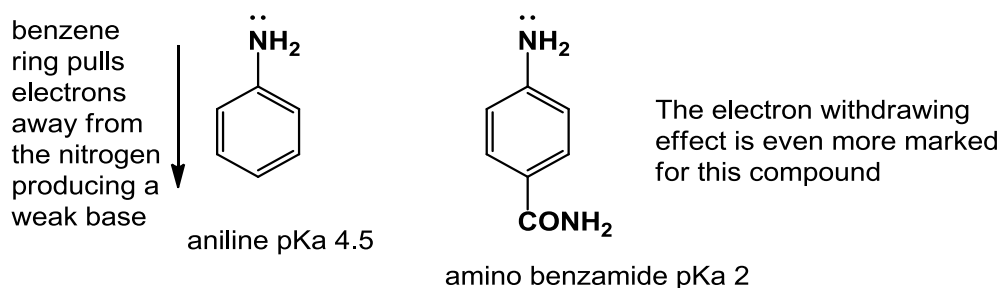


Figure 4.6 Structures of aniline and aminobenzamide

Finally, the third rule is that the reducing agent used to reduce the Schiff's base should be stable under acidic conditions. Sodium borohydride is often used in reductive amination reactions but it is of no use in the current case since it is unstable to acid. A suitable acid-stable reducing agent is 2-methylpyridine borane complex which is stable at low pH.

4.2 Aims

4.2.1 Overall objective

To develop a reductive amination method to enable the chromatographic separation of common sugars.

4.2.2 Specific objectives

- a) Analysis of underivatized neutral sugars and their phosphates
- b) Formation of sugar derivatives by reductive amination with:
 - i. Aniline
 - ii. Deuterated aniline
 - iii. 4-Aminobenzamide and
 - iv. Procainamide
- c) Application of reductive amination with deuterated aniline to the analysis of sugars in brain samples.

4.3 Materials and methods

4.3.1 Test probes and tagging agents

Aniline, $^2\text{H}_5$ -aniline, picoline borane complex, glucose, fructose, mannose, galactose, glucose 1-phosphate, glucose 6-phosphate, fructose 1-phosphate, fructose 6-phosphate were obtained from Sigma Aldrich, Dorset, UK. The test probes consisted of four standard hexose sugars glucose, mannose, galactose and fructose. The derivatising agents were aniline, deuterated aniline, aminobenzamide and procainamide. Exactly 5mg of each of the hexose sugars was separately weighed and dissolved in 5ml of methanol in a vial to form standard stock solutions of 1 mg/ml for each sugar.

4.3.2 Derivatisation of the hexose sugars

Aminobenzamide, procaineamide aniline or deuterated aniline were prepared at 10 mg/ml in methanol/water containing 10% v/v acetic acid (50:50) (solution A) and a solution containing 10 mg/ml of picoline borane in methanol/water (1:1) (solution B) was also prepared. Exactly 50 μg of each sugar was mixed with 40 μl of solution A. The mixture was then heated in a heating block at 40°C for 30 minutes. Then 20 μl of solution B was added and the resulting mixture again heated at 30°C for 45 minutes. The samples were then blown to dryness in a stream of nitrogen gas and re-dissolved in 0.2 ml of water containing 0.1 % formic acid, before adding 1 ml of acetonitrile. Milk was investigated as a model system for derivatisation of sugars. 0.2 ml of milk was mixed with 0.8 ml of acetonitrile and the sample was then centrifuged at 3000 g. An aliquot of supernatant (50 μl) was then treated as described above.

4.3.3 Quantification of sugars in brain samples

Post-mortem brain samples were available from a previous study and were provided by from the Sudden Death Bank collection held in the MRC Edinburgh Brain and Tissue Banks. Full

ethics permission has been granted to the Banks for collection of samples and distribution to approved researchers, the University of Strathclyde Ethics Committee also approved the local study of this material.

4.3.3.1 Internal standard preparation

A stock solution of an internal standard of ^{13}C glucose was prepared at a concentration of 1 mg/ml by dissolving exactly 5 mg of the internal standard in 5 ml of methanol.

4.3.3.2 Standard calibration solutions

Four calibration series were prepared one for each of the sugars fructose, glucose, galactose and mannose in the concentration range of 0.2 $\mu\text{g/mL}$ to 3.2 $\mu\text{g/mL}$ and containing a fixed concentration of ^{13}C glucose internal standard of 5 $\mu\text{g/mL}$. These were prepared as follows: Firstly, the 1mg/ml stock solution of the internal standard was diluted 10-fold by pipetting 500 μl and making it up to 5 ml with methanol. The resulting solution was 0.1 mg/mL (solution A). Secondly, 100 μl aliquots of 1 mg/ml stock solutions of fructose, glucose, galactose and mannose were pipetted into a single separate container and made up to 5 ml with methanol to obtain a 50-fold dilution. The resulting solution mixture was of concentration 0.02 mg/mL for each of the hexose sugars (solution B).

Finally, the calibration series was then prepared as follows:

<i>Calibration sample</i>	<i>Volume of standard added (μL)</i>		<i>Individual sugar concentration ($\mu\text{g/ml}$)</i>
	A (0.1 mg/ml)	B (0.025 mg/ml)	
1	50	0	0.00
2	50	10	0.25
3	50	20	0.5
4	50	40	1.00
5	50	80	2.00
6	50	160	4.00

Each of the resulting solutions was then treated with deuterated aniline using the optimised derivatisation method described above before being analysed using an optimised LC-MS method with a ZIC-HILIC column. For the analysis of the sugars in brain 200 mg of the brain tissue was extracted by homogenising it with 1 ml of acetonitrile/water containing 1 µg/ml of ¹³C₆-glucose internal standard. The sample was centrifuged at 3000 g and then the supernatant was blown to dryness under a stream of nitrogen and the residue was dissolved the 200 µl of methanol and then derivatised as described above.

4.3.4 LC-MS conditions

The final samples were analysed on the Orbitrap Exactive with mobile phases A: 0.01% formic acid in water and B: 0.01% formic acid in acetonitrile using the condition in the table below.

Table 4.1: Gradient conditions in the analysis of hexose sugar derivatives

<i>Time</i>	<i>%A (Water containing 0.01% formic acid)</i>	<i>%B (Acetonitrile containing 0.01% formic acid)</i>	<i>Flow rate (µl/min)</i>
0	20	80	600
30	60	40	600
31	20	80	600
35	20	80	600

4.4 Results

4.4.1 Aniline derivatives of hexose sugars

As already described in section 4.1, the derivatisation reaction between the hexose sugars (e.g. glucose) and aniline (a weak base) was performed at low pH so that the open aldehyde form of the sugar was favoured over the hemi-acetal ring form. In the first step of the

reaction a Schiff's base is formed, of which both the syn- and anti-forms are possible due to the lack of rotation across the C=N double bond. Reduction of the Schiff's base with an acid-stable strong reducing agent such as 2-methylpyridine borane complex produces a final stable product which is then detected by mean of a mass spectrometer.

The chemical formula of the final product can be predicted from the reaction shown in Figure 4.7. For example glucose is $C_6 H_{12} O_6$ (MW=180) and aniline is $C_6 H_7 N$ (MW=93). The first step of the reaction is a condensation reaction with loss of water (H_2O , MW=18), while the second step is a reduction reaction which involves hydrogenation of the Schiff's base with addition of two protons ($2H$, MW=2) to form a saturated product. Thus the final product has a chemical formula of $C_{(6+6=12)} H_{(12+7-2+2=19)} N O_{(6-1=5)}$, that is: $C_{12} H_{19} NO_5$, with expected nominal mass of $(180+93-18+2=257)$ which will be observed at m/z 258 in positive ion ESI mode.

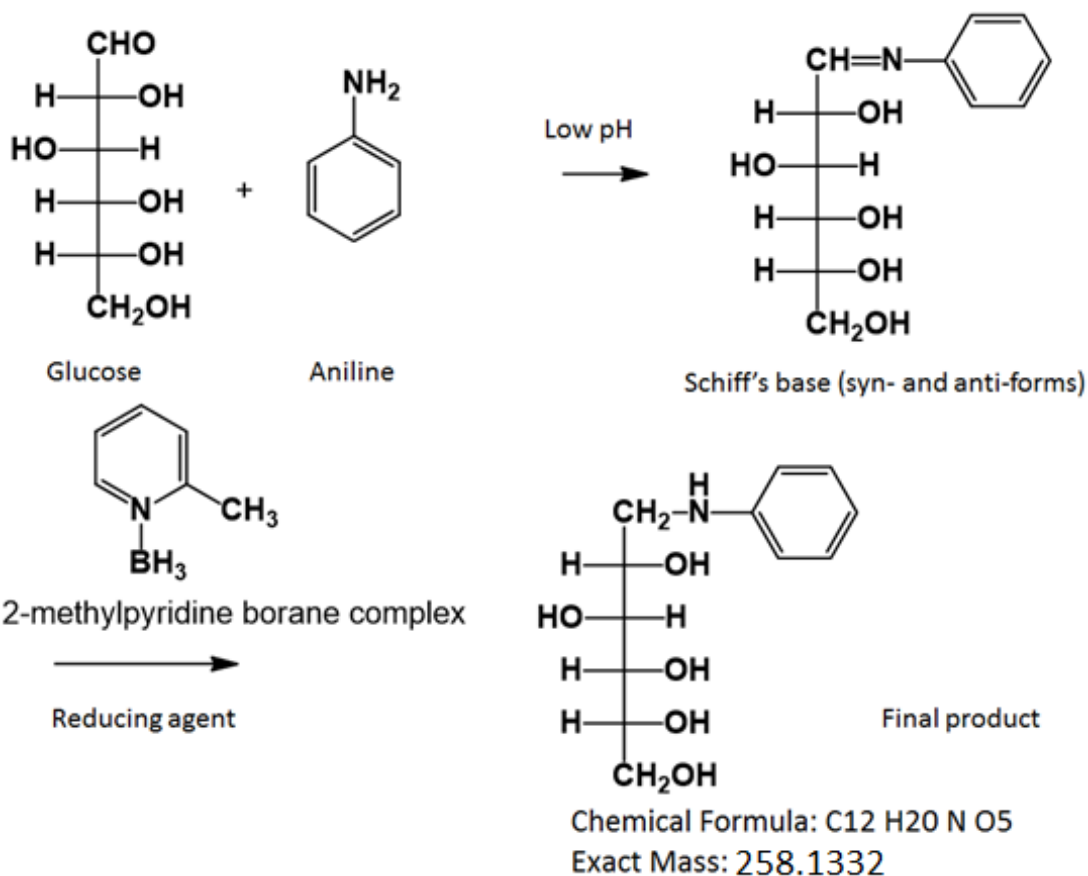
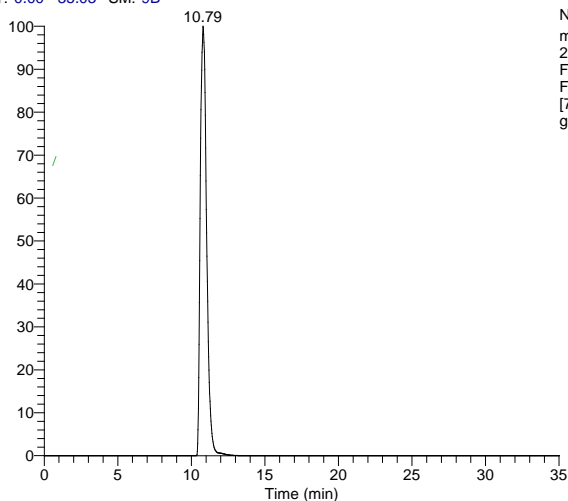


Figure 4.7: Derivatisation reaction for 4-aminobenzamide derivatives. Derivatisation reaction is followed by reduction with 2-methylpyridine borane complex to form a single stable product.

Figure 4.8 shows the chromatogram for the aniline derivative of glucose with its positive ion mass spectrum after acquiring a single proton $[M+H]^+$ in ESI mode. It gives a protonated molecular ion at m/z 258.1332 with an elemental composition of C₁₂H₂₀NO₅. The protonation of the aniline derivative occurs on the ionisable nitrogen atom from the aniline. Due to its attachment to an aromatic group, the amine is less easily protonated compared to a similar amine (secondary amine) in which aliphatic groups are attached. However, the mass spectrometry response for these derivatives is very good.

RT: 0.00 - 35.03 SM: 9B



NL: 3.83E7
m/z=
258.120-258.140 F:
FTMS (1,1) + p ESI
Full lock ms
[75.00-1200.00] MS
glucose

glucose #937 RT: 10.84 AV: 1 SB: 1 10.99 , 14.44 NL: 1.45E7
T: FTMS (1,1) + p ESI Full lock ms [75.00-1200.00]

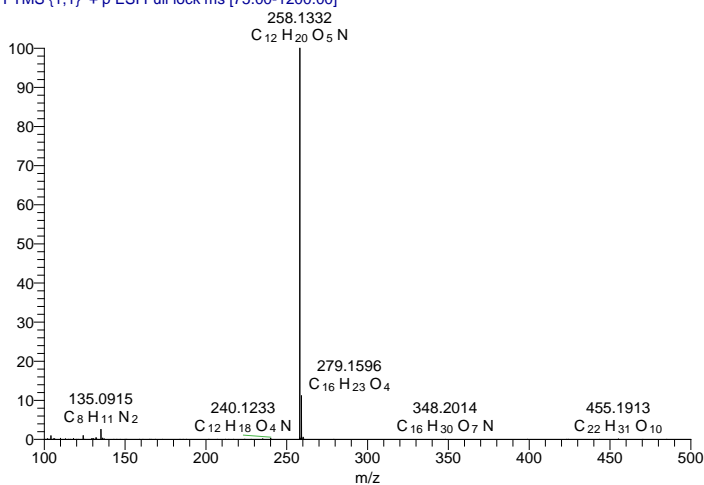


Figure 4.8 Aniline derivative of glucose. The figure shows the extracted ion chromatogram of the aniline derivative with an exact mass of 258.1332 which is the expected mass of a mono-protonated anilide of glucose.

All the four sugars, in form of their aniline derivatives, almost separate from each other as shown in Figure 4.9. In addition, unlike in the underivatized sugars (Figure 4.2), the peak shapes are much improved. Being isomers, all the sugars have the same exact mass for their aniline derivatives which means that their EICs are obtained in the same mass (m/z) range of 258.120-258.140, which is approximately centred about the expected exact mass of the product (258.1332). It can be seen that there is some variation in the peak intensities of the products formed, in the order (from highest to lowest) of mannose, galactose, glucose and

fructose respectively, although this is less than one order of magnitude in each case. This variation may be due to variation in reactivity of the different isomeric sugars and the base, or in the subsequent reductive step. Fructose would be expected to produce two peaks since it is a ketone and reduction of the Schiff base produces an extra asymmetric centre which results in the formation of two diastereomers. However, it is not clear why the second peak for the fructose derivative shows a tendency to split (Figure 4.9d).

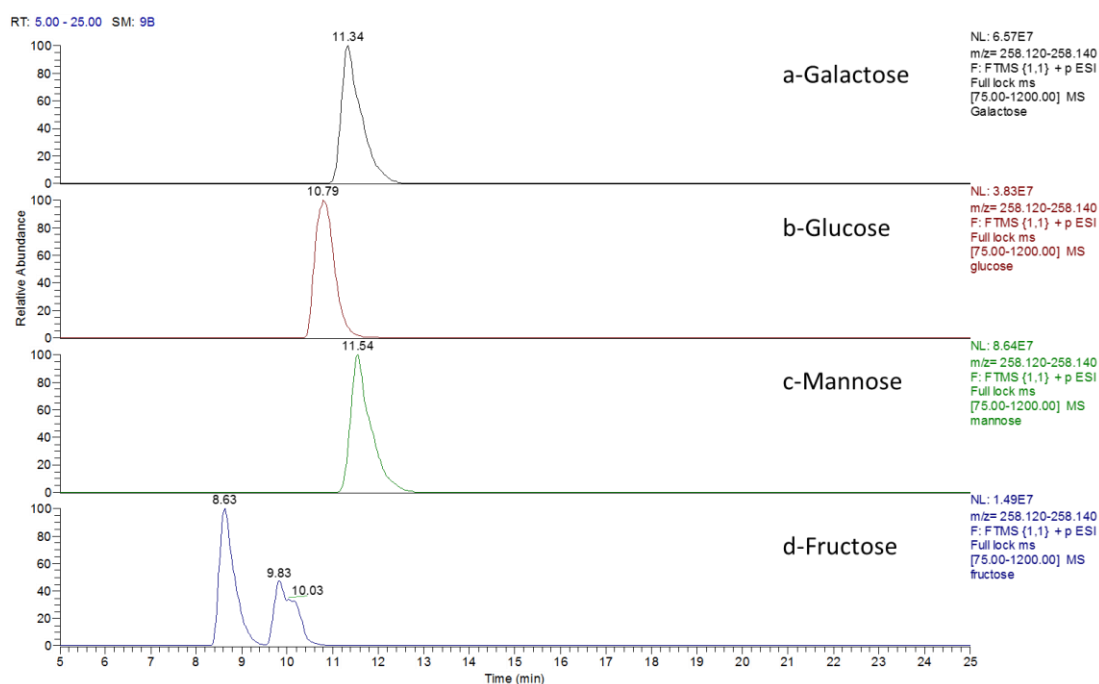


Figure 4.9: Chromatograms of the aniline derivatives of the four sugars galactose, glucose, mannose and fructose. There is almost separation of galactose (a), mannose (c) and fructose (d) peaks from the glucose peak (b). However, galactose (a) and mannose (c) show almost the same retention time.

The formation of aniline derivatives was applied to the profiling of sugars in milk samples. The extracted ion traces in Figure 4.10 for the aniline derivatives of the sugars show that camel milk contains a large amount of lactose (m/z 420.18) with small amounts of glucose (earlier running peak m/z 258.13) and traces of galactose.

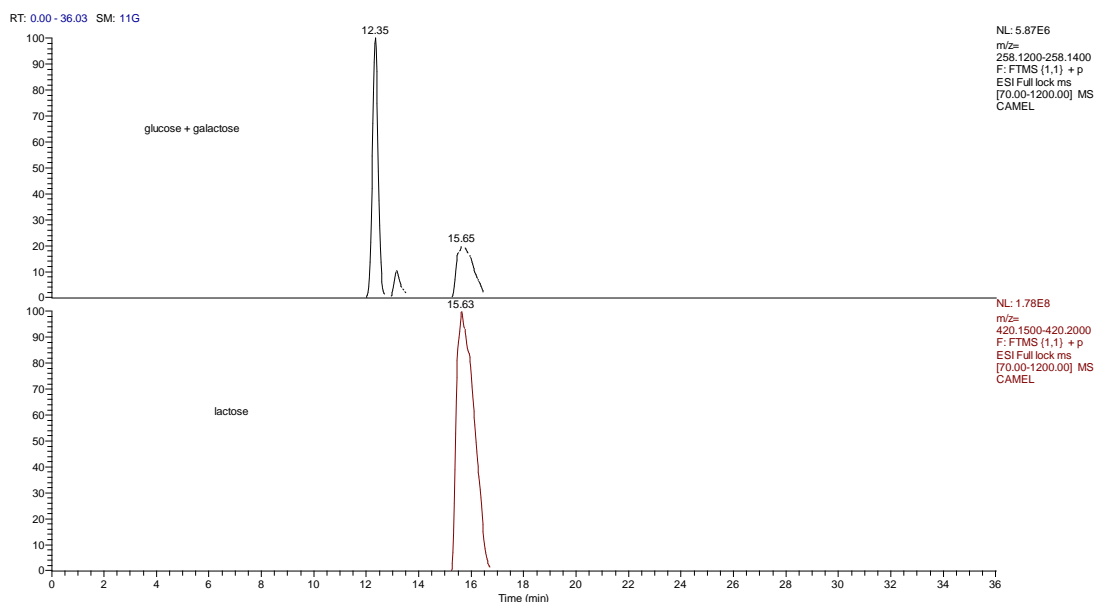
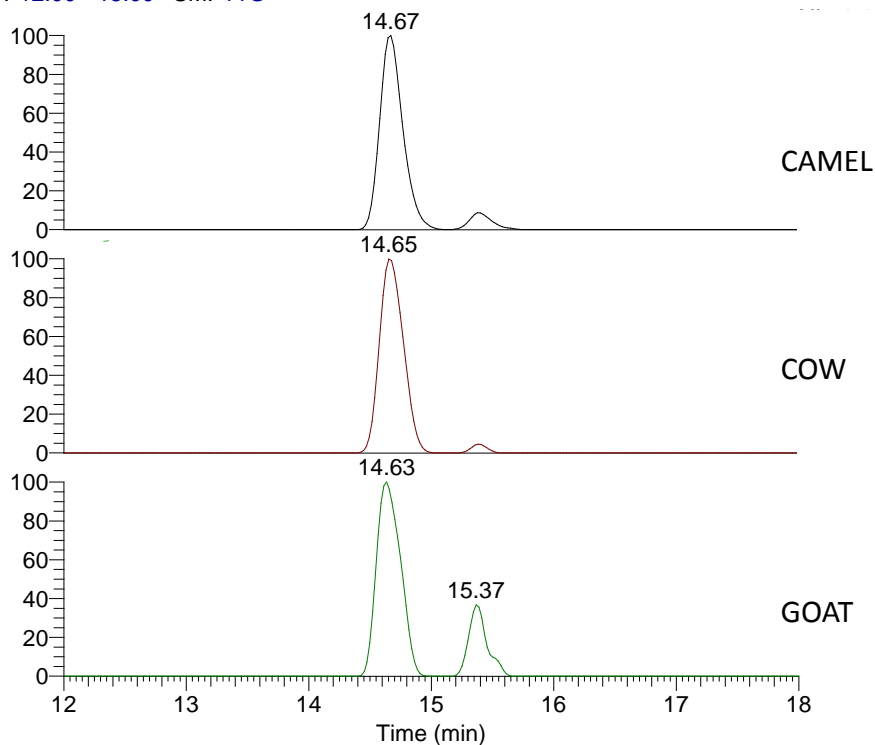


Figure 4.10 Aniline derivatives of the milk sugars showing the presence of glucose, galactose and lactose.

Figure 4.11 shows extracted ion traces for aniline derivatives of sialyl lactoses (Figure 4.12). These antimicrobial sugars are present in many mammalian milks (see chapter 5). It is clear that camel milk contains a much higher concentration of these sugars than cow and goat milks. Tagging these sugars with aniline improves their detectability.

RT: 12.00 - 18.00 SM: 11G



CAMEL #1257 RT: 14.65 AV: 1 SB: 30 33.92-34.59 , 36.03 NL: 1.68E6
T: FTMS {1,1} + p ESI Full lock ms [70.00-1200.00]

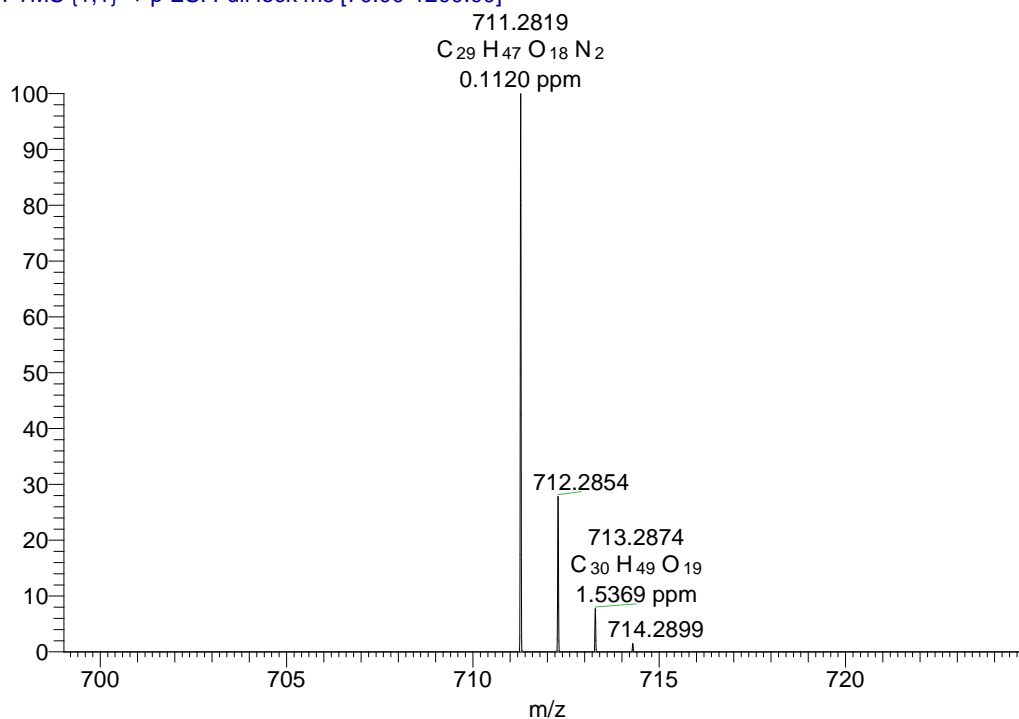
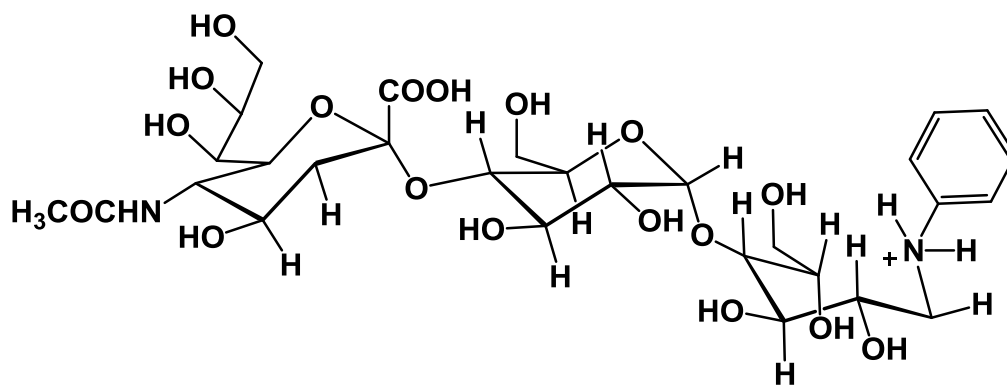


Figure 4.11 Aniline derivatives of sialyl lactose isomers present in milks with the mass spectrum for sialyl lactose.



Chemical Formula: $C_{29}H_{47}N_2O_{18}^+$

Exact Mass: 711.2818

aniline derivative of sialyl lactose antimicrobial sugar

Figure 4.12 Aniline tagged sialyl lactose sugar.

4.4.2 Aniline derivatives of hexose sugar phosphates

Four hexose sugar phosphates of glucose, mannose, galactose and fructose were analysed (Figure 4.13-4.14).

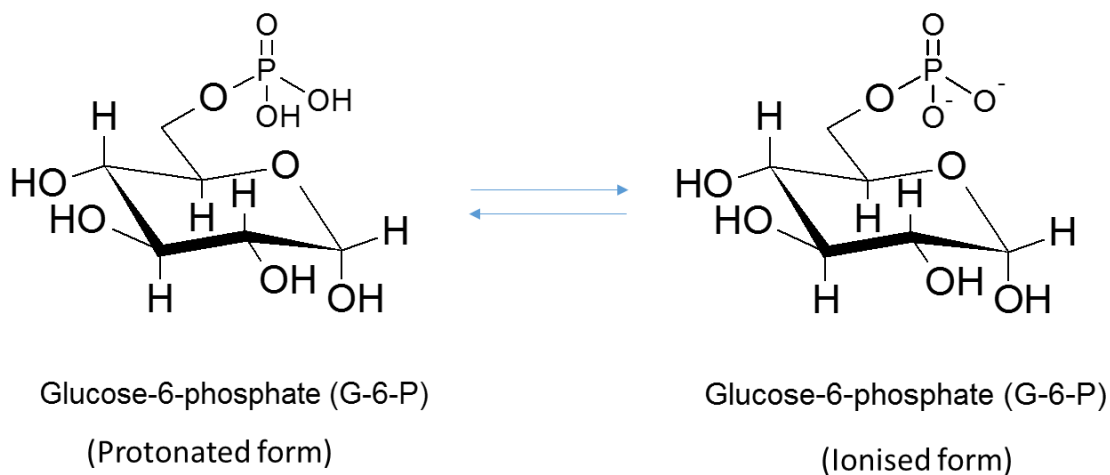


Figure 4.13 Chemical structure of glucose-6-phosphate in its protonated and ionised forms. The former occurs at low pH while the latter occurs at high pH.

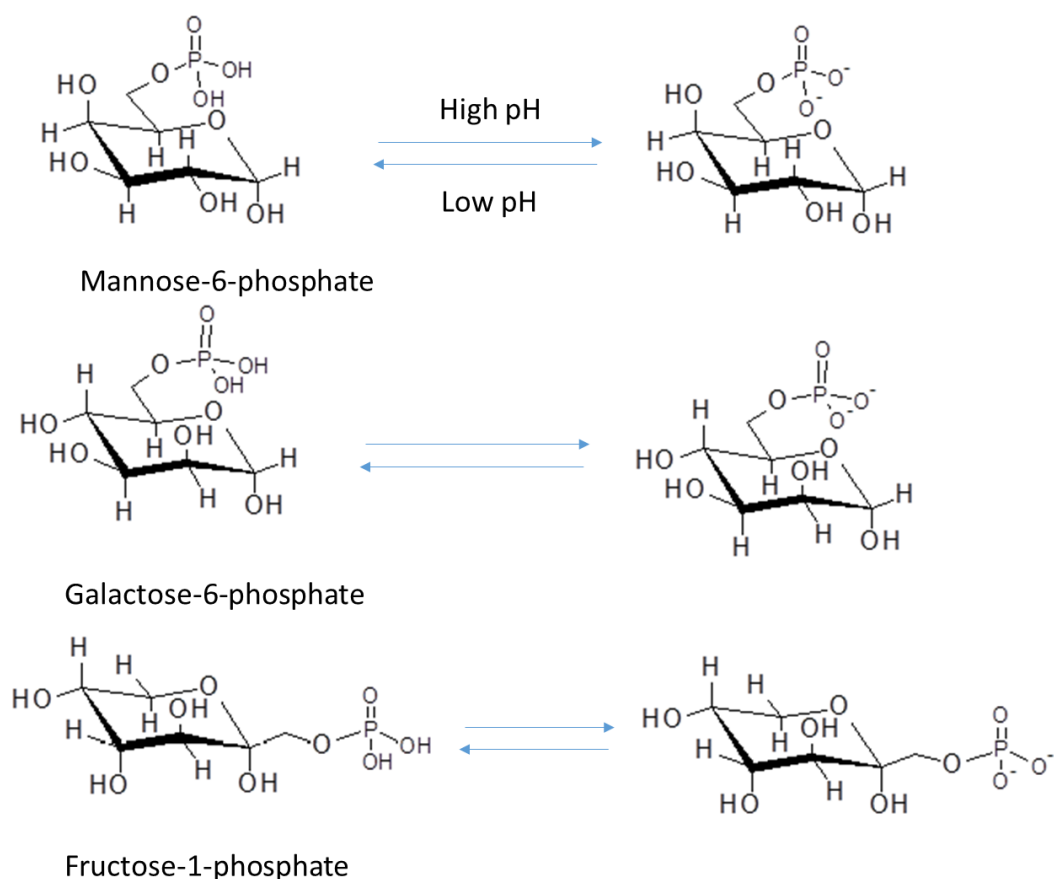


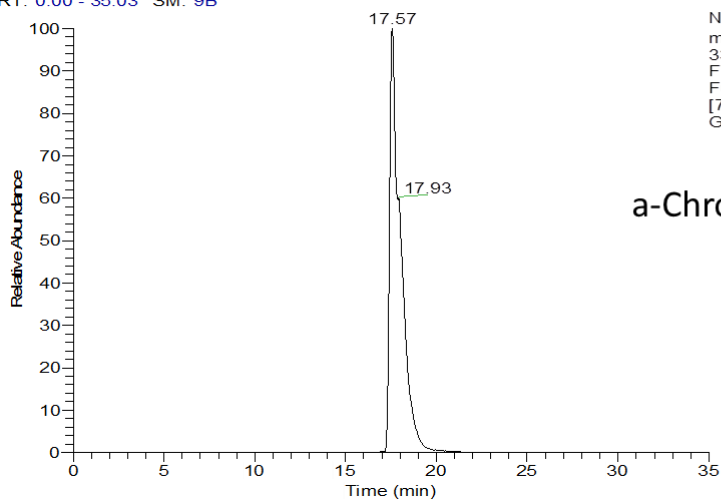
Figure 4.14 Chemical structures of mannose-6, galactose-6 and fructose-1-phosphates. At the low pH conditions used for the derivatisation of the sugars, the sugar is in the ring-open form and the phosphate is in the protonated form shown on the left hand side.

The aniline derivatisation of hexose sugar phosphates follows the same reaction as that shown in Figure 4.7 for the free hexose sugars. It is not possible for the sugar 1-phosphates to form a Schiff's base since the presence of the bond to the phosphate group blocks the reaction, apart from the case of fructose 1-phosphate where phosphate is bonded to the carbon next to the ketone group. The mono-phosphorylated hexoses have chemical formula of $C_6H_{13}O_9P$ (MW=260). Condensation reaction with aniline (C_6H_7N , MW=93), involving loss of a molecule of water (H_2O , MW=18), followed by reduction ($2H$, MW=2) yields a product with a chemical formula, $C_{12}H_{20}O_8NP$ (MW=337). Mono-protonation in the ESI

mode of the mass spectrometer gives an ion with chemical formula $C_{12}H_{21}O_8NP$ and nominal mass of 338.

Figure 4.15 shows the chromatogram for galactose-6-phosphate aniline derivative and Figure 4.16 shows the separation of fructose-1-phosphate and galactose-, glucose- and mannose-6-phosphates as their aniline derivatives. The separation of the phosphates is not as clear as for the neutral sugars and more work would be required to make this a viable method for the separation of the common sugar phosphates.

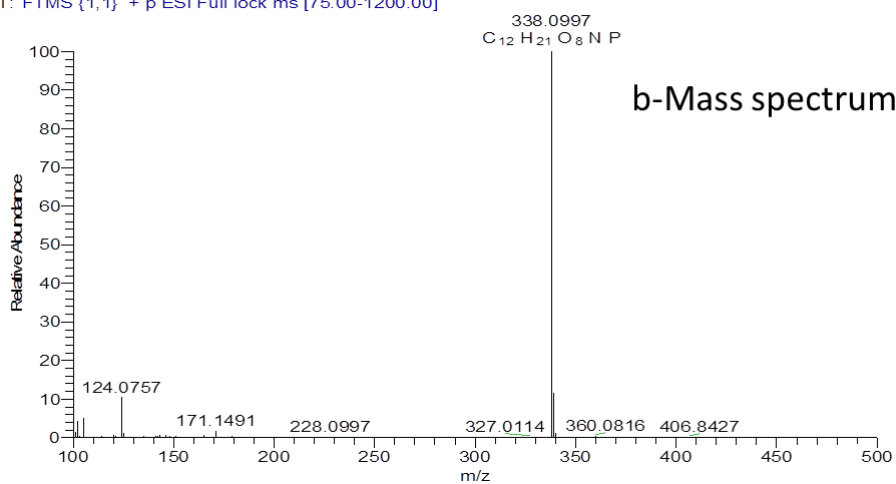
RT: 0.00 - 35.03 SM: 9B



NL: 1.40E7
m/z=
338.090-338.100 F:
FTMS (1,1) + p ESI
Full lock ms
[75.00-1200.00] MS
Glucose-6

a-Chromatogram

Glucose-6 #1583 RT: 18.02 AV: 1 SB: 1 11.00, 14.44 NL: 7.11E6
T: FTMS (1,1) + p ESI Full lock ms [75.00-1200.00]



b-Mass spectrum

Figure 4.15 Extracted ion chromatogram of the aniline derivative of glucose-6-phosphate (a) and its mass spectrum (b) showing the exact mass of the stable derivative product formed.

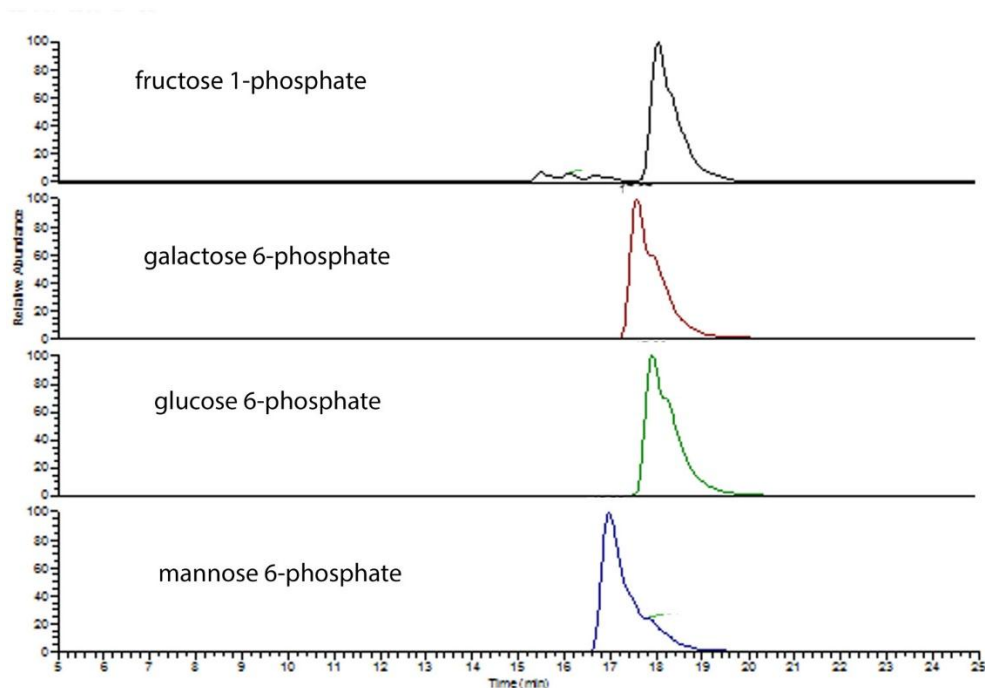


Figure 4.16 Chromatograms showing the separation of aniline derivatives for fructose-1-phosphate and galactose-6, glucose-6 and mannose-6 phosphates.

4.5 Deuterated aniline derivatives

The original intention of the work was to use deuterated aniline to carry out simultaneous analysis of two samples one tagged with aniline and the other tagged with deuterated aniline. However, it was found that when deuterated aniline was used instead of aniline for the derivatisation reaction there was an improvement in the separation of mannose and galactose which largely overlapped when aniline was used as the tag. The reaction proceeds in the same way as with unlabelled aniline to form a final stable product which is 5 mass units higher than the product formed with aniline derivatisation (Figure 4.17). Pentadeuterated aniline is not expensive and very small amounts are required in the formation of derivatives.

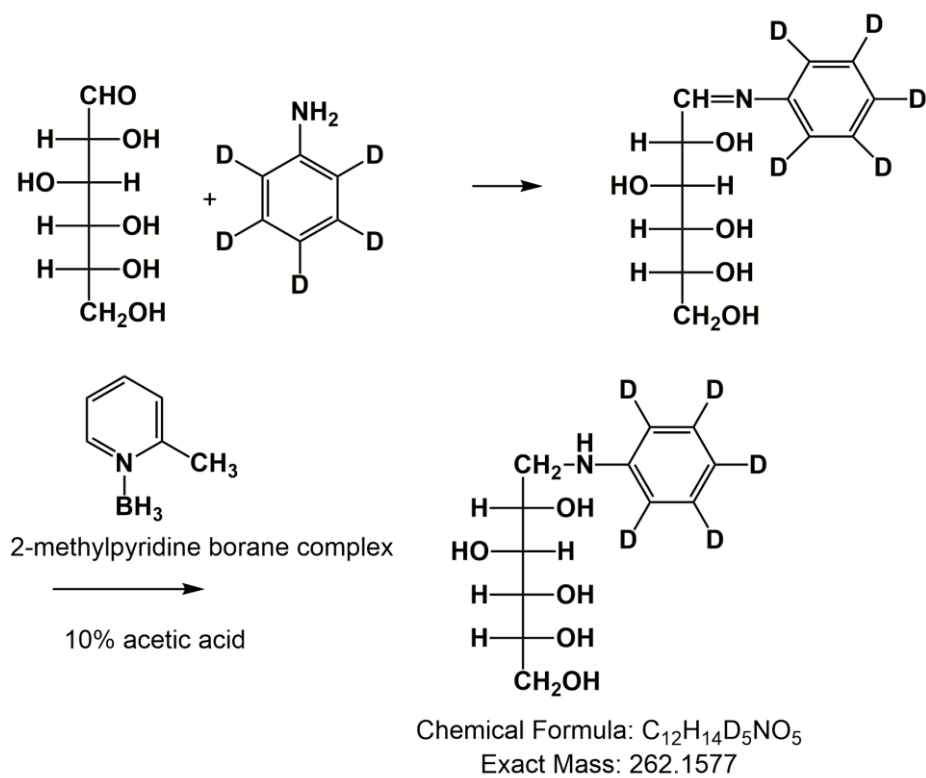


Figure 4.17 Reductive amination of a sugar using pentadeutero aniline and picoline borane.

This method produced derivatives for glucose, mannose and galactose with good peak shapes and high yields. Figure 4.18 below shows an LC-MS trace for the three hexose sugars at a concentration of 0.25 $\mu\text{g/ml}$ in comparison with $^{13}\text{C}_6$ glucose added as an internal standard at 10 $\mu\text{g/ml}$.

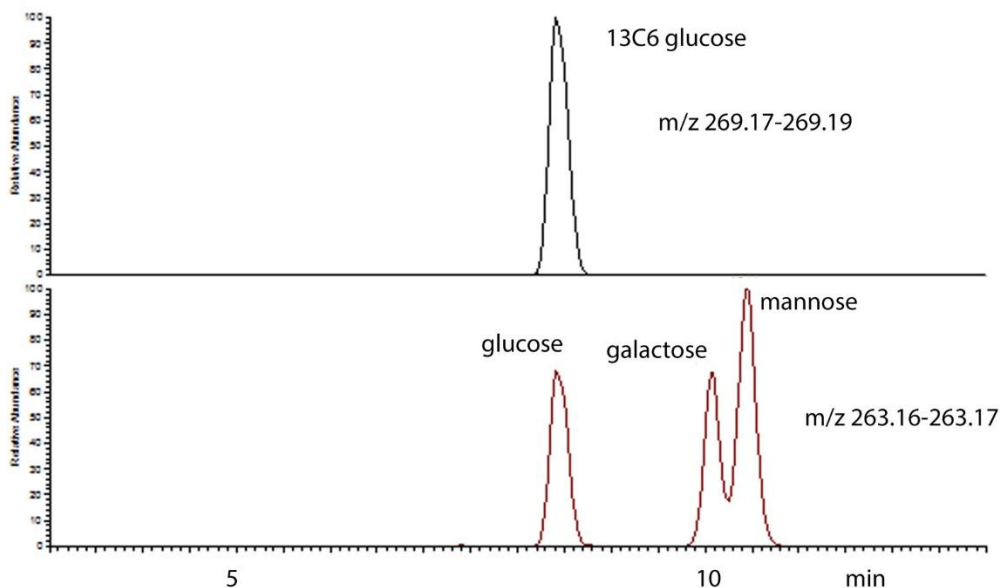


Figure 4.18 Sugar standards as deuterioaniline derivatives analysed on a ZICHILIC column using the conditions described in section 4.3.2.

4.6 Procainamide Derivatives

Several different derivatives were tried using the reductive amination procedure but none produced better separation of the sugar isomers than aniline and deuterio aniline. For example procainamide has two basic nitrogen atoms in its structure, with one being an aromatic primary amine ($pK_a \sim 3.5$) while the other is an aliphatic tertiary amine ($pK_a \sim 8.5$) (Figure 4.19). The amide group is neutral and fairly unreactive. At the acidic conditions ($pH \sim 3.0$) required to keep the hexose sugars in their ring open forms, the aliphatic tertiary amino group in procainamide is fully protonated. This leaves only the aromatic amino group as the nucleophilic site for the initiation of the amination reaction with the sugars.

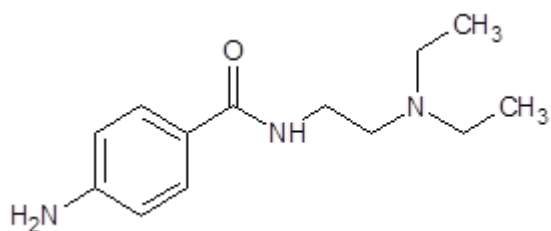


Figure 4.19 The chemical structure of procainamide, whose chemical name is 4-amino-N-(2-diethylaminoethyl) benzamide.

The amination reaction proceeds in the same way as for derivatisation with aniline shown in Figure 4.20. There is initially a condensation reaction between the base and the sugar to form a Schiff's base which is stabilised by hydrogenation using a strong reducing agent that it stable at low pH. The reducing agent is picoline borane and the low pH was attained using 10% acetic acid.

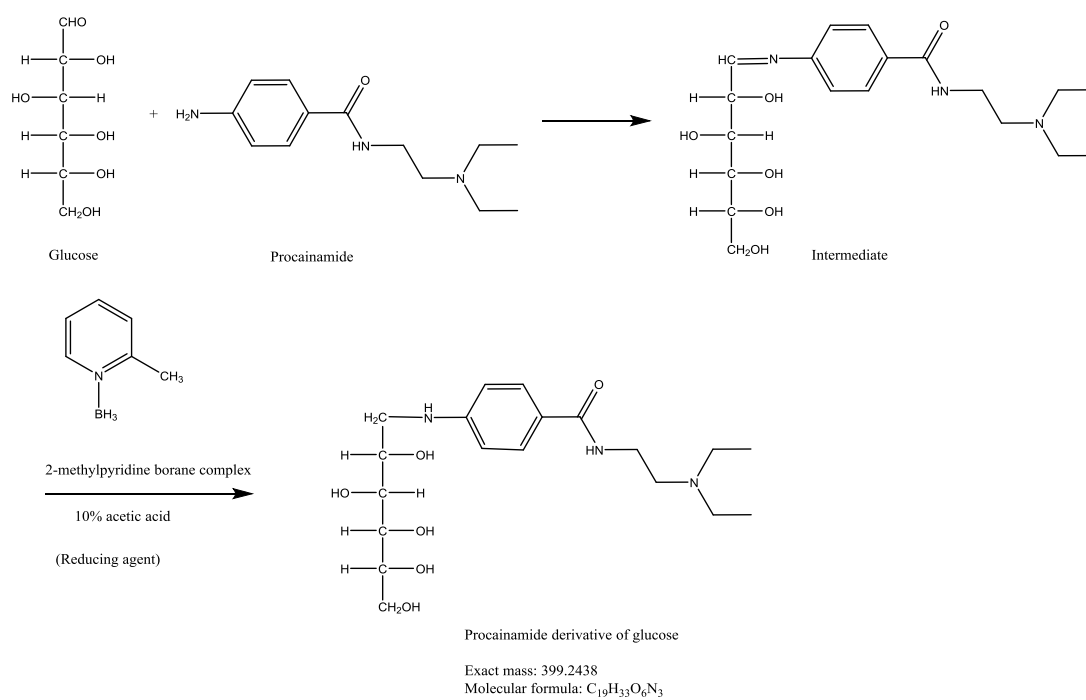


Figure 4.20 Reductive amination of glucose with procainamide in the presence of picoline borane complex.

Figure 4.21 shows an extracted ion trace for galactose procainamide derivative along with the mass spectrum of the derivative. The elemental composition of the protonated molecular ion of the derivative is $C_{19}H_{34}N_3O_6$ (-1.1 ppm).

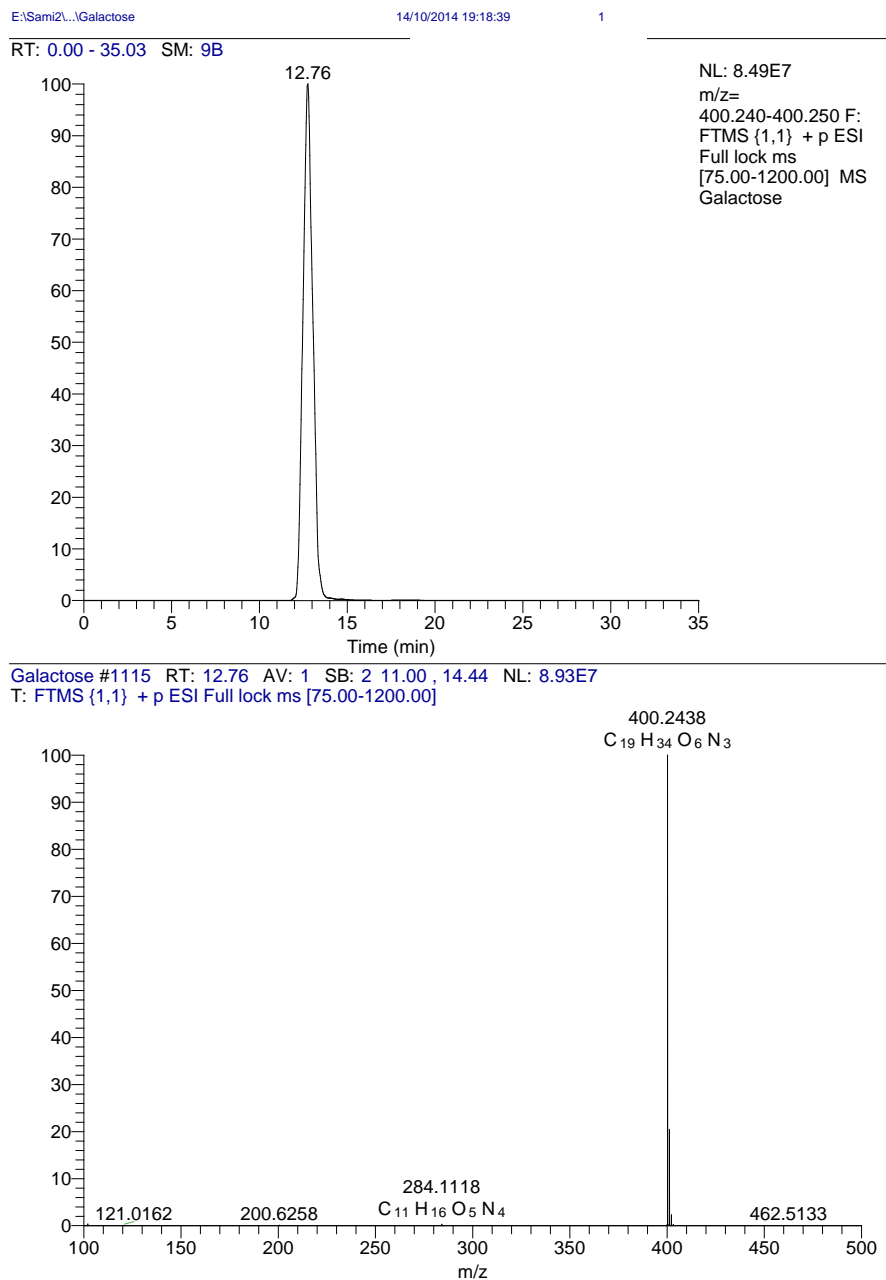


Figure 4.21 Extracted ion chromatogram of the procainamide derivative of galactose

Figure 4.22 shows a comparison between the procainamide derivatives for glucose, galactose, fructose and mannose. There was not much indication that this derivative would be able to separate the sugar isomers.

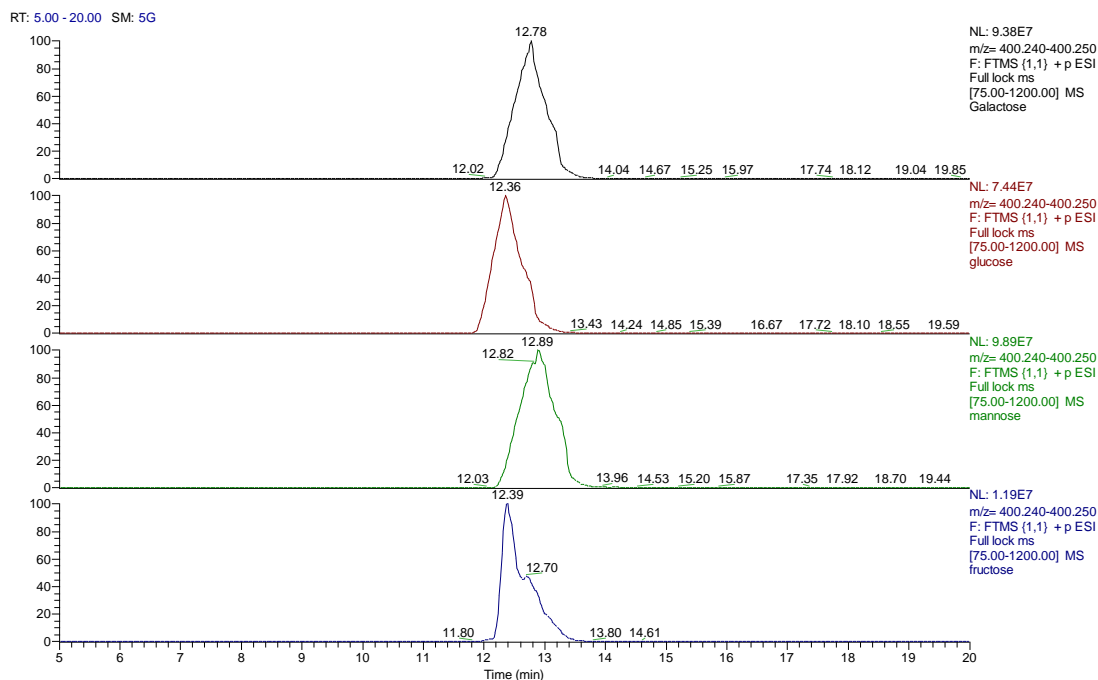
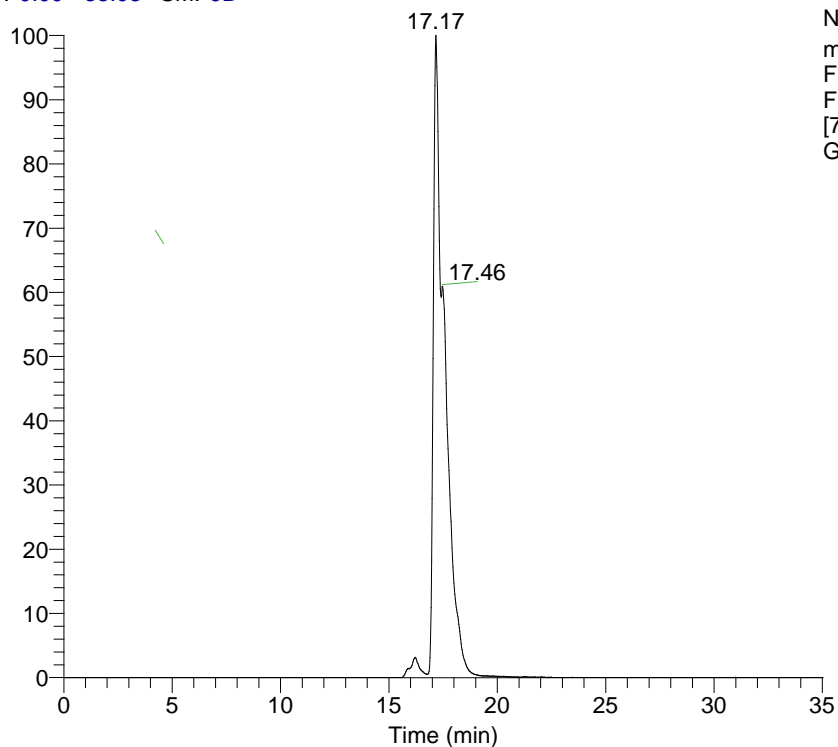


Figure 4.22 Extracted ion chromatograms of the procainamide derivative of galactose, glucose, mannose and fructose.

Figure 4.23 shows the procainamide derivative of galactose-6-phosphate which has a molecular ion at m/z 480.2104 and Figure 4.24 shows the separation of fructose-1-phosphate and galactose, glucose and mannose-6-phosphates as their procainamide derivatives.

RT: 0.00 - 35.03 SM: 9B



NL: 1.99E7
m/z= 480.200-480.220
F: FTMS {1,1} + p ESI
Full lock ms
[75.00-1200.00] MS
Galactose-6

Galactose-6 #1507 RT: 17.15 AV: 1 NL: 2.14E7
T: FTMS {1,1} + p ESI Full lock ms [75.00-1200.00]

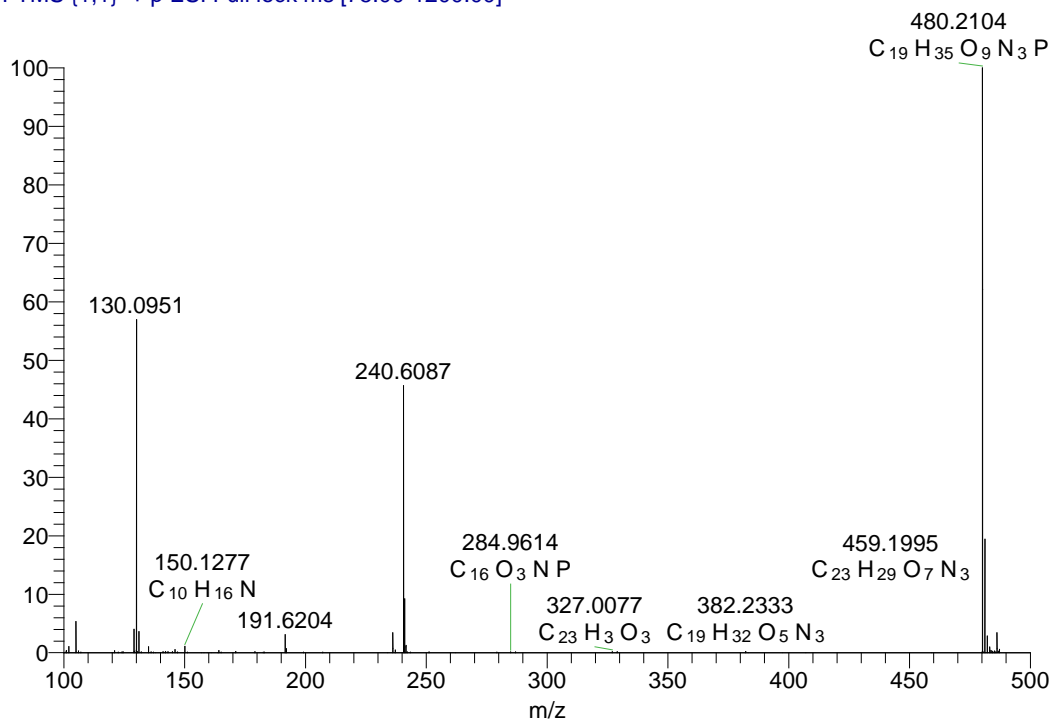


Figure 4.23 Extracted ion chromatograms of the procainamide derivative of galactose-6-phosphate

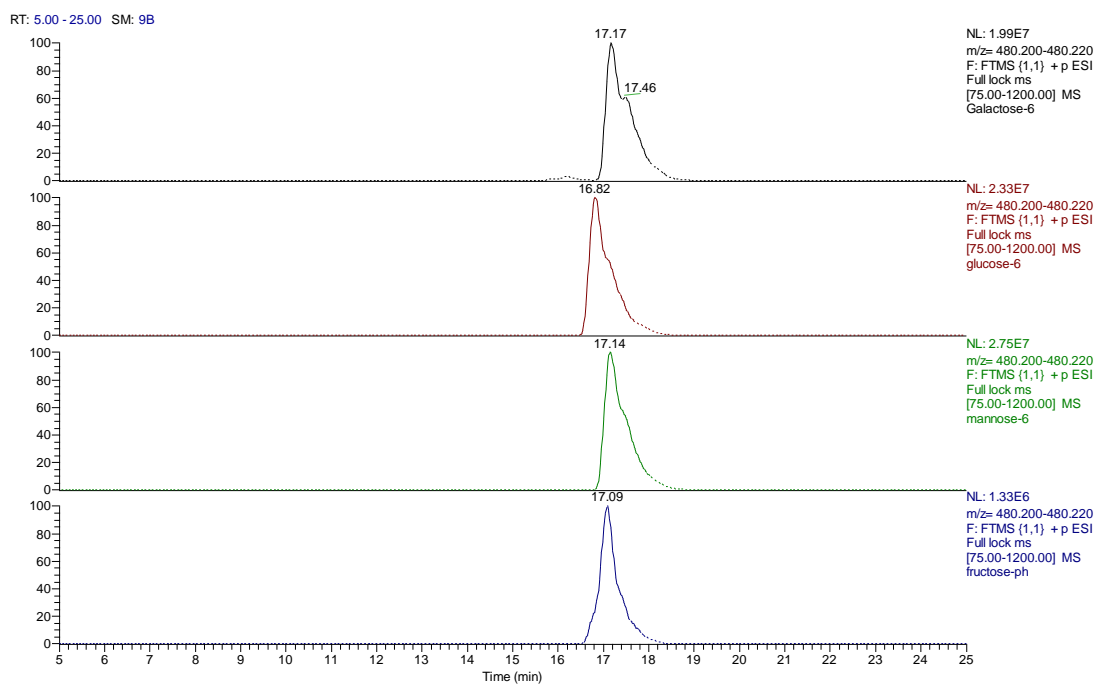


Figure 4.24 Extracted ion chromatograms showing the separation of procainamide derivatives of galactose-6, glucose-6, mannose-6 and fructose-1 phosphates

4.7 Analysis of sugars in brain samples

Figures 4.25 and 4.26 show the chromatograms for glucose, galactose and mannose obtained for the standard mixtures of the sugars. There is ample separation between glucose and galactose and mannose, the latter two being resolved from each other as well, but not quite baseline separated.

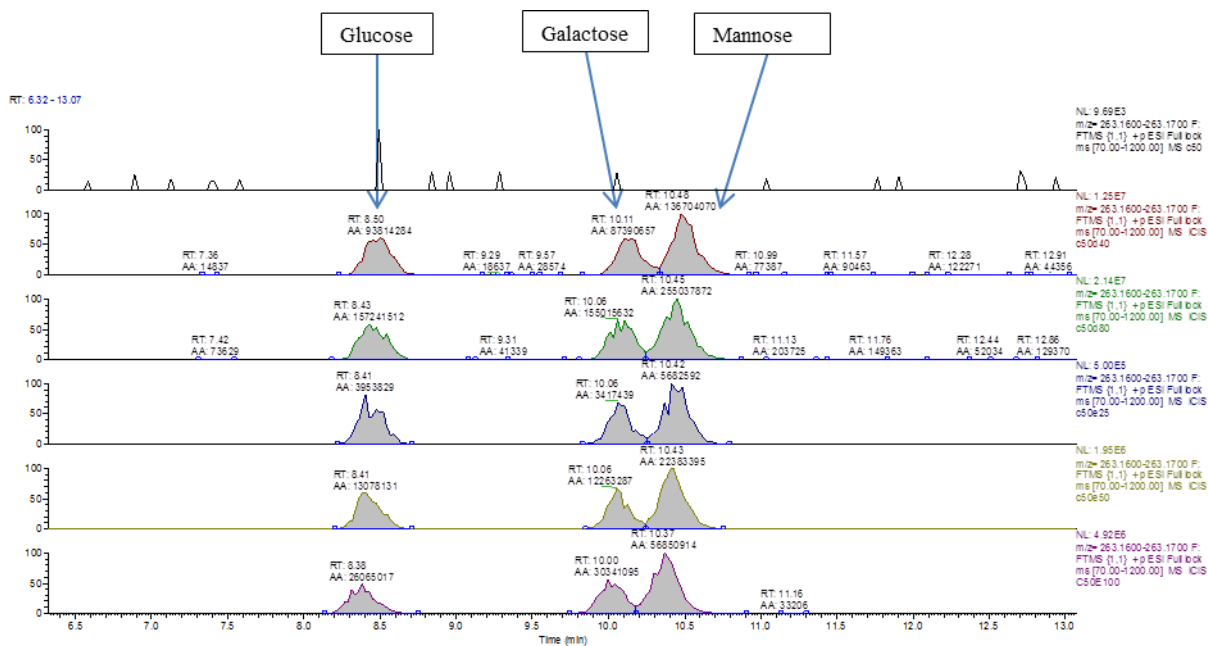


Figure 4.25 Chromatograms showing peaks of glucose, galactose and mannose as derivatives formed reductive amination with pentadeuterated aniline in the calibration series.

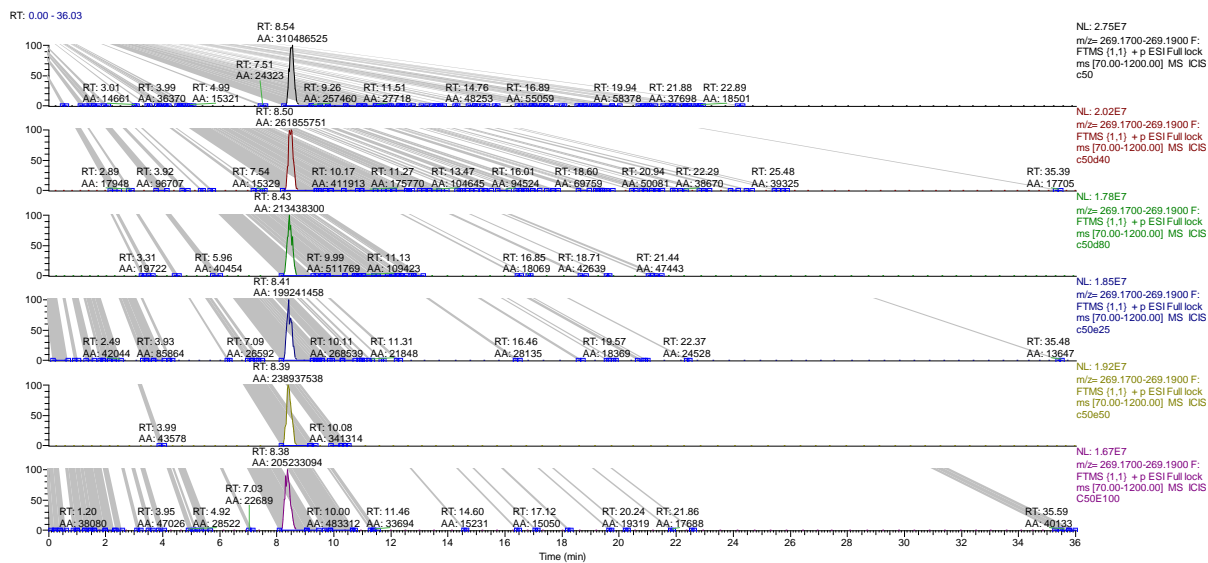


Figure 4.26 Chromatogram showing peaks of ¹³C glucose internal standard as a derivative pentadeuterated aniline spiked into each point in the calibration series.

Table 4.2 summarises the peak areas of each of the sugars and the ¹³C glucose internal standard at each of the five concentrations (0.25, 0.5, 1.0, 2.0 and 4.0 µg/ml) prepared for the

sugars. The internal standard was added in the sample mixtures at a fixed concentration of 10 µg/ml.

Table 4.2 Summary table showing peaks areas and peak area ratios (vs. ^{13}C glucose internal standard) of glucose, galactose and mannose.

Conc. (µg/mL)	^{13}C Glucose	Glucose		Galactose		Mannose	
	Area	Area	Ratio	Area	Ratio	Area	Ratio
0.00	310486525	0	0	0	0	0	0
0.25	199241458	3953829	0.01984	3417439	0.0172	5682592	0.0285
0.50	238937538	13078131	0.05473	12263287	0.0513	22383395	0.0937
1.00	205233094	26065017	0.12700	30341095	0.1478	56850914	0.2770
2.00	261855751	93814284	0.35827	87390657	0.3337	136704070	0.5221
4.00	213438300	157241512	0.73671	155015632	0.7263	255037872	1.1949

The calibration curves of each of the derivatised hexose sugars were plotted as peak area ratios of the derivatised sugar to the $^{13}\text{C}_6$ glucose internal standard. The Figures 4.27-4.29 below show the calibration curves for glucose, galactose and mannose respectively.

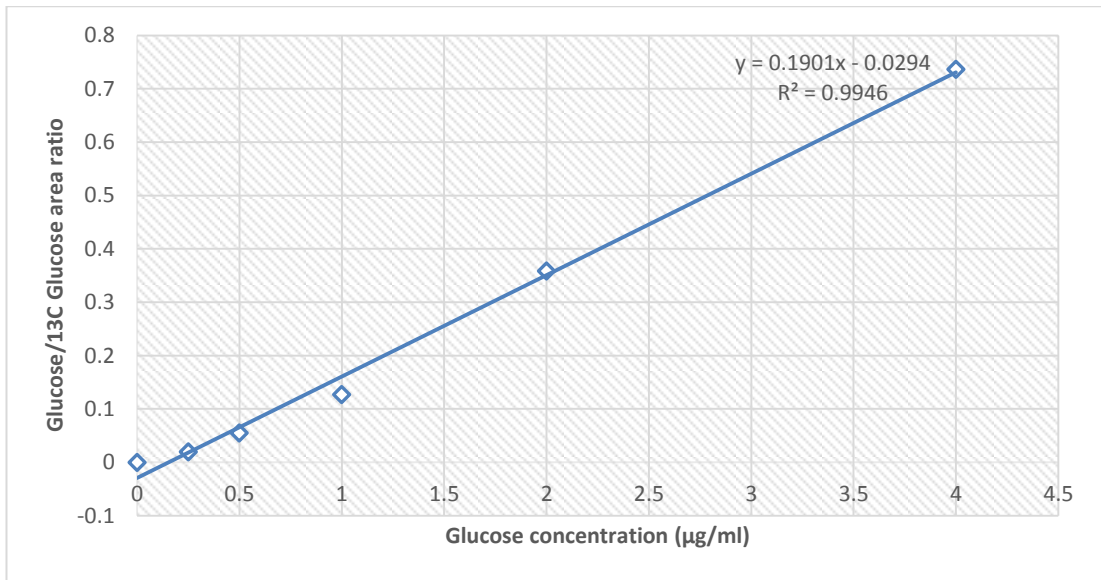


Figure 4.27 Calibration curve for glucose

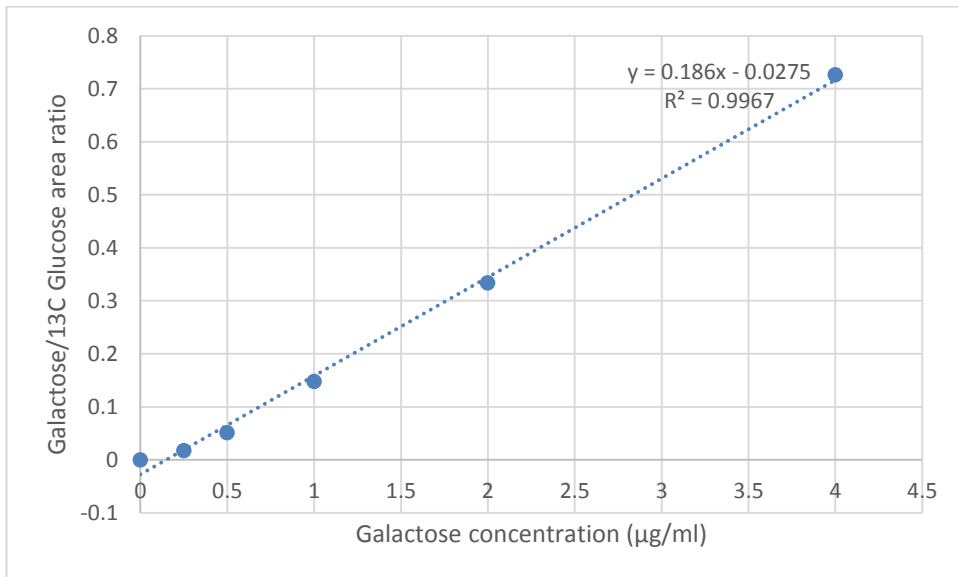


Figure 4.28 Calibration curve for galactose

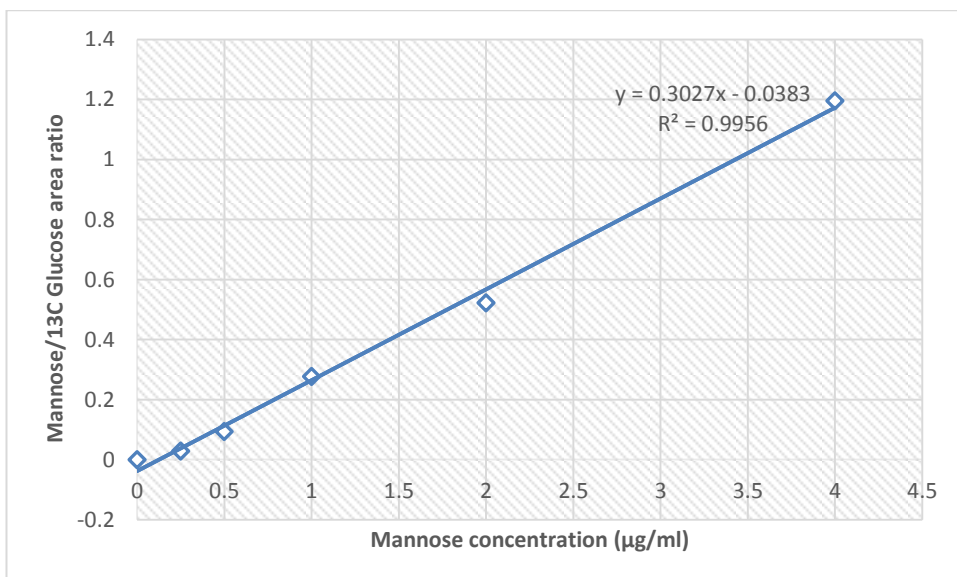


Figure 4.29 Calibration curve for mannose

It can be seen from these calibration curves that linearity (as R^2) was acceptable with values >0.99 in each case. The derivatisation method was then applied to compare sugars in brain samples from normal and schizophrenic patients. The Figure 4.30 below shows the sugar derivatives in a brain sample from a control and schizophrenic brain. There was a trend of higher levels of glucose in brains from people who had suffered from mental illness.

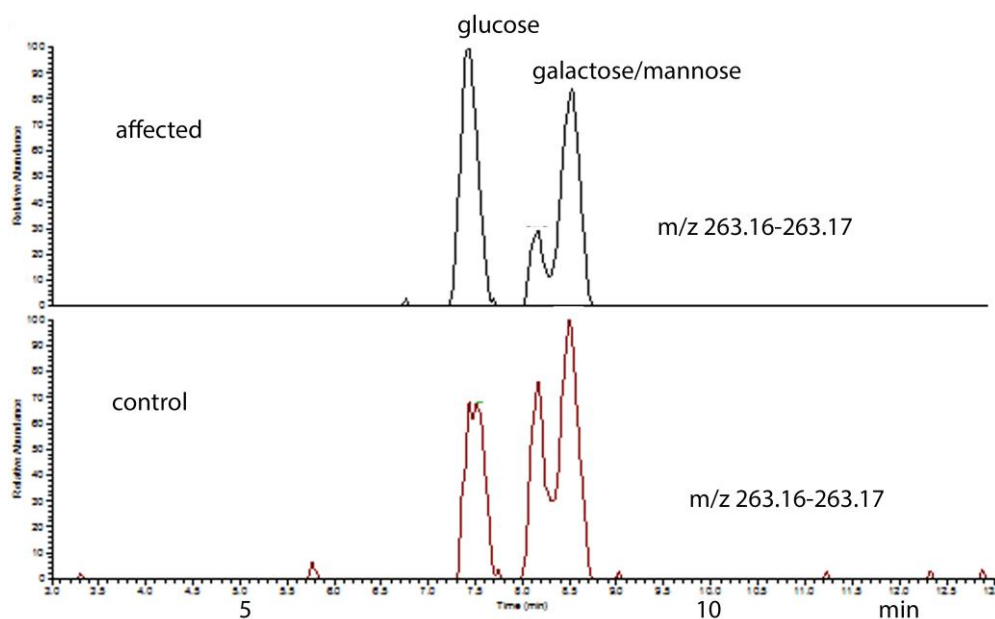


Figure 4.30 Sugars as their deuterioaniline derivatives. The levels of glucose in affected and control samples were estimated as 2.62 μ g/ml and 2.03 μ g/ml respectively.

Thus, in conclusion, the deuterated tag as well as offering the best chromatographic separation was also useful in the characterisation of sugars in the brain as well as additional unknown markers including an abundant unidentified pentose (Figure 4.31). Methods for separating the three common hexoses are rare in the literature. This method is able to do this and has very good potential for monitoring sugar metabolism since the masses of the tagged sugars are very characteristic. For instance metabolism of dietary fibre by the microbiome is complex and the method is currently being applied to the investigation of role that this plays in irritable bowel disease.

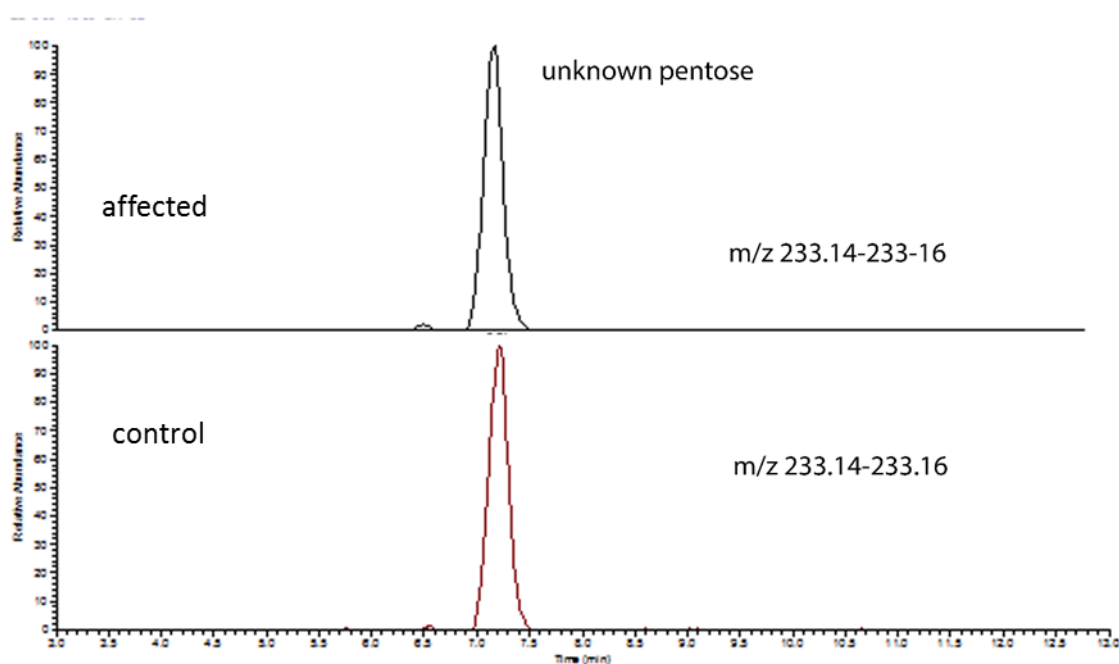


Figure 4.31 An unidentified abundant pentose present in affected and control brain samples.

All pentoses (be it aldopentoses such as arabinose and ribose, or ketopentoses such as ribulose and xylulose) have the same molecular formula ($C_5H_{10}O_5$), implying that they have the same nominal molecular weight (MW) of 150. They are isomers – up to 12 of them. After derivatisation with deuterated aniline (MW 98), the resulting derivatives have nominal MW of 233, due to a net loss of 16 mass units (equivalent to the mass of an oxygen atom). For this reason, it would be impossible to distinguish between these pentoses based on their m/z values. Thus the best way to identify the abundant pentose in the brain tissues analysed would be by use of standards and matching the retention times of their derivatives to the one obtained in this experiment. There is a possibility of coelution of different pentose standards in the ZIC-HILIC column used in this work but this can be overcome by using enantio-specific stationary phases. Alternatively, NMR can be used to confirm the absolute configuration at the chiral centres in order to identify the unknown pentose if it was possible to isolate sufficient material.

Chapter 5:

Metabolomics of Milk Samples

5 Application of hydrophilic interaction chromatography methods to the profiling of mammalian milks

5.1 Introduction

The reasons for the chemical complexity of milk required to support neonatal mammalian development are only partially understood. Beyond the basic functions of nutrition, milk provides immune protection and helps to establish a healthy gut microbiota in young mammals [106-108]. Moreover, the composition of milks must meet the needs of nursing young at changing developmental stages. In previous work the metabolomics profiling of panda milk was carried out and the changes in sugars in the milk post-parturition were found to be very interesting [85, 109] and the composition of oligosaccharides in the milks could be correlated with the growth rate of panda cubs. In the current work samples of seal milk were investigated in order to determine if there were similarities with the milks of land based herbivorous mammals. There has not been extensive work carried out on seal milk and thus it was of interest to determine how milk production is adapted to the environment that seal pups are raised in. It has been previously observed that unlike land based mammals the content of sugars in seal milk is very low. Like pandas seal mothers fast during the early period of lactation and during this time large quantities of lipid are mobilised from their blubber and deposited directly in the blubber of seal pups [110]. It has been observed that metabolism of fatty acids is faster in seals in comparison to other marine mammals and it has been suggested that fat metabolism provides the main source of energy for seals in comparison to other mammals where glycogen stores are depleted prior to the utilisation of fats which only occurs during fasting [111]. It has been observed that the fatty acid content in fur seal milk, since it is derived from the blubber of female seals, reflects the diet of the seals pre-parturition. In fur seals the perinatal fasting period lasts for approximately 7 days

and after this period the females go on foraging trips which may alter the composition of the milk since, during this period, variations in the diet rather than the blubber contributes to the fatty acids in the milk. Table 5.1 shows the variation in the fatty acid composition of seal milk during the different stages of lactation [112]. In the study presented here, untargeted metabolite profiling of milk samples from seals was carried out, using a Hydrophilic Interaction Liquid Chromatography - High Resolution Mass Spectrometry (HILIC-HRMS) method. By using multivariate analysis, principal components analysis (PCA) and hierarchical cluster analysis (HCA) and orthogonal partial least squares (OPLS) regression analysis the changes in small molecule classes were mapped at four time points over 18-19 days post-partum. Further characterisation was conducted using MS/MS for key chemical components discovered from the multivariate analysis.

Table 5.1 Fatty acid content (% of total fat content) of fur seal milk during different periods of lactation (analysed by gas chromatography) by Iverson *et al.*, 1997 [112].

Fatty acid	Perinatal (N = 19)	Early foraging (N = 11)	Mid foraging (N = 11)	Late foraging (N = 8)
Percent fat*	40.8±1.56a	44.0±3.12a	42.1±1.92a	55.1±2.41b
12:0	0.15±0.011	0.16±0.009	0.17±0.007	0.16±0.009
14:0	3.94±0.165	7.65±0.422	8.74±0.347	6.94±0.222
14:1n-9,7	0.12±0.014	0.11±0.019	0.13±0.015	0.14±0.008
14:1n-5	0.28±0.024	0.30±0.019	0.30±0.011	0.21±0.012
Iso15	0.16±0.003	0.19±0.009	0.19±0.012	0.20±0.005
15:0	0.36±0.010	0.31±0.008	0.30±0.007	0.32±0.014
Iso16	0.15±0.005	0.11±0.011	0.11±0.006	0.13±0.004
16:0	15.91±0.306	17.99±0.352	18.49±0.276	16.50±0.216
16:1n-11	0.49±0.021	0.36±0.016	0.35±0.012	0.39±0.005
16:1n-9	0.62±0.022	0.29±0.021	0.26±0.010	0.25±0.013
16:1n-7	6.57±0.262	9.56±0.393	9.44±0.401	7.10±0.213
7Me16:0	0.23±0.008	0.22±0.011	0.25±0.005	0.26±0.004
16:1n-5	0.33±0.006	0.27±0.015	0.26±0.008	0.29±0.004
Iso17	0.18±0.003	0.16±0.008	0.17±0.007	0.20±0.011
16:2n-4	0.32±0.015	0.18±0.030	0.12±0.019	0.20±0.008
16:3n-6	0.22±0.018	0.62±0.049	0.69±0.033	0.49±0.020
17:0	0.40±0.016	0.36±0.017	0.35±0.012	0.35±0.010
17:1	0.56±0.017	0.33±0.020	0.28±0.008	0.29±0.021
16:3n-1	0.31±0.008	0.25±0.012	0.26±0.008	0.26±0.012
16:4n-1	0.09±0.016	0.32±0.034	0.34±0.018	0.42±0.030
18:0	2.12±0.061	1.87±0.083	1.76±0.066	2.10±0.026
18:1n-11	1.93±0.087	0.54±0.116	0.35±0.113	0.62±0.160
18:1n-9	29.86±0.615	18.23±0.977	15.87±0.214	15.57±0.771
18:1n-7	5.23±0.204	6.21±0.392	6.33±0.193	4.83±0.132
18:1n-5	0.48±0.015	0.34±0.041	0.29±0.026	0.50±0.019
18:2n-6	1.69±0.056	1.35±0.040	1.36±0.031	1.31±0.028
18:3n-6	0.08±0.005	0.13±0.008	0.15±0.003	0.16±0.004
18:3n-4	0.22±0.011	0.18±0.010	0.16±0.018	0.14±0.008
18:3n-3	0.46±0.015	0.43±0.012	0.50±0.017	0.57±0.015
18:4n-3	0.38±0.029	0.81±0.051	0.91±0.038	1.06±0.041
18:4n-1	0.23±0.022	0.39±0.022	0.44±0.034	0.57±0.030
20:1n-11	0.91±0.065	0.38±0.056	0.25±0.059	0.08±0.078
20:1n-9	4.79±0.241	2.90±0.381	3.03±0.473	7.38±0.461
20:1n-7	0.31±0.012	0.33±0.014	0.32±0.014	0.40±0.013
20:2n-6	0.22±0.011	0.13±0.019	0.11±0.013	0.18±0.011
20:3n-6	0.16±0.006	0.15±0.008	0.14±0.008	0.17±0.008
20:4n-6	0.72±0.025	0.46±0.027	0.40±0.014	0.46±0.015
20:4n-3	0.92±0.041	0.81±0.038	0.92±0.048	1.24±0.044
20:5n-3	4.77±0.379	11.16±0.573	12.53±0.339	10.37±0.176
22:1n-11	0.76±0.060	0.68±0.186	0.81±0.209	2.65±0.282
22:1n-9	0.51±0.030	0.46±0.068	0.49±0.074	1.09±0.087
22:2n-6	0.13±0.023	0.19±0.036	0.15±0.033	0.22±0.037
21:5n-3	0.24±0.009	0.46±0.020	0.47±0.015	0.46±0.015
22:4n-6	0.07±0.008	0.13±0.060	0.03±0.007	0.03±0.013
22:5n-3	2.20±0.073	2.43±0.100	2.36±0.120	2.04±0.042
22:6n-3	7.58±0.236	8.04±0.518	7.37±0.419	8.18±0.315
24:1	0.23±0.018	0.27±0.049	0.26±0.032	0.60±0.060

5.2 Materials and methods

5.2.1 Chemicals and reagents

Ammonium carbonate and HPLC grade acetonitrile and methanol were purchased from Sigma-Aldrich, UK. HPLC grade water was produced by a Direct-Q 3 Ultrapure Water

System from Millipore, UK. The mixtures of metabolite authentic standards were prepared as previously described [113, 114] from standards obtained from Sigma Aldrich, UK.

5.2.2 Milk Samples

The seal milk samples were provided as part of a collaboration by Dr Paddy Pomeroy and Professor Malcolm Kennedy of Glasgow University. They were obtained from the Isle of May colony of Atlantic grey seals (*Halichoerus grypus*).

5.2.3 Preparation of milk samples

In order to analyse the more polar fraction of the milk samples (0.5 mL) were thawed at room temperature and then centrifuged for 10 minutes at 15,000 rpm at 4°C (Eppendorf 5424 R, maximum RCF = 21.130g). An aliquot of the supernatant (200µl) was mixed with acetonitrile (800µl). The solution was mixed thoroughly and emulsion was centrifuged for 10 minutes at 15,000 rpm at 4°C (Eppendorf 5424 R, maximum RCF = 21.130g). The supernatant was transferred to an HPLC vial for Liquid Chromatography-Mass Spectrometry (LC-MS) analysis. The lipids in the milk were analysed by mixing 200 µl of the whole milk with 800 µl of isopropanol. The solution was mixed thoroughly and emulsion was centrifuged for 10 minutes at 15,000 rpm at 4°C (Eppendorf 5424 R, maximum RCF = 21.130g). The supernatant was transferred to an HPLC vial for Liquid Chromatography-Mass Spectrometry (LC-MS) analysis.

5.2.4 HILIC-HRMS and multiple tandem HRMS analysis and data processing

Sample analysis was carried out on an Accela 600 HPLC system combined with an Exactive (Orbitrap) mass spectrometer (Thermo Fisher Scientific, UK). An aliquot of each sample solution (10µL) was injected onto a ZIC-pHILIC column (150 × 4.6mm, 5µm; HiChrom, Reading UK) with mobile phase A: 20mM ammonium carbonate in HPLC grade water (pH 9.2), and B: HPLC grade acetonitrile. The gradient programme was as follows: 80% B (0

min) 20 % B (30 min) 5% B (36 min) 80% B (37 min) 80% B (45 min). Peak extraction and alignment were calculated by integration of the area under the curve, using MZMine 2.14 software, as previously described [115]. Resulting data were searched against an in house metabolite database and were then exported for multivariate analysis using Simca P 14.

Similar procedures were used for the lipids analysis which was carried out on an ACE Silica gel column (150 x 3 mm, 3 µm particle size) with mobile phase A 20 mM ammonium formate in water isopropanol (80:20) and mobile phase B acetonitrile/isopropanol (20:80). The flow rate was 0.3 mL/min and gradient was as follows: 0–1 min 8% B, 5 min 9% B, 10 min 20% B, 16 min 25% B, 23 min 35% B, 26–40 min 8% B [116].

5.2.5 Multivariate analysis

The mass spectrometry data files were extracted using m/zMine 2.14 and the extracted features were searched against an in house data base drawn from the Human Metabolome Database, KEGG and Lipid Maps. SIMCAP version 14.0 (Umetrics, Umeå, Sweden) was used for multivariate analysis including PCA, HCA, Orthogonal Partial Least Squares Discriminant Analysis (OPLS-DA) and Orthogonal Partial Least Squares (OPLS). The data were mean centred, and Pareto scaled for PCA, HCA and OPLS.

5.3 Results

Figure 5.1 shows a PCA model of seal milk samples in comparison to cow, camel and goat milk. The data was Pareto scaled and the PCA separation is based on 83 variables. As can be seen in Figure 5.2 most of the variation (98.8%) is explained by four components giving a very strong discriminatory model. It is clear that the difference between the milks from the land based mammals and seal milk is much greater than the difference between the milks from cow, goat and camel. Also the changes between 2/8 day seal milk and 13 day seal milk

are very marked. The importance of the major variables can be seen from the VIP scores shown in Table 5.2.

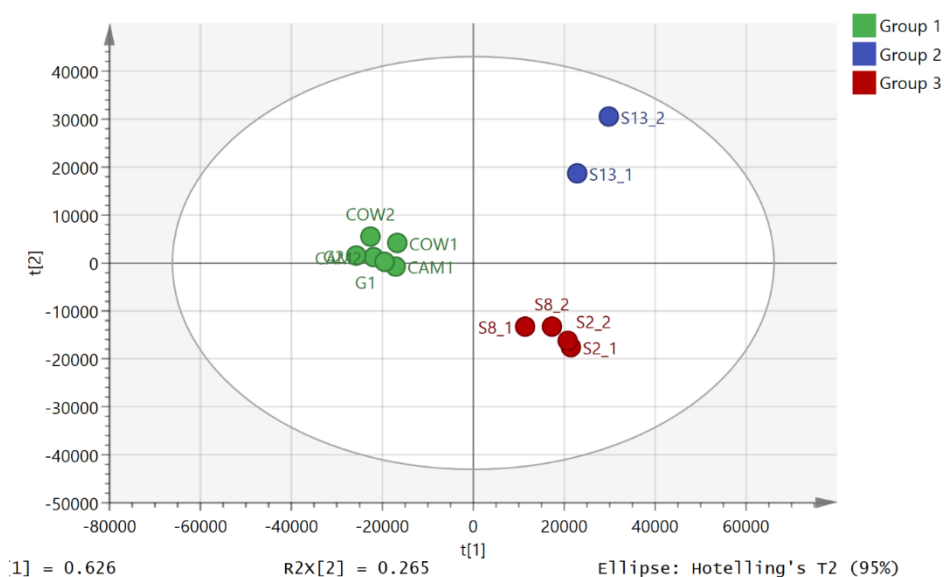


Figure 5.1 PCA analysis of mammalian milks showing the separation between cow, goat and camel and seal milk at 8 and 13 days post-partum. The separation is based on 83 key metabolites.

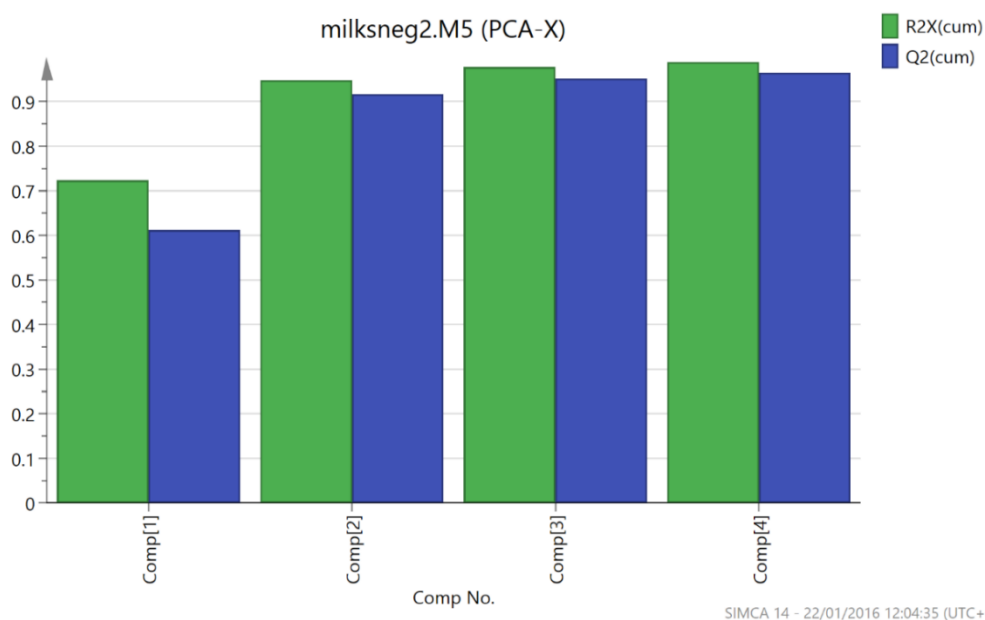


Figure 5.2 Most important components for discriminating land based mammalian milks from seal milk.

Table 5.2 shows the most important metabolites detected in negative ion mode that discriminate between milk from the land based mammals and seal milk. The most striking difference is the lack of lactose in the seal milk which is one of the major components in the milks of the land based mammals. Figure 5.3 shows the extracted ion traces for lactose in cow, camel, goat and seal milk. There are traces of lactose in seal milk at about 0.1% of the levels in the other milks.

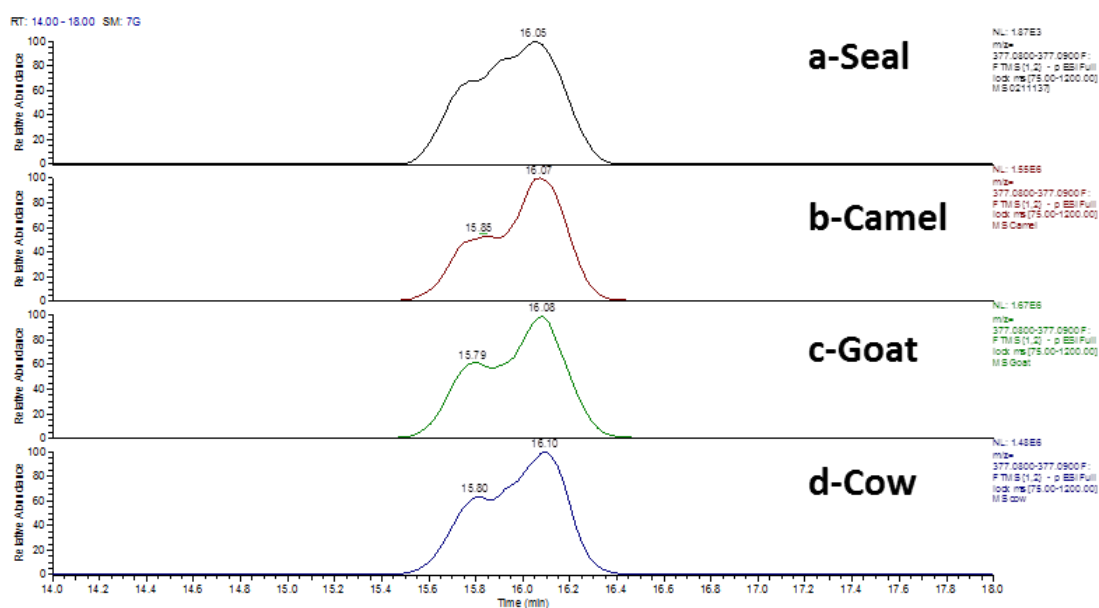


Figure 5.3 Extracted ion traces for lactose as its chloride adduct in seal, camel, goat and cow milks.

Table 5.2 The most important metabolites observed in negative ion mode distinguishing seal milk from camel/goat/cow (CGC) milk. Positive VIPs correlate with seal milk and negative VIP values correlate with CGC milk.

m/z	Rt (min)	Mol formula	Metabolite	VIP score
409.236	4.8	C19H39O7P	LPA 16:0	7.18
255.233	4.8	C16H32O2	Hexadecanoic acid	6.85
435.252	4.8	C21H41O7P	LPA 18:1	5.92
464.278	4.8	C22H44NO7P	LPC 14:1	5.08
494.325	4.8	C24H50NO7P	LPC 16:0	5.07
301.217	3.8	C20H30O2	Eicosapentaenoic acid	4.51
152.996	4.8	C3H7O5P	Propanoyl phosphate	4.50
125.001	4.7	C2H7O4P	Ethyl phosphate	4.28
556.326	4.8	C28H43N7O5	Lys-Lys-Trp-Pro	4.13
480.31	4.7	C23H48NO7P	LPE 18:0	3.54
275.202	3.8	C18H28O2	Octadecatetraenoic acid	3.11
253.218	3.9	C16H30O2	Hexadecenoic acid	3.08
309.28	3.8	C20H38O2	Eicosenoic acid	3.03
124.007	14.8	C2H7NO3S	Taurine	2.88
327.233	3.8	C22H32O2	Docosahexaenoic acid	2.73
419.257	4.7	C21H41O6P	CPA(18:0/0:0)	2.72
437.267	4.6	C21H43O7P	LPA 18:0	2.59
227.202	5.0	C14H28O2	Tetradecanoic acid	2.57
407.221	5.0	C19H37O7P	Palmitoylglycerone phosphate	2.25
303.233	3.8	C20H32O2	Eicosatetraenoic acid	2.20
271.228	5.2	C16H32O3	Hydroxypalmitate	2.20

381.205	5.0	C17H35O7P	LPA 14:0	2.18
212.002	7.1	C8H7NO4S	Indoxylsulfate	2.01
192.067	6.0	C10H11NO3	Phenylacetyl glycine	-1.19
740.524	3.9	C41H76NO8P	PE 36:3	-1.25
126.905	10.3	HI	Hydrogen iodide	-1.36
125.024	16.2	C6H6O3	Phloroglucinol	-1.50
178.051	6.5	C9H9NO3	Hippurate	-1.56
139.976	8.0	CH4NO5P	Carbamoyl phosphate	-1.89
341.11	16.1	C12H22O11	Lactose	-2.74
377.086	16.1	C12H23O11Cl	Lactose chloride adduct	-5.62

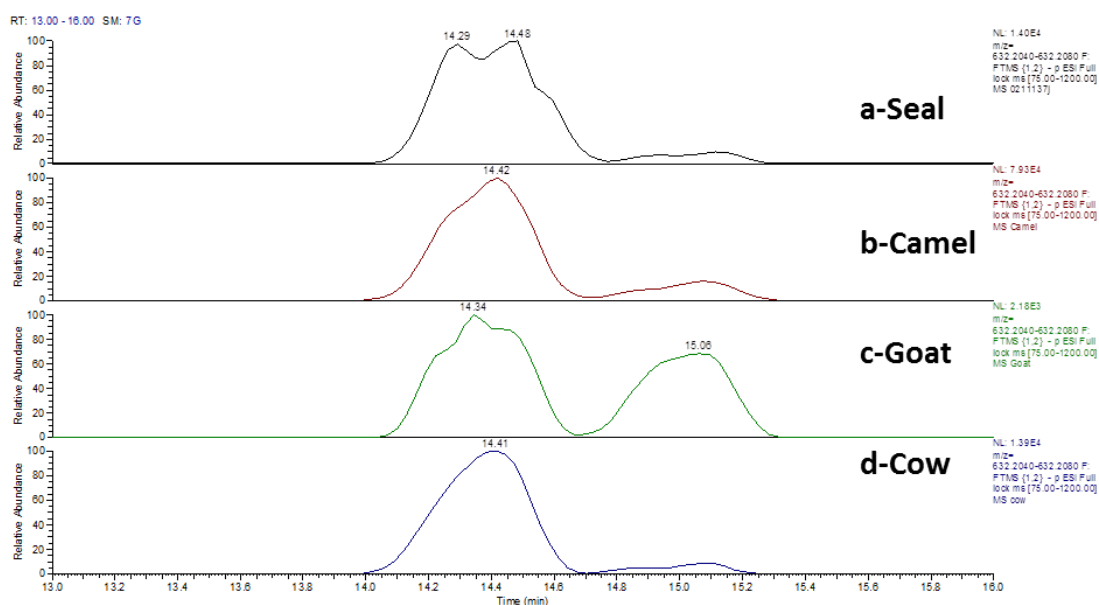


Figure 5.4 Extracted ion traces for sialyl lactose in seal, camel, goat and cow milks.

In seal milk the greatest emphasis is on lipids as an energy source and this reflects earlier studies on fat metabolism in seals [85, 109]. This is a striking contrast which suggests a very different type of energy metabolism in seal pups in comparison with land based mammals,

which does not utilise carbohydrates. Although lactose is absent from seal milk, the antimicrobial carbohydrate sialyl lactose is present at similar levels to those observed for the terrestrial mammals (Figure 5.4). In seals there must be some compensation mechanism that allows production of glycogen stores since during intense physical effort muscles utilise glycogen as a fuel rather than fats [111]. The maximum rate of ATP re-synthesis from fatty acids is about $0.40 \text{ mol min}^{-1}$, while anaerobic breakdown of glycogen can generate from 1.0 to $2.0 \text{ mol of ATP min}^{-1}$ [110]. Thus during high-intensity exercise, the rate of ATP breakdown is too high to be matched by the rate of ATP synthesis from fatty acids. The most important lipids are lysolipids and fatty acids. The most important lyso lipid in the model is C16:0 lysophosphatidic acid (LPA) (extracted ion traces shown in Figure 5.5).

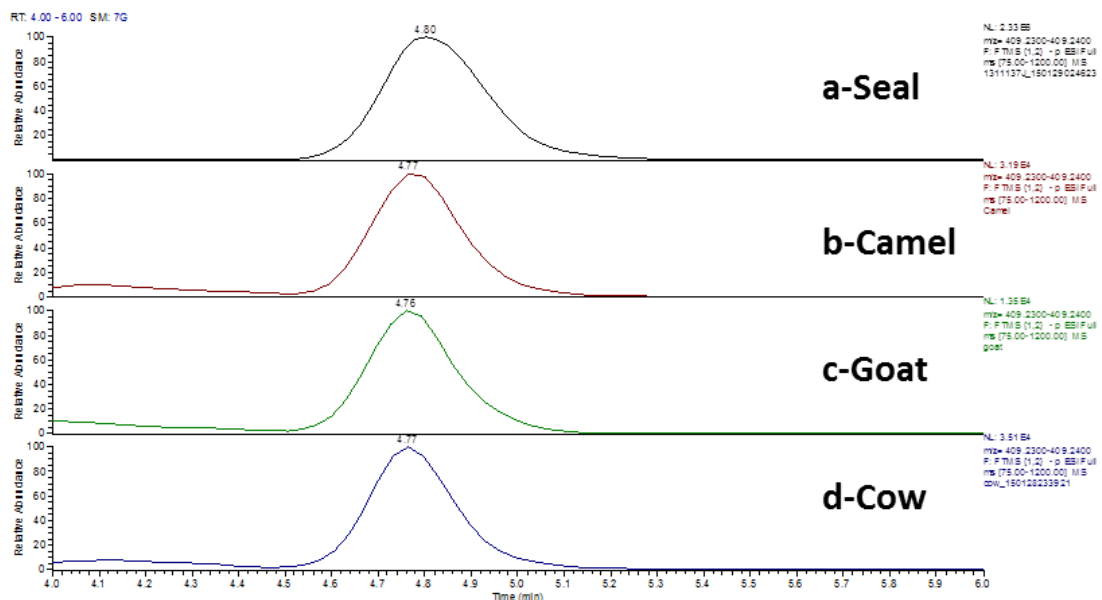


Figure 5.5 Extracted ion traces showing lysophosphatidic acid (LPA; C16:0) in seal, camel, goat and cow milk.

LPAs are important signalling molecules and promote a whole range of functions concerned with cellular growth. Although the PCA model separates the mammalian milks it does not emphasise the relative abundance of different components in the milks. In Table 5.3 the top ten components in each milk sample are listed by their abundance according to mass

spectrometry response. This data suggests that, with regard to the major components, the compositions of the four milks are not that different except for the almost complete absence of lactose in seal milk. All the milks are rich in fatty acids with the land based mammals having abundant C18 and C16 fatty acids whereas eicosapentaenoic and docosahexanoic acids are much more abundant in seal milk reflecting the high content of these fatty acids in the diet of the seals.

Table 5.3 Top ten features by intensity in camel, cow, goat and seal milks in negative ion mode.

Camel	Intensity	Cow	Intensity	Goat	Intensity	Seal 8 days	Intensity
Lactose chloride adduct	2.28E+07	Lactose chloride adduct	2.18E+07	Octadecenoic acid	2.85E+07	Octadecenoic acid	1.50E+08
Octadecenoic acid	1.58E+07	Octadecanoic acid	1.70E+07	Lactose chloride adduct	2.48E+07	Eicosapentaenoic acid	1.15E+08
Hexadecenoic acid	1.51E+07	Linoleate	1.52E+07	Linoleate	7992773	Docosahexaenoic acid	7.84E+07
Linoleate	8241124	Tetradecanoic acid	1.34E+07	Octadecanoic acid	7224366	Hexadecenoic acid	7.47E+07
Hexadecanoic acid	7566466	Hippurate	6419543	Hippurate	7213337	Eicosenoic acid	7.35E+07
Tetradecanoic acid	5014556	Hexadecanoic acid	5533933	Tetradecanoic acid	6244724	Docosapentenoic acid	5.69E+07
Octadecanoic acid	4260767	Chloride adduct N-acetyl glycosamine	5167145	Hypoxanthine	5218183	Octadecatetraenoic acid	4.45E+07
Hydrogen iodide	3991333	Hexadecenoic acid	4867438	Hydrogen iodide	4660091	Hexadecanoyl-glycerophosphate	4.14E+07
Octadecatrienoic acid	3523574	Orotate	4209191	Taurine	4644786	Hexadecanoic acid	3.82E+07

The high level of octadecenoic acid in the seal milk is in agreement with data in shown in Table 5.1 where it is most abundant fatty acid in seal milk during early lactation. This suggests that these acids might be used as energy substrates by the seals as well as being required for cell membrane formation. The metabolism of such long chain fatty acids usually occurs in peroxisomes rather than in the mitochondria and this suggests the metabolism of the seals must be quite different from that of the land based mammals. The seal milks have higher levels of taurine in them (Figure 5.6) and this is probably because the increased dependence on fats for energy metabolism because taurine is required to make taurocholic acid which is a bile acid which is required for the absorption of fats. Taurocholic acid itself is also present in small amounts in milk but does not differ between the milks except for in goat milk where it is much higher (Figure 5.6).

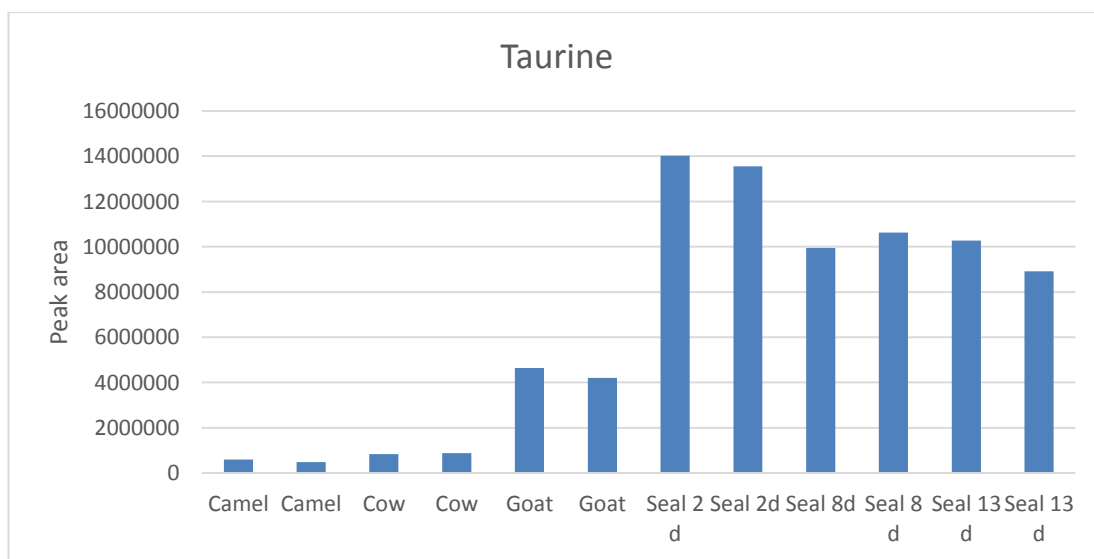


Figure 5.6 The relative levels of taurine in different mammalian milks.

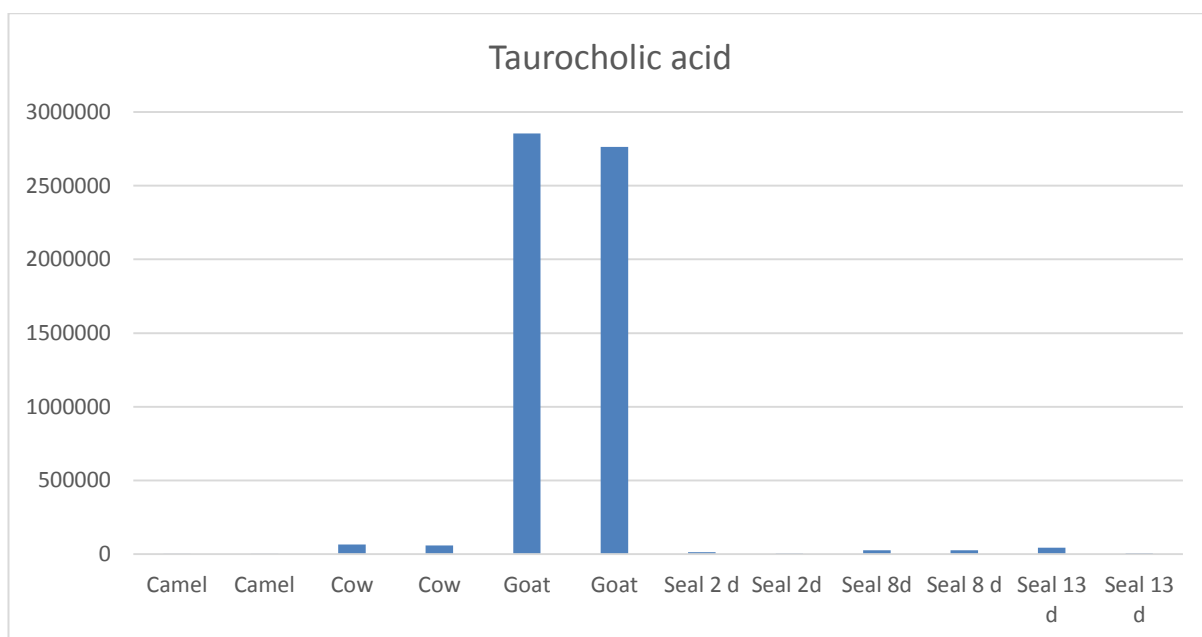


Figure 5.7 The relative levels of taurocholic acid in different mammalian milks.

The levels of iodide in the goat, camel and cow milks are much higher than that in seal milk. Domestic animals receive iodine supplementation in their feedstuffs and another potential source of iodine is from teat washes. There has been some concern that too much iodide is present in milks and that this might not be healthy for those consuming it [113, 114].

Figure 5.8 shows the separation of the different mammalian milks based on positive ion data and Table 5.4 shows the most important metabolites for distinguishing between the milks from the land based mammals and the seal milk. Many of the metabolites are related to the lipids which were observed in the negative ion data but there is a major group of metabolites which have a high biological significance.

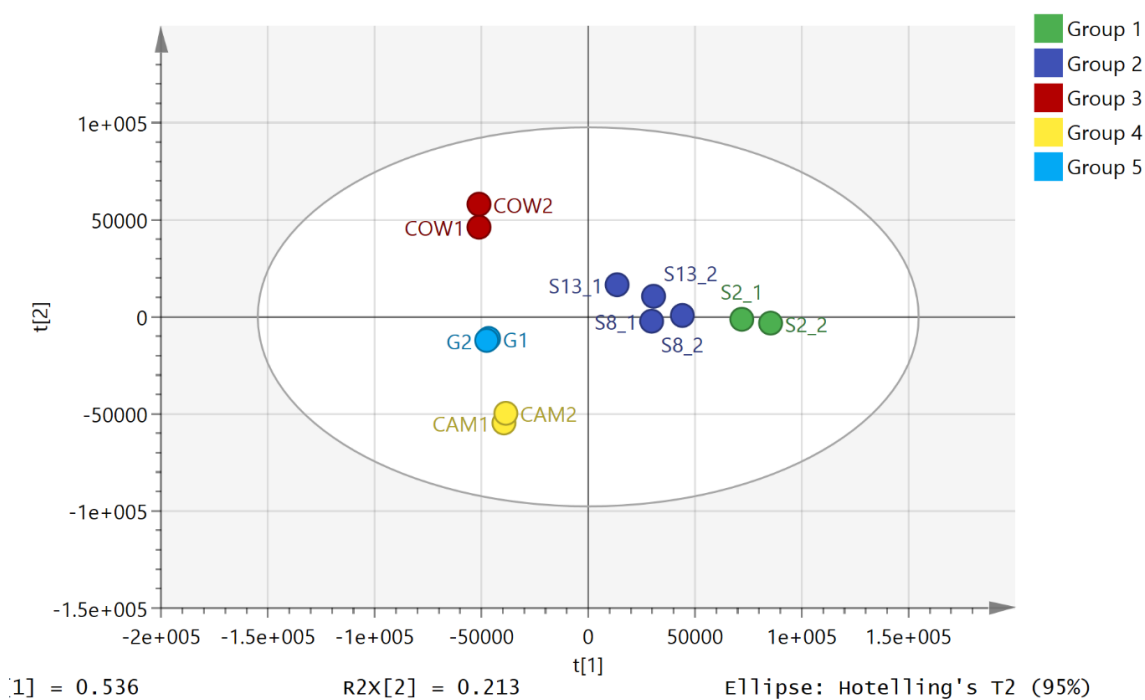


Figure 5.8 PCA separation of cow, goat, camel and seal milks based on positive ion mass spectrometry data.

Table 5.4 The most important metabolites in positive ion mode distinguishing seal milk from camel/goat/cow (CGC) milk. Positive VIPs correlate with seal milk and negative VIP values correlate with CGC milk.

Var ID (Primary)	m/z	Rt	Molecular formula	Metabolite	VIP
262	496.34	4.8	C ₂₄ H ₅₀ NO ₇ P	Hexadecanoyl-glycero-phosphocholine	17.89
194	258.11	14.4	C ₈ H ₂₀ NO ₆ P	Glycero-phosphocholine	16.88
283	524.371	4.6	C ₂₆ H ₅₄ NO ₇ P	Octadecanoyl-glycero-phosphocholine	7.40
252	468.309	5.0	C ₂₂ H ₄₆ NO ₇ P	Tetradecanoyl-glycero-phosphocholine	5.73
71	138.055	11.8	C ₇ H ₇ NO ₂	Anthranilate	5.21
131	174.087	14.1	C ₆ H ₁₁ N ₃ O ₃	Guanidino-oxopentanoate	5.00
33	114.066	9.7	C ₄ H ₇ N ₃ O	Creatinine	4.81
53	127.05	11.7	C ₅ H ₆ N ₂ O ₂	Thymine	4.48

281	522.356	4.7	C26H52NO7P	Oleoylglycerophosphocholine	4.26
46	123.055	7.1	C6H6N2O	Nicotinamide	4.01
824	104.107	14.4	C5H13NO	Choline	3.70
101	155.045	10.4	C6H6N2O3	Imidazol-5-yl-pyruvate	3.41
257	482.324	4.7	C23H48NO7P	Pentadecanoyl-glycero-phosphocholine	3.34
260	494.324	4.8	C24H48NO7P	Hexadecenoyl-glycero-phosphocholine	3.33
57	129.066	13.4	C5H8N2O2	5,6-Dihydrothymine	2.88
271	510.355	4.7	C25H52NO7P	LysoPC(17:0)	2.61
87	146.092	15.0	C5H11N3O2	Guanidinobutanoate	2.55
75	141.066	9.6	C6H8N2O2	Methylimidazoleacetic acid	2.53
126	169.061	7.9	C7H8N2O3	2,3-Diaminosalicylic acid	2.46
150	184.133	11.0	C10H17NO2	Acetylpsudotropine	2.36
199	266.139	8.3	C14H19NO4	Benzyloxycarbonyl-L-leucine	2.08
50	126.022	14.7	C2H7NO3S	Taurine	2.06
52	127.05	8.7	C5H6N2O2	Thymine	1.95
153	188.128	12.1	C9H17NO3	8-Amino-7-oxononanoate	1.90
279	520.34	4.7	C26H50NO7P	Octadecadienoyl-3-phosphocholine	1.85
333	780.554	4.0	C44H78NO8P	Hexadecenoyl-eicosatetraenoyl-glycero-3-phosphocholine	1.81
64	132.077	14.6	C4H9N3O2	Creatine	1.66
560	127.039	16.1	C6H6O3	Phloroglucinol	-1.15
1329	675.497	3.7	C37H71O8P	Hexadecanoyl-2-octadecenoyl-glycero-3-phosphate	-1.17
1259	593.418	3.8	C31H61O8P	Ditetradecanoyl-glycero-3-phosphate	-1.17
322	744.554	3.9	C41H78NO8P	[PE (18:0/18:2)] 1-octadecanoyl-2-(9Z,12Z-octadecadienoyl)-sn-glycero-3-phosphoethanolamine	-1.20
1283	621.45	3.8	C33H65O8P	Dipentadecanoyl-glycero-3-phosphate	-1.23

174	220.118	8.8	C9H17NO5	Pantothenate	-1.26
1306	649.481	3.7	C35H69O8P	PA(16:0/16:0)	-1.27
574	147.076	14.8	C5H10N2O3	L-Glutamine	-1.29
674	703.528	3.7	C39H75O8P	Octadecanoyl-octadecenoyl-glycero-3-phosphate	-1.31
679	706.599	3.7	C39H82N2O6P	SM 34:0	-1.32
628	342.139	16.2	C12H23NO10	Glucosylglucosamine	-1.33
716	742.538	3.9	C41H76NO8P	Octadecenoyl-octadecadienoyl-glycero-3-phosphoethanolamine	-1.36
110	158.117	10.1	C8H15NO2	Homostachydrine	-1.47
329	760.585	4.0	C42H82NO8P	PC 34:1	-1.50
89	146.118	13.4	C7H15NO2	Acetylcholine	-2.41
171	218.139	9.9	C10H19NO4	O-Propanoylcarnitine	-2.84
186	246.17	8.0	C12H23NO4	O-Pentanoylcarnitine	-3.05
183	232.154	8.9	C11H21NO4	O-Butanoylcarnitine	-3.48
165	204.123	11.1	C9H18NO4	O-Acetylcarnitine	-4.90
114	160.133	13.4	C8H17NO2	DL-2-Aminooctanoicacid	-6.35
629	343.123	16.1	C12H22O11	lactose	-7.16

In seal milk metabolites of the nicotinamide pathway are highly evident. Figure 5.9 shows extracted ion traces for anthranilic acid and nicotinamide in 8 day seal milk samples.

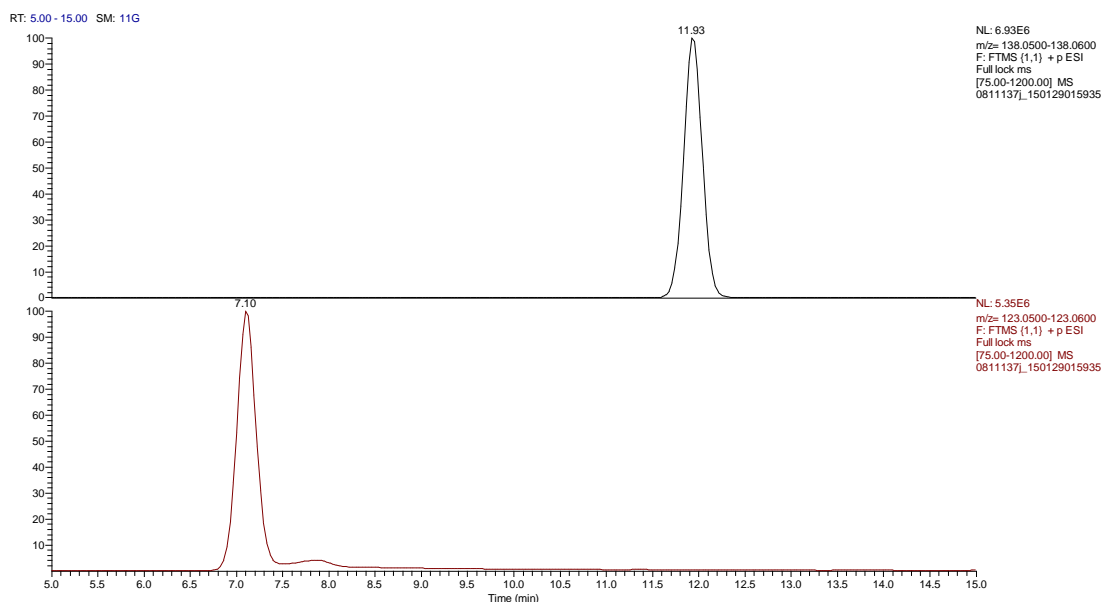


Figure 5.9 Extracted ion traces for anthranilic acid (upper) and nicotinamide in 8 day seal milk samples.

Anthranilic acid is a key intermediate in the biosynthesis of nicotinamide and this is reflected in higher levels of nicotinamide in the seal milk (Figure 5.10). Although nicotinamide is absorbed from the diet it can also be derived from tryptophan. The levels of anthranilate in the seal milk fall as the levels of nicotinamide increase (Figure 5.11). Nicotinamide is probably an important component in seal energy metabolism since it is required for the production of NAD⁺ which is a key co-factor in fatty acid beta-oxidation. Since seal energy metabolism is based on efficient oxidation of fats then it might be expected that there would be a high requirement for NAD⁺.

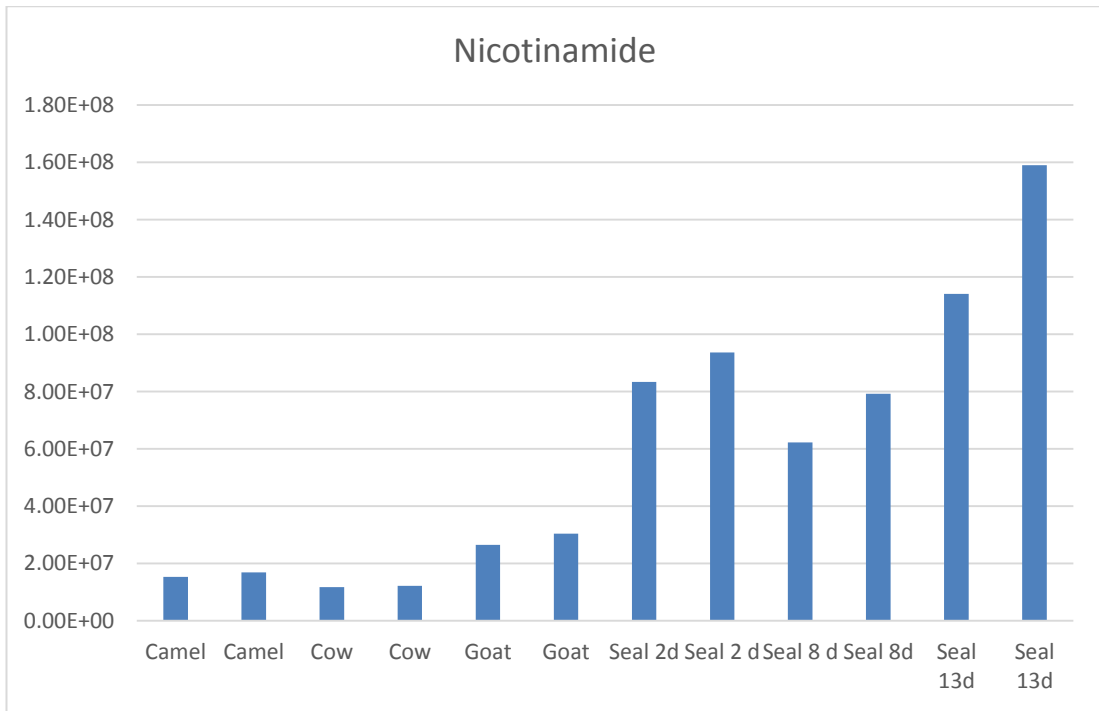


Figure 5.10 Nicotinamide in the milk of terrestrial mammals in comparison with seal milk.

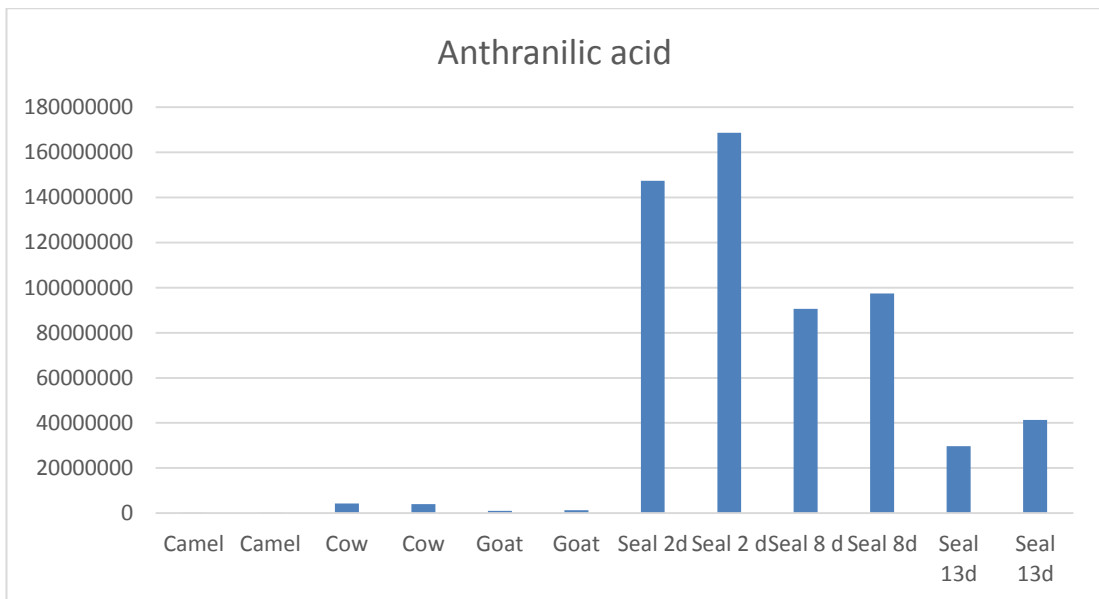


Figure 5.11 Anthranilic acid in the milk of terrestrial mammals in comparison with seal milk.

Nicotinamide can also be converted into N-methylnicotinamide (NMN) (Figure 5.12) which has in the past been viewed as a non-biologically active waste product. However, this compound has attracted increasing interest as a stimulator of peroxisome proliferation [117]. NMN is metabolised into N1-Methyl-2-pyridone-5-carboxamides (Figure 5.13) via the action of aldehyde oxidase and also CYP2E1 and it has been proposed that its levels in urine give an indication of peroxisome proliferation. As mentioned earlier the metabolism of long chain fatty acids takes place in peroxisomes before transfer to the mitochondria. The levels of N1-Methyl-2-pyridone-5-carboxamides are also much higher in seal milk than in the milk of the terrestrial mammals (Figure 5.14). It can be seen in Figures 5.10, 5.12 and 5.14 that these metabolites increase with the length of lactation. This may of course be due to the fact that the mothers have entered a foraging phase at the later time points and thus there is an increased requirement for nicotinamide and increased peroxisome proliferation by their metabolism. However, at the same time the level of nicotinamide being passed onto the seal pups also increases.

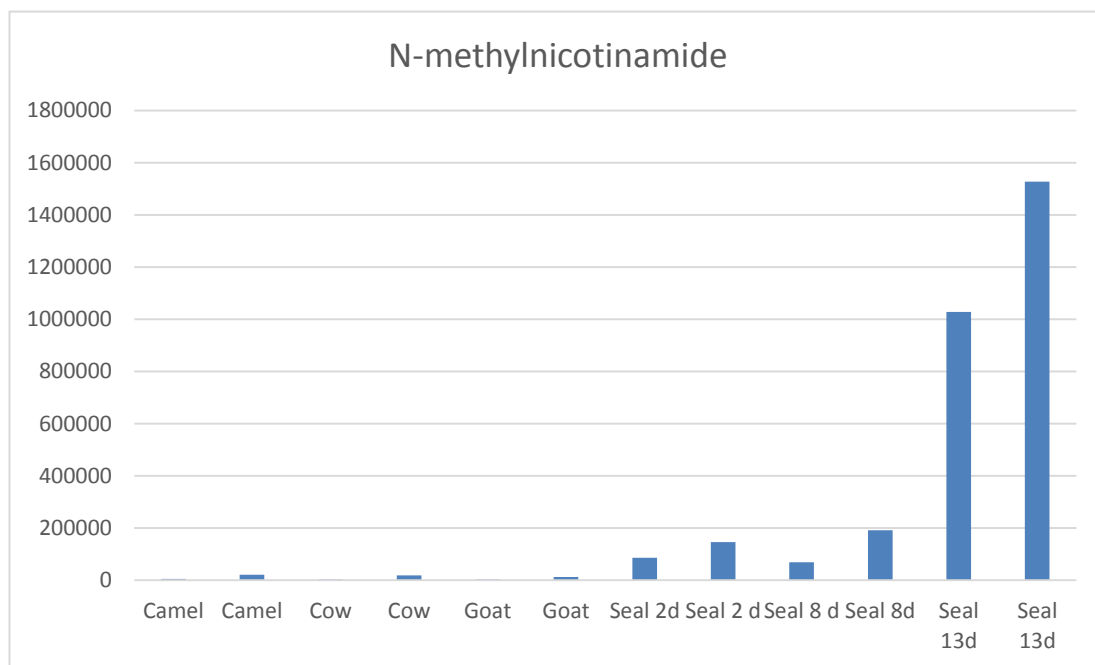


Figure 5.12 N-methyl nicotinamide acid in the milk of terrestrial mammals in comparison with seal milk.

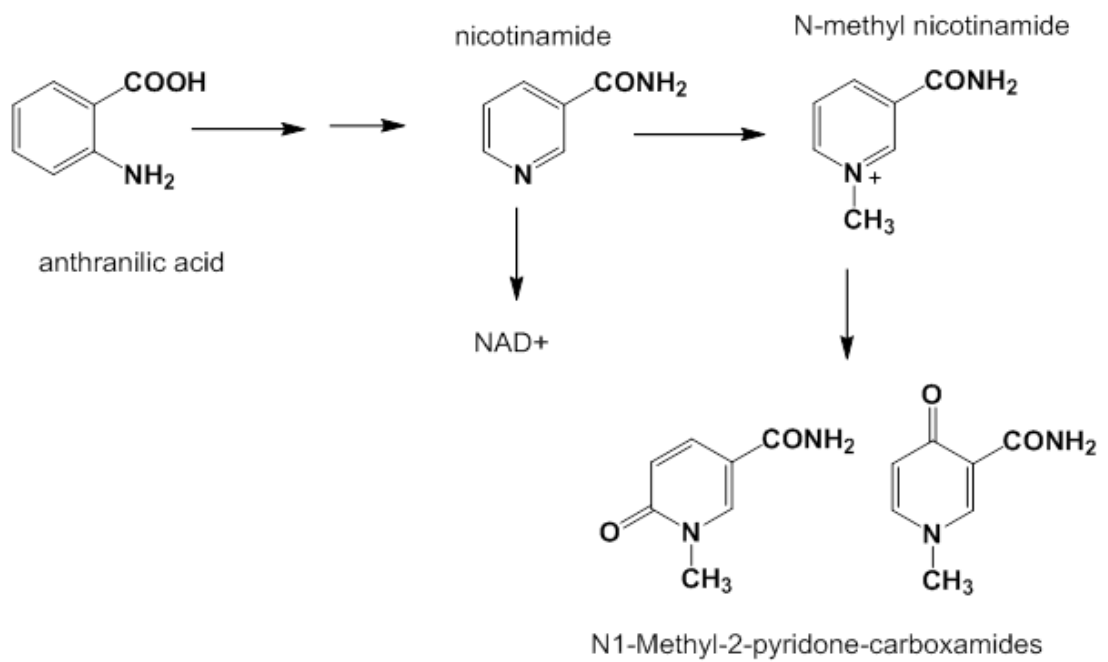


Figure 5.13 Biosynthesis of nicotinamide and N-methylpyridone carboxamides.

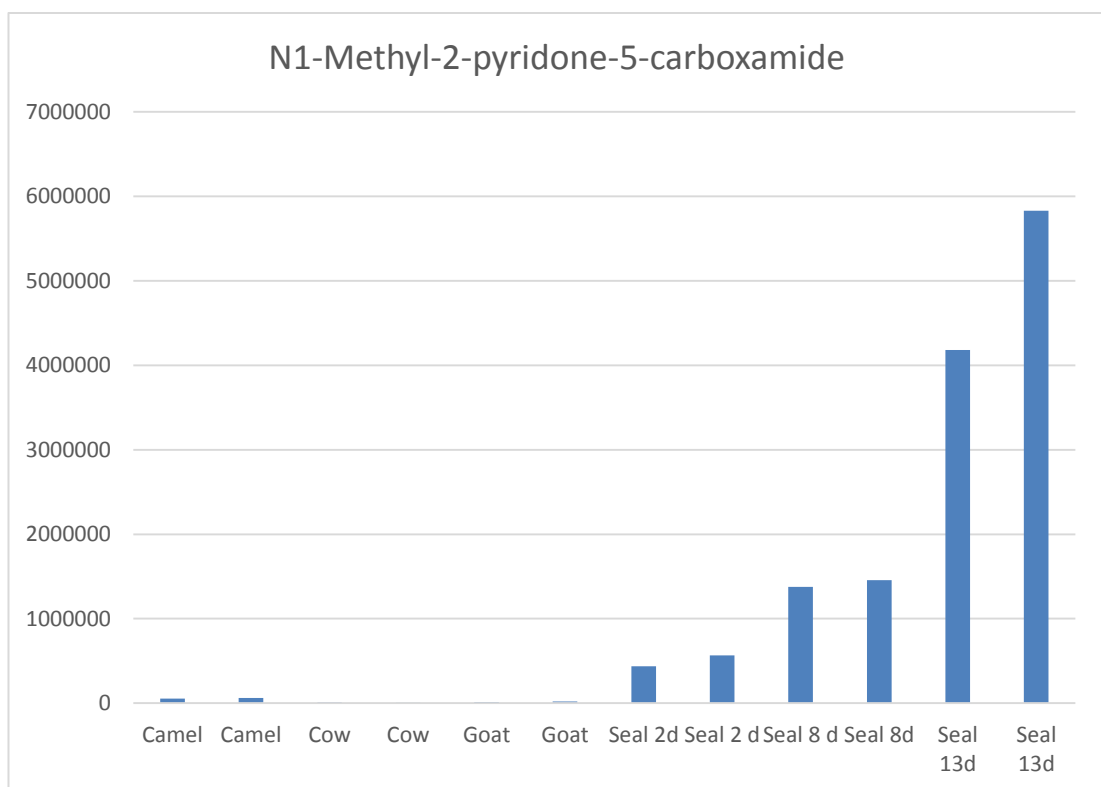


Figure 5.14 N1-methyl-2-pyridone-5-carboxamide in the milk of terrestrial mammals in comparison with seal milk.

As stated above nicotinamide can be acquired from the diet but it can also be produced from tryptophan, the levels of free tryptophan are very low in all of the milk samples but of course it could be derived from the metabolism of proteins present in the milk.

Carnitine is higher in seal milk than in the milk of terrestrial mammals apart from in camel, another mammal that may have a high requirement for fat metabolism, (Figure 5.15) and this might reflect a greater requirement for carnitine where energy metabolism relies more on fats. Carnitine is very important in modulating fatty acid metabolism and fulfils three main functions: it transports fatty acids into the mitochondria so that they can undergo β -oxidation and generate NADH; it removes fatty acids from the mitochondria in order maintain the levels of free CoA within a certain range and it removes waste fatty acids from the body as water soluble carnitine conjugates [118]. It would seem that in seals there would be a high requirement for carnitine since their energy metabolism relies extensively on fatty acid metabolism.

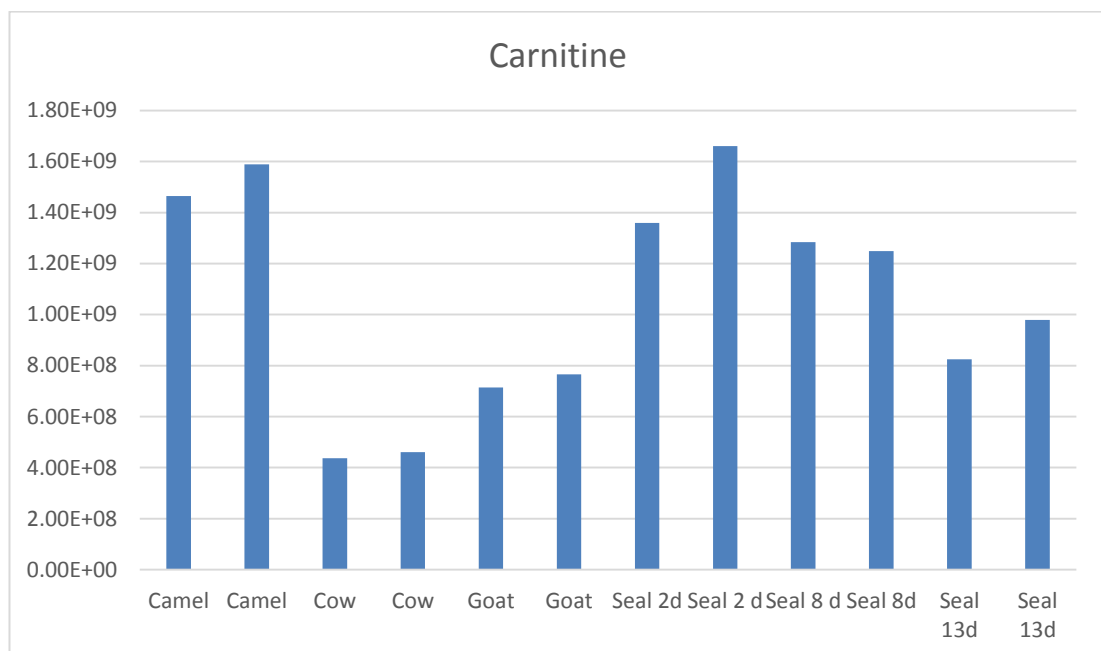


Figure 5.15 Carnitine in the milk of terrestrial mammals in comparison with seal milk.

There are marked differences between the acyl carnitines present in the milk of terrestrial mammals in comparison with seal milk. The milks from the terrestrial mammals are rich in the short chain carnitines, acetyl, propionyl and butyl carnitine, although the differences between the levels of acetyl carnitine are less marked (Figures 5.16-5.19). Dietary carnitine is an important contributor to the carnitine pool and short chain acyl carnitines may have improved bioavailability in comparison with free carnitine. In seal milk there are a large number of long chain fatty acid carnitine conjugates with the longest being the carnitine ester of docosahexanoic acid.

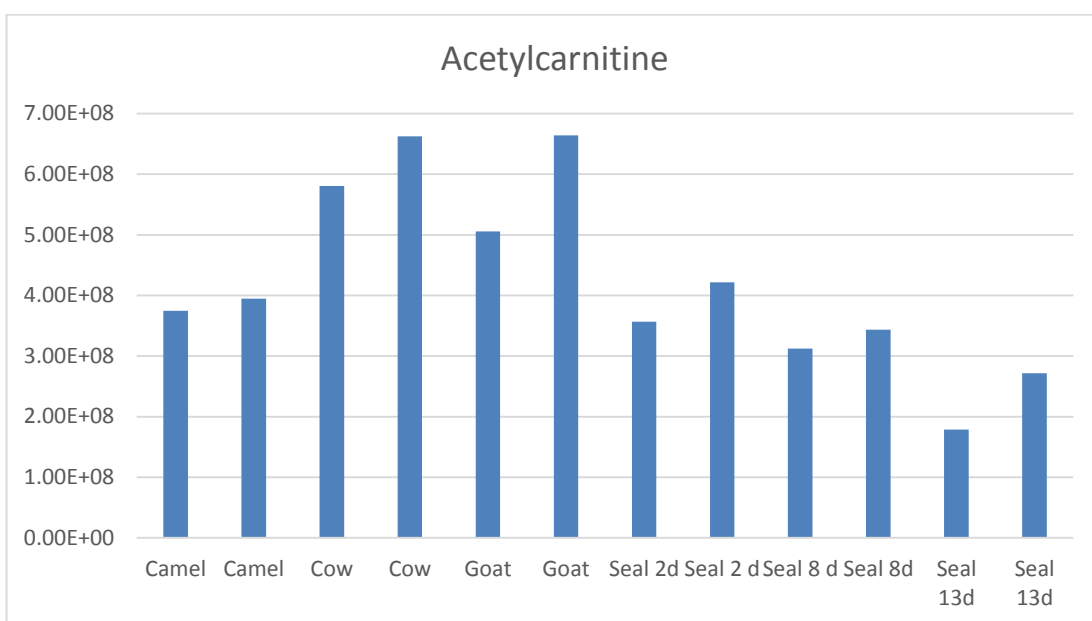


Figure 5.16 Acetyl carnitine in the milk of terrestrial mammals in comparison with seal milk.

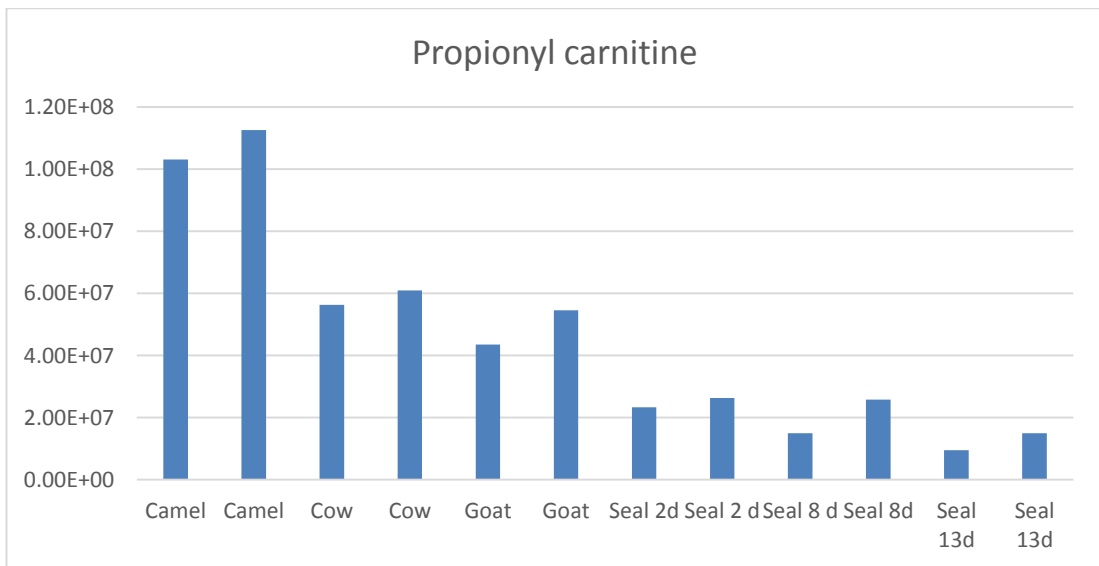


Figure 5.17 Propionyl carnitine in the milk of terrestrial mammals in comparison with seal milk.

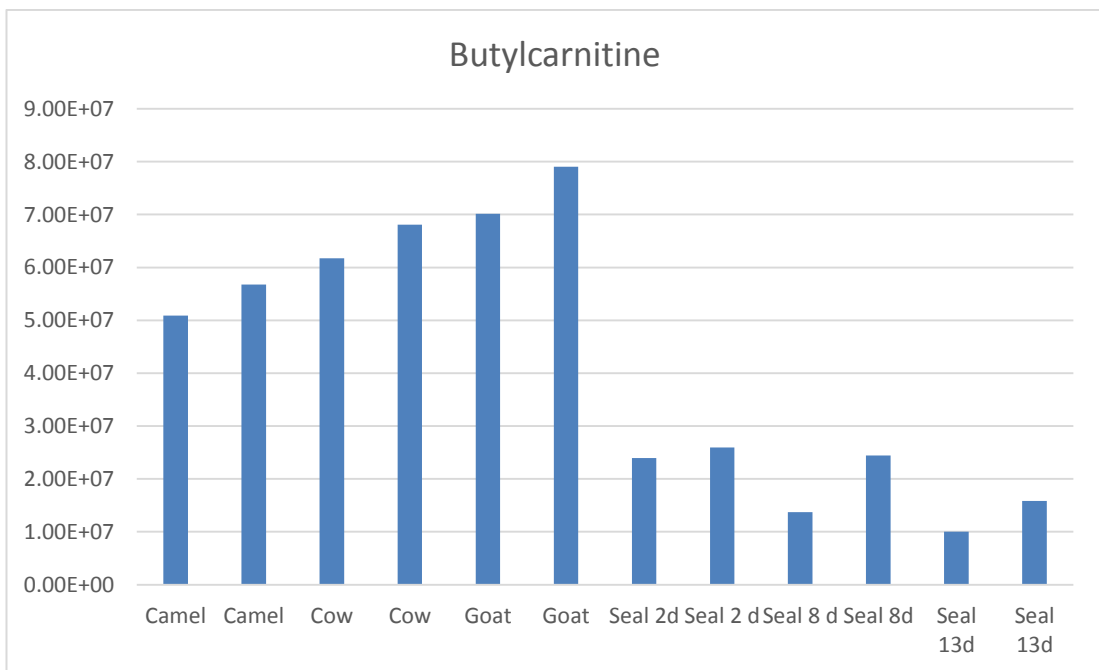


Figure 5.18 Butyl carnitine in the milk of terrestrial mammals in comparison with seal milk.

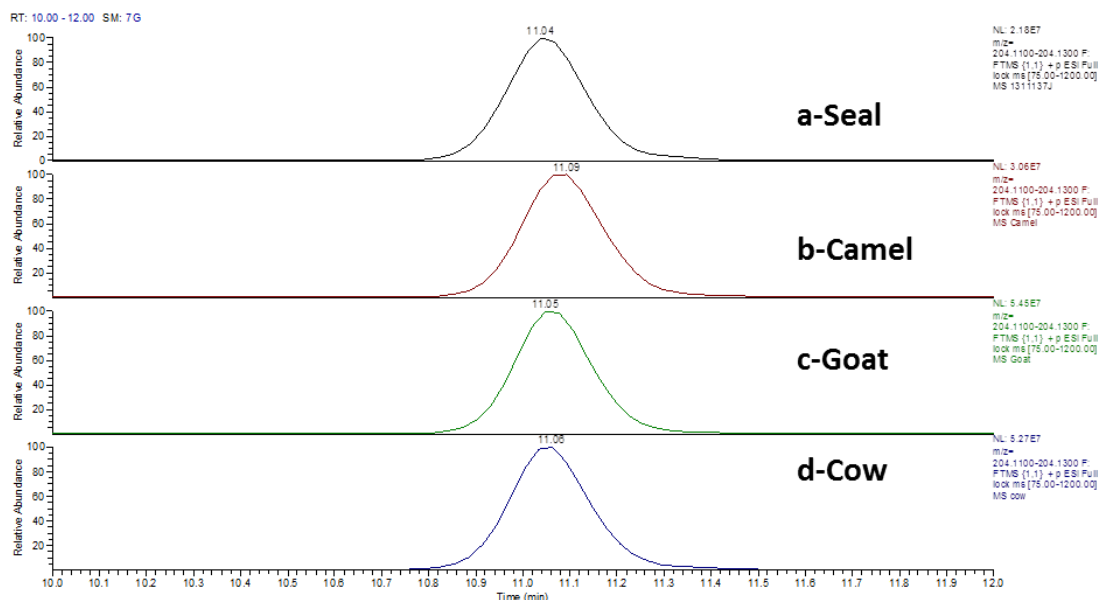


Figure 5.19 Extracted ion trace for acetyl carnitine in seal, camel, goat and cow milk.

There are also carnitine conjugates of oleic acid, palmitic acid and palmitoleic acid plus a number of other long chain carnitine conjugates (Figures 5.20-5.23). It is not clear if these are simply waste products of the mother's metabolism or whether these conjugates are a bioavailable form of carnitine. Such long chain carnitine conjugates are strongly bound to proteins in plasma but removal of the acyl group by esterases would allow them to enter tissues.

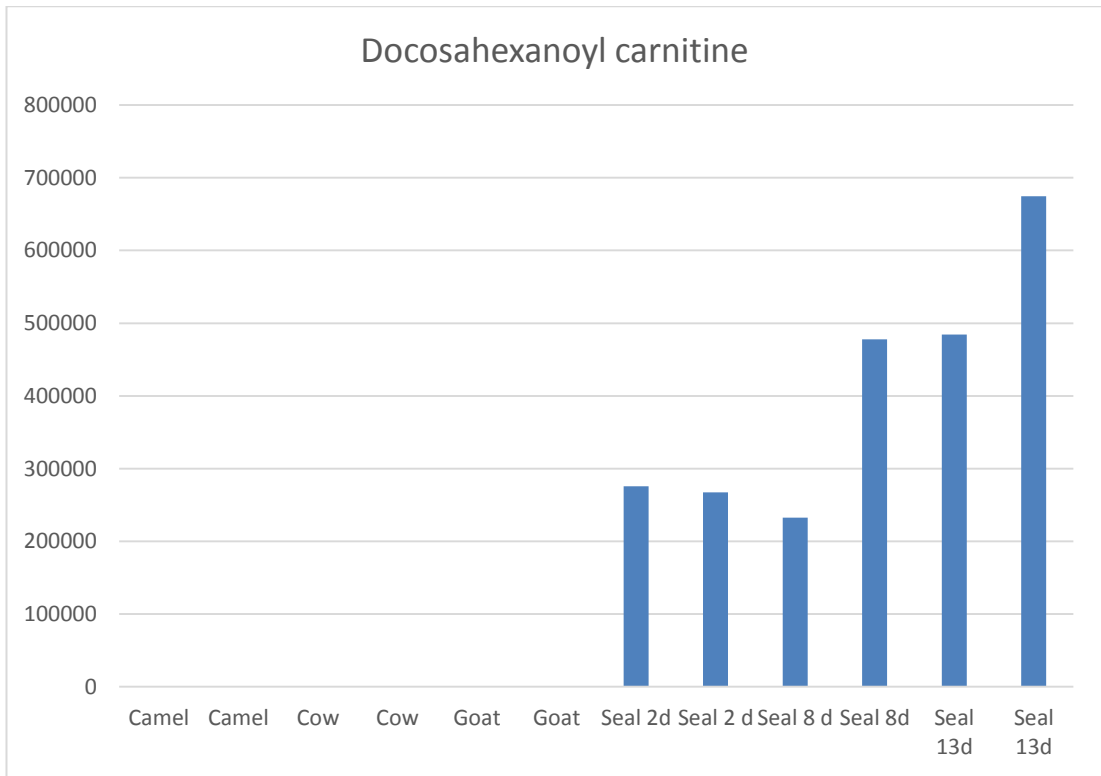


Figure 5.20 Docosahexanoyl carnitine in the milk of terrestrial mammals in comparison with seal milk.

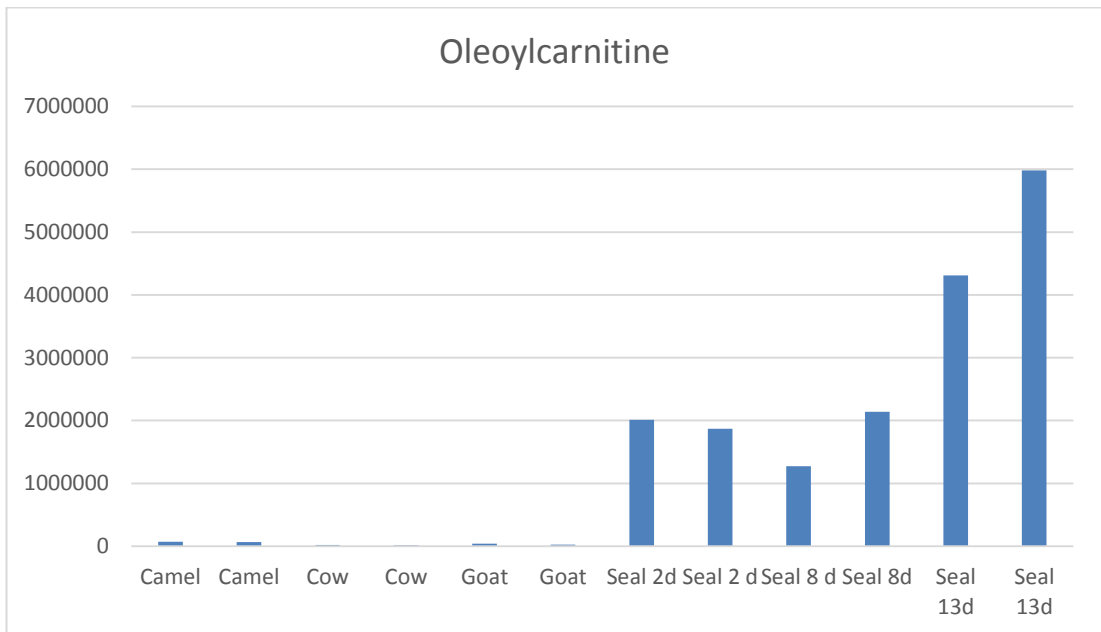


Figure 5.21 Oleoyl carnitine in the milk of terrestrial mammals in comparison with seal milk.

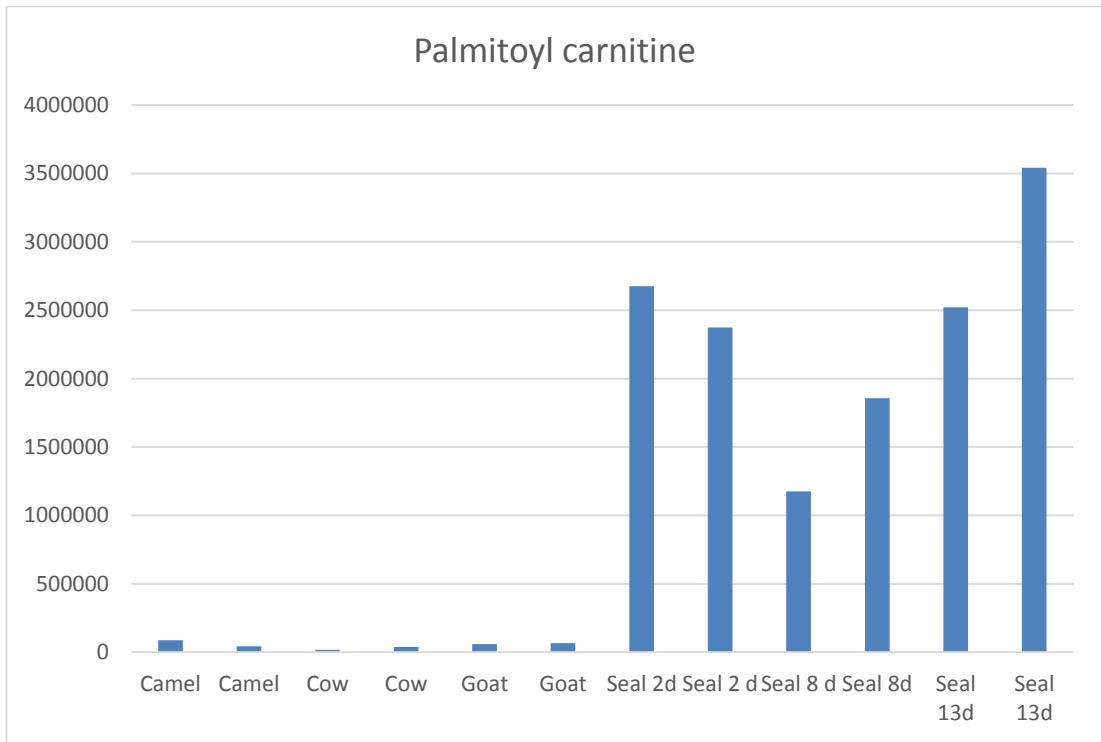


Figure 5.22 Palmitoyl carnitine in the milk of terrestrial mammals in comparison with seal milk.

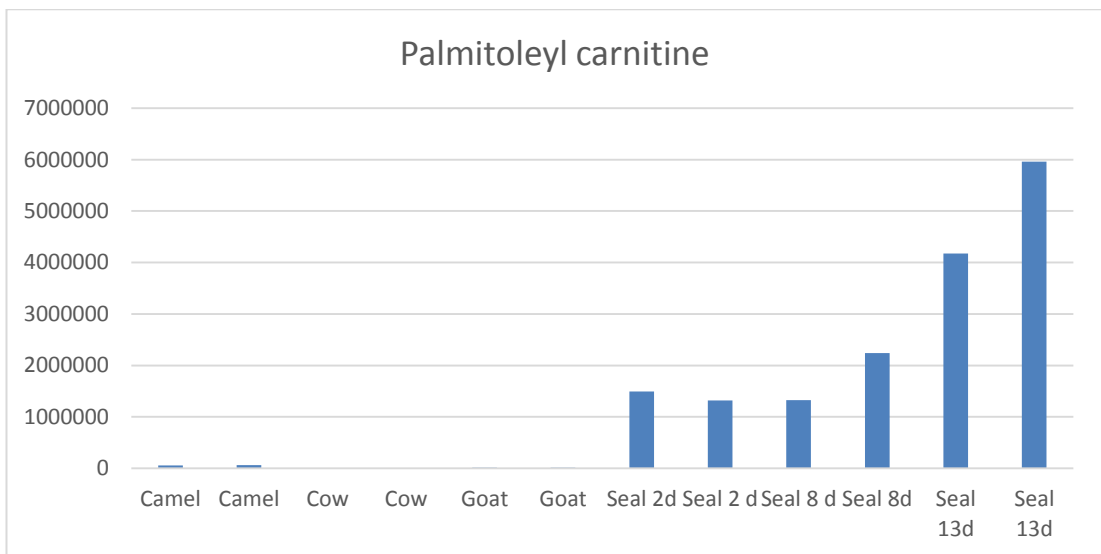


Figure 5.23 Palmitoleyl carnitine in the milk of terrestrial mammals in comparison with seal milk.

Table 5.5 shows the ten most abundant metabolites by response in the milk samples in positive ion mode. There is a large degree of overlap between all the milk samples but in the seal samples there is a particular emphasis on choline and glycerophosphocholine both of which are important in fatty acid metabolism.

Table 5.5 The ten most intense metabolites by absolute response in camel, goat, cow and seal milks

Camel	Intensity	Goat	Intensity	Cow	Intensity	Seal	Intensity
Carnitine	1.59E+09	Creatine	1.03E+09	Choline	1.40E+09	Glycerophosphocholine	1.00E+09
Betaine	7.81E+08	Betaine	9.80E+08	Creatine	9.89E+08	Carnitine	9.79E+08
Creatine	7.67E+08	Carnitine	7.15E+08	Betaine	6.08E+08	Hexadecanoyl-glycero-phosphocholine	7.63E+08
O-Acetylcarnitine	3.95E+08	O-Acetylcarnitine	5.06E+08	O-Acetylcarnitine	5.81E+08	Creatine	7.56E+08
Creatinine	2.12E+08	Creatinine	2.13E+08	L-Carnitine	4.37E+08	Choline	7.53E+08
Lactose	1.61E+08	DL-2-Aminooctanoicacid	1.45E+08	Creatinine	3.05E+08	Betaine	7.31E+08
Acetylcholine	1.24E+08	Lactose	1.43E+08	Glycerophosphocholine	1.89E+08	Creatinine	3.33E+08
Aminooctanoicacid	1.17E+08	Choline	7.34E+07	Aminooctanoicacid	1.55E+08	Acetylcarnitine	2.72E+08
O-Propanoylcarnitine	1.13E+08	Glycerophosphocholine	7.24E+07	Lactose	1.30E+08	Nicotinamide	1.59E+08
5-Guanidino-2-oxopentanoate	9.03E+07	O-Butanoylcarnitine	7.02E+07	O-Butanoylcarnitine	6.98E+07	Guanidino-2-oxopentanoate	1.29E+08

Having compared seal milks against terrestrial mammal milks attention was turned to the analysis of seal milk from six seals taken between 2 and 19 days postpartum. Examining the positive ion data first. Principal component analysis (PCA) of the positive ion data followed by hierarchical cluster analysis gave no clear classification of the samples by day (Figure 5.24). The observations were used to build an OPLS model, this model was refined until a good fit for the plot of day against predicted day was obtained based on 8 variables, samples E2 and A7 were excluded in order to achieve a good fit to the data (Figure 5.25). The eight variables are listed in Table 5.6. Figure 5.26 shows the cross validation plot which indicates a strong model (the separation of the samples in the model is shown in Figure A4.1) with all the blue squares below the green circles. The bar graph plots for the eight variables are shown in Figures 5.27–5.34. It can be seen that the relationship between day and level of metabolites in these samples is not that clear. The clearest trend is for nicotinamide which shows a clear increase and acetyl carnitine which decreases with time. The trend for carnitine is also downwards with time. Thus the important metabolite changes do link to the observations discussed above with regard to the differences between terrestrial mammals and seals concerning the higher reliance on fatty acids as an energy source in seals. There is a fairly clear effect on long chain acyl carnitines which are highest in the day 2 samples and generally fall to low levels in the day 17/18/19 samples. There also appear to be marked variations between individual seals which make it difficult to see clear time dependent changes in milk composition. Table 5.7 shows the variation in terms of absolute response in the top 10 variables in positive ion mode in seal milks with time. There is no marked change in the metabolites in the top ten apart from nicotinamide increasing in importance time which has been discussed above.

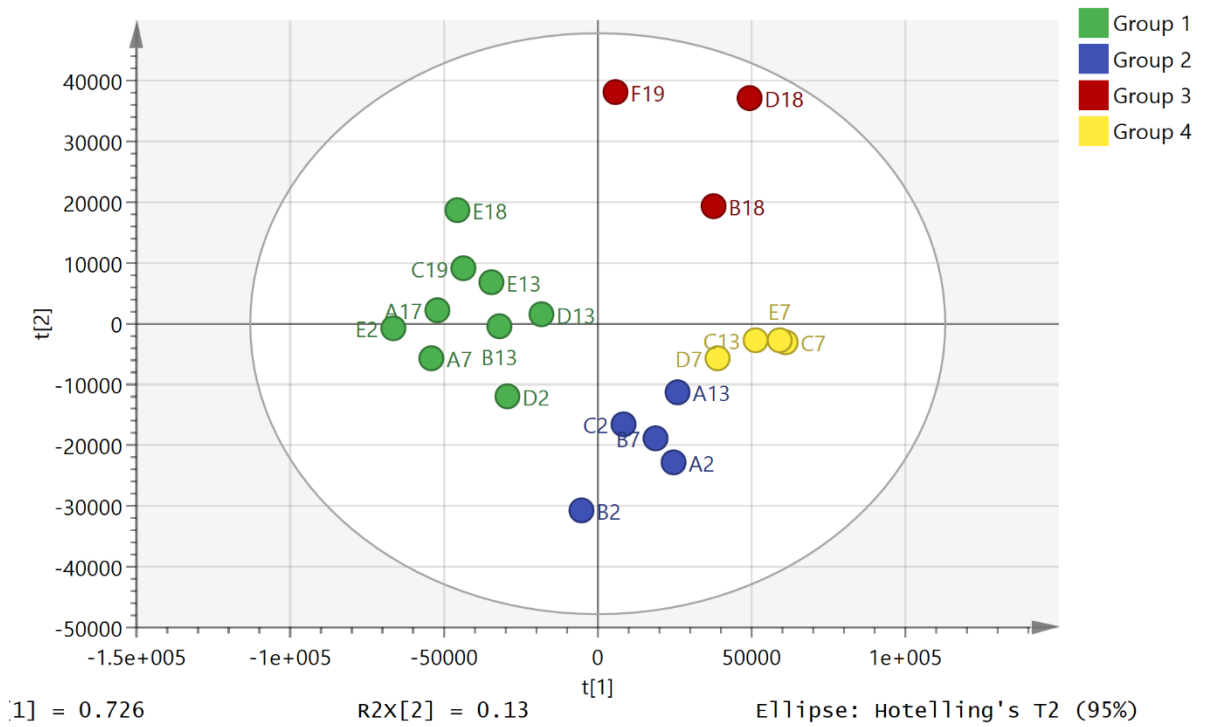


Figure 5.24 PCA with hierarchical cluster analysis (HCA) showing no clear separation between the seal milks with time based on 969 metabolites.

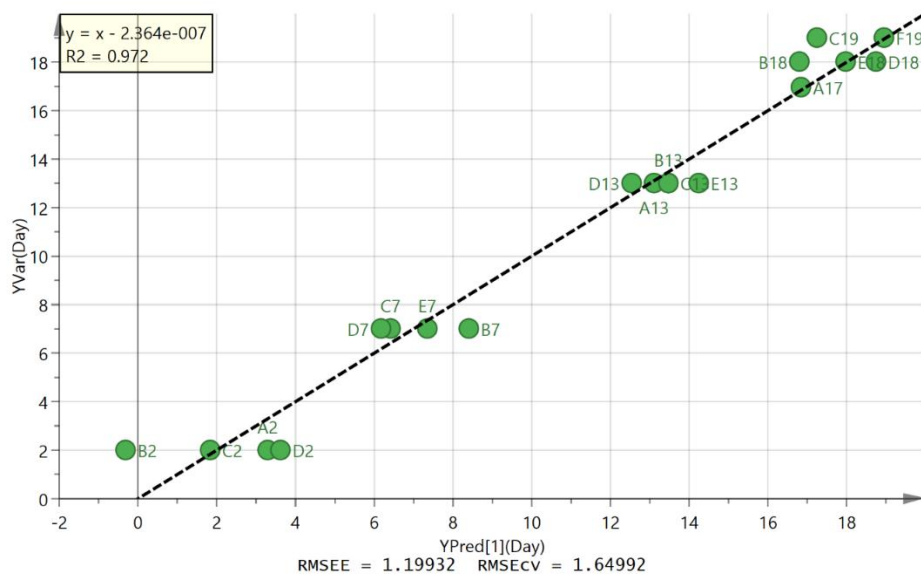


Figure 5.25 OPLS plot based on eight metabolites of day of milk collection versus predicted day of milk collection.

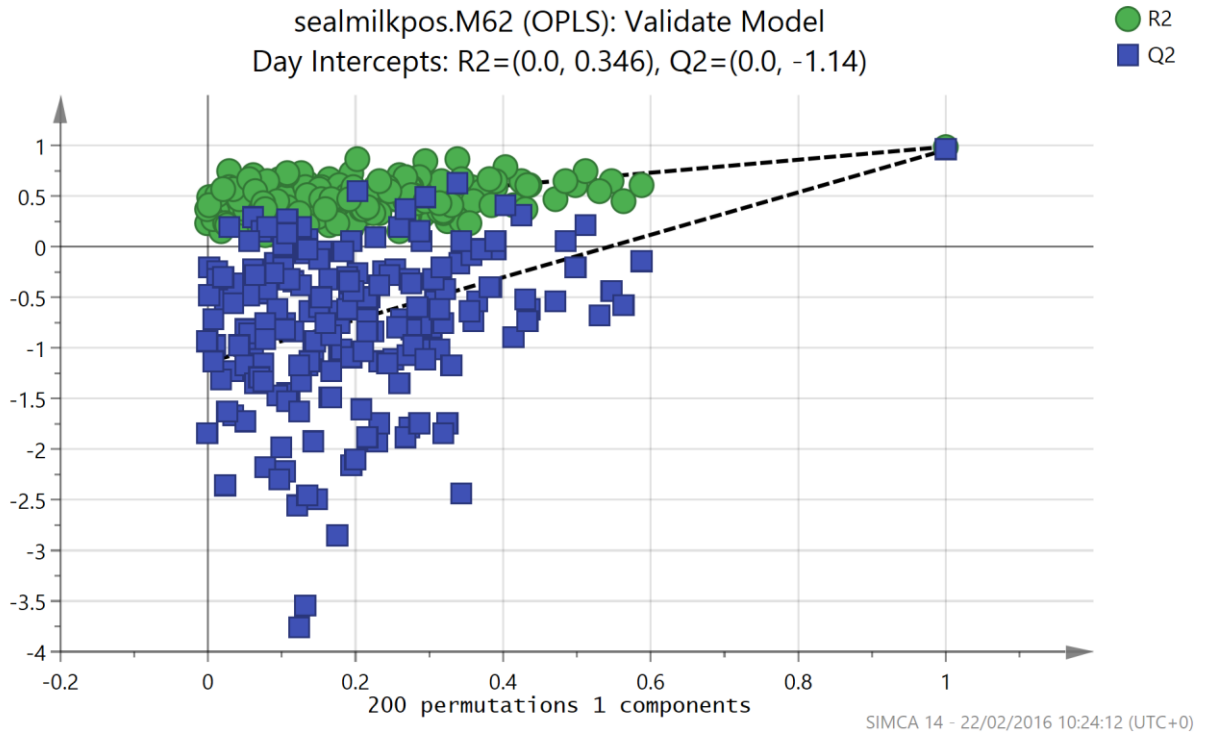


Figure 5.26 Cross validation plot for the OPLS for seal milk composition versus day of collection.

Table 5.6 Eight variables used to classify the seal milk samples according to day of collection.

m/z	Rt min	Metabolite	VIP
132.077	14.5	Creatine	1.36
162.112	13.0	Carnitine	1.33
258.110	14.2	Glycero-3-Phosphocholine	1.30
118.086	11.0	Betaine	1.10
114.066	9.5	Creatinine	0.84
204.123	10.8	Acetylcarnitine	0.76
123.055	7.0	Nicotinamide	0.36
160.133	13.0	Amino octanoic acid	0.25

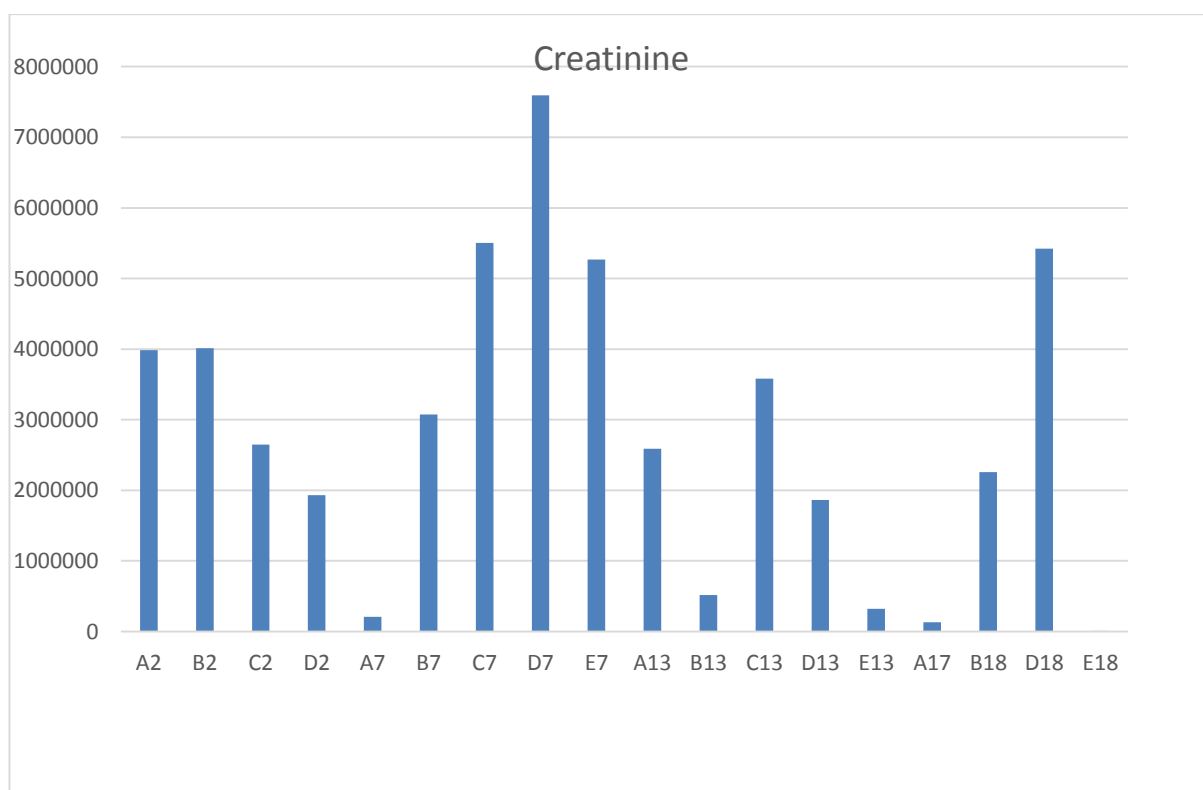


Figure 5.27 Variation of creatinine between day 2 and day 18 in seal milk samples.

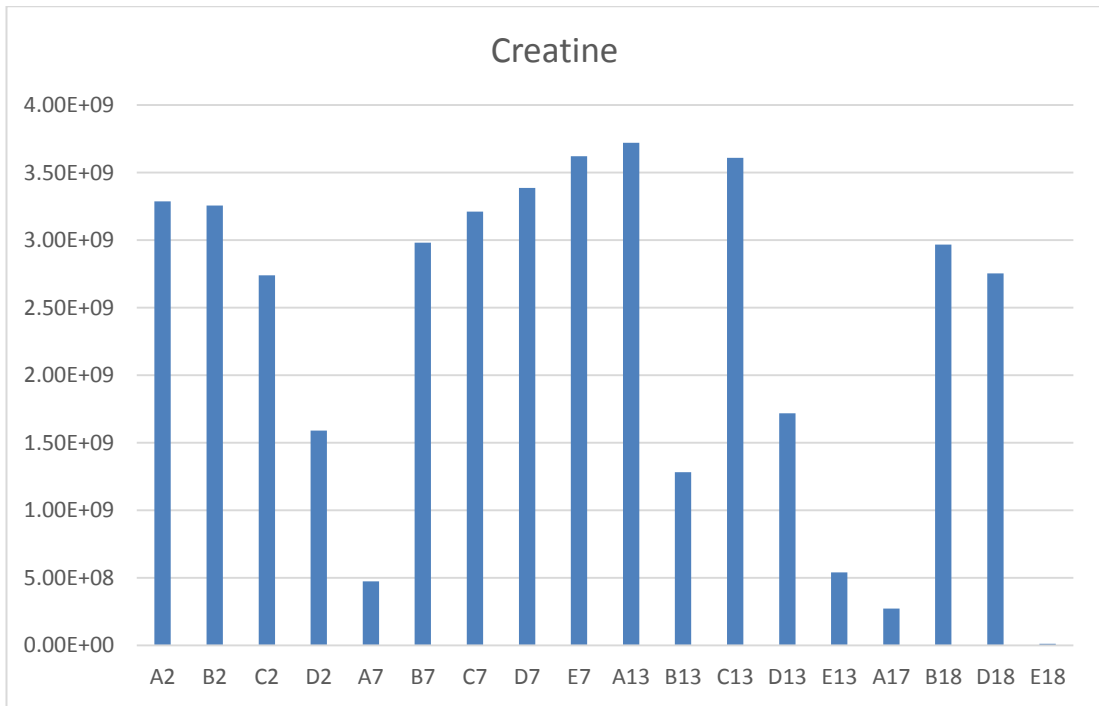


Figure 5.28 Variation of creatine between day 2 and day 18 in seal milk samples

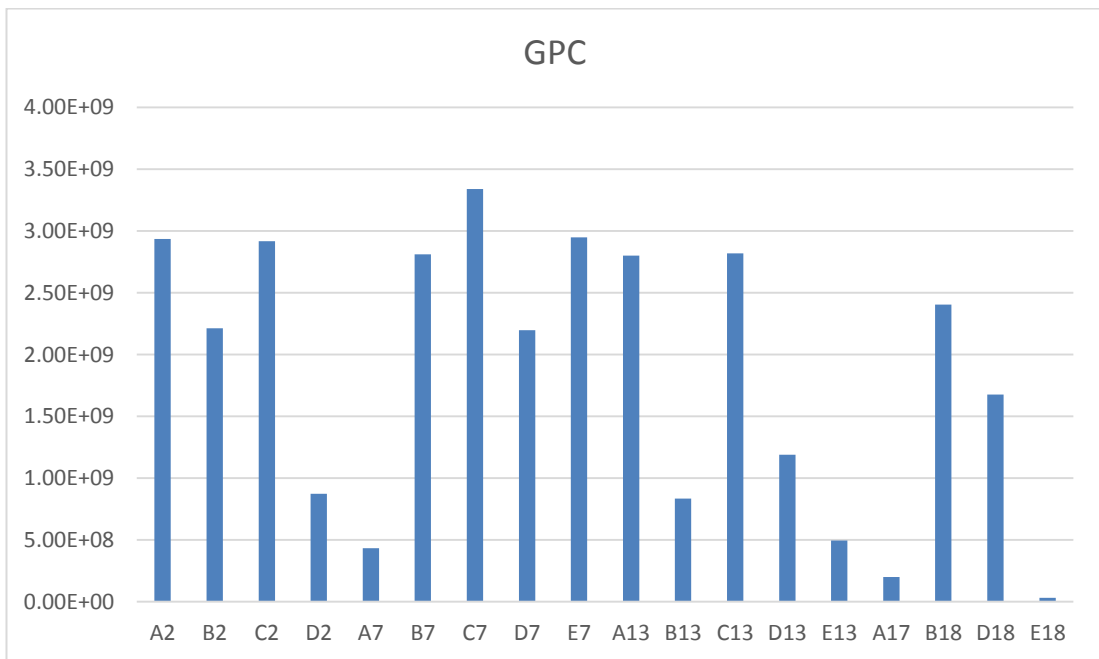


Figure 5.29 Variation of glycerophosphocholine between day 2 and day 18 in seal milk samples.

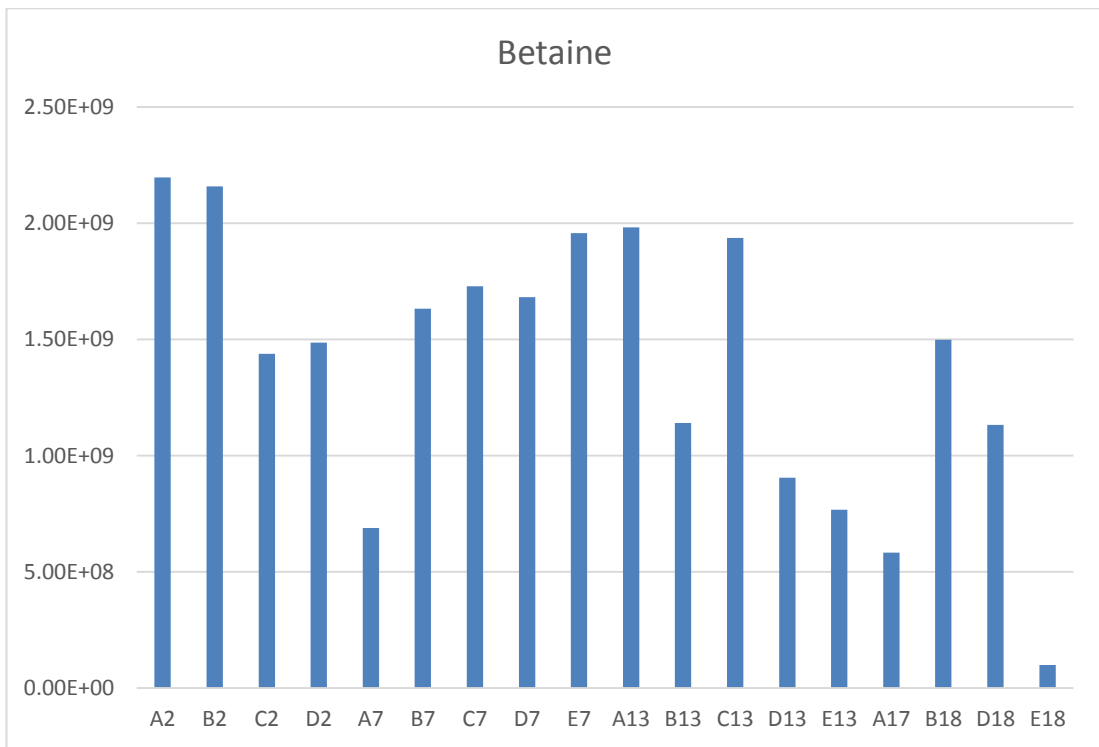


Figure 5.30 Variation of betaine between day 2 and day 18 in seal milk samples.

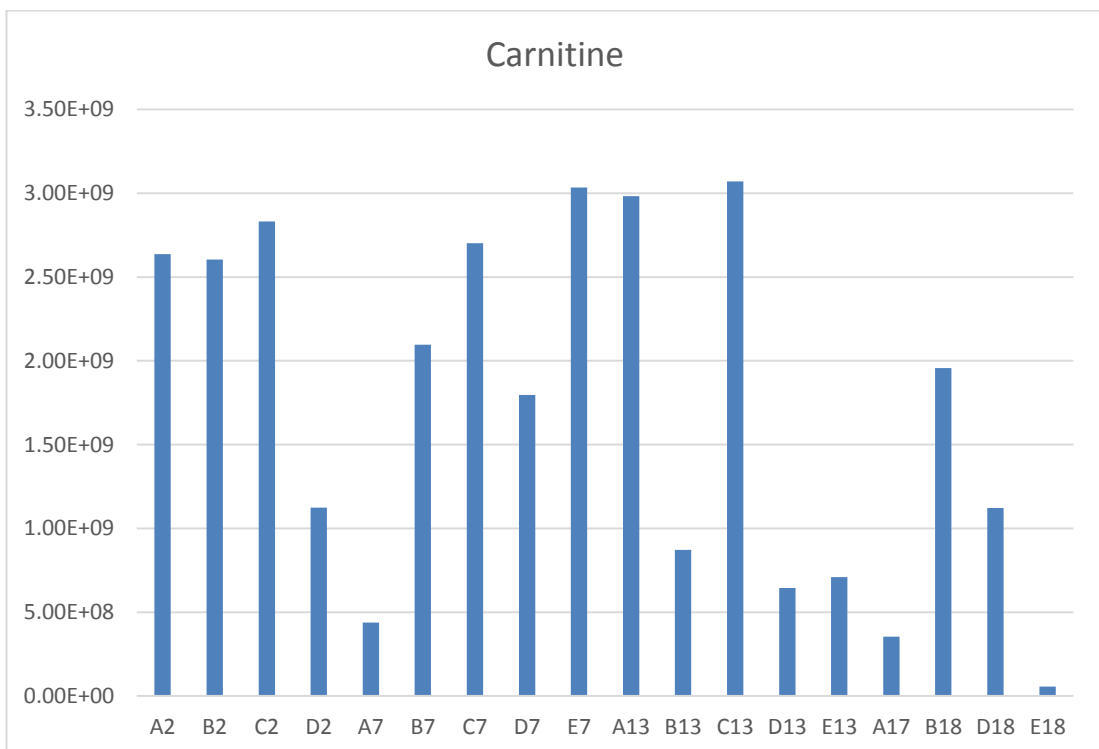


Figure 5.31 Variation of carnitine between day 2 and day 18 in seal milk samples.

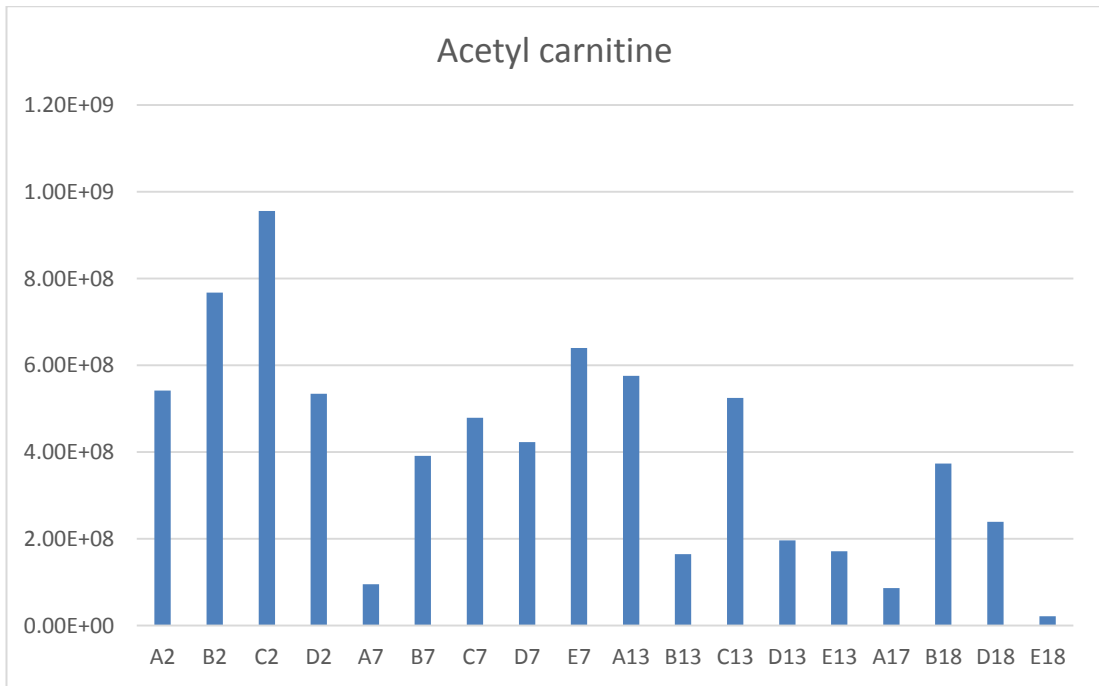


Figure 5.32 Variation of acetyl carnitine between day 2 and day 18 in seal milk samples.

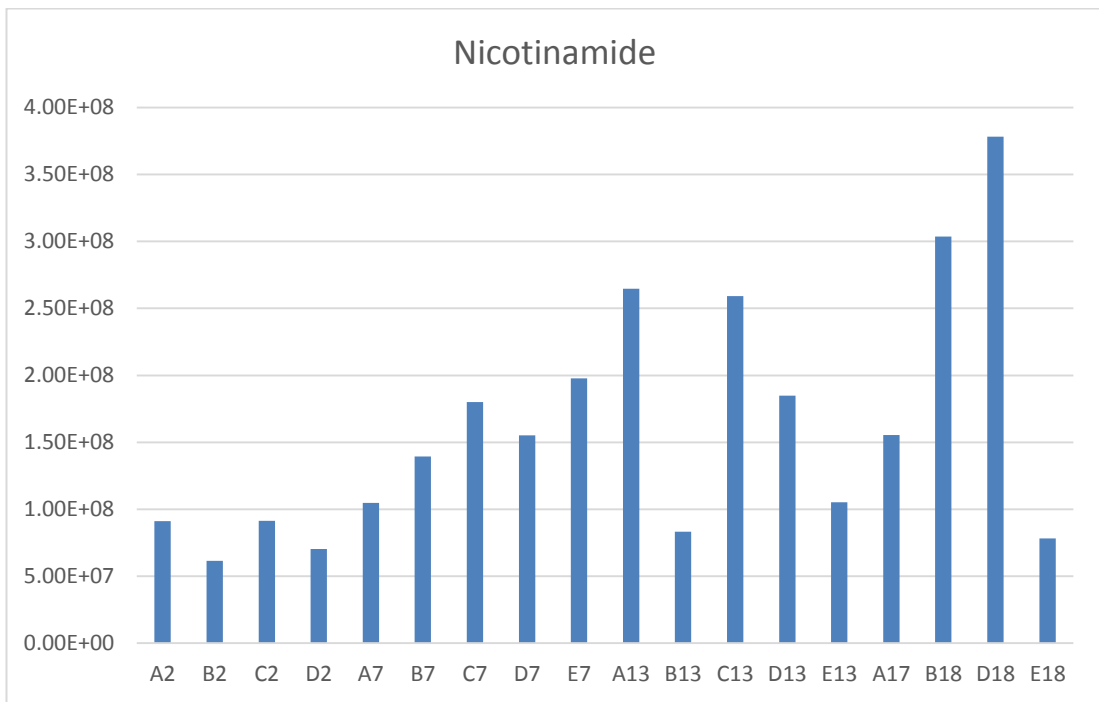


Figure 5.33 Variation of nicotinamide between day 2 and day 18 in seal milk samples.

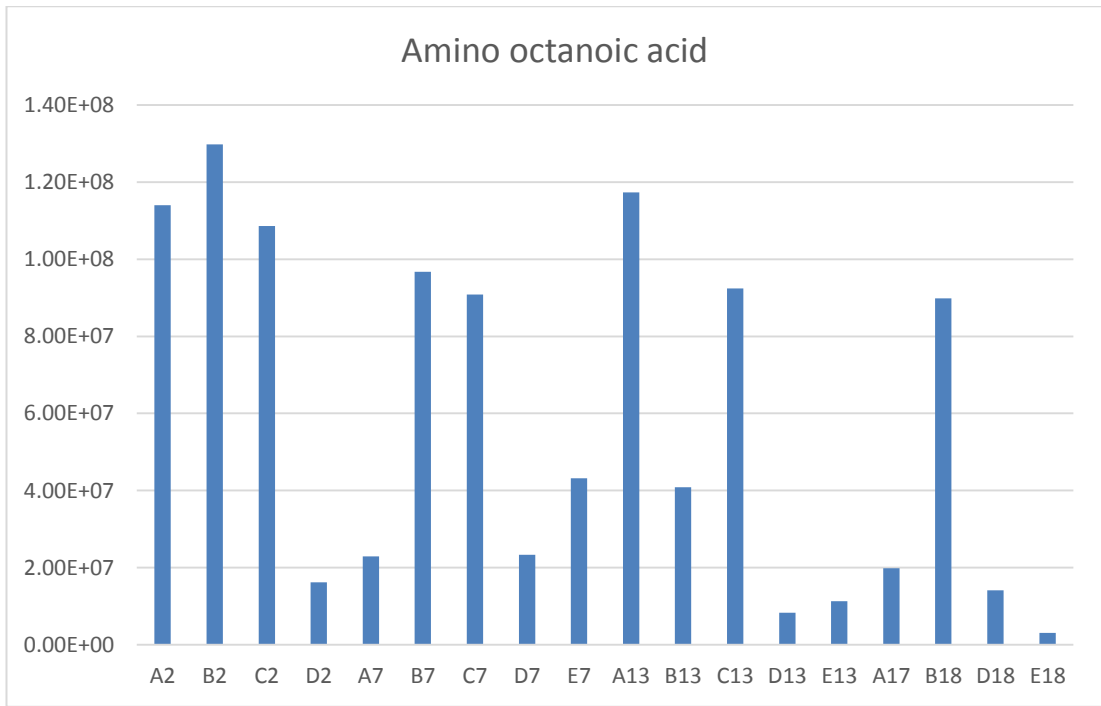


Figure 5.34 Variation of amino octanoic acid between day 2 and day 18 in seal milk samples.

Table 5.7 Ten most abundant metabolites by absolute response in positive ion mode in seal milks at four time points.

Day 2	Mean	Day 7	Mean	Day 13	Mean	Day 17/18/19	Mean
Creatine	2.18E+09	Creatine	2.74E+09	Creatine	2.17E+09	Creatine	1.50E+09
Carnitine	1.86E+09	Glycerophosphocholine	2.35E+09	Carnitine	1.66E+09	Glycerophosphocholine	1.08E+09
Glycerophosphocholine	1.80E+09	Carnitine	2.01E+09	Glycerophosphocholine	1.63E+09	Choline	9.35E+08
Betaine	1.52E+09	Betaine	1.54E+09	Betaine	1.35E+09	Carnitine	8.72E+08
Hexadecanoyl glycerophosphocholine	1.16E+09	Hexadecanoyl glycerophosphocholine	1.51E+09	Hexadecanoyl glycerophosphocholine	1.3E+09	Betaine	8.28E+08
Creatinine	8.37E+08	Creatinine	8.45E+08	Choline	8.18E+08	Hexadecanoyl glycerophosphocholine	7.80E+08
O-Acetylcarnitine	5.82E+08	Choline	7.62E+08	Creatinine	6.02E+08	Creatinine	3.97E+08
Choline	4.21E+08	O-Acetylcarnitine	4.06E+08	O-Acetylcarnitine	3.27E+08	Nicotinamide	2.29E+08
Octadecanoyl glycerophosphocholine	2.06E+08	Octadecanoyl glycerophosphocholine	3.33E+08	Octadecanoyl glycerophosphocholine	3E+08	O-Acetylcarnitine	1.80E+08
Proline	1.47E+08	Thymine	2.51E+08	Nicotinamide	1.79E+08	Octadecanoyl glycerophosphocholine	1.67E+08

Principal component analysis (PCA) of the negative ion data followed by hierarchical cluster analysis did not produce a clear separation of the samples over time although there was a tendency for the day 2 and day 7 samples to cluster together (Figure 5.35).

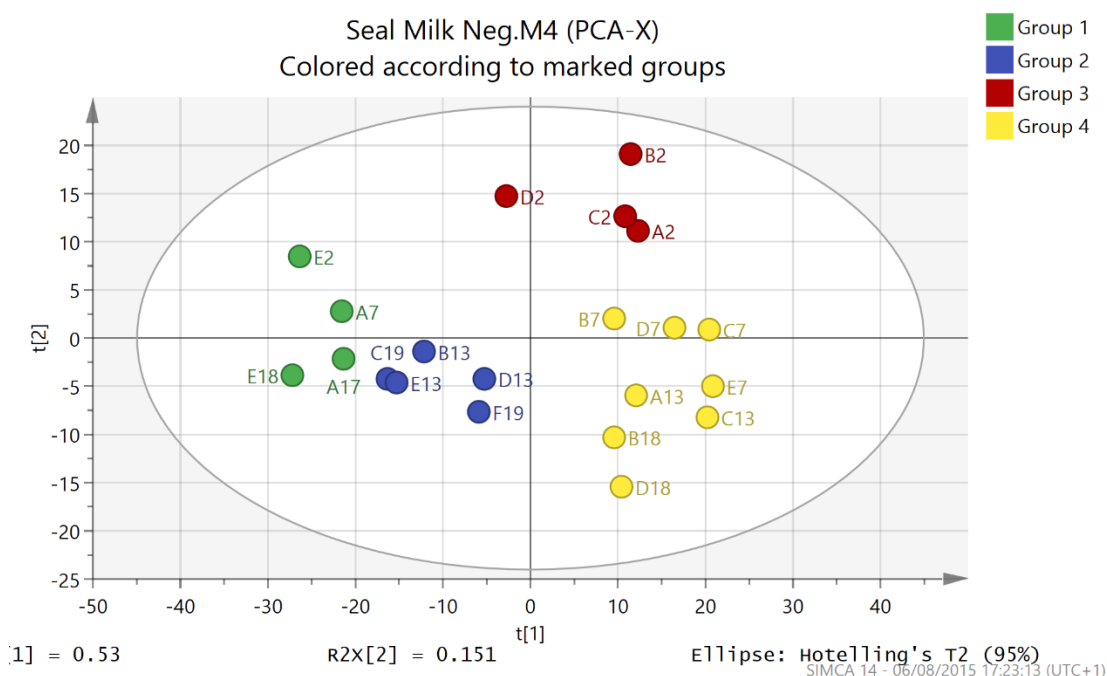


Figure 5.35 PCA analysis with HCA analysis of negative ion data for seal milk samples based on 650 metabolites.

The negative ion data was then modelled using orthogonal partial least squares analysis. A plot was produced which gave a reasonable correlation between day and metabolite profile based on three variables (Figure 5.36). The three metabolites are shown in Table 5.8 and the plots for them over time are shown in Figures 5.37-5.39. There is no particularly strong correlation between metabolites and day and again variations between individual seals may obscure variation with time.

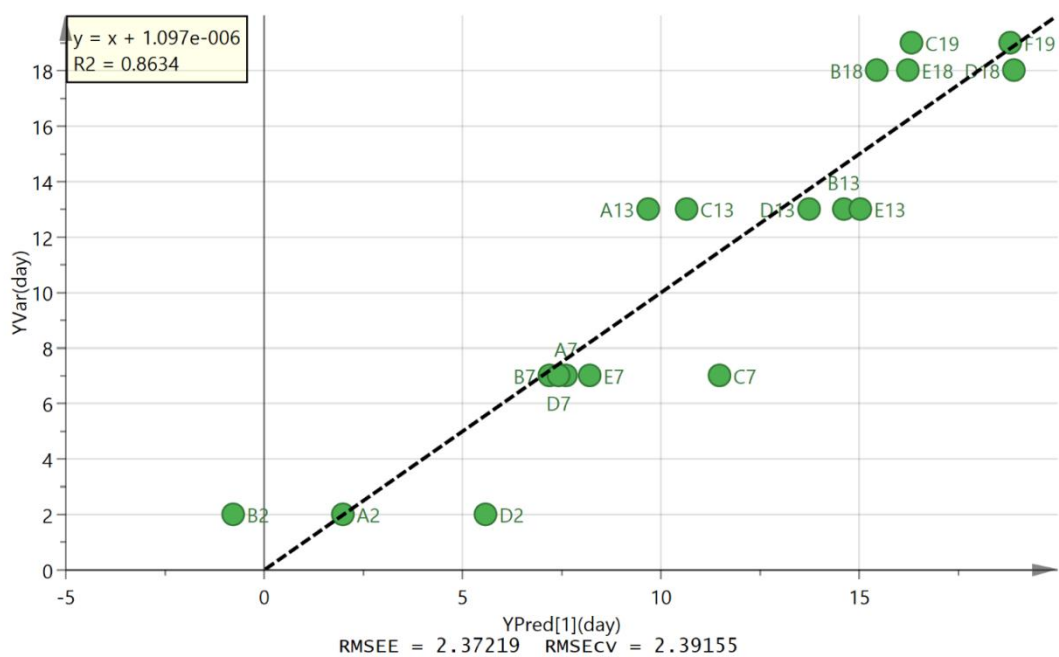


Figure 5.36 OPLS plot for predicted against actual day for seal milk collected over 18 days based on three metabolites detected in negative ion mode.

Table 5.8 Metabolites with the greatest impact on the OPLS model for seal milk samples in relation to day of collection in negative ion mode.

m/z	Rt min	Metabolite	VIP
124.007	14.0	Taurine	1.16
115.077	5.2	Hexanoic acid	1.05
255.233	3.9	Hexadecanoic acid	0.74

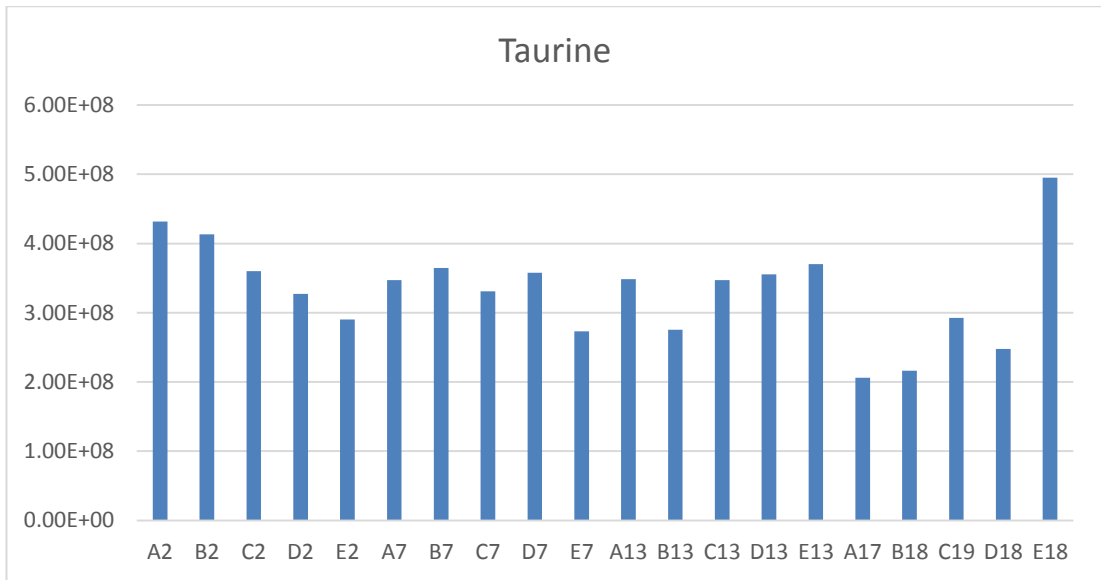


Figure 5.37 Variation of amino taurine between day 2 and day 18 in seal milk samples.

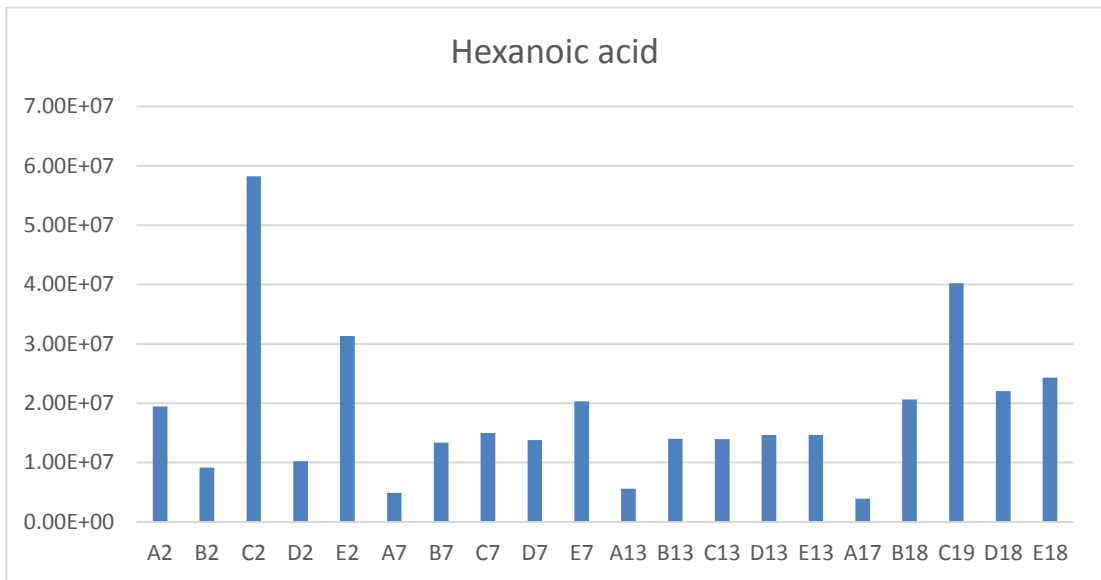


Figure 5.38 Variation of hexanoic acid between day 2 and day 18 in seal milk samples.

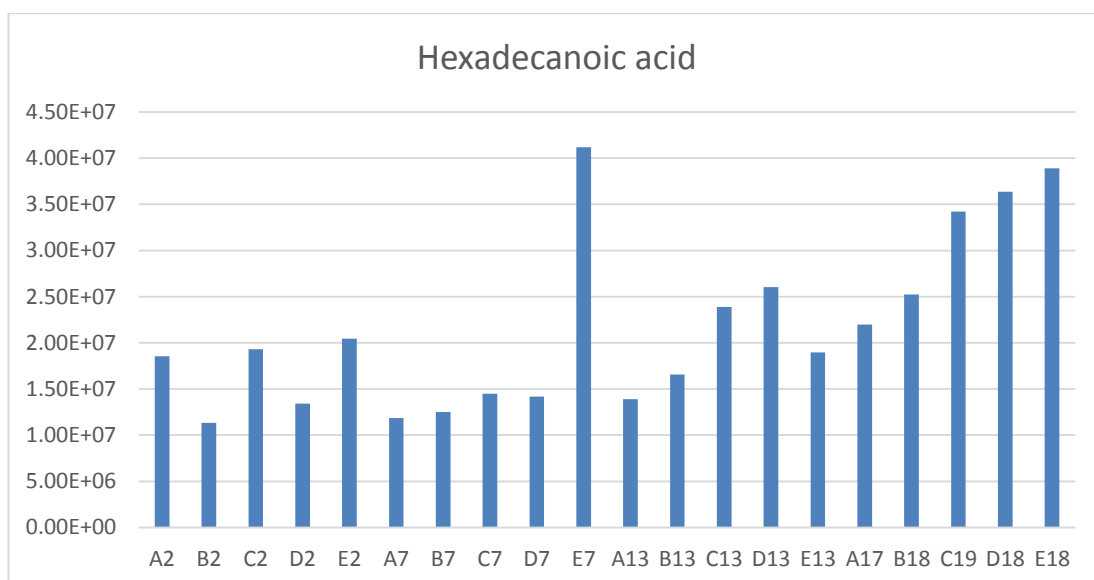


Figure 5.39 Variation of hexadecanoic acid between day 2 and day 18 in seal milk samples.

5.4 Analysis of Lipids in Seal Milk

In order to get a clearer picture of lipid composition in seal milk analysis was carried out by using a lipid profiling method based on chromatography on silica gel. Figure 5.40 shows that there was some separation with time on the basis of PCA analysis with HCA. All of the later samples are in one group along with one of the day 7 samples. OPLS modelling was carried out on the 18 samples included in the PCA model and a very good correlation was found between actual and predicted day based on eight metabolites (Figure 5.41); the 8 metabolites are listed in Table 5.9. The plots of the variation in abundance of these metabolites with time are shown in Figures 5.42-5.49. Most of the free fatty acids show clear increases with time in the milk samples but again there is variation between individual seals.

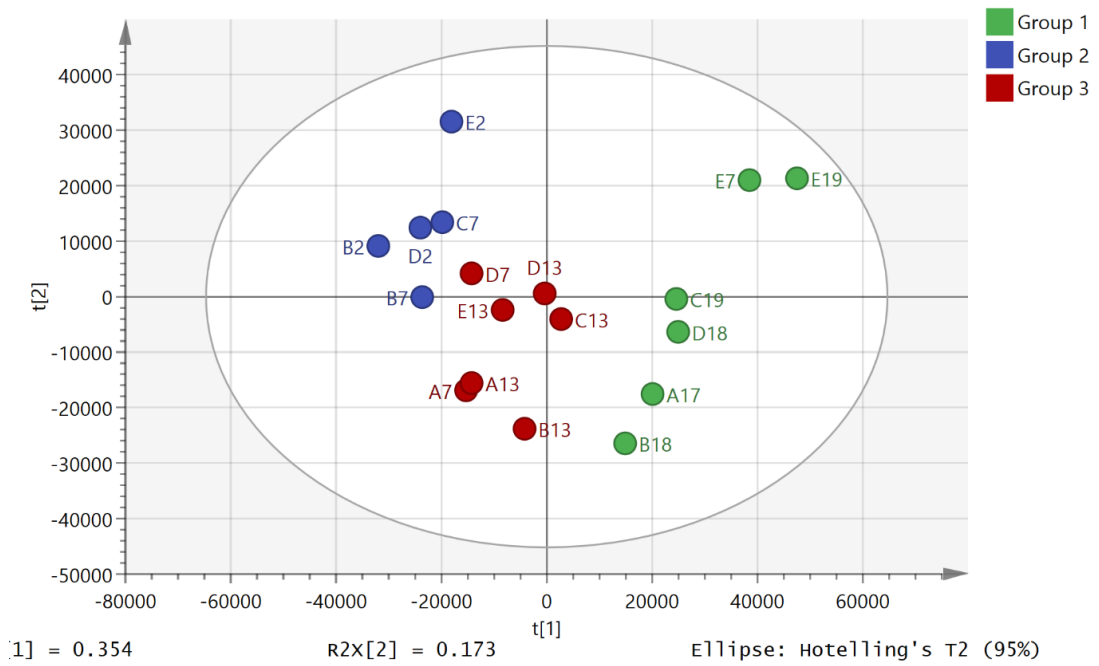


Figure 5.40 Separation of seal milk samples according to day by PCA with HCA analysis based on 1198 metabolites.

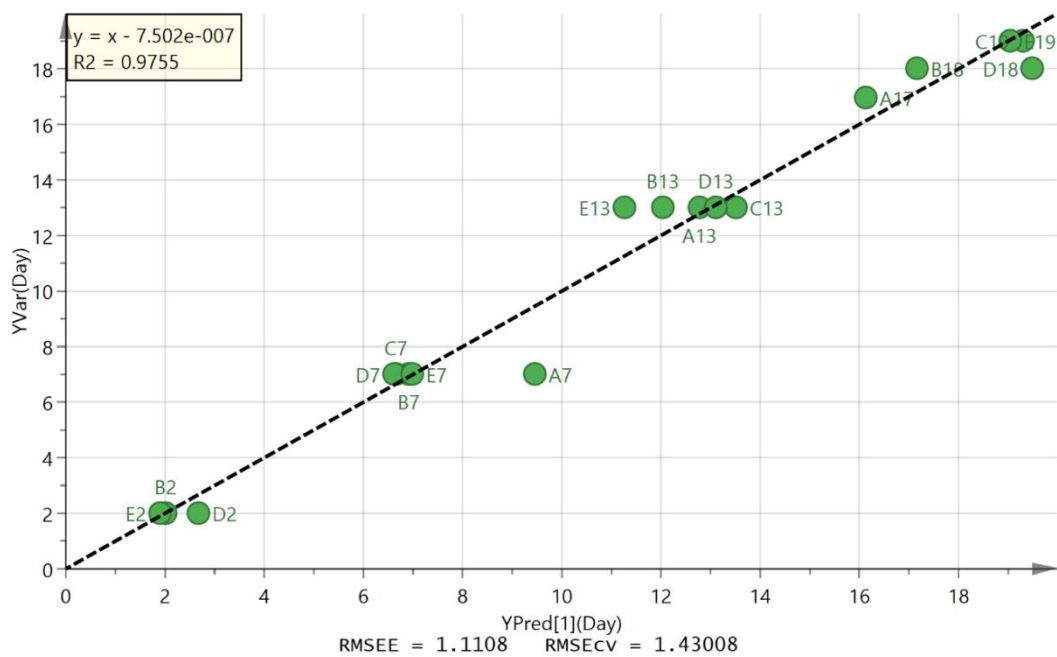


Figure 5.41 OPLS model based on eight metabolites detected in negative ion mode showing predicted against actual day of collection for seal milk samples.

Table 5.9 Metabolites detected in negative ion mode predicting day of collection of seal milk.

m/z)	RT (min)	Metabolite	VIP
327.233	3.2	Docosahexaenoic acid	2.30
129.056	3.0	Oxohexanoic acid	0.83
303.233	3.2	Eicosatetraenoic acid	0.75
297.244	3.5	Oxooctadecanoic acid	0.62
277.218	3.3	Octadecatrienoic acid	0.56
218.103	9.7	Pantothenate	0.54
283.265	3.3	Octadecanoic acid	0.53
331.265	3.2	Docosatetraenoic acid	0.42

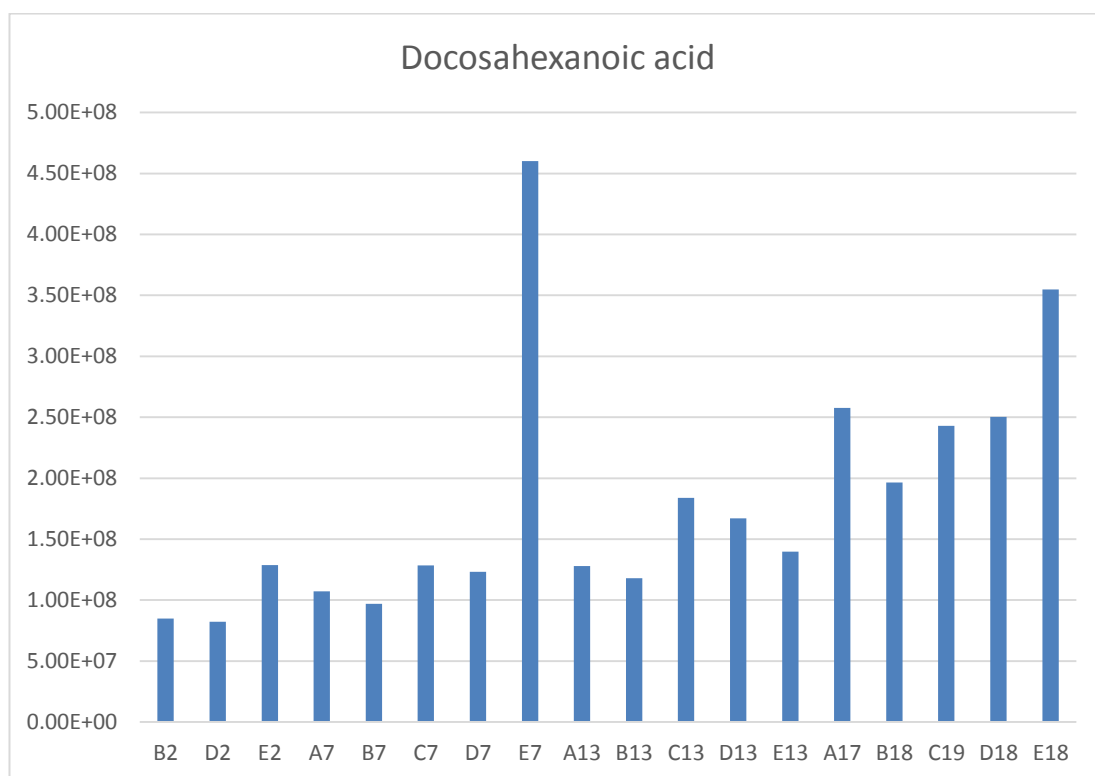


Figure 5.42 Variation of docosahexanoic acid with day of collection of seal milk sample.

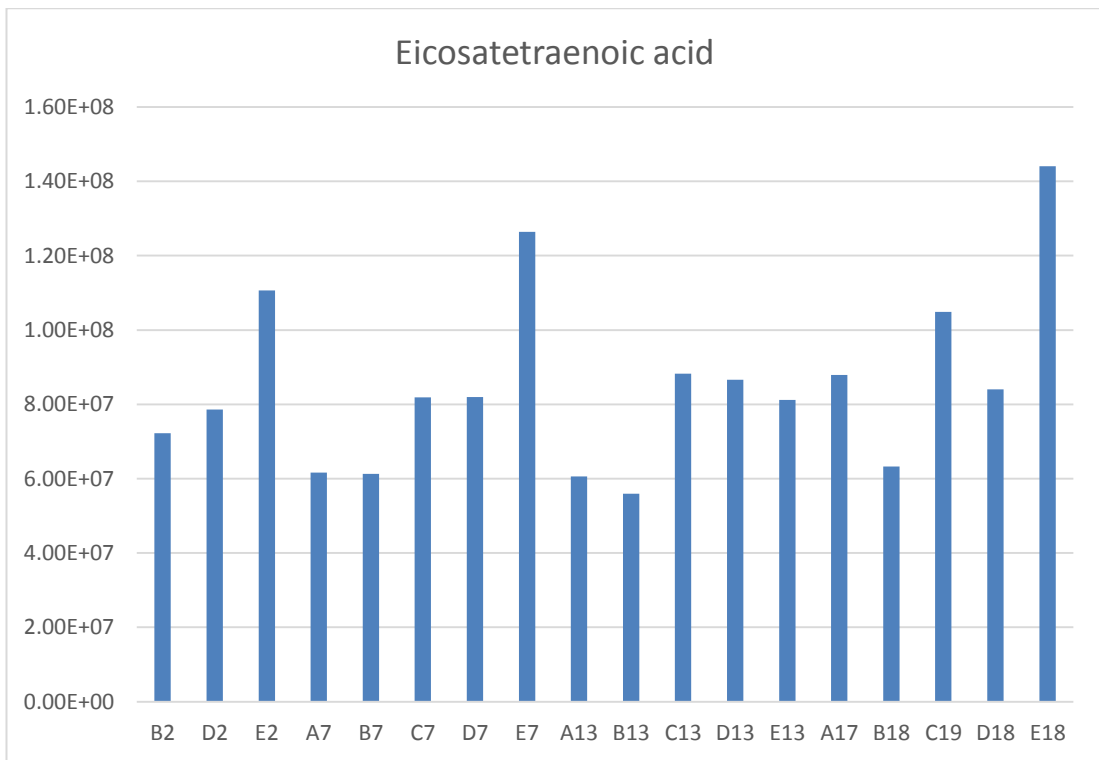


Figure 5.43 Variation of eicosapentanoic acid with day of collection of seal milk sample.

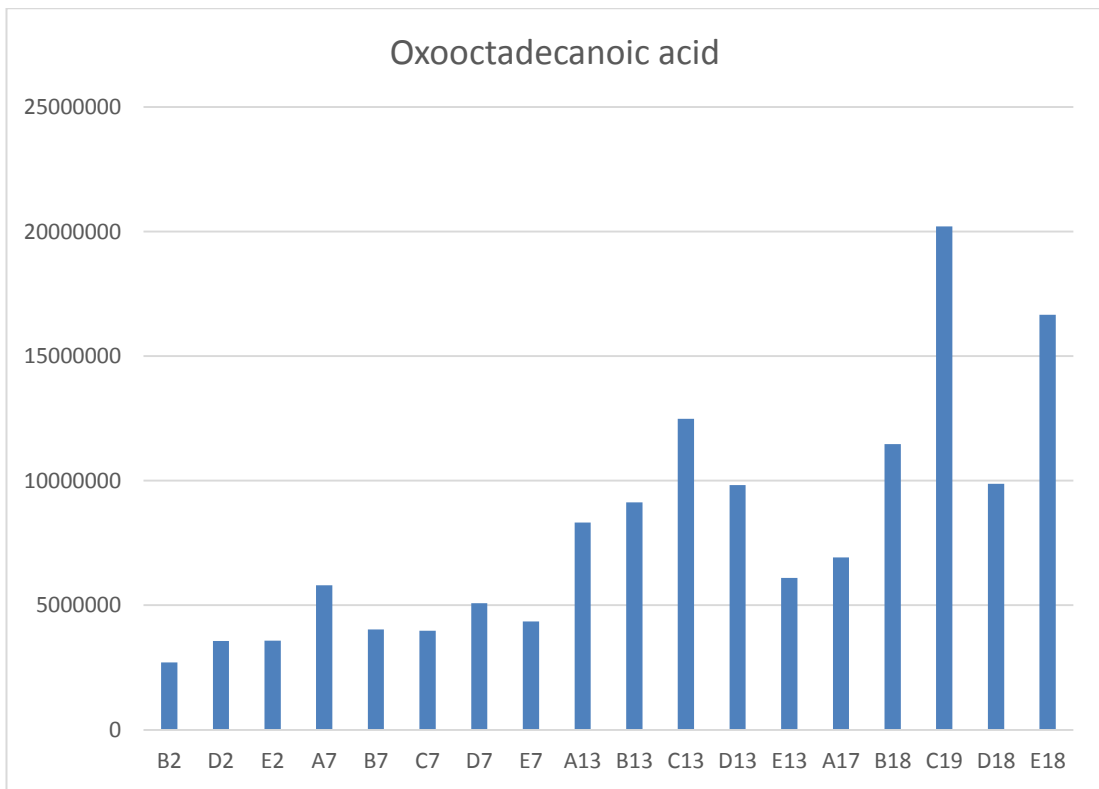


Figure 5.44 Variation of oxoctadecanoic acid with day of collection of seal milk sample.

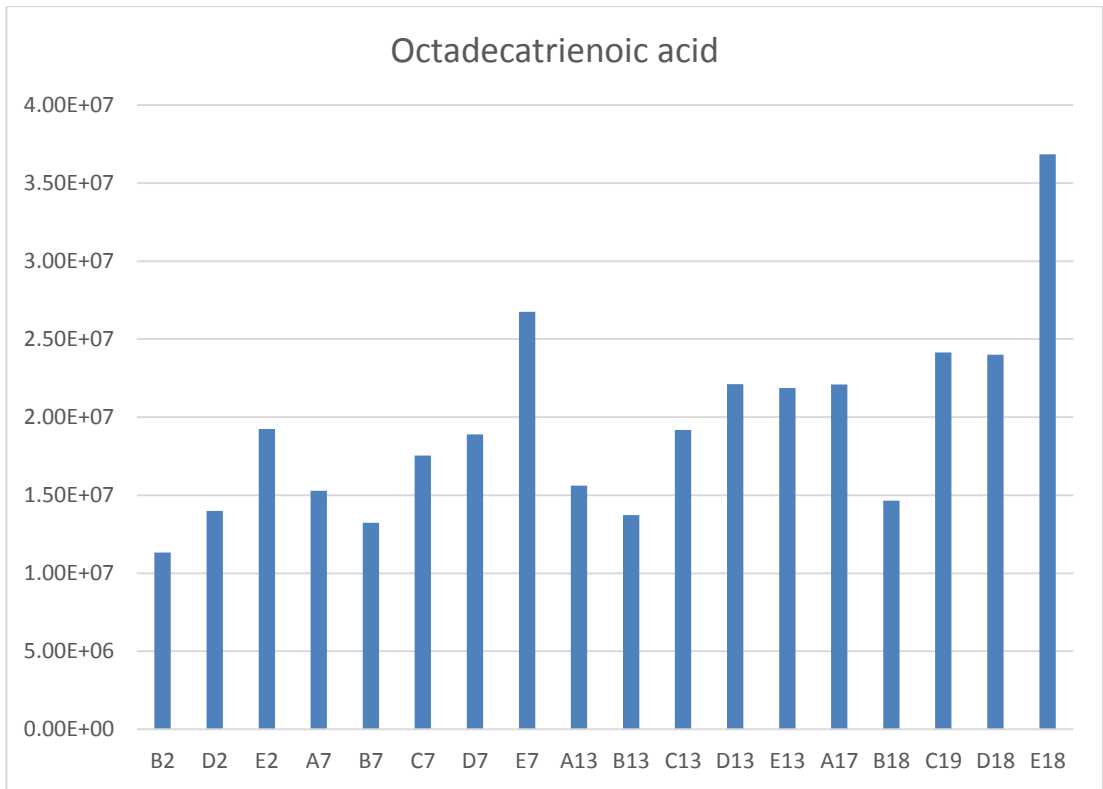


Figure 5.45 Variation of octadecatrienoic acid with day of collection of seal milk sample.

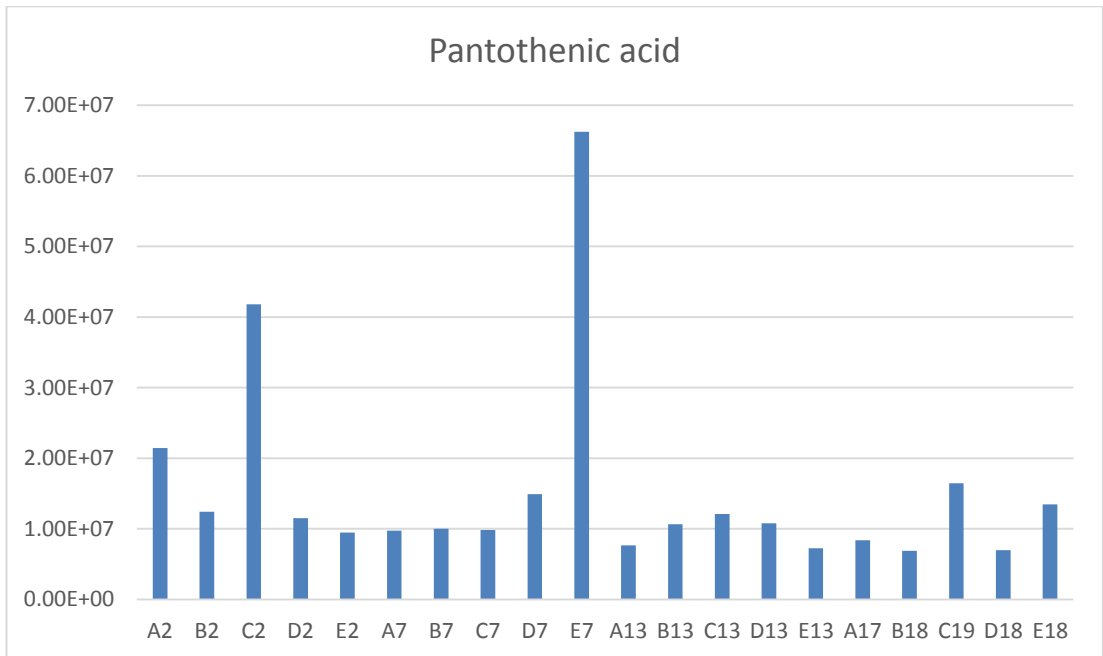


Figure 5.46 Variation of pantothenic acid with day of collection of seal milk sample.

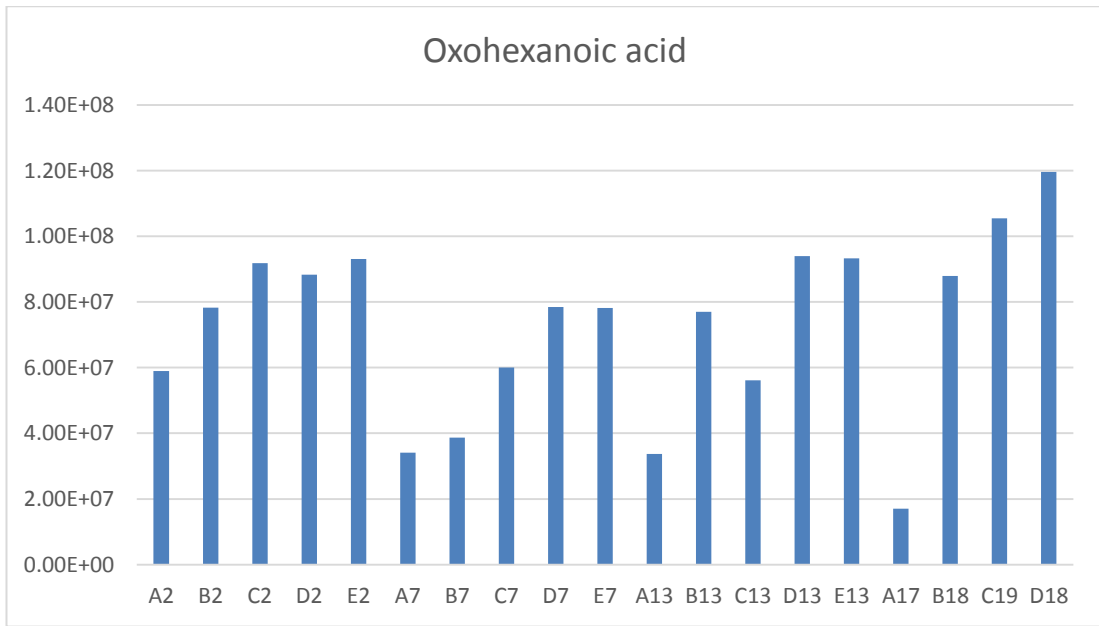


Figure 5.47 Variation of oxohexanoic acid with day of collection of seal milk sample.

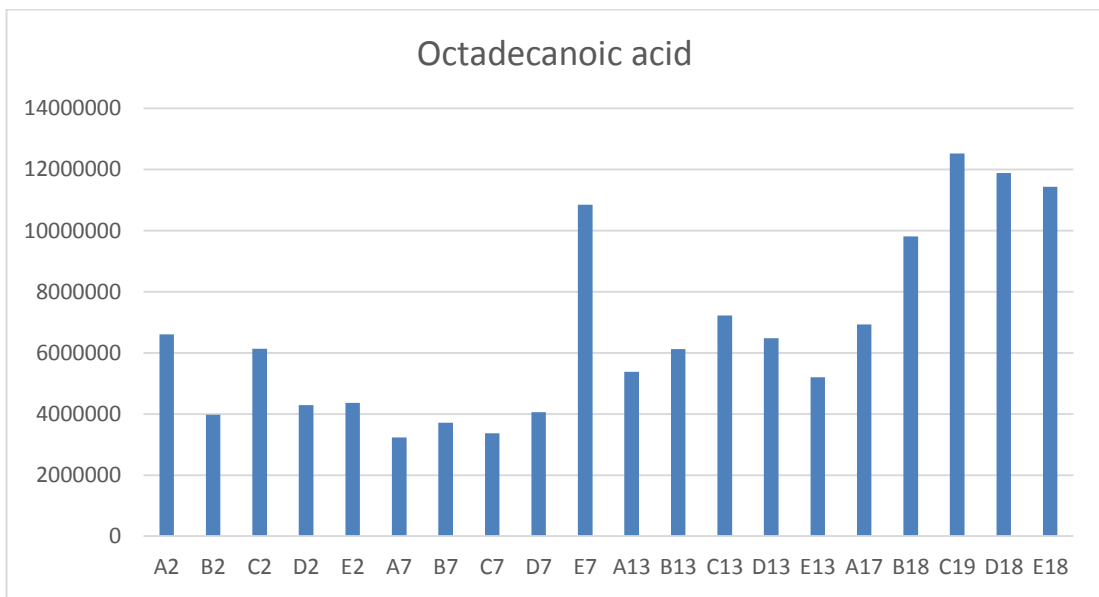


Figure 5.48 Variation of octadecanoic acid with day of collection of seal milk sample.

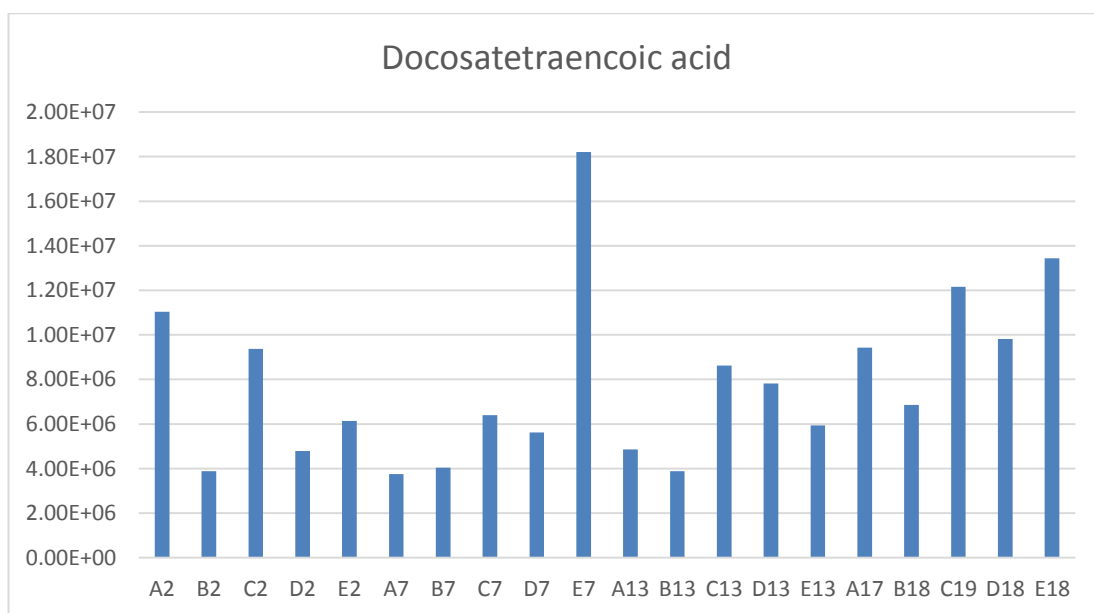


Figure 5.49 Variation of docosatetraenoic acid with day of collection of seal milk sample.

Table 5.10 shows the variation in absolute abundance of metabolites detected in the negative ion mode with time. Although there are some changes in the abundance rankings overall there is no marked variation in composition. One metabolite which does feature in the day 2 samples is sialyl lactose. Although lactose is almost absent from the seal milk samples sialyl lactose does occur. Figure 5.50 shows extracted ion traces for this metabolite from the terrestrial mammals and from seal milk. This metabolite is clearly much higher in the early seal milk samples as can be seen in Figure 5.51. Sialyllactoses and other sialylated oligosaccharides recently have been reported to have potential benefits in promoting resistance to pathogens, maturation of the gut microbiome, immune function and cognitive development [119-122]. In earlier work it was shown that these compounds were very important in panda milk and persisted during the prolonged lactation of this species [109]. These compounds help to promote a healthy microbiome. The short period where they are significant in seal milk reflects the very short lactation period in this species.

Table 5.10 Variation in the absolute abundance of metabolites detected in negative ion mode with day of collection of seal milk.

Day 2		Day 7		Day 13		Day 18/19	
Metabolite	Mean peak area	Metabolite	Mean peak area	Metabolite	Mean peak area	Name	Mean peak area
Eicosapentaenoic acid	9.50E+08	Eicosapentaenoic acid	5.88E+08	Eicosapentaenoic acid	5.80E+08	Eicosapentaenoic acid	6.16E+08
Docosahexaenoic acid	1.52E+08	Docosahexaenoic acid	1.83E+08	Docosahexaenoic acid	1.47E+08	Docosahexaenoic acid	2.89E+08
Octadecenoic acid	1.22E+08	Octadecenoic acid	1.25E+08	Octadecatetraenoic acid	9.99E+07	Octadecenoic acid	1.73E+08
Eicosatetraenoic acid	1.17E+08	Octadecatetraenoic acid	8.85E+07	Octadecenoic acid	9.96E+07	Octadecatetraenoic acid	1.20E+08
Octadecatetraenoic acid	9.56E+07	Eicosatetraenoic acid	8.27E+07	Eicosatetraenoic acid	7.45E+07	Eicosenoic acid	1.20E+08
Leukotriene A4	7.53E+07	Hexadecenoic acid	5.61E+07	Eicosenoic acid	6.01E+07	Eicosatetraenoic acid	1.05E+08
N-(9Z-octadecenoyl)-taurine	6.85E+07	Eicosenoic acid	5.39E+07	Hexadecenoic acid	5.68E+07	Hexadecenoic acid	7.58E+07
Hexadecenoic acid	6.24E+07	Leukotriene A4	3.81E+07	Leukotriene A4	5.17E+07	Leukotriene A4	5.95E+07
Eicosenoic acid	4.21E+07	N-hexadecanoyl-taurine	3.79E+07	Hexadecatetraenoic acid	3.19E+07	Docosenoic acid	5.55E+07
N-hexadecanoyl-taurine	3.97E+07	Docosenoic acid	2.29E+07	LPE 18:0	3.02E+07	N-(9Z-octadecenoyl)-taurine	4.58E+07
LPE 18:0	3.11E+07	LPE 18:0	2.25E+07	Docosenoic acid	2.88E+07	Hexadecatetraenoic acid	3.51E+07
Docosenoic acid	2.32E+07	Hexadecatetraenoic acid	2.17E+07	LPE 18:0	2.58E+07	Dihydroprogesterone	3.21E+07
PS 36:1	2.19E+07	N-hexadecanoyl-taurine	2.07E+07	N-(9Z-octadecenoyl)-taurine	2.29E+07	LPE 18:0	3.07E+07

Dihydroprogesterone	2.17E+07	Dihydroprogesterone	2.03E+07	Dihydroprogesterone	2.15E+07	Linoleate	2.98E+07
Octadecatrienoic acid	2.15E+07	Octadecatrienoic acid	1.83E+07	LPE 16:0	2.03E+07	Octadecatrienoic acid	2.63E+07
Hexadecatetraenoic acid	2.15E+07	Linoleate	1.70E+07	Octadecatrienoic acid	1.85E+07	N-hexadecanoyl-aurine	2.36E+07
Linoleate	1.95E+07	LPE 18:0	1.57E+07	Linoleate	1.78E+07	Oxo-octadecatrienoic acid	2.21E+07
PI 38:4	1.72E+07	Oxo-octadecatrienoic acid	1.38E+07	Oxo-octadecatrienoic acid	1.78E+07	LPE 16:0	2.09E+07
Oxo-octadecatrienoic acid	1.64E+07	LPE 16:0	1.19E+07	N-hexadecanoyl-aurine	1.39E+07	16-hydroxypalmitate	1.75E+07
LPE 16:0	1.41E+07	Lys-Lys-Trp-Pro	1.02E+07	16-hydroxypalmitate	1.20E+07	Tetradecanoic acid	1.60E+07
3'-Sialyllactose	1.32E+07	PE36:1	1.01E+07	PE 40:6	1.17E+07	LPE 16:0	1.60E+07
Hydroxyeicosatetraenoic acid	1.18E+07	PE 36:2	9.65E+06	Tetradecanoic acid	1.04E+07	Hydroxyeicosatetraenoic acid	1.30E+07
PE 36:2	1.07E+07	PE 40:6	9.57E+06	PS 36:2	1.01E+07	2-Oxoctadecanoic acid	1.24E+07
PS 36:2	1.04E+07	PE 38:5	8.90E+06	2-Oxophytanate	9.68E+06	trihydroxy(4:0) -trihydroxy--neuroprostatetraenoic acid-cyclo [7R,11R]	1.22E+07
Prostaglandin A2	1.02E+07	PS36:1	8.28E+06	Prostaglandin A2	9240649	Trhydroxy docosahexaenoic acid	1.21E+07

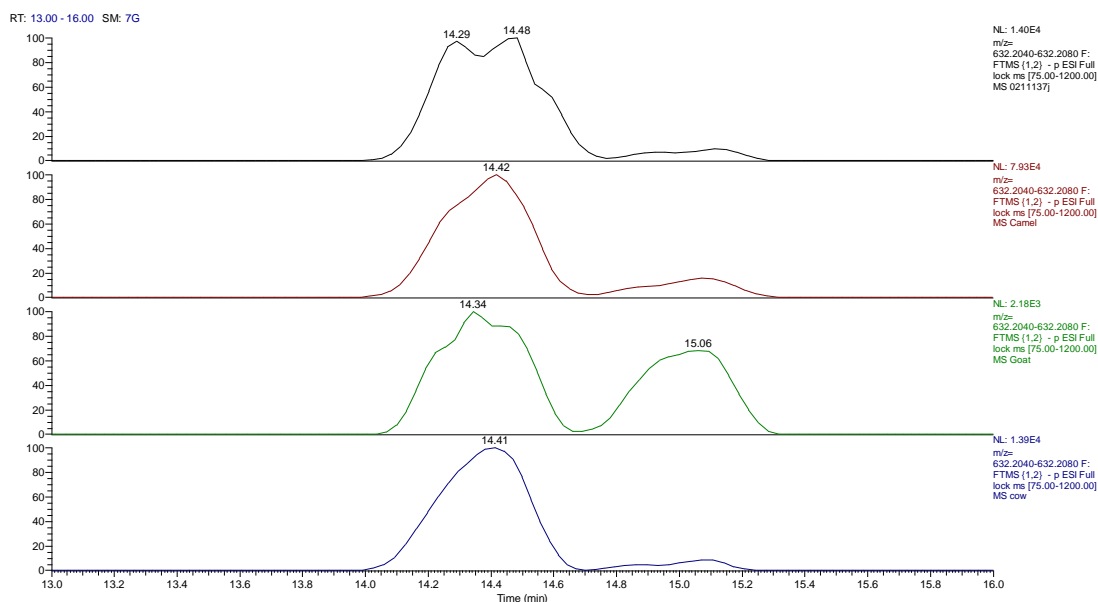


Figure 5.50 Extracted ion traces for sialyl lactose in seal, camel, goat and cow milks.

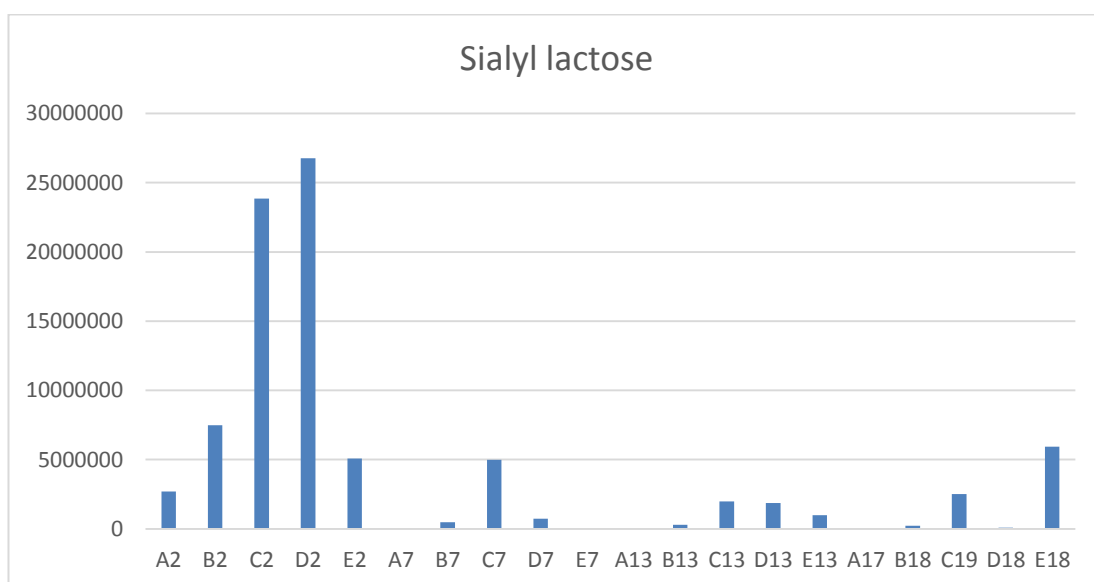


Figure 5.51 Variation in sialyl lactose levels in seal milk with time.

Figure 5.52 shows the PCA separation of seal milk samples in positive ion mode based on the lipid profile. Again there is some clustering of the sample by day but the days are not entirely separated. It was possible to produce an OPLS model based on six variables which produced quite good correlation between actual and predicted day (Figure 5.53). Table 5.11

shows the compounds that the OPLS model is based on. Figures 5.54-65.56 show the variations in the levels of the PC lipids which have the most impact on the model. Table 5.12 shows the variation in the absolute abundance of the lipids detected in positive ion mode with day. Most of the lipids within the top 25 remain stable over time.

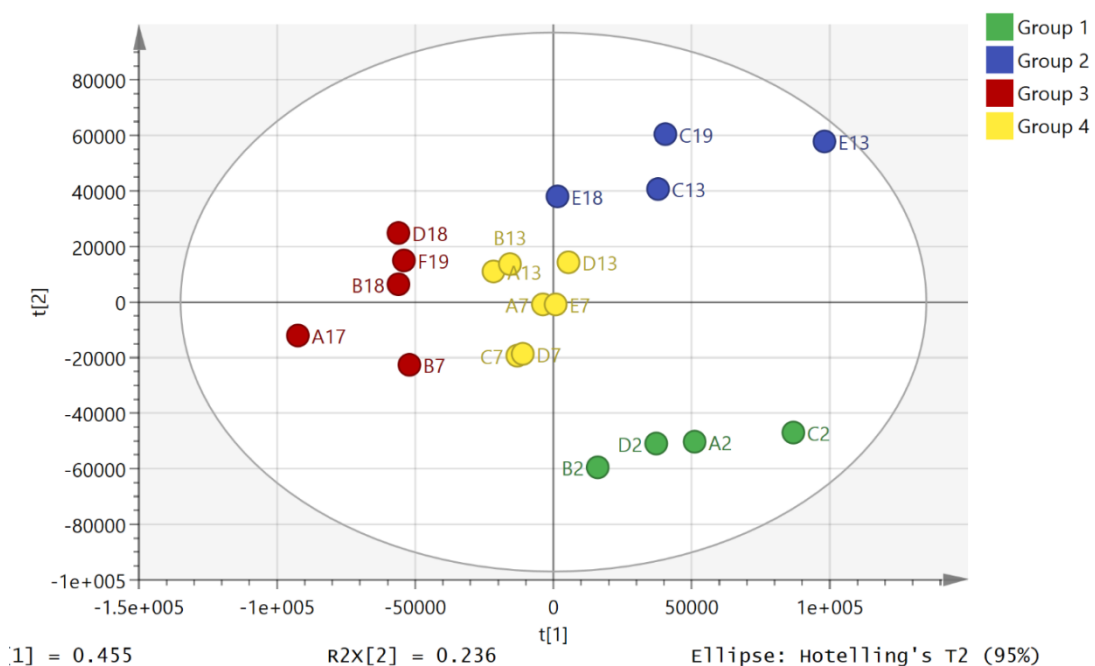


Figure 5.52 PCA with HCA for seal milk sample lipid profiles in positive ion mode.

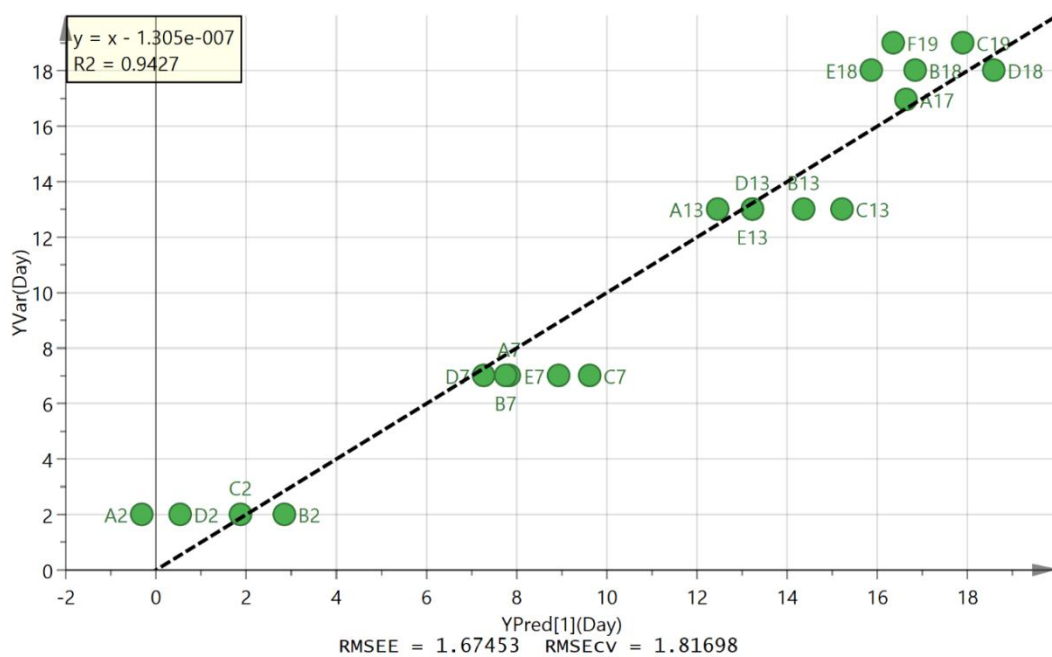


Figure 5.53 Plot of actual against predicted day based on OPLS model of seal milk lipid data in positive ion mode.

Table 5.11 Lipids used to predict the day of collection of seal milk.

m/z	t _R (min)	Metabolite	VIP
732.554	14.8	PC32:1	1.24
760.585	14.8	PC34:1	1.15
734.57	14.9	PC32:0	1.06
706.539	14.9	PC30:0	0.98
768.555	10.2	PE38:4	0.75
731.607	15.3	SM36:1	0.69

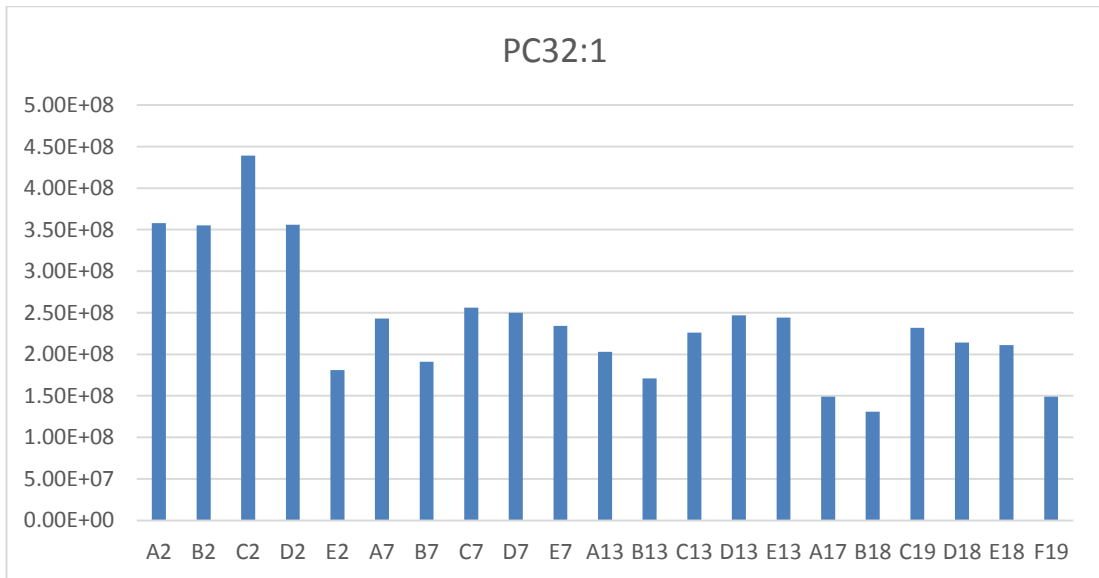


Figure 5.54 Variation in PC 32:1 levels in seal milk with time.

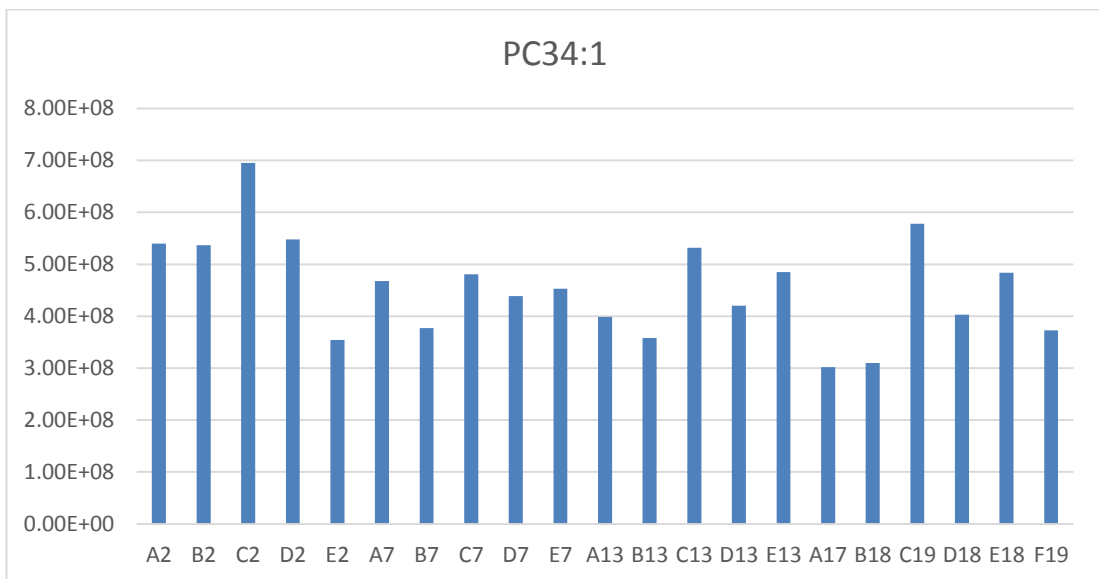


Figure 5.55 Variation in PC 34:1 levels in seal milk with time.

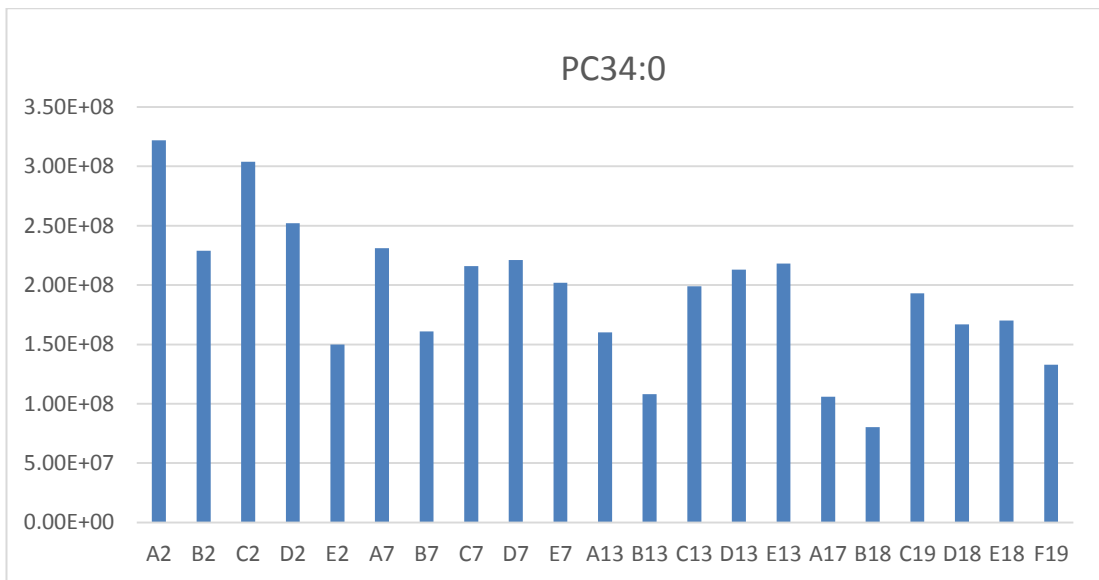


Figure 5.56 Variation in PC 34:0 levels in seal milk with time.

Table 5.12 Variation in the absolute abundance of metabolites detected in negative ion mode with day of collection of seal milk.

Day 2	Mean	Day7	Mean	Day 13	Mean	Day17/18/19	Mean
LPC C16:0	1.2E+09	LPC C16:0	1.16E+09	LPC C16:0	1.46E+09	SM42:2	9.60E+08
PC34:1	5.35E+08	SM42:2	8.56E+08	SM42:2	1.12E+09	LPC C16:0	9.26E+08
SM42:2	3.72E+08	PC34:1	4.44E+08	PC34:1	4.39E+08	LPC C16:0	4.08E+08
PC32:1	3.38E+08	Hexadecanoyl-sphingenine-1-phosphocholine	3.44E+08	LPC C18:0	3.95E+08	hexadecanoyl-sphingenine-1-phosphocholine	3.18E+08
C16:0 sphingenine-1-phosphocholine	2.77E+08	LPC C18:0	2.77E+08	Hexadecanoyl-sphingenine-1-phosphocholine	3.77E+08	LPC C18:0	2.23E+08
PC32:0	2.51E+08	PC32:1	2.35E+08	PC38:5	2.24E+08	PC36:2	1.99E+08
LPC C18:0	2.47E+08	PC32:0	2.06E+08	PC32:1	2.18E+08	PC32:1	1.81E+08
PC36:4	2.22E+08	PC36:4	1.95E+08	PC36:2	2.02E+08	PC34:2	1.73E+08
PC34:2	2.11E+08	PC38:4	1.89E+08	PC36:5	1.94E+08	PC36:1	1.68E+08
PC36:2	1.89E+08	PC38:5	1.88E+08	PC34:2	1.89E+08	PC38:5	1.53E+08
PC38:4	1.8E+08	PC34:2	1.72E+08	PC32:0	1.80E+08	SM38:1	1.46E+08
PC30:0	1.67E+08	PC36:5	1.66E+08	PC36:4	1.79E+08	PC38:4	1.46E+08
PC38:5	1.65E+08	PC36:2	1.61E+08	PC36:1	1.75E+08	PC36:4	1.43E+08
PC36:5	1.48E+08	PC36:1	1.39E+08	PC38:4	1.75E+08	PC32:0	1.42E+08
PC36:1	1.23E+08	SM38:1	1.29E+08	SM38:1	1.61E+08	PC36:4	1.22E+08
PE38:5	1.19E+08	PC30:0	1.11E+08	LPC C14:0	1.58E+08	PE38:6	9.75E+07
LPC C14:0	1.18E+08	LPC C14:0	9.87E+07	PE40:6	1.31E+08	SM42:1	9.16E+07
PE38:4	1.07E+08	PE40:6	8.83E+07	SM42:1	1.31E+08	LPC C14:0	8.31E+07
SM36:1	1.02E+08	PE36:2	8.63E+07	PC30:0	1.03E+08	PE36:1	8.08E+07
PE36:2	1.01E+08	PE38:5	8.17E+07	PE36:1	9.40E+07	PE36:2	7.72E+07
Oleoylglycero-	1E+08	SM36:1	8.09E+07	PE36:2	9.38E+07	PC30:0	7.24E+07

phosphocholine							
SM38:1	8.39E+07	PC36:3	8.00E+07	PE38:5	8.88E+07	PE38:2	6.63E+07
PC36:3	8.25E+07	Oleoylglycero-phosphocholine	7.67E+07	PC38:6	8.41E+07	PC38:2	6.62E+07
Hexadecenoylglycero-phosphocholine	6.96E+07	SM40:2	7.54E+07	SM40:2	8.18E+07	SM40:2	6.45E+07
SM40:2	6.75E+07	PE36:1	7.53E+07	Oleoylglycero-phosphocholine	8.14E+07	PC36:3	6.12E+07

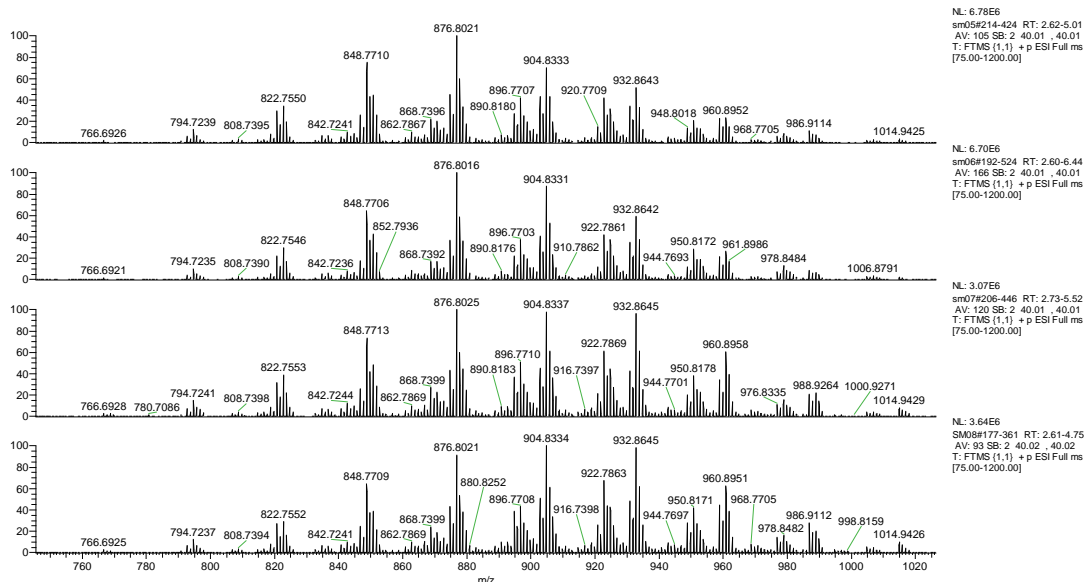


Figure 5.57 Variation in triglycerides with time in seal milk. Triglycerides were detected as ammonium adducts in positive ion mode.

Figure 5.57 shows the variation in the envelope of ions for different triglycerides over the 18 days in which seal milk samples were taken. There is no indication of major changes in the triglyceride composition of the milk with time.

Chapter 6

Conclusion and Future Work

6 Conclusion and Future Work

The work in this thesis has focused on trying to better understand hydrophilic interaction chromatography (HILIC) and on applications of this technique to metabolic profiling. In chapter 2 the effect of different mobile phase modifiers on retention of acidic and neutral test probes on silica gel was studied. The studies supported the proposal that HILIC is due to a combination of hydrophilic interactions and electrostatic interactions. Of the two acidic test probes the more negatively charged probe maleic acid was not strongly retained until the strength of the ammonium ion in the mobile phase was high enough to shield the acid from repulsion by charged silanol groups on the surface of the silica gel. Once charge repulsion was overcome maleic acid was strongly retained by hydrophilic interaction. The neutral test probes were increasingly retained with increasing ionic strength of the mobile phase and gave an indication that the thickness of the water layer on the surface of the silica gel increased with the strength of the ionic modifier. The ability of the silica gel column to separate neutral sugars and sugar phosphates was tested. The sugar isomers were not well separated on silica gel. A Nucleodur zwitterionic column did not prove any more effective at producing separations of sugar isomers. The fundamental work carried out in this chapter is complete enough to form the basis of a paper.

In chapter 3, the utility of three silica hydride columns, Cogent silica C, Cogent Phenyl Hydride and Cogent UDC cholesterol, for separating mixture of metabolites was assessed. It was possible to use these columns with an alternating gradient from high organic to high aqueous and then from high aqueous to high organic. This allowed two selectivities to be obtained on the same column. The columns showed some promise with regard to being able to carry out this type of analysis and further work is required to determine whether or not the method can be generally applied.

In chapter 4, a reductive amination method was developed for the analysis of sugars and sugar phosphates. This method was very successful in that by using deuterated aniline as a tag it was possible to produce separation between the three common hexoses glucose, galactose and mannose. The method was applied to the profiling of sugars in milk and in brain tissue. This was a very successful piece of work and has been submitted to Analytical Chemistry.

In chapter 5, an extensive study was made of seal milk in comparison with other mammalian milks. It was found that unlike the milks of terrestrial mammals seal milk had very little lactose. Thus seal pups appear to rely on fat metabolism to produce energy. A notable feature of the milk was that it provided a high level of nicotinamide which is a required precursor for the production of the cofactor NAD⁺ which is required for the β -oxidation of fats. This is a very interesting study and will be written up into a paper since it is of great interest to mammalian biologists.

6.1 Future Work

The fundamental observations on the behaviour of silica gel in HILIC mode has led to the possibility of a generic HILIC method for metabolomics profiling. This is currently being explored by another PhD student.

The sugars tagging method is currently being applied to examining the complex pattern of sugars in human urine in irritable bowel disease. Variations in the microbiome may produce variations in the pattern of non-mammalian sugars which are derived from microbial breakdown of dietary fibre.

The work on profiling of mammalian milks is of fundamental interest in the design of adequate milk replacers. Comprehensive profiling of human milk could provide some insight into how suitable the current supplements, largely derived from cows milk are.

References

1. Watson, D.G., *Pharmaceutical Analysis, A Textbook for Pharmacy Students and Pharmaceutical Chemists, 3: Pharmaceutical Analysis* 2012: Elsevier Health Sciences.
2. Olsen, B.A., *Hydrophilic interaction chromatography using amino and silica columns for the determination of polar pharmaceuticals and impurities*. Journal of chromatography A, 2001. **913**(1): p. 113-122.
3. Majors, R.E. and M. Przybyciel, *Columns for reversed-phase LC separations in highly aqueous mobile phases*. LC GC NORTH AMERICA, 2002. **20**(7): p. 584-593.
4. Hemström, P. and K. Irgum, *Hydrophilic interaction chromatography*. Journal of separation science, 2006. **29**(12): p. 1784-1821.
5. Alpert, A.J., *Hydrophilic-interaction chromatography for the separation of peptides, nucleic acids and other polar compounds*. Journal of chromatography A, 1990. **499**: p. 177-196.
6. Martin, A. and R.M. Synge, *A new form of chromatogram employing two liquid phases: A theory of chromatography. 2. Application to the micro-determination of the higher monoamino-acids in proteins*. Biochemical Journal, 1941. **35**(12): p. 1358.
7. McCalley, D.V., *Evaluation of the properties of a superficially porous silica stationary phase in hydrophilic interaction chromatography*. Journal of chromatography A, 2008. **1193**(1): p. 85-91.
8. McCalley, D.V., *Study of the selectivity, retention mechanisms and performance of alternative silica-based stationary phases for separation of ionised solutes in hydrophilic interaction chromatography*. Journal of chromatography A, 2010. **1217**(20): p. 3408-3417.
9. McCalley, D.V. and U.D. Neue, *Estimation of the extent of the water-rich layer associated with the silica surface in hydrophilic interaction chromatography*. Journal of chromatography A, 2008. **1192**(2): p. 225-229.
10. Chu, C.H., et al., *A new approach for the preparation of a hydride-modified substrate used as an intermediate in the synthesis of surface-bonded materials*. Analytical Chemistry, 1993. **65**(6): p. 808-816.
11. Molíková, M. and P. Jandera, *Characterization of stationary phases for reversed-phase chromatography*. Journal of separation science, 2010. **33**(4-5): p. 453-463.
12. Pesek, J.J., M.T. Matyska, and S. Larrabee, *HPLC retention behavior on hydride-based stationary phases*. Journal of separation science, 2007. **30**(5): p. 637-647.
13. Soukup, J. and P. Jandera, *The effect of temperature and mobile phase composition on separation mechanism of flavonoid compounds on hydrosilated silica-based columns*. Journal of chromatography A, 2012. **1245**: p. 98-108.
14. West, C. and E. Lesellier, *Characterisation of stationary phases in subcritical fluid chromatography with the solvation parameter model: III. Polar stationary phases*. Journal of chromatography A, 2006. **1110**(1): p. 200-213.

15. Liu, X. and C. Pohl, *New hydrophilic interaction/reversed-phase mixed-mode stationary phase and its application for analysis of nonionic ethoxylated surfactants*. Journal of chromatography A, 2008. **1191**(1): p. 83-89.
16. Pazourek, J., *Monitoring of mutarotation of monosaccharides by hydrophilic interaction chromatography*. Journal of separation science, 2010. **33**(6-7): p. 974-981.
17. Jandera, P., et al., *Dual hydrophilic interaction-RP retention mechanism on polar columns: structural correlations and implementation for 2-D separations on a single column*. J Sep Sci, 2010. **33**(6-7): p. 841-52.
18. Jandera, P. and T. Hajek, *Utilization of dual retention mechanism on columns with bonded PEG and diol stationary phases for adjusting the separation selectivity of phenolic and flavone natural antioxidants*. J Sep Sci, 2009. **32**(21): p. 3603-19.
19. Oyler, A.R., et al., *Hydrophilic interaction chromatography on amino-silica phases complements reversed-phase high-performance liquid chromatography and capillary electrophoresis for peptide analysis*. Journal of chromatography A, 1996. **724**(1): p. 378-383.
20. Valette, J., et al., *Separation of tetracycline antibiotics by hydrophilic interaction chromatography using an amino-propyl stationary phase*. Chromatographia, 2004. **59**(1-2): p. 55-60.
21. Wonnacott, D.M. and E.V. Patton, *Hydrolytic stability of aminopropyl stationary phases used in the size-exclusion chromatography of cationic polymers*. Journal of chromatography A, 1987. **389**: p. 103-113.
22. de Person, M., et al., *Development and validation of a hydrophilic interaction chromatography-mass spectrometry assay for taurine and methionine in matrices rich in carbohydrates*. Journal of chromatography A, 2005. **1081**(2): p. 174-181.
23. Ikegami, T., et al., *Separation efficiencies in hydrophilic interaction chromatography*. Journal of chromatography A, 2008. **1184**(1): p. 474-503.
24. Jandera, P., *Stationary and mobile phases in hydrophilic interaction chromatography: a review*. Analytica chimica acta, 2011. **692**(1): p. 1-25.
25. Karlsson, G., S. Winge, and H. Sandberg, *Separation of monosaccharides by hydrophilic interaction chromatography with evaporative light scattering detection*. Journal of chromatography A, 2005. **1092**(2): p. 246-249.
26. Alpert, A.J., *Cation-exchange high-performance liquid chromatography of proteins on poly (aspartic acid)—silica*. Journal of chromatography A, 1983. **266**: p. 23-37.
27. Tolstikov, V.V. and O. Fiehn, *Analysis of highly polar compounds of plant origin: combination of hydrophilic interaction chromatography and electrospray ion trap mass spectrometry*. Analytical biochemistry, 2002. **301**(2): p. 298-307.
28. Mihailova, A., E. Lundanes, and T. Greibrokk, *Determination and removal of impurities in 2-D LC-MS of peptides*. Journal of separation science, 2006. **29**(4): p. 576-581.
29. Han, S.M., *Direct enantiomeric separations by high performance liquid chromatography using cyclodextrins*. Biomedical Chromatography, 1997. **11**(5): p. 259-271.

30. Berthod, A., et al., *Practice and mechanism of HPLC oligosaccharide separation with a cyclodextrin bonded phase*. Talanta, 1998. **47**(4): p. 1001-1012.
31. Risley, D.S. and M.A. Strege, *Chiral separations of polar compounds by hydrophilic interaction chromatography with evaporative light scattering detection*. Analytical Chemistry, 2000. **72**(8): p. 1736-1739.
32. Daunoravičius, Ž., et al., *Simple and rapid determination of denaturants in alcohol formulations by hydrophilic interaction chromatography*. Chromatographia, 2006. **63**(7-8): p. 373-377.
33. Yoshida, T. and T. Okada, *Peptide separation in normal-phase liquid chromatography: study of selectivity and mobile phase effects on various columns*. Journal of chromatography A, 1999. **840**(1): p. 1-9.
34. Al-Tannak, N.F., et al., *The hydrophilic interaction like properties of some reversed phase high performance liquid chromatography columns in the analysis of basic compounds*. Journal of chromatography A, 2011. **1218**(11): p. 1486-1491.
35. Guo, Y. and S. Gaiki, *Retention behavior of small polar compounds on polar stationary phases in hydrophilic interaction chromatography*. Journal of chromatography A, 2005. **1074**(1): p. 71-80.
36. Jiang, W. and K. Irgum, *Tentacle-type zwitterionic stationary phase prepared by surface-initiated graft polymerization of 3-[N, N-dimethyl-N-(methacryloyloxyethyl)-ammonium] propanesulfonate through peroxide groups tethered on porous silica*. Analytical Chemistry, 2002. **74**(18): p. 4682-4687.
37. Kitano, H., et al., *Raman spectroscopic study on the structure of water in aqueous solution of zwitterionic surfactants*. Journal of colloid and interface science, 2004. **269**(2): p. 459-465.
38. Marrubini, G., B.E.C. Mendoza, and G. Massolini, *Separation of purine and pyrimidine bases and nucleosides by hydrophilic interaction chromatography*. Journal of separation science, 2010. **33**(6-7): p. 803-816.
39. Weber, G., N. von Wirén, and H. Hayen, *Hydrophilic interaction chromatography of small metal species in plants using sulfobetaine- and phosphorylcholine-type zwitterionic stationary phases*. Journal of separation science, 2008. **31**(9): p. 1615-1622.
40. Tanaka, H., X. Zhou, and O. Masayoshi, *Characterization of a novel diol column for high-performance liquid chromatography*. Journal of chromatography A, 2003. **987**(1): p. 119-125.
41. Bell, D.S., H.M. Cramer, and A.D. Jones, *Rational method development strategies on a fluorinated liquid chromatography stationary phase: Mobile phase ion concentration and temperature effects on the separation of ephedrine alkaloids*. Journal of chromatography A, 2005. **1095**(1): p. 113-118.
42. Wade, K.L., I.J. Garrard, and J.W. Fahey, *Improved hydrophilic interaction chromatography method for the identification and quantification of glucosinolates*. Journal of chromatography A, 2007. **1154**(1): p. 469-472.
43. Li, R. and J. Huang, *Chromatographic behavior of epirubicin and its analogues on high-purity silica in hydrophilic interaction chromatography*. Journal of chromatography A, 2004. **1041**(1): p. 163-169.

44. Minotti, G., et al., *Anthracyclines: molecular advances and pharmacologic developments in antitumor activity and cardiotoxicity*. Pharmacological reviews, 2004. **56**(2): p. 185-229.
45. Nesterenko, P.N. and P.R. Haddad, *Zwitterionic Ion-Exchangers in Liquid Chromatography*. Analytical sciences, 2000. **16**(6): p. 565-574.
46. Karatapanis, A.E., Y.C. Fiamegos, and C.D. Stalikas, *HILIC separation and quantitation of water-soluble vitamins using diol column*. Journal of separation science, 2009. **32**(7): p. 909-917.
47. Dell'Aversano, C., P. Hess, and M.A. Quilliam, *Hydrophilic interaction liquid chromatography–mass spectrometry for the analysis of paralytic shellfish poisoning (PSP) toxins*. Journal of chromatography A, 2005. **1081**(2): p. 190-201.
48. Bhaumik, U., et al., *Determination of Drospirenone in Human Plasma by LC–Tandem-MS*. Chromatographia, 2008. **68**(9-10): p. 713-720.
49. Kagan, M., et al., *Optimization of normal-phase chromatographic separation of compounds with primary, secondary and tertiary amino groups*. Journal of chromatography A, 2008. **1194**(1): p. 80-89.
50. McCalley, D.V., *The challenges of the analysis of basic compounds by high performance liquid chromatography: Some possible approaches for improved separations*. Journal of chromatography A, 2010. **1217**(6): p. 858-880.
51. Markopoulou, C., et al., *A Study of the Relative Importance of Lipophilic, π – π and Dipole–Dipole Interactions on Cyanopropyl, Phenyl and Alkyl LC Phases Bonded onto the Same Base Silica*. Chromatographia, 2009. **70**(5-6): p. 705-715.
52. Joshi, S.J., P.A. Karbhari, and S.I. Bhoir, *RP-LC simultaneous determination of nebivolol hydrochloride and amlodipine besilate in bi-layer tablets*. Chromatographia, 2009. **70**(3-4): p. 557-561.
53. Li, W., et al., *Hydrophilic interaction liquid chromatographic tandem mass spectrometric determination of atenolol in human plasma*. Biomedical Chromatography, 2005. **19**(5): p. 385-393.
54. Grumbach, E.S., et al., *Hydrophilic interaction chromatography using silica columns for the retention of polar analytes and enhanced ESI-MS sensitivity*. LC GC NORTH AMERICA, 2004. **22**(10): p. 1010-1023.
55. Hsieh, Y. and J. Chen, *Simultaneous determination of nicotinic acid and its metabolites using hydrophilic interaction chromatography with tandem mass spectrometry*. Rapid communications in mass spectrometry, 2005. **19**(21): p. 3031-3036.
56. Oertel, R., U. Renner, and W. Kirch, *Determination of neomycin by LC–tandem mass spectrometry using hydrophilic interaction chromatography*. Journal of pharmaceutical and biomedical analysis, 2004. **35**(3): p. 633-638.
57. Giroud, C., et al., *A fatal overdose of cocaine associated with coingestion of marijuana, buprenorphine, and fluoxetine. Body fluid and tissue distribution of cocaine and its metabolites determined by hydrophilic interaction chromatography-mass spectrometry (HILIC-MS)*. Journal of analytical toxicology, 2004. **28**(6): p. 464-474.
58. Khreit, O.I., et al., *Elucidation of the phase I and phase II metabolic pathways of (\pm)-4'-methylmethcathinone (4-MMC) and (\pm)-4'*

- (trifluoromethyl) methcathinone (4-TFMMC) in rat liver hepatocytes using LC-MS and LC-MS 2. *Journal of pharmaceutical and biomedical analysis*, 2013. **72**: p. 177-185.
59. Koh, H.L., A.J. Lau, and E.C.Y. Chan, *Hydrophilic interaction liquid chromatography with tandem mass spectrometry for the determination of underivatized dencichine (β -N-oxalyl-L- α , β -diaminopropionic acid) in *Panax medicinal plant species*. *Rapid communications in mass spectrometry*, 2005. **19**(10): p. 1237-1244.*
60. Schlichtherle-Cerny, H., M. Affolter, and C. Cerny, *Hydrophilic interaction liquid chromatography coupled to electrospray mass spectrometry of small polar compounds in food analysis*. *Analytical Chemistry*, 2003. **75**(10): p. 2349-2354.
61. Charlwood, J., et al., *Analysis of oligosaccharides by microbore high-performance liquid chromatography*. *Analytical chemistry*, 2000. **72**(7): p. 1469-1474.
62. Lindner, H., et al., *Separation of acetylated core histones by hydrophilic-interaction liquid chromatography*. *Journal of Chromatography A*, 1996. **743**(1): p. 137-144.
63. Al Bratty, M., et al., *Metabolomic profiling of the effects of allopurinol on *Drosophila melanogaster**. *Metabolomics*, 2011. **7**(4): p. 542-548.
64. Hao, C. and R.E. March, *A survey of recent research activity in quadrupole ion trap mass spectrometry*. *International Journal of Mass Spectrometry*, 2001. **212**(1): p. 337-357.
65. Scigelova, M. and A. Makarov, *Orbitrap mass analyzer—overview and applications in proteomics*. *Proteomics*, 2006. **6**(S2): p. 16-21.
66. Pettus, B.J., et al., *Observation of different ceramide species from crude cellular extracts by normal-phase high-performance liquid chromatography coupled to atmospheric pressure chemical ionization mass spectrometry*. *Rapid communications in mass spectrometry*, 2003. **17**(11): p. 1203-1211.
67. Dams, R., et al., *Influence of the eluent composition on the ionization efficiency for morphine of pneumatically assisted electrospray, atmospheric-pressure chemical ionization and sonic spray*. *Rapid communications in mass spectrometry*, 2002. **16**(11): p. 1072-1077.
68. Kostianen, R. and A.P. Bruins, *Effect of Solvent on Dynamic Range and Sensitivity in Pneumatically-assisted Electrospray (Ion Spray) Mass Spectrometry*. *Rapid communications in mass spectrometry*, 1996. **10**(11): p. 1393-1399.
69. Song, Q. and W. Naidong, *Analysis of omeprazole and 5-OH omeprazole in human plasma using hydrophilic interaction chromatography with tandem mass spectrometry (HILIC-MS/MS)—Eliminating evaporation and reconstitution steps in 96-well liquid/liquid extraction*. *Journal of Chromatography B*, 2006. **830**(1): p. 135-142.
70. Oldiges, M., S. Noack, and N. Paczia, *Metabolomics in Biotechnology (Microbial Metabolomics)*. *Metabolomics in Practice: Successful Strategies to Generate and Analyze Metabolic Data*, 2013: p. 379-391.
71. Fiehn, O., *Combining genomics, metabolome analysis, and biochemical modelling to understand metabolic networks*. *Comparative and Functional Genomics*, 2001. **2**(3): p. 155-168.

72. Fiehn, O., *Metabolomics—the link between genotypes and phenotypes*. Plant molecular biology, 2002. **48**(1-2): p. 155-171.
73. Tomita, M. and T. Nishioka, *Metabolomics: the frontier of systems biology* 2006: Springer.
74. Roessner, U. and J. Bowne, *What is metabolomics all about?* Biotechniques, 2009. **46**(5): p. 363.
75. Dettmer, K., P.A. Aronov, and B.D. Hammock, *Mass spectrometry-based metabolomics*. Mass spectrometry reviews, 2007. **26**(1): p. 51-78.
76. Ellis, D.I., et al., *Metabolic fingerprinting as a diagnostic tool*. 2007.
77. Scalbert, A., et al., *Mass-spectrometry-based metabolomics: limitations and recommendations for future progress with particular focus on nutrition research*. Metabolomics, 2009. **5**(4): p. 435-458.
78. Chen, C., F.J. Gonzalez, and J.R. Idle, *LC-MS-based metabolomics in drug metabolism*. Drug metabolism reviews, 2007. **39**(2-3): p. 581-597.
79. Lindon, J.C., J.K. Nicholson, and E. Holmes, *Metabolic Profiling: Applications in Plant Science*. The Handbook of Metabonomics and Metabolomics, 2011: p. 443.
80. Lewis, G.D., et al., *Metabolite profiling of blood from individuals undergoing planned myocardial infarction reveals early markers of myocardial injury*. The Journal of clinical investigation, 2008. **118**(10): p. 3503-3512.
81. Theodoridis, G.A., H.G. Gika, and I.D. Wilson, *LC-MS-Based Nontargeted Metabolomics*, in *Metabolomics in Practice* 2013, Wiley-VCH Verlag GmbH & Co. KGaA. p. 93-115.
82. Nielsen, J. and M.C. Jewett, *Metabolomics: a powerful tool in systems biology*. Vol. 18. 2007: Springer.
83. Wishart, D.S., *Applications of metabolomics in drug discovery and development*. Drugs in R & D, 2008. **9**(5): p. 307-322.
84. Goodacre, R., et al., *Metabolomics by numbers: acquiring and understanding global metabolite data*. TRENDS in Biotechnology, 2004. **22**(5): p. 245-252.
85. Griffiths, K., et al., *Prolonged transition time between colostrum and mature milk in a bear, the giant panda, *Ailuropoda melanoleuca**. R Soc Open Sci, 2015. **2**(10): p. 150395.
86. Zhang, T., et al., *Changes in the Milk Metabolome of the Giant Panda (*Ailuropoda melanoleuca*) with Time after Birth - Three Phases in Early Lactation and Progressive Individual Differences*. PLoS One, 2015. **10**(12): p. e0143417.
87. Bicker, W., et al., *Retention and selectivity effects caused by bonding of a polar urea-type ligand to silica: A study on mixed-mode retention mechanisms and the pivotal role of solute–silanol interactions in the hydrophilic interaction chromatography elution mode*. Journal of Chromatography A, 2011. **1218**(7): p. 882-895.
88. Santali, E.Y., et al., *A Comparison of Silica C and Silica Gel in HILIC Mode: The Effect of Stationary Phase Surface Area*. Chromatographia, 2014. **77**(13-14): p. 873-881.
89. Kang, Y.K., G. Nemethy, and H.A. Scheraga, *Free energies of hydration of solute molecules. 3. Application of the hydration shell model to charged organic molecules*. Journal of Physical Chemistry, 1987. **91**(15): p. 4118-4120.

90. Guo, K., F. Bamforth, and L. Li, *Qualitative metabolome analysis of human cerebrospinal fluid by ¹³C-/¹²C-isotope dansylation labeling combined with liquid chromatography Fourier transform ion cyclotron resonance mass spectrometry*. J Am Soc Mass Spectrom, 2011. **22**(2): p. 339-47.
91. Liu, P., et al., *Profiling of thiol-containing compounds by stable isotope labeling double precursor ion scan mass spectrometry*. Anal Chem, 2014. **86**(19): p. 9765-73.
92. Bruheim, P., H.F.N. Kvitvang, and S.G. Villas-Boas, *Stable isotope coded derivatizing reagents as internal standards in metabolite profiling*. Journal of Chromatography A, 2013. **1296**: p. 196-203.
93. Zhou, R., K. Guo, and L. Li, *5-Diethylamino-naphthalene-1-sulfonyl chloride (DensCl): a novel triplex isotope labeling reagent for quantitative metabolome analysis by liquid chromatography mass spectrometry*. Anal Chem, 2013. **85**(23): p. 11532-9.
94. Xia, B., et al., *Versatile fluorescent derivatization of glycans for glycomic analysis*. Nature methods, 2005. **2**(11): p. 845-850.
95. Saba, J.A., et al., *Investigation of different combinations of derivatization, separation methods and electrospray ionization mass spectrometry for standard oligosaccharides and glycans from ovalbumin*. Journal of mass spectrometry, 2001. **36**(5): p. 563-574.
96. Ramsay, S.L., et al., *Mild tagging procedures for the structural analysis of glycans*. Carbohydrate research, 2001. **333**(1): p. 59-71.
97. Morelle, W., et al., *Structural characterization of 2-aminobenzamide-derivatized oligosaccharides using a matrix-assisted laser desorption/ionization two-stage time-of-flight tandem mass spectrometer*. Rapid communications in mass spectrometry, 2005. **19**(14): p. 2075-2084.
98. Lamari, F.N., R. Kuhn, and N.K. Karamanos, *Derivatization of carbohydrates for chromatographic, electrophoretic and mass spectrometric structure analysis*. Journal of Chromatography B, 2003. **793**(1): p. 15-36.
99. Harvey, D.J., *Derivatization of carbohydrates for analysis by chromatography; electrophoresis and mass spectrometry*. Journal of Chromatography B, 2011. **879**(17): p. 1196-1225.
100. Gao, X., et al., *Progresses of derivatization techniques for analyses of carbohydrates*. Analytical letters, 2003. **36**(7): p. 1281-1310.
101. Fischer, K., M. Wacht, and A. Meyer, *Simultaneous and Sensitive HPLC Determination of Mono- and Disaccharides, Uronic Acids, and Amino Sugars after Derivatization by Reductive Amination*. Acta hydrochimica et hydrobiologica, 2003. **31**(2): p. 134-144.
102. Cosenza, V.A., D.A. Navarro, and C.A. Stortz, *Usage of α -picoline borane for the reductive amination of carbohydrates*. Arkivoc, 2011. **7**: p. 182-194.
103. Bowman, M.J. and J. Zaia, *Tags for the stable isotopic labeling of carbohydrates and quantitative analysis by mass spectrometry*. Analytical chemistry, 2007. **79**(15): p. 5777-5784.
104. Baxter, E.W. and A.B. Reitz, *Reductive aminations of carbonyl compounds with borohydride and borane reducing agents*. Organic reactions, 2002.
105. Andersen, K.E., C. Bjerregaard, and H. Sørensen, *Analysis of reducing carbohydrates by reductive tryptamine derivatization prior to micellar*

- electrokinetic capillary chromatography*. Journal of Agricultural and Food Chemistry, 2003. **51**(25): p. 7234-7239.
106. Ruhaak, L.R. and C.B. Lebrilla, *Analysis and role of oligosaccharides in milk*. BMB reports, 2012. **45**(8): p. 442-451.
 107. German, J., et al., *Human milk oligosaccharides: evolution, structures and bioselectivity as substrates for intestinal bacteria*. 2008.
 108. ten Bruggencate, S.J., et al., *Functional role and mechanisms of sialyllactose and other sialylated milk oligosaccharides*. Nutrition reviews, 2014. **72**(6): p. 377-389.
 109. Zhang, T., et al., *Changes in the milk metabolome of the giant panda (*Ailuropoda melanoleuca*) with time after birth—Three phases in early lactation and progressive individual differences*. PLoS One, 2015. **10**(12): p. e0143417.
 110. Iverson, S., et al., *Prenatal and postnatal transfer of fatty acids from mother to pup in the hooded seal*. Journal of Comparative Physiology B, 1995. **165**(1): p. 1-12.
 111. Castellini, M., D. Costa, and A. Huntley, *Fatty acid metabolism in fasting elephant seal pups*. Journal of Comparative Physiology B, 1987. **157**(4): p. 445-449.
 112. Iverson, S., J.P. Arnould, and I. Boyd, *Milk fatty acid signatures indicate both major and minor shifts in the diet of lactating Antarctic fur seals*. Canadian Journal of Zoology, 1997. **75**(2): p. 188-197.
 113. Zhang, R., et al., *Evaluation of mobile phase characteristics on three zwitterionic columns in hydrophilic interaction liquid chromatography mode for liquid chromatography-high resolution mass spectrometry based untargeted metabolite profiling of Leishmania parasites*. Journal of Chromatography A, 2014. **1362**: p. 168-179.
 114. Zhang, T., et al., *Evaluation of coupling reversed phase, aqueous normal phase, and hydrophilic interaction liquid chromatography with Orbitrap mass spectrometry for metabolomic studies of human urine*. Analytical chemistry, 2012. **84**(4): p. 1994-2001.
 115. Zhang, T., et al., *Application of holistic liquid chromatography-high resolution mass spectrometry based urinary metabolomics for prostate cancer detection and biomarker discovery*. PLoS One, 2013. **8**(6): p. e65880.
 116. Zheng, L., et al., *Profiling of lipids in Leishmania donovani using hydrophilic interaction chromatography in combination with Fourier transform mass spectrometry*. Rapid communications in mass spectrometry, 2010. **24**(14): p. 2074-2082.
 117. Delaney, J., et al., *Tryptophan–NAD⁺ pathway metabolites as putative biomarkers and predictors of peroxisome proliferation*. Archives of toxicology, 2005. **79**(4): p. 208-223.
 118. Ramsay, R.R. and V.A. Zammit, *Carnitine acyltransferases and their influence on CoA pools in health and disease*. Molecular aspects of medicine, 2004. **25**(5): p. 475-493.
 119. Zivkovic, A.M. and D. Barile, *Bovine milk as a source of functional oligosaccharides for improving human health*. Advances in Nutrition: An International Review Journal, 2011. **2**(3): p. 284-289.

120. Lane, J.A., et al., *Anti-infective bovine colostrum oligosaccharides: Campylobacter jejuni as a case study*. International journal of food microbiology, 2012. **157**(2): p. 182-188.
121. Weiss, G.A. and T. Hennet, *The role of milk sialyllactose in intestinal bacterial colonization*. Advances in Nutrition: An International Review Journal, 2012. **3**(3): p. 483S-488S.
122. Urashima, T., et al., *Recent advances in studies on milk oligosaccharides of cows and other domestic farm animals*. Bioscience, biotechnology, and biochemistry, 2013. **77**(3): p. 455-466.